# TOWARD IMPROVED FLANGE BRACING REQUIREMENTS FOR METAL BUILDING FRAME SYSTEMS

A Thesis

Presented to

The Academic Faculty

By

**Dai Q. Tran**

In Partial Fulfillment

Of the Requirements for Degree

Master of Science in

Civil and Environmental Engineering

**Georgia Institute of Technology**
**May 2009**

# TOWARD IMPROVED FLANGE BRACING REQUIREMENTS FOR METAL BUILDING FRAME SYSTEMS

Approved by:

Dr. Donald W. White, Advisor
School of Civil and Environmental Engineering
*Georgia Institute of Technology*

Dr. Roberto T. Leon
School of Civil and Environmental Engineering
*Georgia Institute of Technology*

Dr. Kenneth M.Will
School of Civil and Environmental Engineering
*Georgia Institute of Technology*

Date Approved: April 6, 2009

To my parents Tran Duc Diep and Nguyen Thi Kieu

# ACKNOWLEDGEMENTS

The author would like to express his appreciation to his advisor, Dr. Donald W. White, for his guidance, patience and encouragement during the course of this study. The appreciation is also extended to the committee members, Dr. Roberto T. Leon and Dr. Kenneth M. Will for their comments.

The sponsorship of this research by Metal Building Manufacturers Association (MBMA) is gratefully acknowledged. In addition, the author would like to thank the following personnel for their help through the research study: Duane Becker and Carl Glanzman.

I would like to thank Vietnam's Ministry of Education and Training for supporting my master study. I want to thank all my friends for all their help, support, interest and valuable hints.

Greatest thanks to the author's family, Tran Duc Diep and Nguyen Thi Kieu, Pham Phu Duc and Nguyen Thi Mai Lan for their unconditional love and support that they provided throughout the study.

# TABLE OF CONTENTS

## CHAPTER 3. REFINED ASSESSMENT OF COLUMN BRACING REQUIREMENTS – APPLICATION OF THE DIRECT ANALYSIS AND PLASTIC ZONE ANALYSIS METHODS...46

# LIST OF TABLES

# LIST OF FIGURES

# CHAPTER 1

# INTRODUCTION

## 1.1 Problem Statement

A brace must be designed to fulfill two main requirements: (1) it must have sufficient stiffness to adequately strengthen the braced members; and (2) it must have sufficient strength itself (Winter, 1958). Reduced bracing stiffness allows greater deformations in the physical imperfect structure; this in turn causes larger forces in the bracing system. If the bracing stiffness is too small, the required bracing forces can be excessive.

The dual requirements for relative and nodal bracing were first captured by AISC in its 1999 LRFD Specification. These achievements have been brought forward in Appendix 6 of the 2005 AISC Specification. The stability bracing provisions in Appendix 6 provide practical simplified design solutions for many bracing situations. However, they involve substantial synthesis, simplification and idealization of many complex bracing considerations. Furthermore, the application of the Appendix 6 equations to general structures can involve significant interpretation and/or extrapolation of the basic rules. As such, the true margin of safety associated with various complex bracing systems is relatively unknown, although it is commonly believed that the current bracing rules can be applied to provide accurate to conservative bracing designs.

This situation is certainly the case for the flange bracing systems in metal building frames. In general, the flange bracing systems for the primary frames in metal building structures are composed of purlins or girts combined with various types of roof and wall systems. The different potential roof and wall systems provide a wide range of diaphragm stiffnesses. In addition, rod, cable or light structural members are commonly employed as

X bracing in a plane parallel to the building envelope. A simplified illustration of two parallel frames with the above systems, minus the roof and wall systems, is shown in Fig. 1.1. Lastly, diagonal braces are commonly employed from the girts or purlins to the inside flanges of the primary frames at various locations where the inside flange of the members needs to be restrained out-of-plane, or where it is desired to brace the top and bottom flange using a torsional brace. Fig. 1.2 is a photo showing typical flange diagonal braces in a metal building.

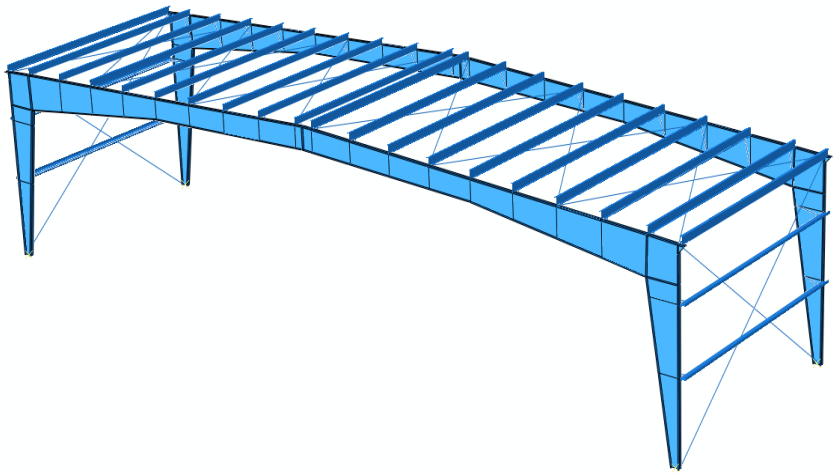

**Fig.1.1. Two representative metal building frames shown with typical outset grits and purlins and X bracing parallel to the building envelope.**

**Fig.1.2. Typical flange diagonal bracing in a metal building.**

There are a number of attributes that place the bracing design for the above types of systems outside of the specific scope of AISC Appendix 6:

1. The primary frame members are generally nonprismatic.
2. The primary frame members are beam-columns transmitting both axial load and moment.
3. The primary frame member axial loads and moments both vary along the member lengths.
4. Although the purlins are often at constant spacing except possibly near areas such as the ridge or the eaves of a typical clear span metal building frame, the girts often are not placed at constant spacing along the columns.

5. The diagonal braces to the inside flanges of the primary frame members are often placed only where the inside flange needs the additional bracing. This results in a non-constant spacing of these braces along the member lengths.
6. Because of the different primary member depths, the specific geometry of the diagonal braces is different at different locations along the primary frames. Because of these different brace geometries, the brace stiffnesses are somewhat different at the different locations.
7. If one considers the lateral bracing from the purlins and girts acting with the X bracing within the roof or walls, as well as the diaphragm bracing from the roof and wall systems, the lateral bracing stiffness provided at the girt and purlin locations is larger where the X bracing connects into the primary frames and smaller at the girt or purlin locations between these points.
8. Although the knee joint is commonly considered as an “end” of a column and an end of a roof girder, the bracing at the joint may not be sufficient such that these points can be assumed to be rigidly braced.
9. The lateral bracing of the primary frame members at the girts and purlins can come from a variety of stiffness contributions involving weak-axis bending and twisting interaction of these members with the shear stiffness of the X bracing truss system, the shear stiffness of the roof and wall diaphragms, and the ability of a more heavily loaded frame to lean-on a more lightly loaded frame in the direction of out-of-plane lateral bending. More lightly loaded unbraced lengths of a given frame may assist the more critically loaded unbraced lengths via the continuity of the members across the brace points.

10. The bracing of the primary frame members generally can come from a combination of both lateral and torsional bracing.

Appendix C of the AISC Stability Design Guide (Griffis and White 2007) discusses in detail how column stability bracing problems may be addressed using the Direct Analysis Method (DM) and provides recommendations for the use of both the 2005 AISC Appendix 6 equations and the DM. Several design examples are provided that show how the DM can lead to substantial savings in certain cases. The two main factors that contribute to these savings are:

1) Quantifying the contribution of the column *EI* to the resistance of the brace point deflections.
2) Allowing for a balancing of the stiffness and strength requirements, providing enough stiffness and strength such that the second-order force demands are smaller than the force requirements in the bracing systems as well as in the primary members.

The sources of the potential inherent conservatism in the Appendix 6 stability bracing equations in certain situations such as the above cases are due largely to a lack of full recognition of various contributors to the stiffness of the combined framing members and their bracing systems.

## 1.2 Research Objectives and Goals

The objective of this research is to investigate the application of the second-order analysis for stability bracing design of columns and beams by using the Direct Analysis Method as well as more refined Distributed Plasticity Analysis procedures. These approaches have the potential to provide improved accuracy and economy relative to the

practical design-based equations of the AISC Appendix 6. Emphasis is placed on out-of-plane flange bracing design in metal building frame systems. Potential improvements and extensions to the AISC 2005 Appendix 6 stability bracing provisions are studied and evaluated. The structural attributes considered include various general conditions encountered in practical metal building design: (1) unequal brace spacing; (2) unequal brace stiffness; (3) nonprismatic member geometry; (4) variable axial load or bending moment along the member length; (5) cross-section double or single symmetry; (6) combined torsional and lateral bracing from girts/purlins with or without diagonal braces from these components to the inside of the bottom flanges; (7) load height; (8) cross-section distortion, and (9) non-rigid end boundary conditions. The research addresses both the simplification to basic bracing design rules as well as direct computation for more complex cases. The primary goal is improved assessment of the demands on flange bracing systems in metal building frames.

The Direct Analysis Method (DM) addressed in the AISC 2005 Appendix 7 is a new method for the stability design. The DM has been developed with the goal of more accurately determining the load effects in the structure in the analysis stage and eliminating the need for calculating buckling effective length factors (*K* factors). The DM can be used to design all types of building frames including moment frames, braced frames, combined systems of braced and moment frames, and other hybrid and/or combined systems such as shear walls and moment frames.

The Distributed Plasticity Analysis (DP) approach is generally as accepted as the most accurate analysis method for assessing the strength of steel frames. Both the DM and the DP procedures applied in this research take into account: (1) flexural, shear, and

axial member deformations, and all other component that contribute to the displacements of the structure; (2) second-order effects (including $P$-$\Delta$ and $P$-$\delta$ effects); (3) geometric imperfections; (4) stiffness reductions due to inelasticity, including the effect of residual stresses and partial yielding; and (5) uncertainty in system, member, and connection strength and stiffness. However, the DP procedures explicitly track the spread of plasticity through the frame members during the loading

Rigorous second-order analyses are applied to investigate potential refinements to the AISC Appendix 6 equations. The above approaches permit the evaluation of individual brace locations based on the demand from the adjacent unsupported lengths. The key attributes of these approaches are:

- They recognize various additional contributions to the combined member and bracing system stiffness that are not included in the 2005 AISC Appendix 6 equations.
- They permit a more balanced accounting of both the available stiffness and the available strength to achieve a more optimum economy of bracing systems. Where the bracing systems and primary members have a reliable and sufficient strength, these approaches allow the designer to relax the stiffness demands on the bracing.

The ultimate goal of this research is to establish a much clearer understanding of the actual demands on flange braces in metal building systems. The specific goals of this thesis are as follows:

- Investigate the influence of a wide range of geometry conditions, applied load, and displacement boundary conditions on the bracing requirements for columns.
- Investigate the effect of the use of significantly smaller bracing stiffness than required for full bracing by Appendix 6 of the AISC Specification.
- Provide assessment of the influence of unequal brace spacing on brace force requirements using representative column nodal bracing problems.
- Benchmark simplified and refined shell-beam analysis solutions against prior eigenvalue buckling solutions for key fundamental beam bracing problems.
- Determine bracing forces using simplified and refined shell-beam second-order load-deflection solutions.
- Investigate the influence of combined lateral and torsional bracing on cases similar to the fundamental benchmark beams, but with bracing models representative of the torisonal and lateral bracing from purlins or girts.
- Investigate the stability bracing behavior for select beam problems using refined distributed plasticity shell FEA solutions. These solutions may be considered as rigorous virtual test simulations.
- Determine whether reduced bracing stiffness responses observed for columns apply to selected lateral and torsional beam bracing problems.
- Provide a preliminary assessment of the influence of tapered beam geometry on bracing requirements using a basic variation on one of the key beam bracing benchmark problems.

The structural analysis programs Mastan 2, GTSabre, SAP 2000, and ABAQUS (2007) are used as the analysis tools for this research.

## 1.3 Organization

The study is organized into six chapters. Chapter 2 discusses the general literature on bracing and reviews key background information. Chapter 3 investigates the bracing requirements in various column problems using second-order elastic analysis by the Direct Analysis Method requirements and using the Distributed Plasticity Analysis approaches. A wide range of column examples is considered. Chapter 4 focuses on the assessment of beam bracing requirements based on second-order elastic analysis. This chapter also discusses combined lateral and torsional bracing. Chapter 5 presents the assessment of beam bracing requirements based on shell finite element distributed plasticity analyses. Finally, Chapter 6 provides conclusions and recommendations from this research.

# CHAPTER 2

# BACKGROUND

## 2.1 Introduction

This chapter presents background information on bracing requirements for columns and beams and discusses previous research results on column and beam bracing. Braces are used to increase the buckling strength of structural members and framing systems. An adequate bracing system requires both brace stiffness and strength. The purpose of the stiffness requirement is to limit deformation of the braced member or structure and the purpose of the strength requirement is to provide essential stabilizing forces. Winter (1958) was among the first to recognize and develop these dual requirements for bracing design. Subsequently, much research has been conducted to investigate the bracing design requirements for elastic and inelastic members. The bracing requirements for columns and beams in Appendix 6 of the 2005 AISC Specification are largely due to these research advances.

This chapter is organized as follows. First, Section 2.2 presents the background to the column bracing requirements in the current AISC Specification. This includes both refined and simplified elastic eigenvalue buckling and second-order elastic load-deflection solutions. Section 2.2 concludes with a synthesis of the AISC (2005) Appendix 6 column bracing requirements. Section 2.3 then addresses the calculation of column elastic or inelastic strengths by a general (elastic or inelastic) eigenvalue buckling analysis. An example with four intermediate nodal braces is used to illustrate buckling solutions to determine the influence of bracing stiffness on the member strength. Then beam bracing requirements are summarized in Section 2.4.

It is important to recognize that the calculation of column design strengths via effective length factors in essence always involves some sort of eigenvalue buckling analysis. This solution is often hidden within tools such as the AISC alignment charts or the use of tabulated values of effective length factors. The procedure discussed in Section 2.3 is a refinement upon the ordinary effective length calculation of column strengths by embedding all the attributes of the AISC column curve in the calculation of the member flexural rigidities *(EI)* used in the buckling analysis. This approach can be used with general matrix analysis models of members or frames and their bracing systems to obtain column design capacities including the influence of the bracing system flexibility. This eigenvalue bucking calculation of the column strengths is referred to in this thesis as the *Effective Length Method*, although it never actually involves the calculation of any column effective length. This approach can be used to determine the column strengths in either "braced" or "unbraced" members and frames.

Chapter 2 concludes with a synthesis of beam bracing stiffness and strength requirements developed largely by Yura and Phillips (1992) and Yura (1993 and 2001), and an overview of related requirements in the 2005 AISC Appendix 6 provisions.

## 2.2 Bracing Requirements for Columns

Column bracing systems are commonly categorized into four types: relative, nodal, continuous, and lean-on. Discussions of these bracing types can be found in Yura (1993 and 1995), Yura and Helwig (1996), Galambos (1998), and Griffis and White (2008). Nodal bracing requirements for columns with equally spaced brace points have been presented by Winter (1958), McGuire (1968), Salmon and Johnson (1996), and others. The behavior of perfectly-straight pinned-pinned columns with one internal brace has

been discussed by Timoshenko and Gere (1961), Mutton and Trahair (1975), O'Connor (1979), Trahair and Nethercot (1984), Stanway (1992), Plaut (1993), Chen and Tong (1994) and Yura (1995a & b, 1996). Stanway (1992), Plaut (1993) and Yura (1996) have addressed the behavior of these types of idealized columns considering an arbitrary location of the intermediate brace. The background to the development of the dual strength and stiffness criteria for column bracing is discussed below.

### 2.2.1 Bracing Stiffness Requirements

Consider the perfectly-straight column with a single intermediate brace at its mid-height shown in Fig. 2.1. When the stiffness of the brace is very small or zero, the column will buckle in a symmetric mode. As the brace stiffness is increased, the buckling load increases but the column still fails in a symmetric mode involving displacement at the brace point. In this case, the column is said to be *partially braced*. When the brace stiffness is large enough, the perfectly straight column will buckle into the anti-symmetric *S*-shape with zero displacement at the brace point as shown in Fig. 2.1(b). In this case, the column is considered to be *fully braced*. The *full bracing stiffness* is defined as the minimum value that allows the column to support an axial load corresponding to an unbraced length of $KL_b = L_b$, where $L_b$ is the distance between braces and $K$ is the effective length factor equal to 1.0. For the perfectly-straight column, this stiffness is also the *ideal bracing stiffness*. And the ideal bracing stiffness is defined as the stiffness corresponding to incipient buckling of the bracing system for a perfectly-straight column subjected to an axial load $P$, where $P$ is a general applied load value. For a column containing initial geometric imperfections, the bracing stiffness generally must be larger

than the above ideal bracing stiffness for full bracing for the column to fail in an anti-symmetric mode corresponding to a relatively high axial load capacity.

In this research, the ideal *full* bracing stiffness is defined as the smallest brace stiffness for which the buckling strength of the ideal member is developed based on $KL_b = L_b$ $(K = 1)$. This stiffness is denoted by the symbol $\beta_{iF}$. This may be contrasted with the general ideal stiffness, $\beta_i$, which includes $\beta_{iF}$, as well as various stiffness values for partial bracing, where the bracing is sufficient to develop a particular buckling load level smaller than that associated with the fully braced member.

In general, there are many different ideal brace stiffnesses corresponding to different degrees of partial bracing. However, in cases involving partial bracing, the bracing stiffness is not sufficient to develop the member buckling strength associated with $K = 1$. In addition, in some situations, member buckling loads larger than that associated with $K = 1$ (i.e., buckling loads associated with $K < 1$) may be developed by providing braces with a stiffness larger than $\beta_{iF}$. In many cases, $\beta_{iF}$ is a well defined value. For all stiffnesses larger than this value, the buckling strength is a constant maximum value and the buckling displacement at the brace point(s) is zero. For stiffnesses smaller than this value, the buckling strength is reduced and the displacement at the brace point(s) is non-zero. However, for some problems, the member buckling strength approaches the maximum strength only asymptotically with increasing brace stiffness. For these types of problems, the brace displacements also are often non-zero in the governing buckling mode. In these situations, $\beta_{iF}$ must be determined as a stiffness such as the value at which, for instance, 98% of the strength corresponding to a rigid brace is achieved.

The behavior of columns with multiple intermediate braces is similar in many respects to the behavior of columns with a single brace. However, due to the reduced effect of the rigid end braces (if the end braces are assumed to be rigid), the bracing requirements for a column with multiple intermediate braces are larger than those of a column with single brace. And it is interesting to note that if the end braces in a column such as the one in Fig. 2.1 were to have only one-half the stiffness of the intermediate brace(s), the bracing stiffness requirement is actually identical to that for a column with an infinite number of intermediate braces spaced at the length $L_b$. In this section, the bracing requirements for a column with single brace at the mid-height and rigid end braces are examined thoroughly. The behavior of a column with four intermediate braces is discussed later.

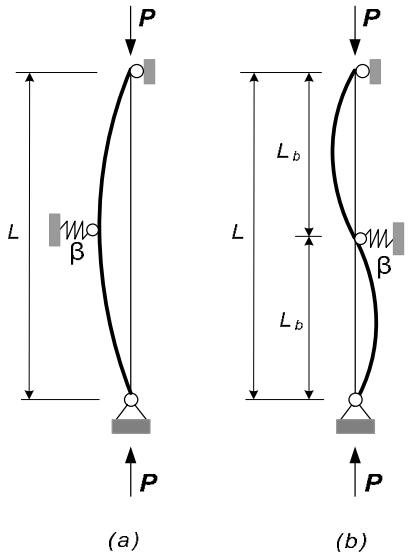


**Fig. 2.1. Columns with a single intermediate brace: (a) partially-braced column and (b) fully-braced column.**

2.2.1.1 Exact Buckling Solution for a Column with a Single Intermediate Brace

Timoshenko and Gere (1961) solved the governing differential equation of equilibrium to find the brace stiffness requirement for the perfectly straight axially loaded column with a single lateral brace at the mid-height shown in Fig. 2.1.The relationship between the elastic buckling load $P_{cr}$ and the brace stiffness β for this column can be expressed as

$$\sin 2u\left[-\sin 2u + 8u\cos 2u\left(\frac{1}{4} - \frac{P}{\beta L}\right)\right] = 0 \tag{2-1}$$

where: $u = \frac{L_b}{2}\sqrt{\frac{P}{EI}}$

β = the brace stiffness

In this problem, the upper limit for the critical value of the compressive force is obtained by assuming that the intermediate support is rigid (β = ∞). The corresponding buckling shape is shown in Fig. 2.1(b). The corresponding critical value of the compressive force determined from Eq. (2-1) is

$$P_{cr} = \frac{4\pi^2 EI}{L^2} \tag{2-2}$$

One can observe from the analytical solution associated with Eq. (2-1) that the smallest value of the brace rigidity for which the column buckles into the *S*-shape shown in Fig. 2.1(b) is

$$\beta = \frac{16\pi^2 EI}{L^3} \tag{2-3}$$

Also, the lower limit for the column buckling capacity is obtained by assuming that the intermediate brace has zero stiffness (β = 0). The corresponding buckling mode shape

is shown in Fig. 2.1(a). The corresponding critical value of the compressive force determined from Eq. (2-1) is

$$P_{cr} = \frac{\pi^2 EI}{L^2} \tag{2-4}$$

For brace stiffnesses between the above extremes, the relationship between the buckling load $P_{cr}$ and the brace stiffness β may be approximated accurately by:

$$P_{cr} = \frac{\pi^2 EI}{L^2} + \frac{3}{16}\beta L = P_{eL} + \frac{3}{16}\beta L \tag{2-5}$$

where: $P_{eL} = \frac{\pi^2 EI}{L^2}$ , the buckling load of the unbraced column

This relationship is plotted in Fig. 2.2

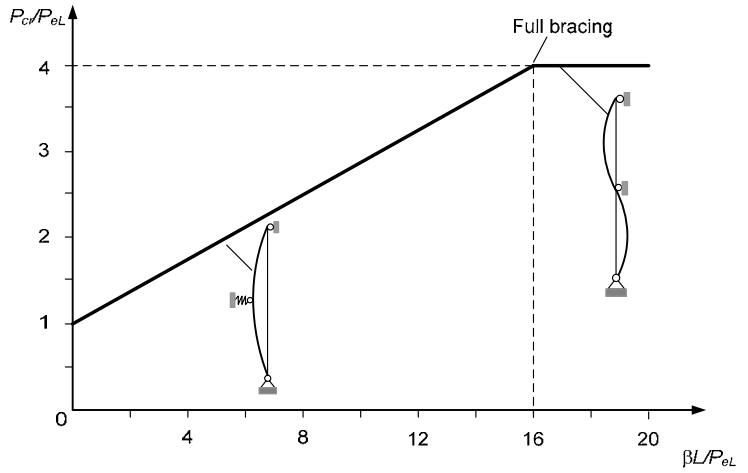


**Fig. 2.2. Buckling load vs. brace stiffness from Timoshenko and Gere (1961).**

The ideal bracing stiffness for this column (equal to the full bracing stiffness for the ideal initially straight column) is obtained by substituting $P_{cr} = P_e = \frac{\pi^2 EI}{L_b^2}$ into Eq. (2-5) and solving for β. The result is

$$\beta = \frac{16\pi^2 EI}{L^3} = \frac{16\pi^2 EI}{(2L_b)^3} = \frac{2P_e}{L_b} \tag{2-6}$$

where: $P_e = \dfrac{\pi^2 EI}{L_b^2}$ , the buckling load of the braced column.

2.2.1.2 Winter's Solution

Winter (1958) introduced a simple method to find the stiffness and strength requirements corresponding to full bracing. He recommended a simple rigid link model with fictitious hinges at the brace points for this calculation. Winter's model is shown for the case of a single intermediate brace in Fig. 2.3. This simplification is based on the fact that a perfectly straight column (with equally spaced braces) that buckles in a fully-braced mode will have inflection points and zero moment at the brace points.

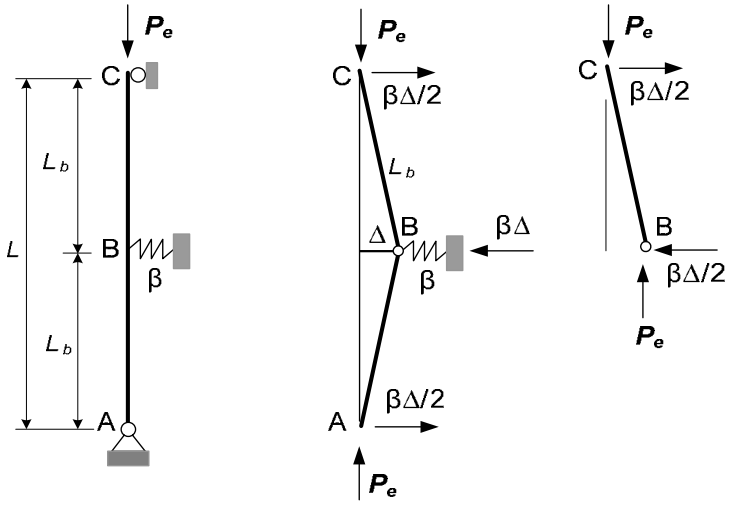


**Fig. 2.3. Winter's fictitious hinge model – Perfect column.**

In Fig. 2.3, if moment equilibrium is taken at the fictitious hinge (point B) in the right most free body diagram, the ideal brace stiffness (corresponding to $P = P_e$) is obtained as

$$\beta_i = \frac{2P_e}{L_b} \tag{2-7}$$

Equation (2-7) is the same as Eq. (2-6). That is, for the pinned-pinned column with a single lateral brace at the mid-height of column, the ideal brace stiffness calculated from Winter's model, Eq. (2-7), is the same as the ideal brace stiffness determined exactly by Timoshenko and Gere (1961), Eq. (2-6).

Interestingly, per Winter's model, the required brace stiffness for full bracing is larger for a column with an initial geometric imperfection. For the idealized column with an initial imperfection shown in Fig. 2.4, the required brace stiffness for full bracing at $P = P_e$ can be determined from fundamental equilibrium on the deflected geometry as

$$\beta = \frac{2P_e}{L_b}\left(1 + \frac{\Delta_o}{\Delta}\right) = \beta_i\left(1 + \frac{\Delta_o}{\Delta}\right) \tag{2-8a}$$

where: $\Delta_o$ = the initial imperfection amplitude.

$\Delta$ = the lateral displacement of column at the brace point.

Stated alternately, by solving this equation for $\Delta/\Delta_o$, one can determine the normalized deflection $\Delta/\Delta_o$ of the idealized column, containing a pin at the intermediate brace point, as a function of the column load $P = P_e$ and the ratio of the brace stiffness to the ideal stiffness (for full bracing) $\beta_i$:

$$\frac{\Delta}{\Delta_o} = \left[\frac{\beta}{\beta_i} - 1\right]^{-1} \tag{2-8b}$$

Note that if $\beta = \beta_i$ is selected, one obtains $\Delta = \infty$ from Eq. (2-8b). The corresponding large deflections would result in failure of the brace before reaching the load $P_e$.

One should note that Eq. (2-8) is actually valid at any axial load level $P$ for Winter's idealized model. That is, the ideal bracing stiffness at any axial load level for the pinned model is given generally by Eq. (2-7) but with $P_e = P$. Winter assumes $P = P_e$ to justify

his idealization of placing an internal hinge in the column at the brace point. In other words, Winter's model is fictitious for $P < P_e$.

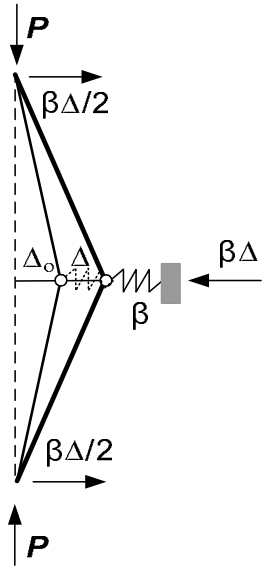


**Fig. 2.4. Winter's fictitious hinge model - Imperfect column.**

Yura (1996) emphasizes that Winter's model can be used to determine the ideal bracing stiffness corresponding to $P = P_e$ for a column with unequal unbraced lengths. This problem is considered subsequently in Section 3.7.4.2.2. Yura also shows an application of Winter's model to generate approximate solutions for column partial bracing. The application of Winter's model to analyze a column with four intermediate nodal braces for a complete range of brace stiffnesses is presented in Section 2.3.

2.2.1.3 Plaut's Solution

Plaut (1993) found that Winter's model does not always give a conservative estimate of the brace stiffness requirements. He showed that the assumed fictitious hinges at the brace points fail to account for the influence of column internal bending moments (or continuity effects) at these points in an imperfect column.

By assuming quadratic and sinusoidal initial imperfections and solving the differential equations of equilibrium, Plaut and Yang (1993) derived exact solutions to construct the relationship between the column strength and the brace stiffness. Based on these solutions, Plaut (1993) modified Winter's solution for the column with single brace at mid-height. Plaut (1993) suggested the factor "1.5" multiplier on $\Delta_o$ in Eq. (2-8a) to account for the effects of various potential shapes of the initial imperfections. That is Plaut (1993) recommended that the brace stiffness requirement for a column with a single brace at its mid-height should be

$$\beta = \frac{2P_e}{L_b}\left(1 + 1.5\frac{\Delta_o}{\Delta}\right) = \beta_i\left(1 + 1.5\frac{\Delta_o}{\Delta}\right) \tag{2-9}$$

### 2.2.2 Bracing Strength Requirements

As discussed earlier, braces also need to satisfy a strength requirement. Many previous studies have shown the interrelationship between stiffness and strength. Nair (1992) stated that "reduced stiffness allows greater deformation, which in turn results in increased force on the bracing." Winter (1958) in a discussion of experimental results also noted that greater bracing rigidity leads to smaller bracing strength requirements to produce a given column capacity. However, Plaut (1993) found that an increase in the bracing stiffness sometimes causes the bracing force to increase and sometimes causes it to decrease.

#### 2.2.2.1 Traditional 2 % Rule

Traditionally, engineers have taken 2% of the column compression force, i.e.,

$$P_{br} = 0.02\,P \tag{2-10}$$

where: $P_{br}$ = brace force

$P$ = axial compression load in column

as the column bracing strength requirement, Throop (1947) and Zuk (1956), who were the first to consider bracing strength requirements, found that this rule provided an adequate strength requirement. Required brace strengths ranging from 1.2% to 2.5% of the compressive load were identified by Throop (1947), Zuk (1956), McGuire (1968), Medland (1977), and O'Connor (1979).

2.2.2.2 Winter's Solution

According to Winter (1958), the brace force is a function of the initial column out-of-straightness, $\Delta_o$, and the brace stiffness, $\beta$. By writing the brace force-deformation and equilibrium equations for the initially imperfect column shown in Fig. 2.4, based on Winter's "pinned" idealization, the strength requirement of the brace may be expressed as:

$$P_{br} = \beta\Delta = \beta_i\left(\Delta + \Delta_o\right) = \beta_i \frac{\Delta_o}{1 - \frac{\beta_i}{\beta}} \tag{2-11}$$

where: $P_{br}$ = the brace force

$\beta$ = the actual brace stiffness

$\beta_i$ = the ideal brace stiffness given by Eq. (2-7), determined using $P = P_e$ in the previous developments, but calculated generally by using the applied axial load $P$; in this general case, $\beta_i$ is the brace stiffness corresponding to incipient buckling of the bracing system at the applied load level $P$.

$\Delta_o$ = initial lateral displacement at the brace point

$\Delta$ = additional lateral displacement at the brace point upon application of the axial load

The corresponding relationship between the column buckling load and the brace strength based on Eq. (2-11) is plotted in Fig. 2.5 for three different brace stiffnesses, $\beta = 2P_e/L_b$, $2(2P_e/L_b)$ and $3(2P_e/L_b)$. The initial imperfection at the brace point is assumed as $0.002L_b = L_b/500$. Fig. 2.5 shows that an increase in brace stiffness reduces the brace force. For example, if the brace stiffness is $\beta = 2(2P_e/L_b)$, then when $P$ reaches $P_e$, the brace force is only 0.8% of $P_e$. For design, Yura (1993) recommended a brace strength requirement equal to 1% of the applied load $P$. The increase from 0.8% to 1% is in recognition of the type of behavior observed by Plaut (1993). This requirement is based on the use of a brace stiffness equal to two times the ideal brace stiffness *for full bracing*, i.e., $\beta = 2(2P_e/L_b)$, and an initial out-of-straightness of $L_b/500$.

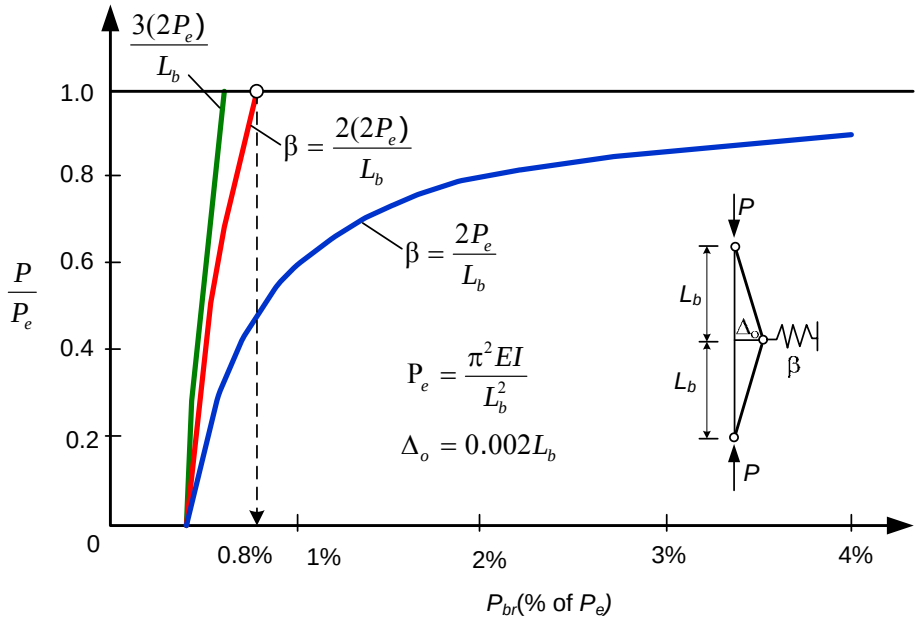


**Fig. 2.5. Brace stiffness and brace force relationship from Winter's model (1958).**

2.2.2.3 Plaut's Solution

As mentioned above, Plaut (1993) recommended a modification to Winter's solution to conservatively estimate the bracing force requirements. For the case with a brace at the column mid-height, he suggested the factor "1.5" multiplier on $\Delta_o$ to account for the effects of various shapes of initial imperfection and the effects of the continuity across the brace point location. Plaut's brace strength requirement is expressed as:

$$\beta = \frac{2P_e}{L_b}\left(1 + 1.5\frac{\Delta_o}{\Delta}\right) = \beta_i\left(1 + 1.5\frac{\Delta_o}{\Delta}\right) \qquad (2\text{-}12)$$

### 2.2.3 Summary of Brace Requirements from the AISC (2005) Appendix 6

The AISC (2005) Appendix 6 addresses only two types of column bracing: relative and nodal. The requirements for the strength and stiffness for these bracing types are summarized below:

2.2.3.1 Relative Bracing

The requirements for relative bracing are as follows:

Strength requirement:

$P_{br} = 0.004\, P_r$ (2-13, AISC A-6-1)

$P_r$ = required axial strength in the column from LRFD or ASD load combinations

$P_{br}$ = required axial strength in the brace

Stiffness requirement:

$$\beta_{br} = \frac{1}{\phi}\left(\frac{2P_r}{L_b}\right)\text{(LRFD)} \qquad \beta_{br} = \Omega\left(\frac{2P_r}{L_b}\right)\text{(ASD)} \qquad (2\text{-}14, \text{AISC A-6-2})$$

$\phi = 0.75$ $\Omega = 2.00$

$L_b$ = distance between brace points

The fundamental assumptions behind the relative bracing equations, discussed in detail in (Griffis and White 2008), are as follows:

- The relative bracing requirements address the shear force that must be resolved in a given panel of a bracing system.
- The relative bracing requirements neglect the help from the flexural stiffness *EI* of the column(s). Therefore, the $L_q$ concept (discussed below) is not applied for relative bracing.

2.2.3.2 Nodal Bracing

The requirements for nodal bracing are as follows:

Strength requirement:

$$P_{br} = 0.01\, P_r \qquad \text{(2-15, AISC A-6-3)}$$

Stiffness requirement:

$$\beta_{br} = \frac{1}{\phi}\left(\frac{8P_r}{L_b}\right)\text{(LRFD)} \qquad \beta_{br} = \Omega\left(\frac{8P_r}{L_b}\right)\text{(ASD)} \qquad \text{(2-16, AISC A-6-4)}$$

Based on the discussion in the AISC Commentary, Eq. (AISC A-6-4) may be written more generally as:

$$\beta_{br} = \frac{1}{\phi}\left[2\left(4-\frac{2}{n}\right)\right]\left(\frac{P_r}{L_q}\right)\text{(LRFD)} \qquad \beta_{br} = \Omega\left[2\left(4-\frac{2}{n}\right)\right]\left(\frac{P_r}{L_q}\right)\text{(ASD)}$$

(2-17, AISC-C 6-4)

where: $n$ = number of brace points within the column length (not including end points)

$L_q$ = the maximum braced length for which the member can support the required axial load using $K = 1$

In contrast to the assumptions behind the relative bracing equations, the fundamental assumptions behind the nodal bracing equations are as follows (Griffis and White 2008):

- The nodal bracing requirements address the absolute or direct force that must be transferred from a brace point to the bracing system.
- The nodal bracing requirements include the help from the *EI* of the column(s) in an approximate fashion via the $L_q$ parameter.

It should be noted that the AISC (2005) Appendix 6 uses the *applied load* $P_r$ to estimate the brace stiffness and strength requirements as shown in the equations from Eq. (AISC A-6-1) to Eq. (AISC A-6-4). This should be contrasted with the equations in Winter's solution, which are derived based on assuming that the column is loaded at the *critical load* $P_e$. This subtle change in variables is based on the following assumptions:

1) The relationship between the necessary brace strength and stiffness and the column axial force at $P_u = \phi_c P_n$ (LRFD), or $P_a = P_n/\Omega_c$ (ASD), is the same form as the relationship between the brace strength and stiffness at $P = P_e$ in the idealized second-order elastic analysis solutions, and
2) For $P_u < \phi_c P_n$ (LRFD) or $P_a < P_n/\Omega_c$ (ASD), the brace strength and stiffness requirements are estimated conservatively by using the axial force ($P_u$ or $P_a$) with the same brace strength and stiffness equations, which were developed by targeting the ultimate strength limit state.

The brace stiffness and brace strength requirements based on the above equations are compared to the results from Finite Element Analysis in Chapter 3.

## 2.3 Calculation of Column Design Strength from an Eigenvalue Buckling Analysis -- the AISC Effective Length Method (ELM)

As discussed in Section 2.1, the calculation of column elastic or inelastic strengths by an elastic or inelastic eigenvalue buckling analysis is helpful in gaining an understanding of the bracing requirements for columns and the relationship between the bracing requirements and column strengths. In this section, a column with four intermediate nodal braces is investigated. First, the elastic buckling strength of the column is studied using Winter's model. Then, the effective length method (ELM) procedure for determining the column flexural buckling strength is presented. This ELM procedure is a generalized one based on an eigenvalue buckling analysis, as explained in Section 2.1. Finally, solutions that focus on the elastic and inelastic behavior of a column with four equally spaced nodal braces are examined.

### 2.3.1 Elastic Buckling Strength of a Column with Four Equally Spaced Nodal Braces

Fig. 2.6 shows a column with four intermediate nodal braces having equal stiffnesses $\beta$ and with five equal unbraced lengths, $L_b$. The elastic behavior of the column based on Winter's model is discussed below.

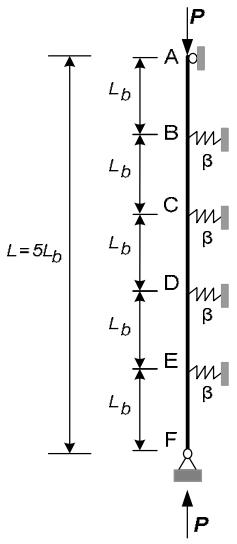


**Fig. 2.6. Column with four intermediate nodal braces.**

The rigid-link model shown in Fig. 2.7 has four unknown displacements, $\Delta_B$, $\Delta_C$, $\Delta_D$ and $\Delta_E$. These are the displacements at each of the intermediate brace points. Fictitious hinges are inserted at each of these points.

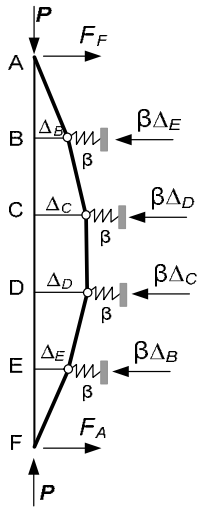


**Fig. 2.7. Winter's model - Column with four intermediate nodal braces.**

Moment equilibrium equations are written about each of the fictitious hinges in the following developments. Cutting the structure at B and summing moments gives:

$$P = \frac{\beta L_b}{5}(4 + 3X1 + 2X2 + X3) \tag{2-18}$$

where: $X1 = \frac{\Delta_C}{\Delta_B}$ ; $X2 = \frac{\Delta_D}{\Delta_B}$; $X3 = \frac{\Delta_E}{\Delta_B}$ Cutting the structure at C and summing moments gives:

$$P = \frac{\beta L_b}{5}(6 + \frac{3}{X1} + 4\frac{X2}{X1} + 2\frac{X3}{X1}) \tag{2-19}$$

Cutting the structure at D and summing moments gives:

$$P = \frac{\beta L_b}{5}(6 + \frac{2}{X2} + 4\frac{X1}{X2} + 3\frac{X3}{X2}) \tag{2-20}$$

Lastly, cutting the structure at E and summing moments gives:

$$P = \frac{\beta L_b}{5}(4 + \frac{1}{X3} + 2\frac{X1}{X3} + 3\frac{X2}{X3}) \tag{2-21}$$

Simultaneously solving Eqs. (2-19) through (2-21) gives the following four solutions:

1) $X3 = 1,\ X1 = X2 = \frac{1+\sqrt{5}}{2}$ and $\beta L_b/P = 0.382$ (mode 1)

2) $X3 = -1,\ X2 = -X1 = \frac{1-\sqrt{5}}{2}$ and $\beta L_b/P = 1.382$ (mode 2)

3) $X3 = 1,\ X2 = X1 = \frac{1-\sqrt{5}}{2}$ and $\beta L_b/P = 2.618$ (mode 3)

4) $X3 = -1,\ X2 = -X1 = \frac{1+\sqrt{5}}{2}$ and $\beta L_b/P = 3.62$ (mode 4)

The buckling modes corresponding to these four solutions are plotted in Fig. 2.8.

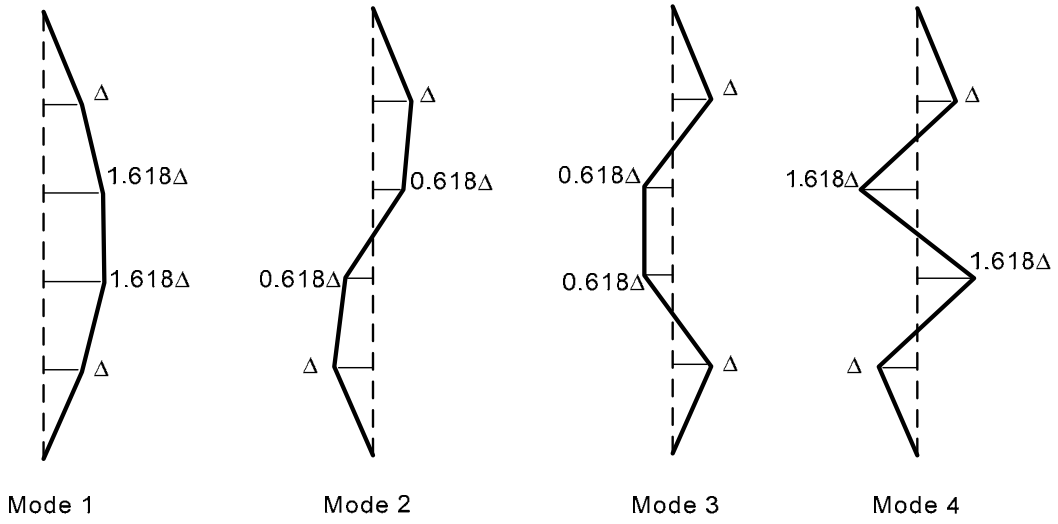


**Fig. 2.8. Winter's model – Buckling modes.**

The exact analytical solution for the buckling load of the above column versus the brace stiffness β is approximated quite well by the solid multi-segment curve shown in Fig. 2.9. This curve is constructed by assuming that the load P at buckling is given by the smallest value from the dashed lines AB, CD, EF, and GH shown in the figure. Line AB is constructed using:

1. The buckling solution for the column with no braces (point A), where the buckling load is $P_e/25$, and
2. The above solution for $P = P_e$ corresponding to mode 1 (point B).

Similarly, lines CD, EF, and GH are constructed by connecting the anchor points obtained by:

1. Using the higher-order eigenvalue buckling solutions for a pinned-ended column with no internal braces ($\beta = 0$) corresponding to the column buckling into two, three, or four half sine waves (points C, E, and G in the figure), and

2. The anchor points obtained using the above solutions from Winter's model corresponding to buckling of the bracing system at $P = P_e$ in modes 2, 3 and 4 (points D, E and H).

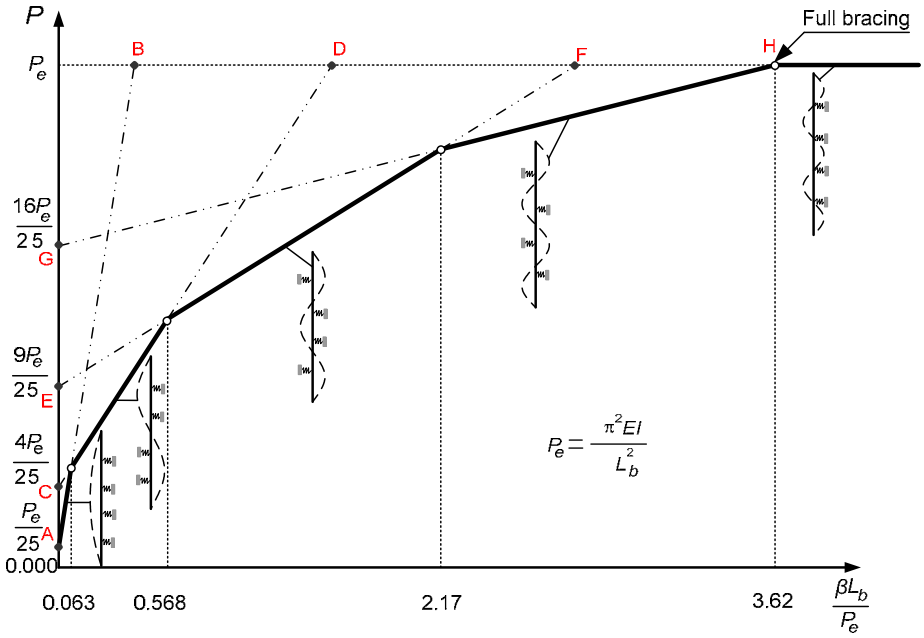


**Fig. 2.9. Buckling strength of elastic column with four equally spaced nodal braces.**

The solutions for points A, C, E and G are based on the analytical eigenvalue buckling solutions for the pinned-pinned Euler column with no internal braces ($\beta = 0$), while the solutions for points B, D, F and H are based on the above separate eigenvalue buckling solution using Winter's model. It turns out that the analytical column strength for $\beta > 0$ is represented reasonably well by drawing a straight line between each of these corresponding solutions and then taking the lower bound of all the curves (Yura 1996).

In the above problem, when the brace stiffness is very small such that $\beta L_b/P_e \leq 0.063$ the column buckles into a single wave (mode 1). As the brace stiffness is increased, the buckling mode changes. Full bracing, i.e., incipient buckling of the bracing system at $P = P_{cr} = P_e = \pi^2 EI/L_b$ corresponds to $\beta L_b/P_e = 3.62$.

### 2.3.2 Inelastic Buckling Strength Procedure for Determining Column Flexural Buckling Strength

The equations used to calculate column elastic or inelastic flexural buckling strengths are presented in Section E3 of the 2005 AISC Specification The column strength for both elastic and inelastic bucking may be expressed as one equation as the following single equation:

$$\phi_c P_n = \phi_c (0.877\tau_a P_e) \qquad (2\text{-}22)$$

where: $\tau_a$ =inelastic column stiffness reduction based on AISC column curve

For elastic buckling, $\tau_a = 1.0$.

For inelastic buckling,

$$\tau_a = -2.724 \frac{P_n}{P_y} \ln\left(\frac{P_n}{P_y}\right) \qquad (2\text{-}23, \text{AISC C-C2-12})$$

The expression for $\tau_a$ given by Eq. (2-23) is derived in Griffis and White (2008).

The stiffness reduction $\tau_a$ is plotted in Fig. 2.9.

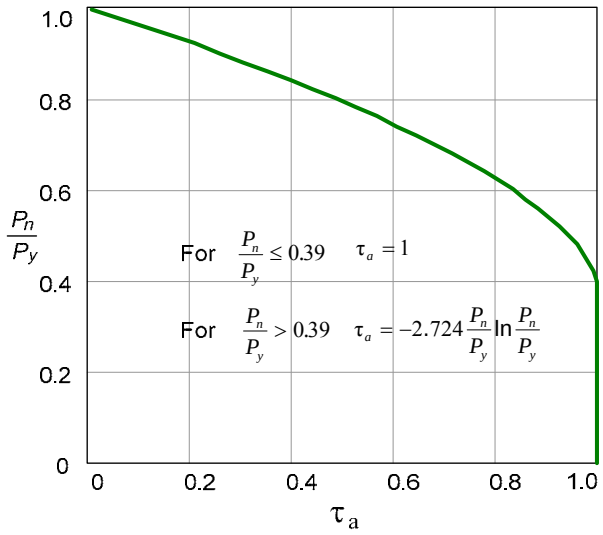


**Fig. 2.10. Stiffness reduction factor $\tau_a$.**

Eqs. (2-22) and (2-23) may be used with eigenvalue buckling analysis to determine a refined estimate of the column flexural buckling strength considering the influence of any degree of column inelasticity. The procedure to calculate the column maximum strength using rigorous inelastic eigenvalue buckling analysis is as follows:

*Step 1: Define the overall structural layout.*

*Step 2: Use the reduced elastic stiffness*

$$\phi_c\,(0.877E) = 0.9\,(0.877E) = 0.7893E$$

*Step 3:*

- Estimate $(\phi_c P_n)_o$ and $\dfrac{\phi_c P_n}{\phi_c P_y} = \dfrac{P_n}{P_y}$
- Calculate $\tau_a$ for all the members using Eq. (2-23)
- Apply the $\tau_a$ reduction to members with heavy axial loads, i.e., use a reduced member flexural rigidity of

$$I^* = \tau_a I \text{ when } \frac{\phi_c P_n}{\phi_c P_y} > 0.39 \text{ with } \tau_a = -2.724\frac{P_n}{P_y}\ln\left(\frac{P_n}{P_y}\right)$$

but note that there is no $\tau_a$ reduction, i.e.,

$$I^* = I \text{ when } \frac{\phi_c P_n}{\phi_c P_y} \le 0.39$$

*Step 4:*

- Determine the buckling load $(\phi_c P_{nb})_o$ using the member flexural rigidities

$$EI^* = 0.7893\,\tau_a EI$$

throughout the structure.

*Step 5: Check convergence of the solution*

- Select $(\phi_c P_n)_1 = (\phi_c P_{nb})_o$ and repeat until $(\phi_c P_n)_i = (\phi_c P_{nb})_i$

As mentioned in Section 2.1, the Eigenvalue bucking calculation of the column strengths is referred to here as the *Effective Length Method* (ELM)

### 2.3.3 Example Calculation of Elastic and Inelastic Buckling Strengths for a Column with Four Equally Spaced Nodal Braces

Shown in Fig. 2.10 is a W14x90 column with four intermediate nodal braces, equal unbraced lengths $L_b = L_{by}$ = 15 ft, and equal brace stiffness, β = 20 kips/inch. The column yield stress is $F_y$ = 50 ksi, and the member is subjected to a concentric axial load *P*.

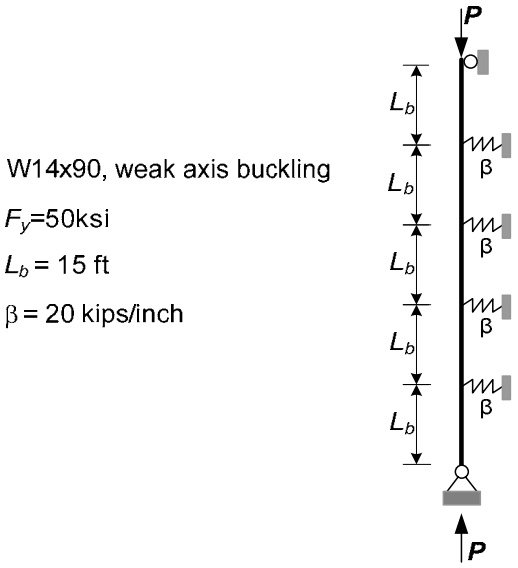


**Fig. 2.11. Column with four intermediate nodal braces – Example.**

This section illustrates the calculation of the maximum load capacity using the ELM procedure. The steps of the procedure are:

*Step 1: Determine overall structural layout.*

- As shown in Fig. 2.10.

*Step 2: Use the reduced elastic stiffnesses.*

$$0.7893E = 22{,}890 \text{ ksi}$$

$$0.7893\beta = 15.79 \text{ kips/inch}$$

*Step 3:*

- Estimate $(\phi_c P_n)_o$ = 994.1 kips. Thus, $\frac{P_n}{P_y} = \frac{\phi_c P_n}{\phi_c P_y} = \frac{994.1}{1192.5} = 0.8336$

- Calculate $\tau_a$

$$\tau_a = -2.724(0.83\ 36)\ln(0.8336) = 0.4133$$

*Step 4:*

- Determine the buckling load $(\phi_c P_{nb})_o$ using the column flexural rigidities

$$EI^* = 0.7893\ \tau_a EI$$

$$(\phi_c P_{nb})_o = 994.1 \text{ kips}$$

*Step 5: Check convergence of the solution*

The assumed $(\phi_c P_n)_o$ = 994.1 kips is equal to the calculated buckling load. Therefore, the solution has converged. This inelastic buckling load is a precise calculation of the design load capacity $\phi_c P_n$ (LRFD) using the ELM.

An accurate estimate of the elastic buckling strength of the above column is derived in Section 2.3.1. The elastic buckling strength based on the nominal elastic stiffness is plotted in Fig. 2.12. This curve is determined using the eigenvalue buckling solution capabilities in Mastan 2 (Ziemian and McGuire 2007).

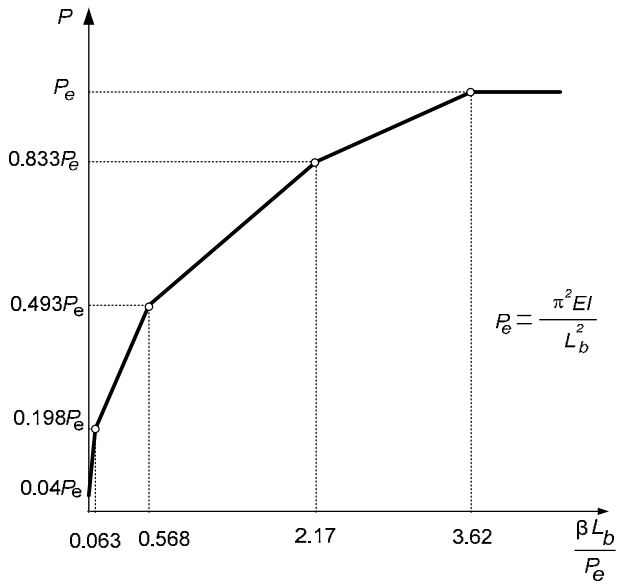


**Fig. 2.12. Elastic buckling strength.**

Fig. 2.13 shows the corresponding AISC column design strengths (LRFD) as a function of the variable bracing stiffness β, assuming that the yield stress is infinite, i.e., $F_y = \infty$. In other words, the AISC column elastic buckling design strength is $\phi_c P_n = \phi_c (0.877 P_e) = 0.789 P_e$ for full bracing.

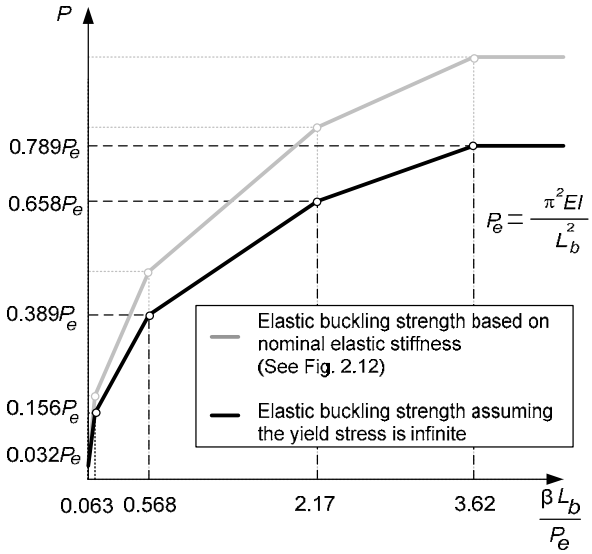


**Fig. 2.13. Elastic column bucking strength, $F_y = \infty$.**

The AISC column design strength for $F_y$ = 50 ksi is plotted in Fig. 2.14.

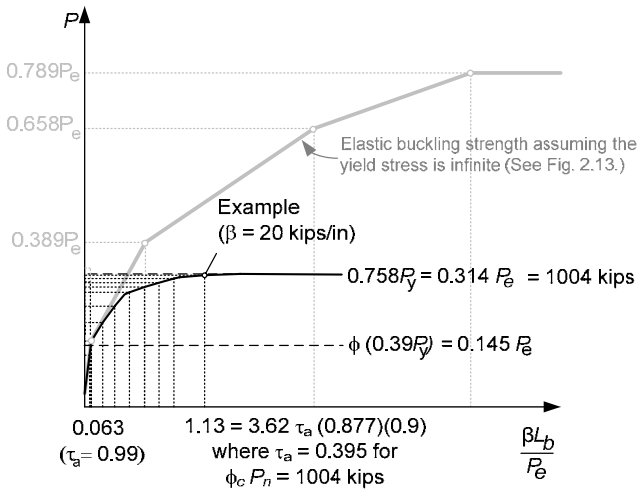


**Fig. 2.14. Inelastic buckling strength with $F_y$ =50ksi.**

One can observe that the "fully-braced strength" ($\phi_c P_n$ = 1004 kips = 0.314 $P_e$ based on $K$ = 1, $KL_b$ = 15 ft) is developed using a brace stiffness of $\beta_i = 3.62\ \phi_c P_n / L_b$ = = 3.62 (1004) / 180 = 20 kips/in. This brace stiffness $\beta_i$ = 20 kips/in is also used to determine the brace forces and column capacity in illustrative examples of the application of the Direct Analysis Method (DM) and the Distributed Plasticity (DP) Method in Chapter 3. The column strength with rigid bracing and $KL_b$ = 15 ft is determined from the AISC equations as $\phi_c P_n$ = 1004 kips where $\tau_a$ = 0.395 as shown in Fig. 2.14.

The above ELM procedure provides an effective "exact" flexural buckling resistance $\phi_c P_n$ based on inelastic eigenvalue buckling solutions. However, the ELM procedure only gives the column capacity for a given configuration and stiffness of a member and its bracing system. The ELM procedure does not provide any information about the forces in order to design the braces.

Only column bracing requirements have been discussed thus far. The corresponding beam bracing requirements are reviewed in the next section.

## 2.4 Bracing Requirements for Beams

The behavior of beam bracing systems is more complicated than that of column bracing systems, since the beam buckling capacity involves both bending and torsion while the column flexural buckling capacity depends only on the column flexural rigidity and the resistance of the braces to the transverse displacements due to column bending. In this section, the lateral and torsional bracing requirements for relative and nodal bracing of beams are summarized.

### 2.4.1 Lateral Bracing Requirements

Similar to the column bracing requirements, Winter also proposed lateral bracing requirements for beams. He considered the compressed portion of a flange as an independent strut. The strut acts like a column and the same method used for the column bracing is applied to find the requirements for the beam lateral bracing. However, beam bracing is much more complicated than column bracing due to load height effects, cross-section distortion, moment gradient effects, and the influence of brace position through the cross-section depth.

Yura (1993b and 2001) has provided numerous refinements to the base model developed by Winter. These refinements have served as the primary basis for the beam lateral bracing provisions in the 2005 AISC Appendix 6. The AISC beam lateral bracing stiffness and strength requirements are summarized below.

*a) Stiffness Requirement*

The commentary to the 2005 AISC Appendix 6 gives a refined version of its brace stiffness requirement expressed for LRFD as

$$\beta_{br} = \frac{1}{\phi}\frac{2\,N_i\left(C_b P_f\right)C_t C_d}{L_b} \qquad \text{(2-24, AISC C-A-6-3)}$$

where: $N_i$ = 1.0 for relative bracing

= (4-2/$n$) for discrete bracing

$n$ = number of intermediate braces

$P_f$ = beam compression flange force. This force is shown as $\pi^2 EI_{yc}/L_b^2$ in the AISC Commentary. However, if designers were to use this expression, the beam lateral bracing stiffness requirements would be excessive for most practical problems. In the implementation of the AISC beam lateral bracing requirements, $C_b P_f$ is expressed as $M_u / h_o$ in LRFD, where $M_u$ is the required flexural strength of the beam. The maximum permitted value of $M_u$ is of course $\phi_b M_n$. Hence, the beam lateral bracing stiffness requirements are based on the same type of assumptions as those discussed previously for columns. That is, the bracing stiffness necessary to develop $M_u = \phi_b M_n$ is assumed to be the same form as the bracing stiffness necessary to develop the buckling strength in second-order elastic solutions. Also, the bracing requirements for $M_u < \phi_b M_n$ are estimated conservatively by this same form.

$I_{yc}$ = out-of-plane moment of inertia of the compression flange

= $I_y$/2 for doubly symmetric cross sections

$C_b$ = moment gradient modifier

$C_t$ = factor accounting for top flange loading

$= 1 + (1.2/n)$

= 1 for centroidal loading

= 1.2 for top flange loading

$C_d$ = double curvature factor (compression in both flanges)

$= 1 + (M_S/M_L)^2$

= 1 for bending in single curvature

= 2 for double curvature

= 2 for the brace closest to the inflection point

$M_S$ = smallest moment causing compression in each flange

$M_L$ = largest moment causing compression in each flange

These requirements are similar for ASD, but $M_u$ is replaced by the required ASD flexural strength and $1/\phi = 1/0.75$ is replaced by $\Omega = 2.00$.

*b) Strength Requirement*

The refined strength requirements for relative and nodal bracing are specified in the AISC Appendix 6 commentary as follows.

For relative bracing (LRFD):

$$P_{br} = \frac{0.004 M_u C_t C_d}{h_o} \qquad \text{(2-25, AISC C-A-6-4a)}$$

For nodal bracing (LRFD):

$$P_{br} = \frac{0.001 M_u C_t C_d}{h_o} \qquad \text{(2-26, AISC C-A-6-4b)}$$

where $M_u$ is the required flexural strength.

### 2.4.2 Torsional Bracing Requirements

Taylor and Ojalvo (1966) investigated the elastic buckling strength of torsionally braced beams. They considered the effects of both continuous and nodal torsional bracing on simply-supported beams subjected to three types of loading: uniform bending moment, a transverse point load at mid-span, and a transverse uniformly distributed load. They developed the following theoretical equation for the critical moment of a doubly-symmetric beam with continuous torsional bracing subjected to uniform bending moment:

$$M_{cr} = \sqrt{M_o + \overline{\beta_T} EI_y} \tag{2-27}$$

where: $M_o$ = buckling capacity without any intermediate bracing

$\overline{\beta_T}$ = continuous torsional brace stiffness

One can observe from Eq. (2-27) that with continuous torsional bracing, the critical moment increases without any limit as the brace stiffness increases.

Yura and Phillips (1992) expanded upon the work by Taylor and Ojalvo and developed detailed design requirements for both continuous and discrete beam torsional bracing. Their study examined the effects of cross section distortion, position of loading, and torsional brace location on the buckling behavior of *I*-section beams. This study showed that cross-section distortion has a substantial effect on the behavior of torsional braces. Yura and Phillips (1992) modified Eq. (2-27) from Taylor and Ojalvo by including the effects of position of loading and cross section and distortion as shown below:

$$M_{cr} = \sqrt{C_{bu}^2 M_o^2 + \frac{C_{bb}^2 \overline{\beta_T} EI_y}{C_t}} \leq M_y \text{ or } M_{bp} \tag{2-28}$$

where:

$M_o$ = buckling capacity of the unbraced beam subjected to uniform moment loading

$C_{bu}$ = $C_b$ factor for the unbraced beam

$C_{bb}$ = $C_b$ factor for the fully braced beam

$C_t$ = top flange loading modifier

$\overline{\beta_T}$ = continuous torsional brace stiffness accounting for cross section distortion

$M_y$ = beam yield moment

$M_{bp}$ = moment corresponding to buckling between the braces with $KL_b = L_b$.

Based on the definition of $\overline{\beta_T}$ , Eq. (2-28) applies directly for continuous torsional bracing. However, it can also be utilized for discrete (or nodal) torsional bracing by using the following expression to convert the nodal bracing stiffnesses to the continuous bracing stiffness (Yura and Phillips 1992).

$$\overline{\beta_T} = \frac{n\beta_T}{\alpha L} \tag{2-29}$$

where: $n$ = number of intermediate braces

$L$ = span length

$\alpha$ = 0.75 for a single mid-span torsional brace in beams subjected to centroidal loading

= 1.0 for all other cases

As mentioned above, cross-section distortion can affect the torsional bracing requirements significantly. For cases with a torsional brace attached to the beam cross-

section at a single discrete location, a web stiffener at the brace point reduces the cross-sectional distortion and greatly improves the effectiveness of the torsional bracing. The total stiffness of the torsional bracing system is a function of the torsional bracing stiffness and the cross-section distortional stiffness. The individual stiffness components may be considered as the springs in series. Therefore, the total bracing system stiffness can be predicted by using the following expression:

$$\frac{1}{\beta_T} = \frac{1}{\beta_{Tb}} + \frac{1}{\beta_{sec}} \qquad \text{(2-30, AISC C-A-6-10)}$$

where: $\beta_T$ = total torsional bracing system stiffness

$\beta_{Tb}$ = torsional brace stiffness (required bracing stiffness)

$\beta_{sec}$ = cross-section stiffness (accounts for cross-section distortion)

Expressions for $\beta_{sec}$ are provided in the following sections. Several sections in Chapters 4 and 5 address the calculations for torsional bracing provided by girts or purlins combined with flange diagonal bracing in metal building structures.

2.4.2.1 Brace Requirements Based on Refined Equations from Yura and Phillips (1992)

The brace stiffness and strength requirements developed by Yura and Phillips (1992) are as follows:

*a) Stiffness Requirement*

- The ideal discrete torsional bracing stiffness is estimated as

$$\beta_{Ti} = (M_{cr}{}^2 - C_{bu}^2 M_o^2)\frac{C_t}{C_{bb}^2 EI_{eff}}\frac{\alpha L}{n} \qquad \text{(2-31)}$$

where: $I_{eff} = I_y$ for doubly symmetric sections

$= I_{yc} + \frac{t}{c} I_{yt}$ for singly symmetric sections

$c$ = distance between cross section centroid and centroid of compression flange

$t$ = distance between cross section centroid and centroid of tension flange

It should be noted that this equation gives the brace stiffness requirement necessary to develop the beam elastic buckling resistance. The modifications implemented in AISC to address general cases of $M_u \leq \phi_b M_n$ (LRFD) are discussed in the next section.

- The brace stiffness excluding web distortion is

$$\beta_T = \frac{2\beta_{Ti}}{\phi} \tag{2-32}$$

- The web distortional stiffness is

$$\beta_{sec} = \frac{3.3E}{h_o}\left(\frac{1.5h_o t_w^3}{12} + \frac{t_s b_s^3}{12}\right) \tag{2-33}$$

where: $t_w$ = beam web thickness

$t_s$ = web stiffener thickness

$b_s$ = stiffener width for one-sided stiffeners ( use twice the individual stiffener width for pairs of stiffeners)

- The required brace stiffness, including the influence of web distortion, is

$$\beta_{Tb} = \frac{\beta_T}{\left(1 - \frac{\beta_T}{\beta_{sec}}\right)} \tag{2-34}$$

*b) Strength Requirement*

$$M_{br} = \beta_T \theta_o = \beta_T \frac{L_b}{500 h_o} \tag{2-35}$$

2.4.2.2 Brace Requirements Based on the AISC 2005 Appendix 6

The brace stiffness and strength requirements from the AISC (2005) Appendix 6 are summarized as follows:

*a) Stiffness Requirement*

- The brace stiffness excluding web distortion is

$$\beta_T = \frac{1}{\phi}\left(\frac{2.4 L M_r^2}{n E I_y C_b^2}\right) \tag{2-36, AISC A-6-11}$$

  This equation is derived from Eq. (2-28) by neglecting the unbraced beam buckling term $(C_{bu}M_o)$, using $C_t = 1.2$ for top flange loading, replacing the critical moment $M_{cr}$ by the applied moment $M_t$. and multiplying the resulting estimate of the ideal bracing stiffness by 2.0 .

- The web distortional stiffness is

$$\beta_{sec} = \frac{3.3E}{h_o}\left(\frac{1.5 h_o t_w^3}{12} + \frac{t_s b_s^3}{12}\right) \tag{2-37, AISC A-6-12}$$

  This equation is the same as the corresponding Eq. (2-33) from Yura and Phillips (1992)

- Required brace stiffness

$$\beta_{Tb} = \frac{\beta_T}{\left(1 - \frac{\beta_T}{\beta_{sec}}\right)} \qquad \text{(2-38, AISC A-6-10)}$$

*b) Strength Requirement*

$$M_{br} = \frac{0.024 M_r L}{n C_b L_b} \qquad \text{(2-39, AISC A-6-9)}$$

This equation is derived by substituting Eq. (2-36) into Eq. (2-35), assuming that the beam compression flange force is $P_f = M_r/h_o$, replacing $C_b\pi^2 EI_y/L_b^2$ by $2P_f$, and using $C_t = 1.2$ for top flange loading. It is applicable only for doubly-symmetric cross-section where $I_{yc} = I_y/2$. For singly-symmetric cross-sections, this equation will generally be conservative. However, better estimates of the strength requirement can be obtained by using Eqs. (2-31), (2-32) and (2-35) in Section 2.4.2.1.

The brace stiffness and brace strength requirements based on the above equations are compared to the results from Finite Element Analysis in Chapters 4 and 5.

# CHAPTER 3

# REFINED ASSESSMENT OF COLUMN BRACING REQUIREMENTS - APPLICATION OF THE DIRECT ANALYSIS AND PLASTIC ZONE ANALYSIS METHODS

## 3.1 Introduction

As addressed in Chapter 2, there have been numerous important prior studies regarding column bracing. Many of the previous developments have been based on Winter's idealization (Winter 1958), in which the member unbraced segments are modeled as rigid links connected by hinges at the brace points. The resulting developments have the advantage of simplicity, and they work well in many cases. However, Plaut (1993) showed analytically that Winter's model does not always estimate the required brace strength and stiffness conservatively. The results from Winter's model may be either unconservative or conservative due to the fact that Winter's model does not account for member continuity effects on the bracing requirements.

This chapter focuses on investigating and understanding key issues and considerations in the context of column bracing prior to tackling these issues in the context of beams. Lateral bracing requirements for beam compression flanges are in many respects similar to column bracing requirements. In other words, column bracing design is in certain respects a microcosm of beam and beam-column bracing design. Many of the current beam bracing design requirements are extensions of column bracing rules.

The organization of this chapter is as follows. First, Section 3.2 gives an overview of a suite of column bracing problems studied in this research and the rationale for each of

these problems. Then, Section 3.3 discusses the appropriate magnitude and pattern of geometric imperfections that should be considered in refined analysis of columns and their bracing systems. After that, the specific procedures for applying the Direct Analysis Method (DM) to the solution of general column bracing problems are outlined. Then, a column with four intermediate nodal braces and a range of different brace stiffnesses is analyzed to demonstrate these procedures. This is followed by a summary of the procedure for applying the Distributed Plasticity (DP) analysis method to general column bracing problems and the presentation of the DP solution for the above example. The chapter then presents results for each of the column bracing problems described in Section 3.2 using the DM and DP methods.

## 3.2 Overview of Example Column Bracing Problems

The column bracing problems considered in this chapter are summarized in Figs. 3.2.1 to 3.2.3. Fig. 3.2.1 shows five cases of a column with four intermediate nodal braces, labeled as problems NB1 to NB5. Fig. 3.2.2 shows two different columns with a single intermediate nodal brace. Case NB1 in Fig. 3.2.1 is an AISC Specification Appendix 6 compliant example. That is, Appendix 6 addresses all the attributes of this problem. This case is studied in Section 3.8.1. Case NB1 exhibits substantial effects from the continuity of the column across multiple interior brace points. Furthermore, it also includes the common nodal bracing assumptions of:

1) Rigid end braces
2) Equal spacing of all the braces,
3) Equal stiffness of all the braces,
4) Constant axial load along the member length, and

5) Constant member rigidity *EI* along the member length.

The other problems shown in Fig. 3.2.1 deviate from these common bracing assumptions.

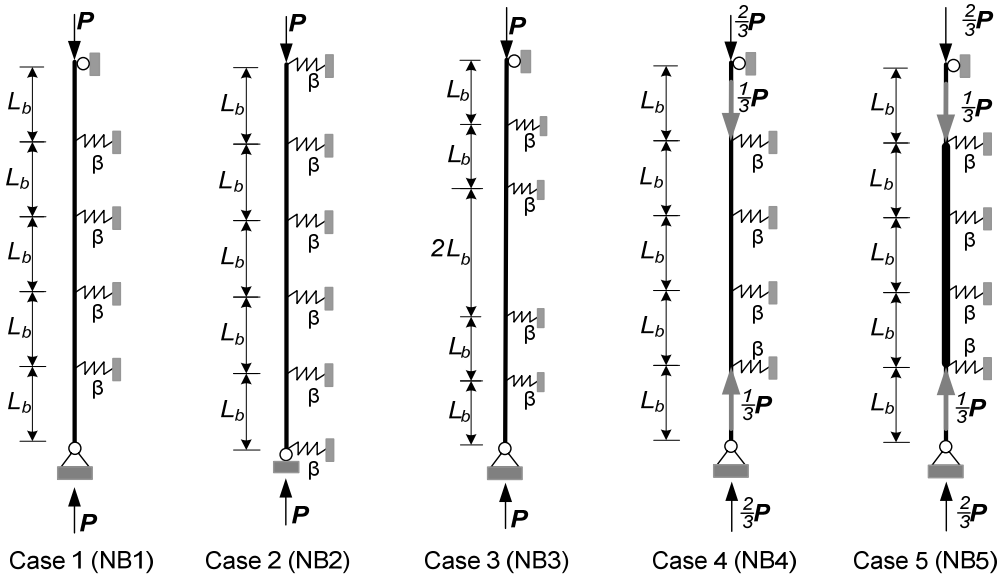


**Fig. 3.2.1. Nodally-braced columns with multiple intermediate braces.**

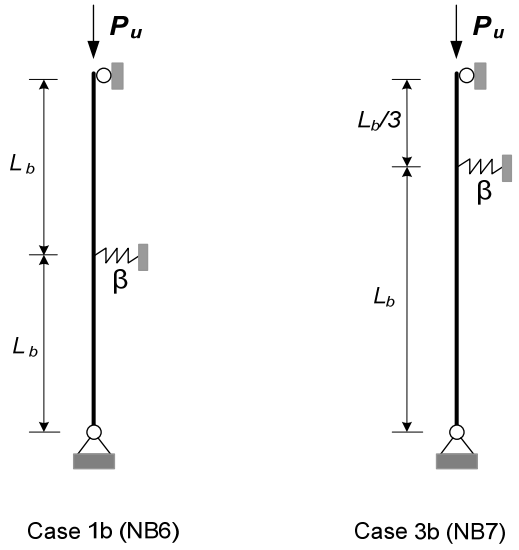


**Fig. 3.2.2. Nodally-braced columns with a single intermediate brace.**

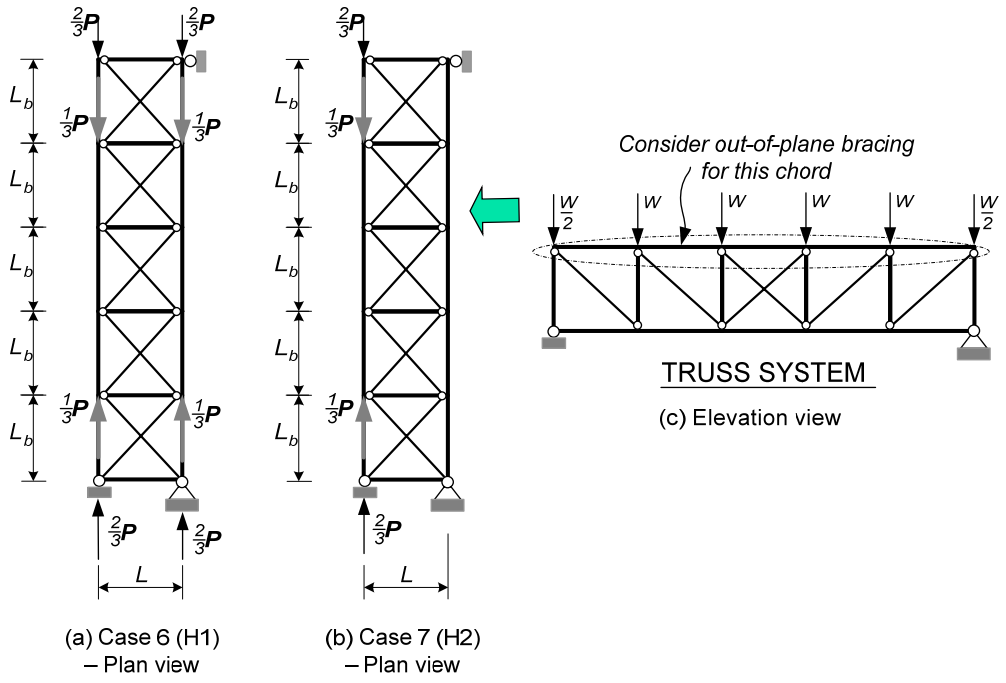


**Fig. 3.2.3. Hybrid bracing problems.**

The column with the single nodal brace labeled as NB6 in Fig. 3.2.2 is studied in Section 3.8.2. This problem investigates the effect of minimal member continuity (continuity across only one interior brace point) on the bracing system behavior. The behavior of columns and their bracing systems having minimal continuity across interior brace points (only one intermediate interior brace) is significantly different from the behavior of columns having continuity across a relatively large number of interior brace points. These differences in behavior may be observed by comparing the responses for NB6 with the responses for problem NB1 of Fig. 3.2.1.

Problem NB2 (Fig. 3.2.1) replaces the rigid end braces of problem NB1 by flexible end braces having the same stiffness as the intermediate interior braces. This allows some assessment of the influence of end brace flexibility in the case of a column with a larger number of equal stiffness interior braces. This problem is studied in Section 3.8.3.

Problem NB3 focuses on the influence of unequal brace spacing in a column with a substantial number of intermediate brace points. This problem is studied in Section 3.8.4.1. In addition, in parallel with the above solutions for problems NB1 and NB6, problem NB7, shown in Fig. 3.2.2, is considered to address the effects of unequal brace spacing for a column having only a single intermediate nodal brace (and hence lesser continuity effects across interior braces). This problem is studied in Section 3.8.4.2.

Column NB4 is studied in Section 3.8.5 to investigate the bracing requirements for a situation with non-constant internal axial force. Finally, Problem NB5, a column with four intermediate nodal braces with varying internal axial force and stepped cross-section geometry is studied in Section 3.8.6. Problems NB4 and NB5 may be considered as idealizations of the chord of a truss loaded by a uniform distributed load and braced out of the plane of the truss by hypothetical nodal braces of stiffness $\beta$. This hypothetical case is explained in more detail in the following discussions of "hybrid" bracing systems.

Fig. 3.2.3 shows several hybrid bracing systems involving a combination of relative bracing, nodal bracing and/or lean-on bracing. Problem H1 shown in Fig. 3.2.3(a) may be considered as a combination of relative and nodal bracing while problem H2 shown in Fig. 3.2.3(b) may be considered as a combination of relative, nodal and lean-on bracing. These problems are studied in detail in Section 3.8.7. Both of these examples are intended to represent the plan bracing of the top-chord of the truss shown in Fig. 3.2.3(c). It should be noted that the distribution of the internal axial forces in the two columns of Problem H1 and in the left-hand column of Problem H2 is the same as the distribution of the axial forces for Problems NB4 and NB5 of Fig. 3.2.1. However, the bracing system models shown in Fig. 3.2.3 are a more realistic representation of the bracing typically

provided along the length of a column or truss chord than the springs of equal stiffness β shown in Fig. 3.2.1. It should be noted that nodal bracing springs of equal stiffness β are not equivalent to the lateral bracing provided to the top chord of the truss in Fig. 3.2.3(c) by the plan view of bracing shown in Fig. 3.2.3(a) or (b). In fact, it is difficult to come up with any physical situation specifically corresponding to equal stiffness nodal lateral column braces as shown in Fig. 3.2.1, other than the bracing of a light column by struts tying the column to a relatively massive diaphragm or wall.

Problem H1 in Fig. 3.2.3 involves combined relative and nodal bracing because the lateral stability of the top chords of the two adjacent trusses, both loaded as shown in Fig. 3.2.3(c), depends both upon the flexural rigidity of the individual chords, *EI*, as well as the overall stiffness developed by the action of the truss chords with the other members of the plan bracing system. Problem H2 in Fig. 3.2.3 involves combined relative, nodal and lean-on bracing because, in this case, only one of the truss chords is loaded. The other truss is assumed to support zero vertical load. This corresponds to a general situation where an adjacent truss is less heavily loaded, and thus its top chord can assist in providing lateral stability to the more heavily loaded truss chord.

## 3.3 General Geometric Imperfection Modeling Considerations

### 3.3.1 Types of Imperfections for Assessment of Column Flexural Buckling Strength

In general, two types of geometric imperfections must be considered in any analysis assessment of columns and their bracing systems: the member out-of-straightness between the brace, end or interconnection points, $\delta_o$, and the member out-of-plumbness, i.e., the angular out-of-alignment with respect to the member working line, $\Delta_o/L_b$. Both of these imperfections can have a significant effect on column flexural buckling strengths.

Fig. 3.3.1 shows a model of each of these imperfections, within a given unbraced length $L_b$, commonly recommended for the analysis of columns and their bracing systems. The appropriate pattern of the out-of-straightness and out-of-plumbness imperfections along the overall member length is discussed subsequently.

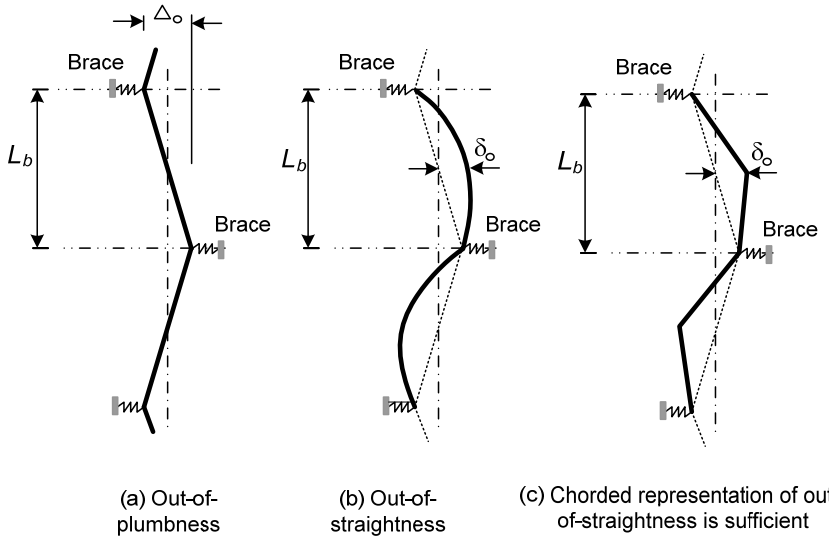


**Fig. 3.3.1. Imperfections based on the AISC (2005) Code of Standard Practice Tolerances.**

### 3.3.2 Appropriate Magnitude of Column Imperfections

The Code of Standard Practice for Steel Buildings and Bridges (AISC 2005) specifies fabrication and erection tolerances that may be used as a basis for determining the appropriate magnitude of the above imperfections. With respect to out-of-straightness, the Code of Standard Practice specifies, "For straight compression members, whether or a Standard Structural Shape or built-up, the variation in straightness shall be equal to or less than 1/1000 of the axial length between points that are to be laterally supported." With respect to out-of-plumbness or out-of-alignment, the Code of Standard Practice specifies multiple requirements. The base tolerance is an angular misalignment of 1/500 relative to the member working line. For vertical columns, the member working line is

taken as a plumb line. For horizontal members, the working line is taken as a straight line between work points defined at the center of the top flange and at the ends of a shipping piece. For other members, the working line is taken as a straight line between the center of the member cross-section at the ends of a shipping piece.

In general, the above definitions of out-of-plumbness from the Code of Standard Practice are different than that shown in Fig. 3.3.1. However, the definitions become the same if each unbraced length $L_b$ is simplistically taken as a shipping piece. Given this simplification, one can state that the maximum out-of-straightness permitted by the Code of Standard Practice is a physical transverse displacement $\delta_o$ normal to the working line of $L_b/1000$, and the maximum out-of-plumbness permitted by the Code of Standard Practice is an angle relative to the working line of $\Delta_o / L_b = 1/500$. Common practice is to use these values as the base magnitudes of the initial geometric imperfections for the assessment of columns and their bracing systems. The AISC Specification and Commentary allow the use of smaller magnitudes of the initial geometric imperfections when reduced values can be justified. Previous studies (Winter 1958; Yura 1995) have shown that the forces in the brace members are directly proportional to the magnitude of the initial imperfections.

### 3.3.3 Simplified Representation of Out-of-Straightness Imperfections

When analyzing columns and their bracing systems for the effects of out-of-straightness and out-of-plumbness, Fig. 3.3.1(c) shows a practical simplification recommended in this research. The out-of-straightness between brace points can be represented sufficiently by a chorded or "kinked" geometry with an offset from a chord between the brace points of $\delta_o = L_b/1000$ at the chord mid-length.

### 3.3.4 Overview of General Considerations Necessary in Selecting an Appropriate Pattern of Out-of-Straightness and Out-of-Plumbness

The above discussions address the two types of imperfections that should be considered in any single column unbraced length, as well as the recommended magnitude of these imperfections. However, there is one additional decision that must be addressed in any analysis that explicitly determines the physical stability behavior and strength of an imperfect column and its bracing system. Generally, one must also select an appropriate distribution (i.e., the $\pm$ and – directions) of the out-of-straightness ($\delta_o$) and out-of-plumbness ($\Delta_o/L_b$) from unbraced length to unbraced length throughout the system. This distribution must be selected to generate the maximum strength demand on a given brace or set of braces, as well as to produce the maximum "destabilizing" effect on the column as a whole (similar to the way that different ASD or LRFD load combinations are applied to produce the maximum strength requirement on any given component).

Unfortunately, similar to the fact that different ASD or LRFD load combinations generate the maximum strength requirements on different members or components, different patterns of $\delta_o$ and $\Delta_o/L_b$ create the maximum strength demands on different braces and on the member as a whole. Furthermore, for a given brace or for determining the strength of the member as a whole, the critical distributions of $\delta_o$ and $\Delta_o/L_b$ along the member length depend in general on the stiffness of the bracing system relative to the stiffness of the column. In addition, characteristics such as nonuniform brace stiffness and strength along the length of the column and/or non-constant brace spacing along the column length can have an important influence on which $\delta_o$ and $\Delta_o/L_b$ distributions are the most critical.

It is interesting to note that for members with more than one intermediate brace, the AISC Appendix 6 equations are derived as an estimate of the largest strength requirement for all the braces. In addition, these derivations are based predominantly on the assumption of constant brace stiffness and strength, constant spacing of the braces, and full bracing (some consideration of partial bracing is accommodated via the parameter $L_q$). If all the braces are indeed of equal strength and stiffness, then the determination of a single maximum strength requirement that can be applied for all of the braces is all that is needed. Nevertheless, only one of the braces will be subjected to the maximum strength demand in most situations. The other braces are loaded less critically. If one wishes to relax the AISC full bracing stiffness and strength requirements by use of refined methods of analysis, or if one needs to address cases involving unequal brace stiffness, strength and/or spacing, one must select an appropriate distribution of $\delta_o$ and $\Delta_o/L_b$ along the member length for the corresponding analysis.

For some bracing problems, the critical imperfection is relatively obvious. One example of this is a column with single nodal brace at its mid-height. The critical imperfection pattern for the calculation of the strength requirement on the intermediate brace is a single wave between the ends of column as shown in Fig. 3.3.2(a).

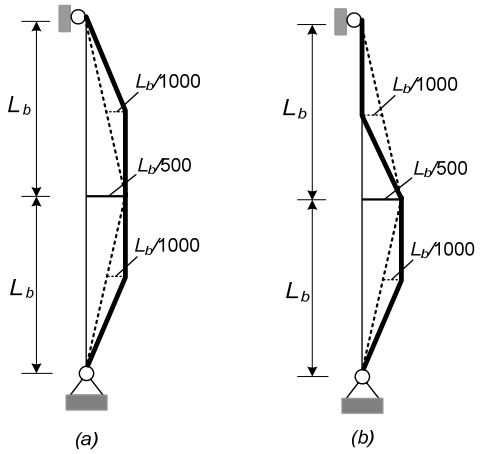


**Fig. 3.3.2. Imperfections for a column with single nodal brace at its midheight based on the AISC (2005) Code of Standard Practice Tolerances.**

In this pattern, the magnitude of the out-of-plumbness $\Delta_o/L_b$ is specified according to the AISC Code of Standard Practice as 1/500 in opposite directions in each of the column unbraced lengths. In addition, the critical column out-of-straightness $\delta_o$ is specified as $L_b/1000$ in each of the column unbraced lengths and in the same direction as the above out-of-plumb displacements. This pattern of $\delta_o$ and $\Delta_o/L_b$ will always produce the largest strength requirement on the single intermediate brace compared to the other possible combination of the base $\delta_o$ and $\Delta_o/L_b$ values shown in Fig. 3.3.2(b). One does not need to consider $\delta_o = L_b/1000$ in opposite directions in each of the column unbraced lengths as shown in Fig. 3.3.2(b) if the goal is to determine the critical strength requirement for the intermediate brace.

However, if the goal is to determine the distributions of $\delta_o$ and $\Delta_o/L_b$ that give the maximum destabilizing effect on the overall column strength, either of the distributions shown in Fig. 3.3.2 can be the critical one. If the brace is relatively flexible compared to the column, the distribution shown in Fig. 3.3.2(a) is the crtical one. On the other hand, when the brace has a sufficient stiffness and strength to "fully brace" the column, the

distribution shown in Fig. 3.3.2(b) will give the maximum destabilizing effect on the column strength. This means that for the case where the single intermediate brace has a stiffness and strength approaching that required for "full bracing," two different geometric imperfections must be considered if the column and its bracing system are to be assessed via a refined analysis: (1) The geometric imperfection shown in Fig. 3.3.2(a) must be considered when calculating the strength requirement for the intermediate brace, and (2), the geometric imperfection shown in Fig. 3.3.2(b) must be considered when calculating the strength requirements (i.e., the axial force and internal bending moment demands) for the column.

When the column has more than one brace, the determination of the critical imperfection pattern is as not straightforward as in the above case. Furthermore, determining the critical imperfection in general beam bracing problems is more complex than in column bracing problems because of the effects of moment gradient, load height effects, and cross-section distortional flexibility. The procedure described below may be used to determine the critical imperfection for both column and beam bracing. However, this chapter focuses on column bracing. Geometric imperfections for beam bracing are discussed further in Chapters 4 and 5.

It should be noted that the selection of an appropriate distribution of $\delta_o$ and $\Delta_o/L_b$ for assessment of the strength of a column and its bracing system by refined analysis is generally a subset of the broader problem of selecting appropriate geometric imperfections for refined analysis. For the broader problem, there are often cases where the displacement "mode" of the structure under the applied loads has substantial affinity with the displacement mode corresponding to the ultimate strength limit state. In these

cases, the response is a load-deflection problem, and the ultimate strength is associated with a progressive growth of the deflections. The appropriate directions of the member $\delta_o$ and $\Delta_o/L_b$ values in these cases are usually the directions of the corresponding displacements in the structural system at the start of the applied loading.

Conversely, in cases where the strength limit states, neglecting initial geometric imperfections, involve a bifurcation from a primary equilibrium path, distributions of $\delta_o$ and $\Delta_o/L_b$ that have significant affinity with the corresponding buckling modes must be considered. The bracing of a column subjected solely to concentric axial compression falls within this second class of problems. Generally, the buckling modes of the column and its bracing system must be considered in some fashion in determining the appropriate distributions of $\delta_o$ and $\Delta_o/L_b$. This problem is the focus of the following discussions.

### 3.3.5 Specific Procedures for Selecting an Overall Pattern of Out-of-Straightness and Out-of-Plumbness Imperfections

The appropriate pattern of the $\delta_o$ and $\Delta_o/L_b$ geometric imperfections for checking of a given brace, or for checking the overall column strength, is the one that satisfies the Code of Standard Practice tolerances while also maximizing the corresponding destabilizing effects, i.e., maximizing the brace force or column internal moment respectively. This pattern is generally a function of:

1) The relative stiffness properties of the various column segments and of the various braces.
2) The level of axial load in the column, since the column axial load affects the relative stiffness of the column compared to that of the braces.

The following discussions introduce and detail a formal procedure for determining the appropriate geometric imperfections for general problems involving column flexural buckling and corresponding bracing systems. Once one understands this formal procedure, the critical geometric imperfections can be determined in many situations based simply on inspection. However, particularly for more complex problems, the formal procedure can be very useful. This section introduces and outlines the procedure. The following section presents an example showing its application.

a) Affinity with buckling modes

In the limit that the axial load in the column is at the buckling load of the column and/or the column and its bracing system, the global tangent stiffness of the analysis model becomes singular. As this load is approached, the column incremental displacements will tend to be dominated by the corresponding eigenvalue buckling mode. However, the maximum strength of any imperfect column is reached generally prior to the axial load level reaching the buckling load. The buckling load corresponds to bifurcation of the ideally straight member from its initial straight configuration into a buckled configuration. The imperfect column will tend to deflect into a pattern that becomes increasingly like the lowest eigenvalue buckling mode of the column, or of the column and its bracing system, as the buckling mode is approached. Since the tangent stiffness neglects the bending effects associated with the geometric imperfections, the global tangent stiffness of the column and its bracing system (including the influence of geometric nonlinearity) will be positive definite at the maximum axial strength load level.

In cases where several column buckling eigenvalues (i.e., column buckling loads) are equal or nearly the same, the deflections of the column and its bracing system will tend to

be dominated by some combination of the corresponding buckling modes as the lowest eigenvalue buckling load is approached.

The above discussions also apply in cases involving the strength assessment of a group of columns, or the strength assessment of a general structural system. However, in these cases, the response is affected by the interactions between various axially compressed members.

b) Influence lines

Given a positive definite global tangent stiffness matrix for a column and its bracing system, or of a general structural system, influence line concepts provide the most straight-forward way to determine the imperfection pattern that maximizes a given brace force, or maximizes the internal moment at a particular location in a given column. In the context of the "chorded" geometric imperfections shown in Fig. 3.3.1(c), one only needs the influence line ordinates corresponding to the brace points and the mid-lengths between the brace points. This is because the effect of these kinked geometric imperfections is approximately equivalent to a set of self-equilibrating lateral loads applied transverse to the axis of the column. At any given "kink" in the column, the corresponding equivalent lateral load is as shown in Fig. 3.3.3. Given an initial angular deviation of $\theta_{o1}$ and $\theta_{o2}$" this lateral load is

$$N = P_1\theta_{o1} + P_2\theta_{o2}, \tag{3-1}$$

where $P_1$ and $P_2$ are assumed to be constant axial forces in segments 1 and 2 (if $P_1 \neq P_2$, then an applied force of $P_2 - P_1$ must exist tangent to the working line at the kink). If for example $\theta_{o1}$ and $\theta_{o2}$ are both equal to $L_b/500$ (in opposite directions) and $P_1 = P_2 = P$, then $N = P\,(L_b/250)$.

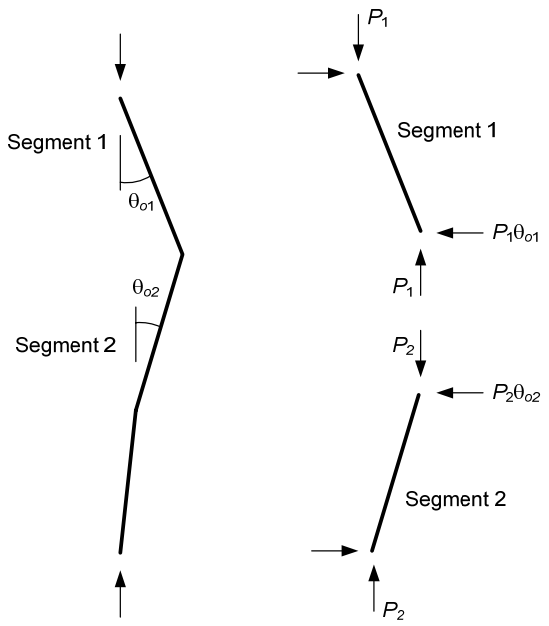


**Fig. 3.3.3. Equivalent lateral load corresponding to kinked geometric imperfections.**

For any given pattern of combined out-of-plumbness and out-of-straightness along the length of a column, one can create a corresponding set of equivalent lateral loads. In addition, one can generate the necessary influence line ordinates for a given brace force or column internal moment by applying transverse unit loads at each of the brace locations and at the mid-lengths between the braces in a model of the perfectly straight column. The force or moment at a given location corresponding to each unit load gives the influence line ordinate for that node. This is denoted by the symbol $r_i$. Correspondingly the brace force or internal moment given by any geometric imperfection pattern may be determined by the sum of the products of the equivalent notional loads and the influence line ordinates, i.e.,

$$R = \Sigma N_i \, r_i \tag{3-2}$$

Engineers accustomed to designing for moving loads are accustomed to the use of influence lines for first-order analysis of the moving load effects. The above application of Eq. (3-2) is exactly as in the analysis for moving loads. However, as opposed to the analysis of structures for moving loads, the global tangent stiffness at the axial load level under consideration is the appropriate stiffness for determining the influence line ordinates in the above problems. This is because the column flexural stiffness can be affected substantially by the axial load effects. Also, note that given the axial forces in the column or columns, and assuming no changes in these axial forces during the application of loads on the structure, the second-order (geometric nonlinear) analysis problem is completely linear.

Given the influence line from the second-order (geometric nonlinear) tangent stiffness, the engineer can then determine the pattern of geometric imperfections that maximizes the result from Eq. (3-2) while not exceeding the geometric imperfection tolerances on $\delta_o$ or $\Delta_o/L_b$ anywhere within the column or structural system.

When the engineer determines the influence line for a given brace force or internal moment as described above, and then determines a critical geometric imperfection by maximizing the value from Eq. (3-2), the affinity of the geometric imperfection pattern with the lowest eigenvalue buckling mode or modes, as well as with other higher eigenvalue buckling modes, is automatically and naturally included. Therefore, although one may in some cases wish to calculate the eigenvalue buckling loads and buckling modes to ascertain a better understanding of the structural response, this is generally not required. One only needs to determine the influence line for a given brace or internal

moment location under consideration, then maximize the value from Eq. (3-2) to determine the appropriate geometric imperfection causing the largest destabilizing effect.

### 3.3.6 Example Determination of Geometric Imperfection Pattern

The above specific considerations can be understood most easily by examining a specific representative example. As such, consider the W14x90 column with four intermediate nodal braces each of stiffness β shown in Fig. 3.3.4. This problem has the general configuration shown as case NB1 in Fig. 3.2.1. For this specific example, we will assume a W14x90 column subjected to weak-axis bending in the plane of the bracing, $L_b$ = 15 ft, $F_y$ = 50 ksi, and a nominal elastic bracing stiffness of β = 20.0 kips/inch. The behavior for other values of β will be studied for this same column in subsequent examples.

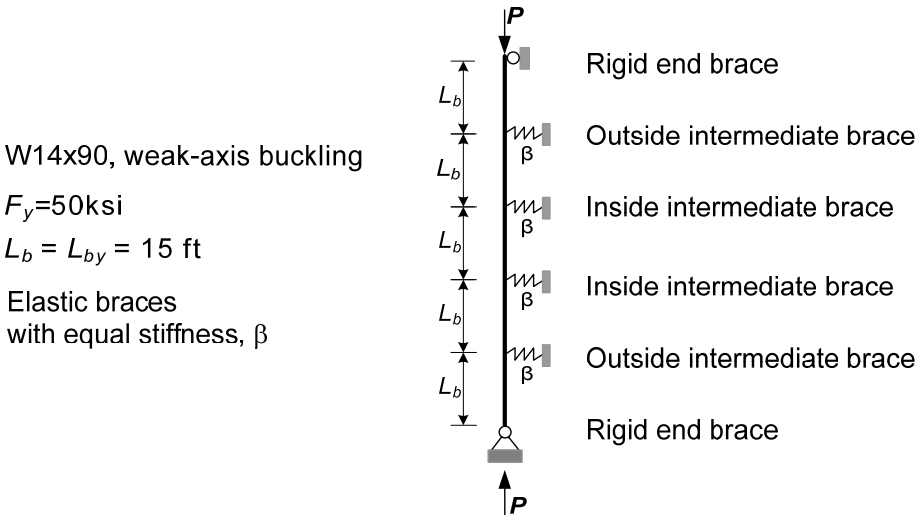


**Fig. 3.3.4. Pinned-pinned column with four intermediate nodal braces.**

Suppose that one is interested in evaluating the maximum strength requirement for the outside intermediate braces labeled in Fig. 3.3.3. One would execute the following steps to determine the required strength for these braces:

1) First, the column axial load corresponding to the maximum strength condition must be determined. For this purpose, we assume in this example that the brace stiffnesses are sufficient to develop a load capacity of the column of $P_{max} = \phi_c P_n =$ = 1000 kips based on $KL_b$ = 15 ft, $K$ = 1 in the weak-axis direction. The 2005 AISC LRFD column strength equations are used directly to determine this value of the axial capacity. The above value $\phi_c P_n$ can be read from Table 4-1 on page 4-13 of the AISC 13th Edition Manual.

2) Utilize a reduced elastic stiffness of $0.8E$ = 23,200 ksi and a reduced elastic brace stiffness of $0.8\beta$ = 16.0 kips/inch for the second-order analyses to determine the influence line for the top outside brace. The influence line for the bottom brace is similar due to symmetry.

3) Given an axial force $P_u = \phi_c P_n$, determine the inelastic stiffness reduction factor for the column. The AISC $\tau_b$ equation is used for this purpose:

$$\tau_b = 4\frac{P_{max}}{P_y}\left(1 - \frac{P_{max}}{P_y}\right) = 0.74$$

Given this value for $\tau_b$, the flexural rigidity of the column utilized for the caculation of the brace influence line is

$0.8\tau_b EI_y$ = 0.8 (0.74) (29,000 ksi) (362 in$^4$) = 6,215,000 kip-in$^2$

The above values are all consistent with the analysis of general structures by the Direct Analysis Method. If the above assumption that $\phi_c P_n$ is achievable given the elastic brace stiffnesses of $\beta$ = 20.0 kips/inch is correct, then the above stiffnesses provide a reasonable approximation of the stiffness characteristics of the structure at its maximum strength limit.

4) Apply a unit load at each of the four intermediate brace locations as well as at the mid-length between the braces, and determine the top outside brace force for each of these loadings. Apply the axial load of $P_u$ = 1000 kips in conjunction with each of these unit loads so that the influence lines include the approximate reductions in the column stiffness due to stability effects. The resulting influence line for the top outside brace force is shown in Fig. 3.3.5.

5) Consider the possible combinations of $\Delta_o/L_b$ and $\delta_o$ that will maximize the value from Eq. 3-2. Figure 3.3.5 shows the influence line generated from step 4, several potential geometric imperfections, the equivalent notional loads, and the calculated values of *R*. The critical geometric imperfection usually can be defined by first setting the out-of-plumbness in each unbraced length to maximize the positive contribution to R (Eq. 3-2) from the corresponding notional loads at the brace points. Once the out-of-plumbness is set, the out-of-straightness values are specified in each unbraced segment such that the value of *R* from Eq. 3-2 is increased further.

   The imperfections are shown in a normalized form in Fig. 3.3.5. One can obtain the angular imperfection in each half-segment ($L_b/2$) by multiplying the values shown in the figure by 1/250. Also, the notional loads are shown in normalized form. One can obtain the actual notional load values by multiplying the values shown in the figure by $P_u/250$. The imperfection "1o" gives the largest estimated brace force of *R* = 9.9 kips, based on the assumption that $P_u$ = 1000 kips can be developed and given the specified nominal bracing stiffness of $\beta$ = 20 kips/inch.

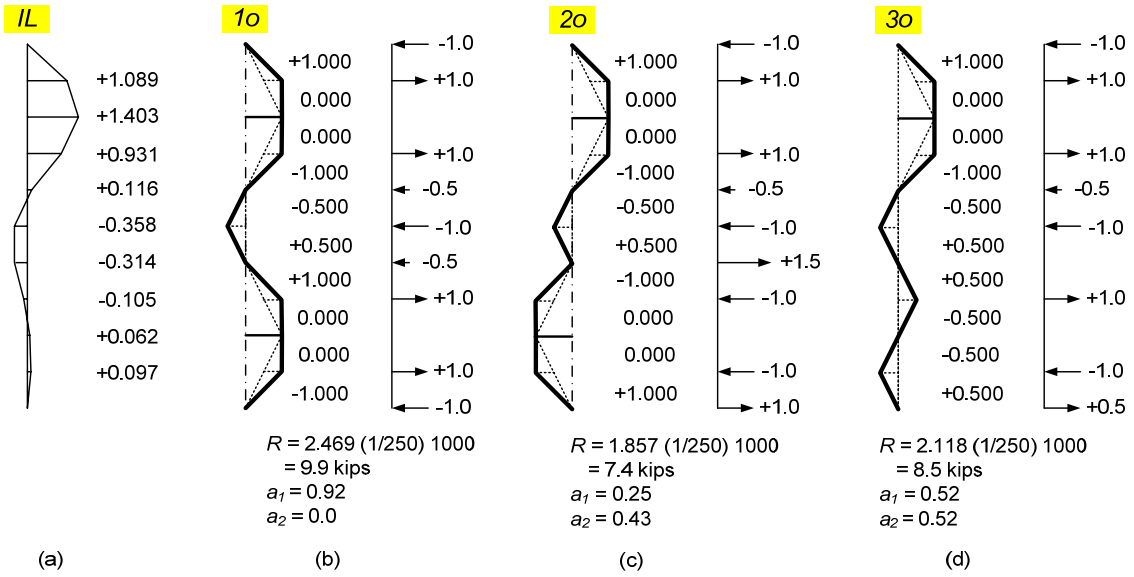


**Fig. 3.3.5. Geometric imperfections potentially causing the largest outside brace force with β = 20.0 kips/inch.**

It is informative in many situations (particularly response is deviated by column stability effects) to consider the affinity with several of the lowest eigenvalue buckling modes and the corresponding eigenvectors in selecting the appropriate geometric imperfection. As an approximate rule of thumb, the engineer may wish to consider any eigenmodes for which the eigenvalue is within 20 % of the lowest buckling load. Fig. 3.3.6 shows the results of an inelastic eigenvalue buckling analysis of the above problem. The first buckling mode of the structure occurs an eigenvalue of $P_{cr1}$ = 1442 kips while the second mode occurs at an eigenvalue of $P_{cr2}$ = 1604 kips. The third buckling mode is not shown but corresponds to an eigenvalue of $P_{cr3}$ = 1907 kips. It should be noted that the first two buckling modes correspond to significant displacements of the brace points (see Fig. 3.3.6). The normalized relative transverse displacement in each of the column half-unbraced lengths are labeled next to each of the buckling modes. These relative displacements are normalized such that the square root of the sum of their

squares is equal to 1.0. The third mode (not shown) involves zero displacement at all of the brace points as well as inflection points at each of the brace-points and a single half-sine wave in each unbraced length. One can observe that the ratio $P_{cr2}/P_{cr1}$ is 1.11 whereas $P_{cr3}/P_{cr1}$ = 1.32. Therefore, one would expect substantial amplification of any geometric imperfection pattern that has affinity with either of the first two modes. For instance, if one assumes that the displacement amplification in each of the eigenmodes is approximated by

$$AF_i = \frac{1}{1 - P_{\max} / P_{cri}}$$

We obtain $AF_1$ = 3.26 and $AF_2$ = 2.66 at $P_u$ = 1000 kips. However, for the third mode, $AF_3$ = 2.10 at $P_u$ = 1000 kips.

Fig. 3.3.5 shows the values for the calculated affinity of each of the geometric imperfection patterns 1o, 2o and 3o with the two eigenvalue buckling modes. The affinity is measured as the projection of the vector of the normalized chord rotations (or "layovers") in each half length onto the normalized unit eigenvectors shown in Fig. 3.3.6. The 10x1 chord rotation vector is normalized by dividing by its Euclidean norm prior to taking its projection on the unit 10x1 eigenvectors (i.e., the normalized buckling modes). The imperfections in Fig. 3.3.5 are actually selected to have maximum affinity with the first two buckling modes, and with the average of the first two buckling modes shown in Fig. 3.3.6. This is accomplished typically by orienting the chord rotation (layover) in each half length in the same direction as the chord rotation in the desired mode.

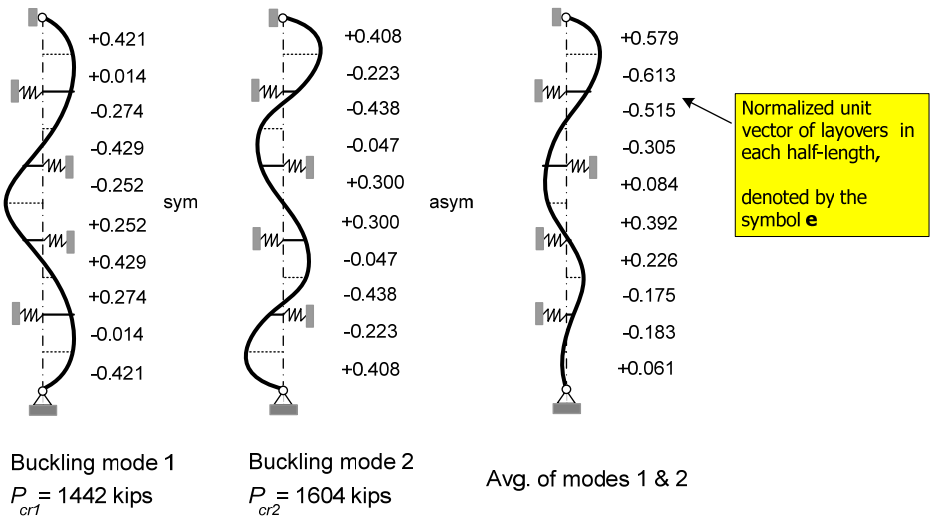


**Fig. 3.3.6. Buckling mode shapes for the W14x90 column and its bracing system using a reduced elastic stiffness of $0.8E$ = 23,200 ksi, $0.8\beta$ = 16.0 kips/inch, and $\tau_b$ = 0.74 determined assuming $P_u = \phi_c P_n$ = 1000 kips based on $K$ = 1 in the weak-axis bending direction.**

Recall that in this example the goal is to estimate the maximum strength requirement of the outside intermediate braces labeled in Fig. 3.3.3. If one were to use a geometric imperfection that causes essentially zero force at these brace points of the imperfect column, one would still have essentially zero force at these braces once the geometric imperfection is amplified due to the second-order stability effects. This is the case for the third buckling mode in this problem, and is always the case for any buckling mode that involves zero brace displacements.

In this example, the imperfection that has the largest affinity with the first buckling mode causes the largest strength demand on the top outside brace. However, this is not always the case. For instance, as noted earlier, if the brace displacements are zero in the lowest eigenvalue buckling mode, then geometric imperfections that have significant affinity with the subsequent one or several modes will generate the largest strength demands on the braces. Generally speaking, the eigenmodes can be used as discussed

above to help focus on the geometric imperfection pattern that will maximize the value of $R$ in Eq. 3-2.

For general problems, the complexities of determining the worst-case geometric imperfections to maximize the brace forces are such that the application of the above procedures is suited only for research studies and specialized design problems. As a simplification, it is considered sufficient to neglect the out-of-straightness, consider only the out-of-plumbness, and calculate $P_n$ based on the unsupported lengths $L_b$ (with $K = 1$). Out-of-straighness is modeled explicitly in this research. The critical imperfections are generally different for the different braces.

### 3.4 Direct Analysis Method (DM) Procedure

The Direct Analysis Method has been developed with the goals of more accurately determining the load effects in the structure and eliminating the calculation of the flexural buckling effective length factors for columns. This method is applicable to all types of frame structures including braced, moment, combined braced and moment frames, and other hybrid or combined systems. The detailed procedure for the use of this method is described in Appendix 7 of the 2005 AISC Specification and in Chapter 3 of Griffis and White (2008).

*Step 1: Determine overall structural layout and the required loads.*

*Step 2: Use reduced member properties.*

- Use reduced elastic stiffnesses: $E^* = 0.8E$
- Apply $\tau_b$ reduction to members with heavy axial loads

$$I^* = I \quad \text{when} \quad \frac{\alpha P_r}{P_y} \leq 0.5$$

$$I^{*} = \tau_b I \quad \text{when} \quad \frac{\alpha P_r}{P_y} > 0.5 \quad \text{with} \qquad \tau_b = 4\frac{\alpha P_r}{P_y}\left(1 - \frac{\alpha P_r}{P_y}\right) \quad (3.1)$$

where $I$ = moment of inertia about the axis of bending, inches$^4$.

$P_r$ = required axial compressive strength under LRFD or ASD load combinations, kips.

$P_y = AF_y$, member yield strength, kips.

$\alpha$ = 1.0 (LRFD) and $\alpha$ = 1.6 (ASD).

$\tau_b$ = stiffness reduction factor as shown in Fig. 3.4.1.

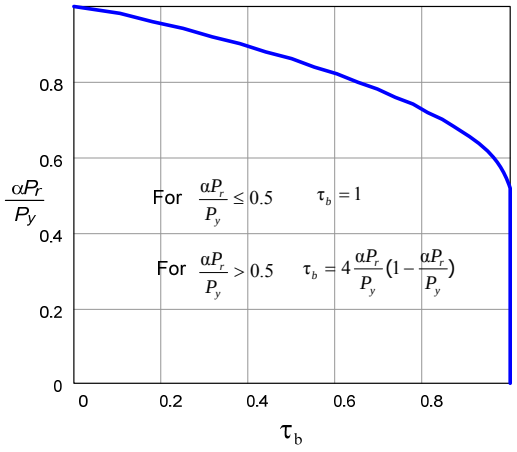


**Fig. 3.4.1. Stiffness reduction factor $\tau_b$.**

*Step 3: Determine influence lines for the forces in the bracing elements. If desired, also calculate the buckling eigenvalues and mode shapes.*

These analyses are conducted with 0.8 of the nominal elastic stiffness and with $\tau_b$ applied to the moment of inertia for members with heavy axial loads.

*Step 4: Apply geometric imperfections.*

According to the procedure described in Section 3.3, several imperfections may need to be examined to determine the critical one. However, given an understanding of the above fundamentals influencing the critical imperfections, the critical imperfection associated with each brace often can be identified by inspection.

*Step 5: Perform a second-order analysis.*

A second-order analysis including both $P$-$\Delta$ and $P$-$\delta$ effects is conducted using the above reduced stiffness and geometric imperfections. In this Chapter, Mastan 2 Version 3 is used.

*Step 6: Check the column(s) using the AISC interaction equations.*

For $P_r/P_c \geq 0.2$

$$P_r/P_c + 8/9(M_{rx}/M_{cx} + M_{ry}/M_{cy}) \leq 1.0 \qquad \text{(3-2 H1-1a)}$$

For $P_r/P_c < 0.2$

$$P_r/2P_c + (M_{rx}/M_{cx} + M_{ry}/M_{cy}) \leq 1.0 \qquad \text{(3-3 H1-1b)}$$

where $P_c = \phi P_y$ (LRFD), $P_c = P_y/\Omega$ (ASD) (Since out-of-straightness is included in the analysis model and braces are assumed initially elastic.)

*Step 7: Check the amplification of brace point displacements at the maximum load level.*

Where the amplification becomes "large", the system response becomes sensitive to small changes in the system characteristics. Amplification values larger than 4.0 based on the reduced stiffness, or 2.5 based on the nominal stiffness, are inadvisable. A typical influence of nominal stiffness reduction on second-order amplification is illustrated in Fig. 3.4.2.

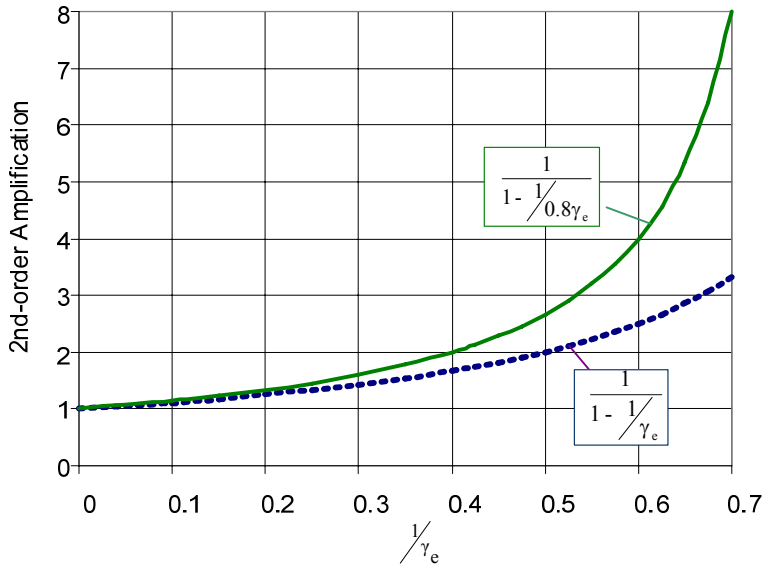


**Fig. 3.4.2. Influence of nominal stiffness reduction on 2nd-order amplification.**

In Fig. 3.4.2, $\gamma_e$ is defined as the ratio of the member elastic buckling load or moment to the required strength.

*Step 8: If the brace point displacements at service load levels cause serviceability concerns, check the brace point displacements at the service load levels.*

## 3.5 DM Example

The column previously introduced in Fig. 3.3.4 is considered further in this section. The purpose of this section is to illustrate the application of the DM procedure to column bracing. The DM is used here to determine the column maximum load capacity as well as the brace forces as a function of the brace stiffness. Note that in selecting the appropriate geometric imperfections in Seciton 3.3, the value of $P$ is assumed to be equal to $\phi_c P_n$ based on $K = 1$ ($KL_b = L_b$). For partial bracing, the column load capacity is generally smaller than this value. If one is conducting design, then typically accurate estimates of $P_u$ can be determined from the structural analysis for the design load

combinations. If one is considering the maximum overall load capacity of a column and its bracing system, the solution is generally an iterative one of estimating the axial load(s) at the system capacity, then subsequently checking the accuracy of this estimate. The solutions below are conducted assuming $P_u$ = 982.7 kips. This is the maximum load capacity of the column calculated using the DM, given a selected example brace stiffness of $\beta$ = 20 kips/inch.

It should be noted that for the column shown in Fig. 3.3.4, the brace requirements based on the AISC Appendix 6 are calculated as follows:

Based on the AISC (2005) LFRD provisions, for the section W14x90 with effective length $KL = L_b$ = 15 ft, the column strength is $\phi_c P_n$ = 1000 kips. For $P_u = \phi_c P_n$ = 1000 kips, the brace stiffness and strength requirements are:

Brace stiffness: $$\beta_{br} = \frac{1}{\phi} 2(4 - 2/n)\frac{P_u}{L_q} \qquad \text{(3-4 A.6.2 Comm.)}$$

$$\beta_{br} = \frac{1}{0.75} 2(4 - 2/4)\frac{1000}{180} = 51.9 \text{ kips/inch}$$

Brace strength: $P_{br} = 0.01\, P_u$ (3-5 A-6-3)

$$P_{br} = 0.01(1000) = 10 \text{ kips}$$

Using the DM procedure described above, this problem is analyzed in this research by considering six different brace stiffnesses, $\beta$ = 0.8, 5, 10, 20, 30 and 50 kips/inch. The aim to consider this complete range of brace stiffness is to study a complete range of partial and full bracing. For the smallest brace stiffness, $\beta$ = 0.8 kips/inch, the buckling load is similar to that of the pinned-pinned column without bracing; the fundamental buckling mode for this brace stiffness is a single wave between the ends of column. For the largest brace stiffness considered, $\beta$ = 50 kips/inch, the column buckles between the

brace points; this brace stiffness is practically equal to the brace stiffness required by AISC Appendix 6 for full bracing. The different bracing stiffnesses (and the corresponding column buckling mode shapes) lead to different critical geometric imperfections and to different values for the required brace forces. In this Section, the detailed solution for the case with brace stiffness of $\beta = 20$ kips/inch is studied. The results for the other brace stiffnesses, $\beta = 0.8$, 5, 10, 30, and 50 kips/inch are presented in Section 3.8.1.

*Step 2: Use reduced member properties.*

- Use reduced elastic stiffnesses: $0.8E = 23{,}200$ ksi

  $0.8\beta = 16.0$ kips/inch

- Apply $\tau_b$ reduction to members with heavy axial loads

  Since $\dfrac{P_u}{P_y} = \dfrac{982.7}{1325} = 0.7417 > 0.5$

  $$\tau_b = 4\frac{P_u}{P_y}\left(1 - \frac{P_u}{P_y}\right) = 0.7664$$

  $$I^* = \tau_b I = 0.7664 I$$

*Step 3: Determine the influence lines for the forces in the bracing elements. If desired, also calculate the buckling eigenvalues and mode shapes.*

The eigenvalue buckling results and the influence line for the outside brace forces presented in Section 3.3 are for all practical purposes the same as the ones based on $P_u = 982.7$ kips. In this section, the only difference is that the buckling modes in Section 3.3 are based on $P_u = \phi P_n = 1000$ kips. Therefore, the prior results are reused here. The influence line for the top inside brace force and the identification of the critical geometric imperfection corresponding to these braces are presented below.

*Step 4: Apply geometric imperfections*

As described in Section 3.3, the selection of the critical imperfection can be guided by considering the affinity with the buckling modes. The previously defined affinity parameters "$a_i$" and the estimated brace forces from Eq. 3-2, "$R$", are shown in Fig. 3.5.1 for the top inside brace below. The affinity parameter "$a_i$" is determined by multiplying the normalized unit vector of buckling mode layovers in the half-lengths, $e_i$ by the corresponding normalized unit vector of imperfection layovers $i_o$, $a_i = e_i^T i_o$. The results for the outside braces are shown previously in Fig. 3.3.5.

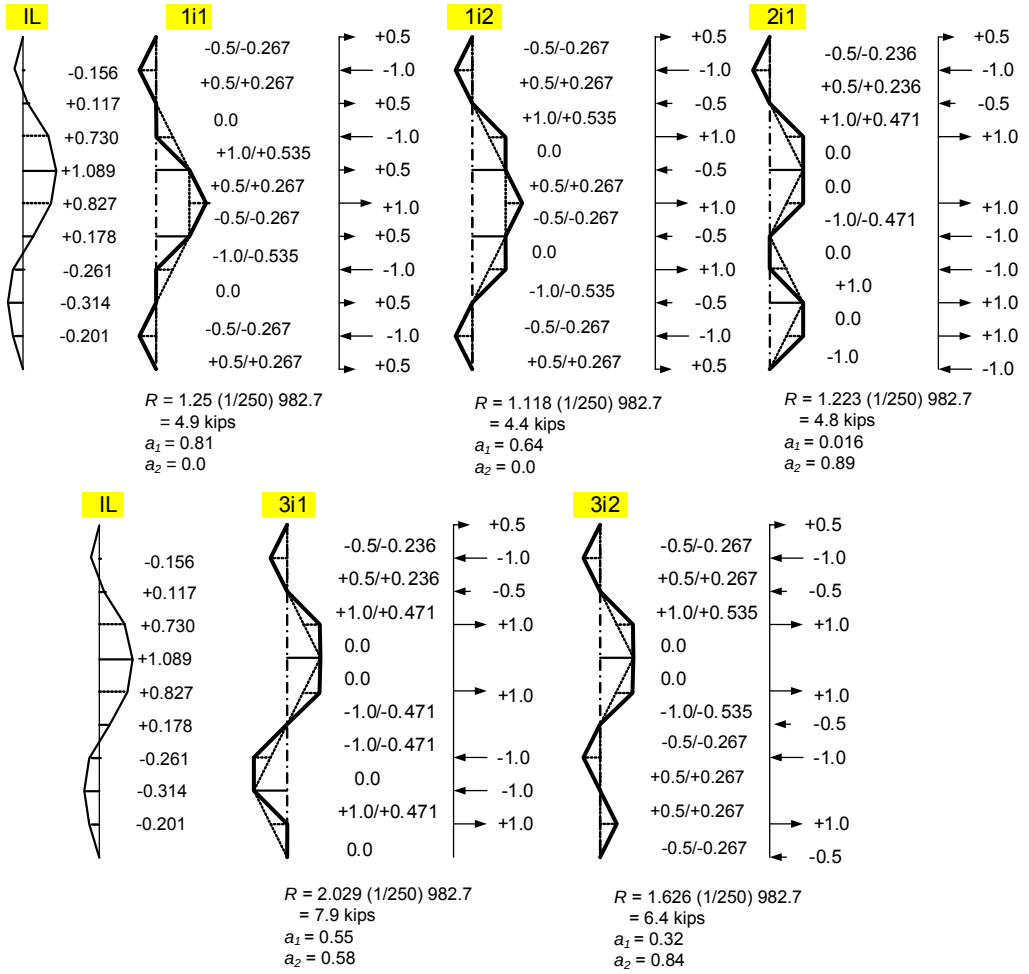


**Fig. 3.5.1. Geometric imperfection potentially causing the largest inside brace force with β = 20.0 kips/inch.**

The imperfections are labeled in Fig. 3.3.5 (for the outside braces) and Fig. 3.5.4 (for the inside braces) using the following convention. For example, for the imperfection "*1o*":

- "1" stands for affinity with buckling mode "*1*".
- "*o*" indicates this is an imperfection potentially causing a maximum force at one of the two "outer" intermediate brace points.

Similarly, "*2o*" denotes an imperfection having affinity with buckling mode "*2*" and potentially causing maximum force at one of the "outer" intermediate brace points. And "*3o*" denotes affinity with the combination of modes 1 and 2 and potentially causing maximum force at one of the "outer" intermediate brace points. The notations for the imperfections potentially producing the maximum force at the inside brace also follow this convention. The term "*i*" indicates a geometric imperfection potentially causing maximum force at one of the "inner" intermediate brace points.

The critical imperfection causing the largest outside brace force is imperfection "*1o*" and the critical imperfection causing the largest inside brace force is imperfection "*3i1*". These are demonstrated by the results from second-order analysis in Steps 5 and 6.

*Step 5: Perform a second-order analysis*

A second–order load deflection analysis is conducted.

*Step 6: Check members using the AISC interaction equations*

The results from second-order analysis are shown in Table 3.5.1. In this Table, UC stands for the Unity Check given by Eqs. (3-2) or (3-3). The term $\Delta_b$ is the maximum displacement at the brace points from the second-order analysis; $\Delta_{bo}$ is the initial

imperfection at this point. $P_{out}$ and $P_{in}$ are the corresponding brace forces at the outside and inside braces respectively. $P_u$ is the maximum load capacity of the column.

**Table 3.5.1. Second order analysis results, DM example with β = 20.0 kips/inch and $P_u$ = 982.7 kips**

| No | Imperfection | *UC* | $P_{out}$ (kips) | $P_{in}$ (kips) | $\Delta_b$ (in) | $(\Delta_b+\Delta_{bo})/\Delta_{bo}$ |
|---|---|---|---|---|---|---|
| 1 | 1o | 1.0000 | 8.90 | 4.81 | 0.5561 | 2.54 |
| 2 | 2o | 0.9249 | 6.98 | 1.29 | 0.4363 | 2.21 |
| 3 | 3o | 0.9527 | 7.77 | 2.99 | 0.4856 | 2.34 |
| 4 | 2i | 0.9669 | 3.16 | 4.46 | 0.2788 | 1.77 |
| 5 | 1i1 | 0.9727 | 6.20 | 4.53 | 0.3875 | 2.07 |
| 6 | 1i2 | 0.9527 | 4.81 | 4.09 | 0.3006 | 1.83 |
| 7 | 3i1 | 0.9702 | 6.80 | 7.43 | 0.4644 | 2.29 |
| 8 | 3i2 | 0.9612 | 2.99 | 5.95 | 0.3719 | 2.03 |

Table 3.5.1 shows that the imperfection "*1o*" causes the maximum "outer" intermediate brace force, $P_{out}$ = 8.90 kips and the imperfection "*3i1*" causes the maximum "inner" intermediate brace force, $P_{in}$ = 7.43 kips. This imperfection also gives the largest beam-column unity check of 1.0 at $P_u$ = 982.7 kips. These results are consistent with the determination of the critical imperfections discussed in Section 3.3.5. The key responses at the maximum load for imperfection "*1o*" and "*3i1*" are plotted in Fig. 3.5.5.

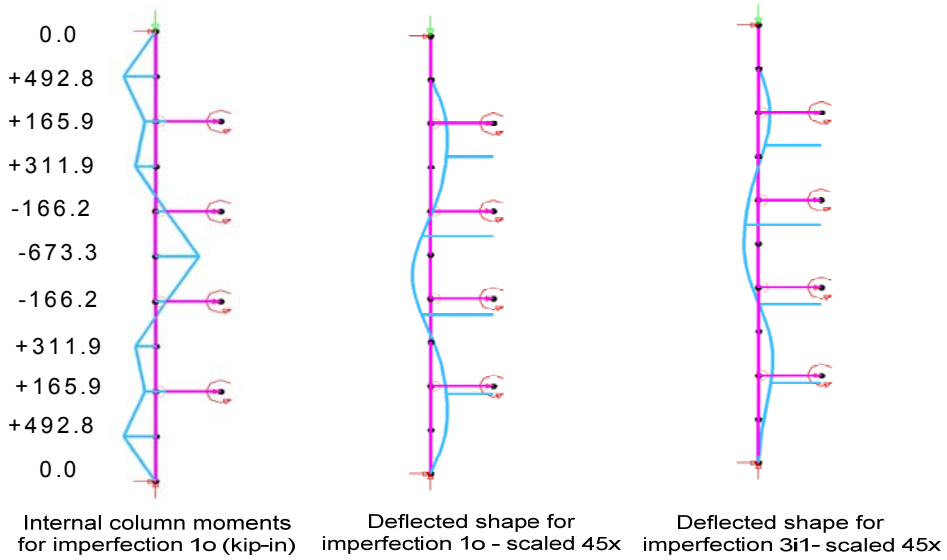


**Fig. 3.5.2. Responses at the maximum load with β = 20.0 kips/inch.**

*Step 7: Check amplification of brace point displacements at maximum load level*

From the Table 3.5.1, the maximum amplification of brace point displacement is

$$(\Delta_b + \Delta_{bo})/\Delta_{bo} = 2.54$$

This is an acceptable level of amplification (i.e., it is smaller than 4.0)

## 3.6 Distributed Plasticity (DP) Procedure

Distributed Plasticity Analysis has become a routine research tool for development and validation of various simplified analysis and design methods (ASCE 1997; Galambos and Ketter (1959), Ketter (1961), Chen and Atsuta (1976), and Kanchanalai (1977), Maleck and White (2003); Martinez-Garcia and Ziemian (2006). In a Distributed Plasticity Analysis, the spread of plasticity through the member cross-section and along the member length is explicitly tracked in a model of structure including geometric imperfections, initial residual stresses, and typically assuming elastic-perfectly plastic material stress-strain response. A common residual stress pattern used in rolled wide

flange members is the so-called Lehigh pattern as shown in Fig. 3.6.1. This residual stress pattern which has a maximum value of $0.3F_y$ in compression and linear variation across the flanges and uniform tension in the web induces early yielding in compression at the flange tips.

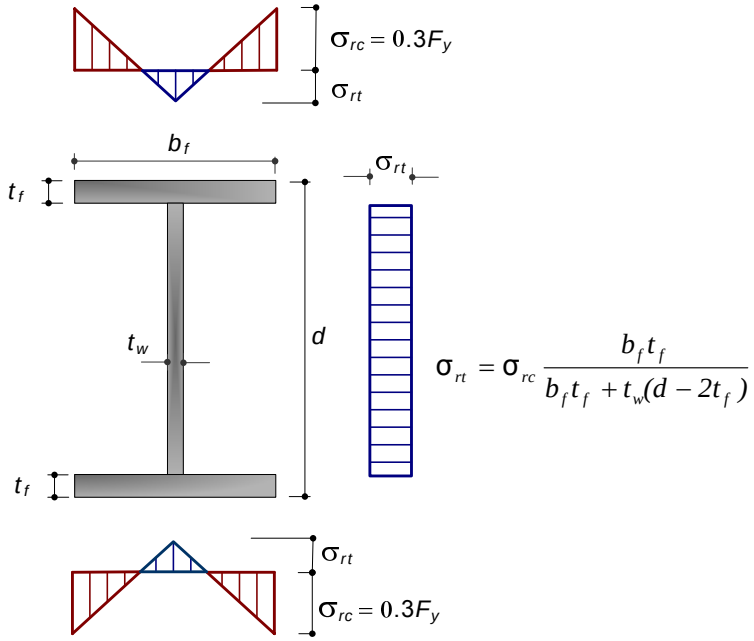


**Fig. 3.6.1. Typical assumed residual stress pattern for rolled wide-flange shapes (Galambos and Ketter 1959).**

The analysis model in the DM is simply an approximate DP analysis. The detailed procedure for the use of the Distributed Plasticity Analysis to determine the column flexural buckling strength and the corresponding brace forces in the column bracing problem is as follows:

*Step 1: Determine overall structural layout and required loads.*

*Step 2: Use reduced member properties.*

- Use reduced stiffnesses of $0.9E$ and $0.9F_y$ for column members. The factor of 0.9 accounts for the uncertainty in the strength and stiffness of the members, connections, and structural system.
- Use reduced stiffnesses of $0.8E$ for bracing members (to maintain the same level of reliability with respect to the design of the elastic bracing system components as in the DM)

*Step 3: Determine the buckling eigenvalues and mode shapes using the DM model*

*Step 4: Apply geometric imperfections.*

Geometric imperfections is applied based on the AISC Code of Standard Practice Tolerances, affinity with the lowest eigenvalue buckling modes, and affinity of the equivalent lateral loads with the influence lines for the brace forces. Use the same calculations as presented for the DM.

*Step 5: Perform a distributed plasticity analysis*

- Tracks the spread of yielding due to applied plus residual stresses
- The column capacity ($\phi_c P_n$) is the limit load obtained from the analysis

## 3.7 DP Example

The column considered in this section is the same as the one considered in the DM example in Section 3.5.

*Step 1: Determine overall structural layout and the required loads*

This step is the same as step 1 in DM solution.

*Step 2: Use reduced member properties.*

- Use reduced stiffnesses: $0.9E$ = 26,100 ksi and $0.8\beta$ = 16.0 kips/inch.
- Use reduced yield strength: $0.9F_y$ = 45 ksi.

*Step 3: Determine the buckling eigenvalues and mode shapes using the DM model.*

This step is the same as step 3 in DM solution in Section 3.5.

*Step 4: Apply geometric imperfections.*

As discussed previously, the critical imperfection "*1o*" causing the largest "outer" intermediate brace force and smallest column axial resistance and imperfection "*3i1*" causing the largest force at one of the "inner" intermediate brace points are shown again in Fig. 3.7.1.

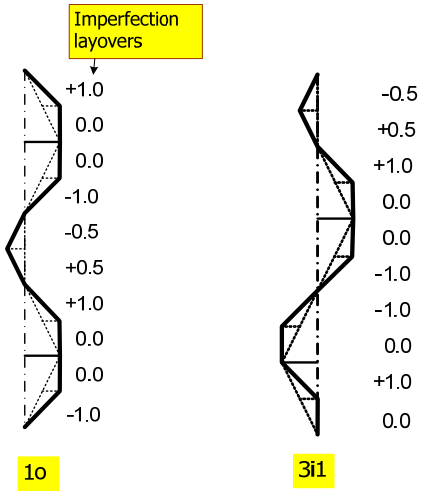


**Fig. 3.7.1. Critical imperfections for the DP example.**

As noted in the DM example above, the denotation "1.0" in the vectors of imperfection layovers in Fig. 3.7.1 indicates $1.0(L_b / 500)$.

*Step 5: Perform a distributed plasticity analysis*

GT-Sabre (Chang 2006) acronym for Georgia Tech Structural Analysis and Bridge Evaluation is used in this research for DP solutions. The results from GT-Sabre are plotted from Fig. 3.7.2 to Fig. 3.7.5. One can observe from Fig. 3.7.2 that the column capacity ($\phi_c P_n$) is equal to 940 kips. This value is smaller than the column capacity obtained from the DM solution, $P_{max}$ = 982.7kips. This type of result is common for

weak-axis bending problems. Also, the brace force corresponding to the limit load from DP is 19.3 kips for imperfection *"1o"* as indicated in Fig. 3.7.3. Note that this brace force is significantly larger than the brace force determined from the DM of 8.9 kips. This difference is discussed in Section 3.8.1.2.

The diagrams of moment, equivalent area $A_{eq}$, equivalent elastic section modulus $Q_{eq}$, and the equivalent of moment inertia $I_{eq}$ from the Distributed Plasticity Method due to the spread of plasticity through the member cross-section and along the member length at the maximum load are displayed in Fig. 3.7.4 and 3.7.5.

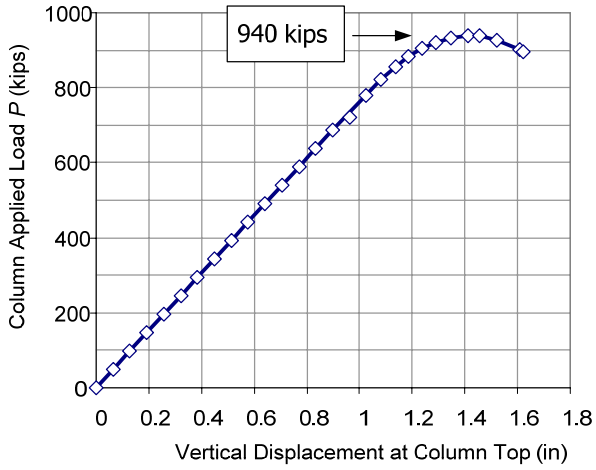


**Fig. 3.7.2. Trace for load vs. displacement - Imperfection 1o, DP example.**

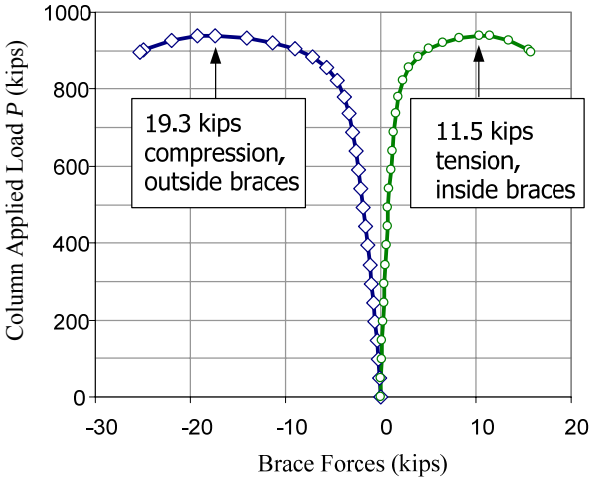


**Fig. 3.7.3. Trace for load vs. brace forces - Imperfection 1o, DP example.**

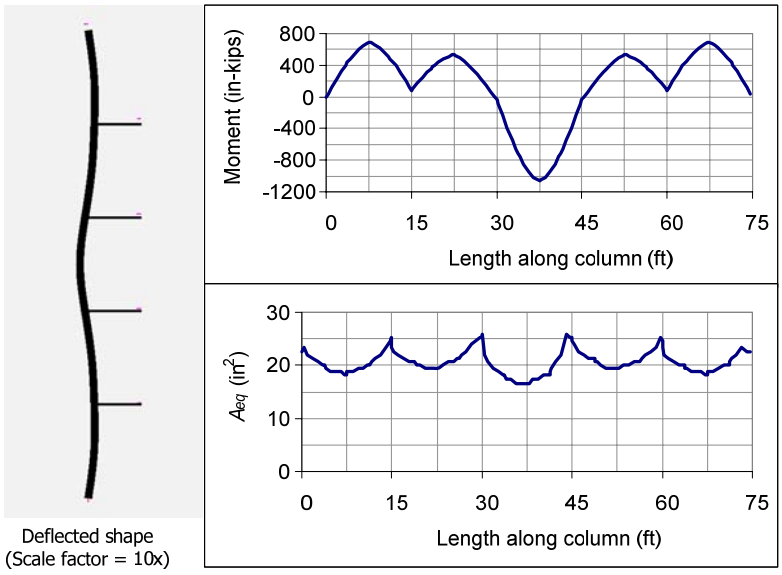


**Fig. 3.7.4. Response at maximum load (1) - Imperfection 1o, DP example.**

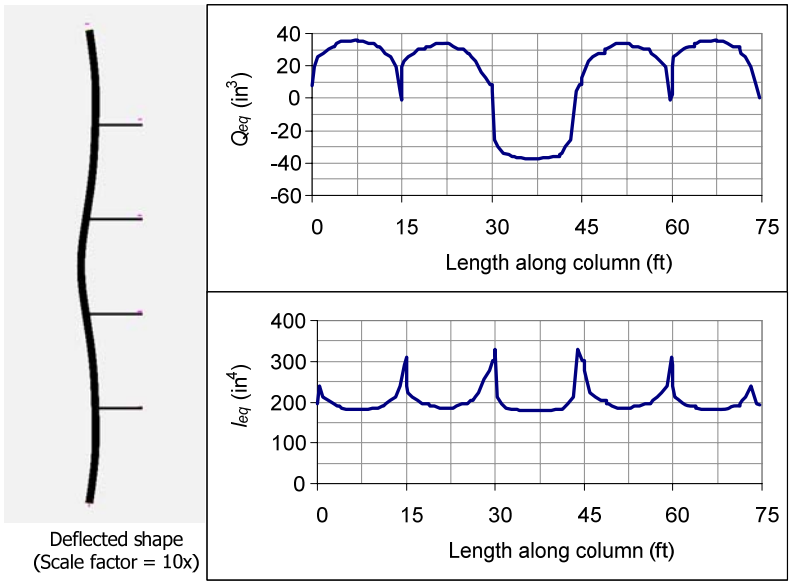


**Fig. 3.7.5. Response at maximum load (2) - Imperfection 1o, DP example.**

The DM and DP solutions for a column with four intermediate nodal braces under the brace stiffness approximately equal to the brace stiffness to develop the "fully-braced strength" in the Effective Length Method are presented above. In order to understand the

complete behavior of this column as a fact of the brace stiffness, five other brace stiffnesses $\beta = 0.8$, 5, 10, 30, and 50 kips/inch are investigated in Section 3.8.1.

## 3.8 Illustrative Examples - Column Bracing

As discussed previously, the DM and DP solutions can be used to predict the bracing requirements for all types of bracing problems. In this section, the behavior of several complex problems that fall outside the scope of AISC Appendix 6 is investigated. These problems which cover column bracing case studies accounting for the different parameters such as continuity effects, unequal brace spacing, and different end boundary conditions as well as non-constant axial stress along the length of member, nonprismatic geometry, and combinations of relative and nodal bracing are addressed from Section 3.8.1 to 3.8.7.

### 3.8.1 Case 1: Column with Four Intermediate Nodal Braces

This problem is based on the column considered in the DM and DP examples in Section 3.5 and 3.7. However, here the column is analyzed with five other brace stiffnesses $\beta = 0.8$, 5, 10, 30, and 50 kips/inch. The description of this benchmark problem is repeated in Fig. 3.8.1.1.

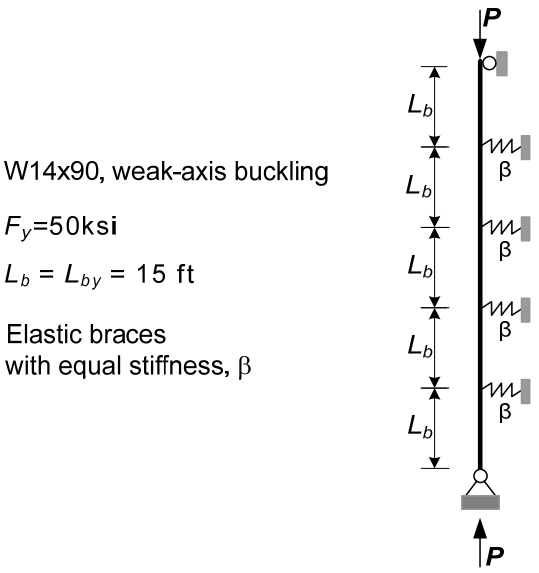


**Fig. 3.8.1.1. Pinned-pinned column with four intermediate nodal braces, case 1.**

3.8.1.1 DM and DP Solutions

*a. Brace stiffness $\beta = 0.8$ kips/inch.*

The buckling modes for this brace stiffness are shown in Fig. 3.8.1.2.

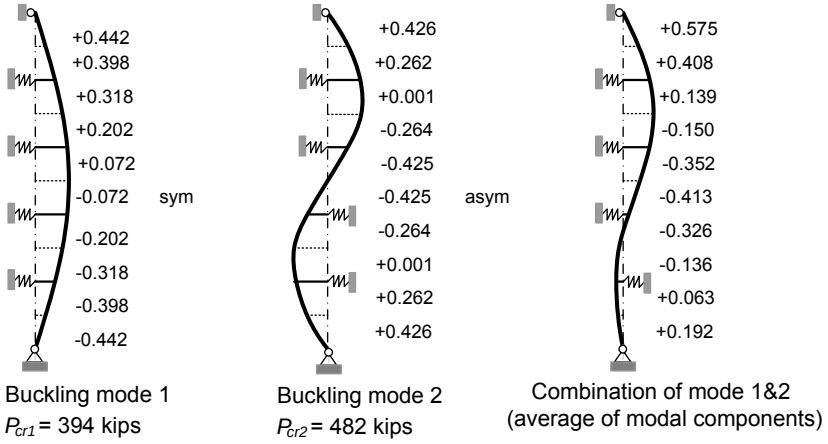


**Fig. 3.8.1.2. Buckling mode shapes with β = 0.8 kips/inch.**

The critical imperfection for this case is the imperfection "*1o=1i*" shown in Fig. 3.8.1.3. This imperfection has maximum affinity with mode 1.

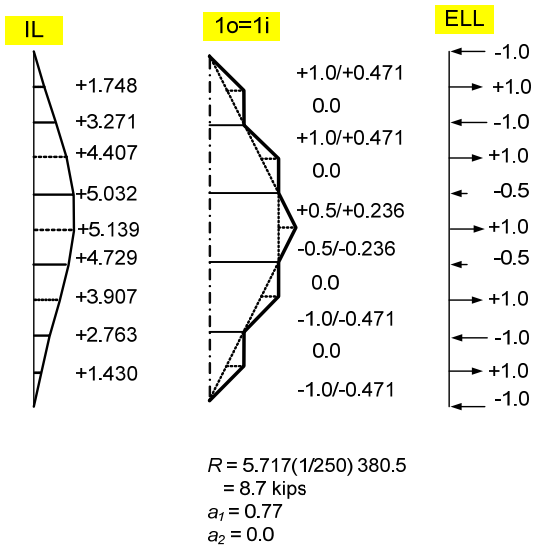


**Fig. 3.8.1.3. Critical imperfections with β = 0.8 kips/inch.**

Using the DM and DP procedures, the results are summarized as follows:

The maximum load from the DM is 380.5 kips while the maximum load from the DP is 376.1 kips. The maximum brace force at the inside braces from the DM is 14.5 kips and from the DP is 7.45 kips; the maximum brace force at the outside braces from the DM is 8.94 kips and from the DP is 4.55 kips. The amplification for this stiffness is very large, $(\Delta_b + \Delta_{bo})/\Delta_{bo} = 32.4$. It is much bigger than the acceptable level of 4.0.

*b. Brace stiffness $\beta = 5.0$ kips/inch.*

The buckling modes for this brace stiffness are plotted as Fig. 3.8.1.4.

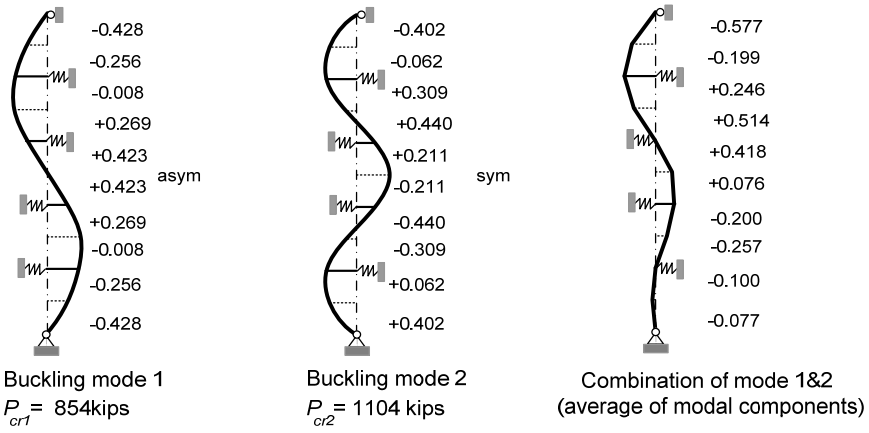


**Fig. 3.8.1.4. Buckling mode shapes with β = 5.0 kips/inch.**

The critical imperfection for this case is the imperfection "*1o3*" shown in Fig. 3.8.1.5.

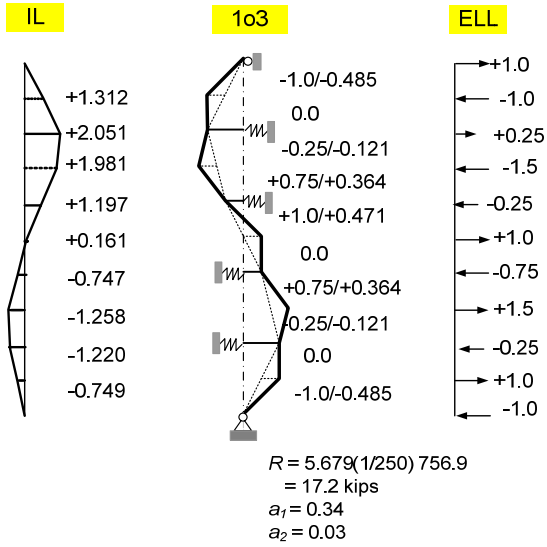


**Fig. 3.8.1.5. Critical imperfections with β = 5.0 kips/inch.**

The maximum load from the DM is 756.9 kips while the maximum load from the DP is 698.3 kips. The maximum brace force at the inside braces from the DM is 7.41 kips and from the DP is 5.68 kips; the maximum brace force at the outside braces from the DM is 12.2 kips and from the DP is 9.46 kips. The amplification for this stiffness is still excessive, $(\Delta_b + \Delta_{bo})/\Delta_{bo} = 9.39$.

*c. Brace stiffness $\beta$ = 10.0 kips/inch.*

The buckling modes for this brace stiffness are plotted as Fig. 3.8.1.6.

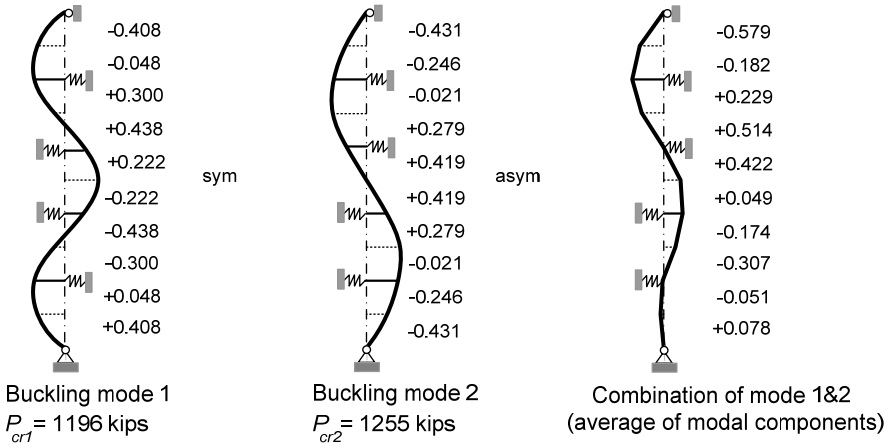


**Fig. 3.8.1.6. Buckling mode shapes with β = 10.0 kips/inch.**

The critical imperfection for this case is the imperfection "*3o=3i*" shown in Fig. 3.8.1.7.

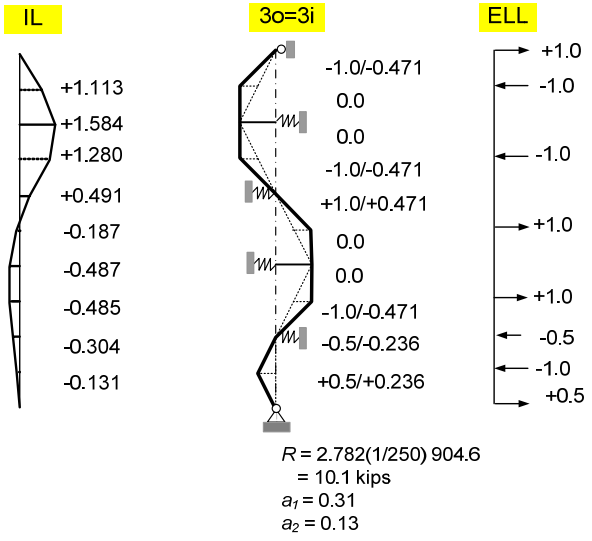


**Fig. 3.8.1.7. Critical imperfections with β = 10.0 kips/inch.**

The maximum load from the DM is 904.6 kips while the maximum load from the DP is 837.1 kips. The maximum brace force at the inside braces from the DM is 7.14 kips

and from the DP is 8.05 kips; the maximum brace force at the outside braces from the DM is 10.0 kips and from the DP is 11.7 kips. The amplification for this stiffness is still large, $(\Delta_b + \Delta_{bo})/\Delta_{bo} = 4.48$.

*d. Brace stiffness $\beta$ = 30.0 kips/inch.*

The buckling modes for this brace stiffness are plotted as Fig. 3.8.1.8.

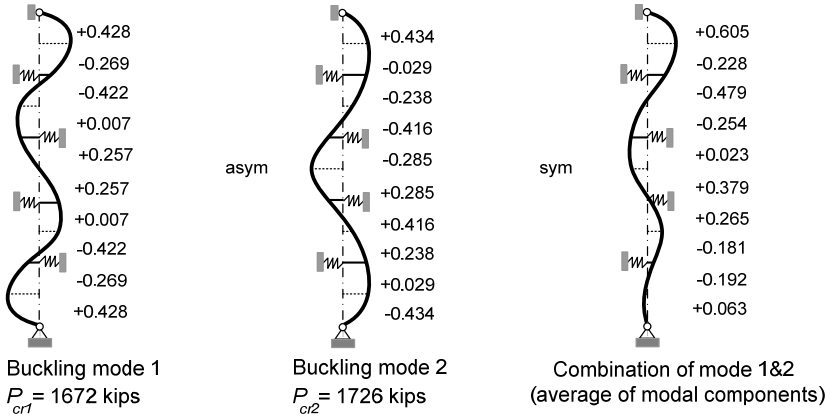


**Fig. 3.8.1.8. Buckling mode shapes with β = 30.0 kips/inch.**

The imperfections "*2o*" and "*3i*"shown in Fig. 3.8.1.9 give the largest outside and inside brace forces.

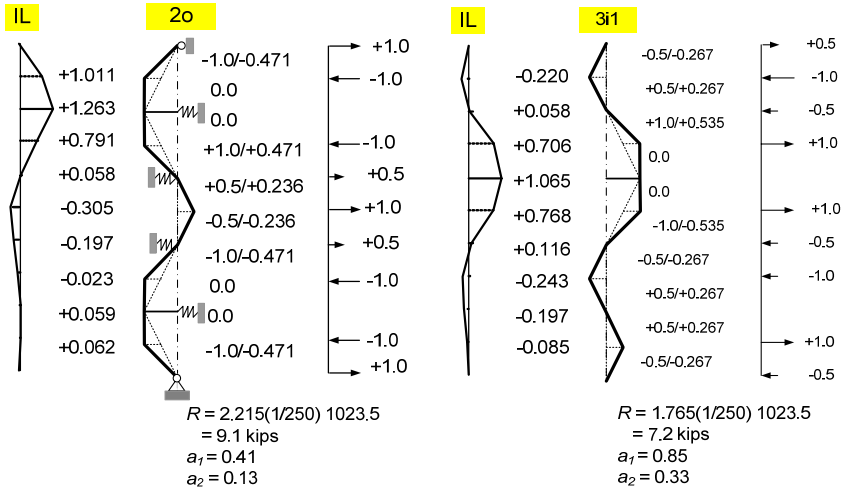


**Fig. 3.8.1.9. Critical imperfections with β = 30.0 kips/inch.**

The maximum load from the DM is 1023.0 kips while the maximum load from the DP is 976.3 kips. The maximum brace force at the inside braces from the DM is 8.32 kips and from the DP is 14.4 kips; the maximum brace force at the outside braces from the DM is 9.12 kips and from the DP is 14.9 kips. The amplification for this stiffness is $(\Delta_b + \Delta_{bo})/\Delta_{bo} = 2.06$.

*e. Brace stiffness $\beta = 50.0$ kips/inch.*

The buckling modes for this brace stiffness are plotted as Fig. 3.8.1.10.

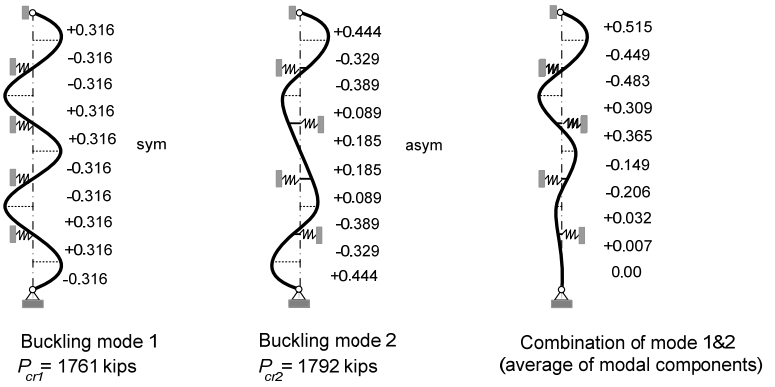


**Fig. 3.8.1.10. Buckling mode shapes with β = 50.0 kips/inch.**

The imperfections "*2o1*" and "*2i*" shown in Fig. 3.8.1.11 give the largest outside and inside brace forces.

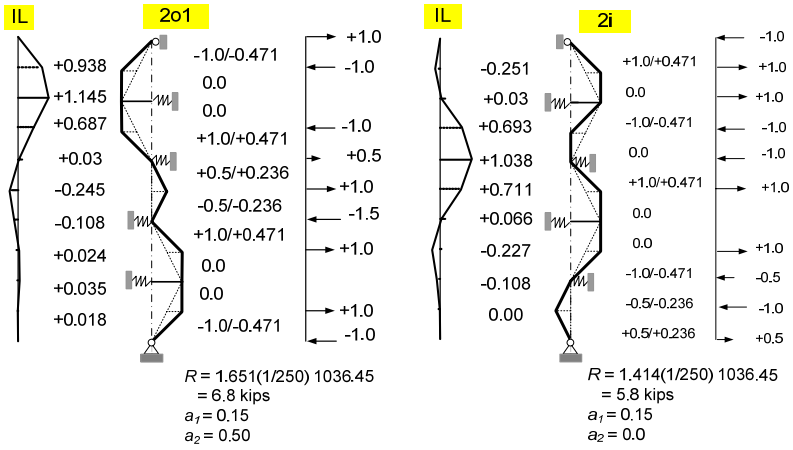


**Fig. 3.8.1.11. Critical imperfections with β = 50.0 kips/inch.**

The maximum load from the DM is 1036.0 kips while the maximum load from DP is 989.7 kips. The maximum brace force at inside braces from DM is 7.11 kips and from DP is 9.87 kips; the maximum brace force at outside braces from DM is 6.90 kips and from DP is 9.47 kips. The amplification for this stiffness is acceptable, $(\Delta_b + \Delta_{bo})/\Delta_{bo} = 1.49$.

3.8.1.2 Comparison of the results between the DM, DP, ELM and AISC (2005) Appendix 6 Solutions

The column capacity and maximum brace forces calculated from the DM, DP, and the AISC (2005) Appendix 6 as well as from the Effective Length Method for the case study 1 with a brace stiffness $\beta = 20.0$ kips/inch are shown in the Table 3.8.1.

**Table 3.8.1. Column capacity and maximum brace forces.**

| Method | Column Capacity | Maximum brace force | |
|---|---|---|---|
| | (kips) | (kips) | %*P* |
| Effective Length Method (ELM) | 994.0 | NA | NA |
| AISC Appendix 6 | 688.0 | 6.9 | 1.0 |
| Direct Analysis Method (DM) | 983.0 | 8.9 | 0.9 |
| Distributed Plasticity Method (DP) | 940.0 | 19.3 | 2.1 |

Table 3.8.1 indicates that the column capacity from the Distributed Plasticity Solution is lower than that from the Direct Analysis Method as well as from the Effective Length Method. This can be explained by noting that the Distributed Plasticity solution tends to give a slightly lower column capacity than the AISC column curve for WA flexural buckling. It tends to give a slightly higher column capacity than the AISC curve for SA flexural buckling. Also, the brace force from the Distributed Plasticity Solution is higher than the brace force from the Direct Analysis Method and from the AISC (2005)

Appendix 6 calculations. However, the larger brace forces in Distributed Plasticity Solution occur only at $P > 0.95P_{max}$.

**Table 3.8.2. ELM and DM results - Column capacity and maximum brace forces with β = 0.8, 5, 10, 20, 30, 50 kips/inch.**

| Case | β (kips/in) | $P_{max.ELM}$ (kips) | $P_{max.DM}$ (kips) | $P_{max.DM} / P_{max.ELM}$ | $P_{br.out.DM}$ (kips) | $P_{br.in.DM}$ (kips) | $P_{br.out.DM} / P_{max.DM}$ (%) | $P_{br.in.DM} / P_{max.DM}$ (%) |
|---|---|---|---|---|---|---|---|---|
| A | 0.8 | 388.7 | 380.5 | 0.979 | 8.94 | 14.5 | 2.35 | 3.81 |
| B | 5 | 761.7 | 759.0 | 0.996 | 12.2 | 7.41 | 1.61 | 0.98 |
| C | 10 | 904.5 | 904.6 | 1.000 | 10.0 | 7.14 | 1.11 | 0.79 |
| | 20 | 994.1 | 982.7 | 0.989 | 8.90 | 7.43 | 0.91 | 0.76 |
| D | 30 | 1004 | 1023 | 1.019 | 9.12 | 8.32 | 0.76 | 0.81 |
| E | 50 | 1004 | 1036 | 1.032 | 6.90 | 7.11 | 0.67 | 0.69 |

**Table 3.8.3. DP and DM results - Column capacity and maximum brace forces with β = 0.8, 5, 10, 20, 30, 50 kips/inch.**

| Case | β (kips/in) | $P_{max.ELM}$ (kips) | $P_{max.DM}$ (kips) | $P_{max.DM} / P_{max.ELM}$ | $P_{br.out.DM}$ (kips) | $P_{br.in.DM}$ (kips) | $P_{br.out.DM} / P_{max.DM}$ (%) | $P_{br.in.DM} / P_{max.DM}$ (%) |
|---|---|---|---|---|---|---|---|---|
| A | 0.8 | 388.7 | 380.5 | 0.979 | 8.94 | 14.5 | 2.35 | 3.81 |
| B | 5 | 761.7 | 759.0 | 0.996 | 12.2 | 7.41 | 1.61 | 0.98 |
| C | 10 | 904.5 | 904.6 | 1.000 | 10.0 | 7.14 | 1.11 | 0.79 |
| | 20 | 994.1 | 982.7 | 0.989 | 8.90 | 7.43 | 0.91 | 0.76 |
| D | 30 | 1004 | 1023 | 1.019 | 9.12 | 8.32 | 0.76 | 0.81 |
| E | 50 | 1004 | 1036 | 1.032 | 6.90 | 7.11 | 0.67 | 0.69 |

**Obtained using the imperfection pattern that maximizes the listed brace force(s) in the DM solution. $P_{max.DP}$ is otherwise obtained using the imperfection pattern that maximizes the column unity check in the DM solution*

**Table 3.8.4. Amplification of brace point displacements from DM.**

| Case | Maximum $(\Delta_b + \Delta_{bo})/\Delta_{bo}$ |
|---|---|
| A (β = 0.8 kips/in) | 32.4 |
| B (β = 5 kips/in) | 9.39 |
| C (β = 10 kips/in) | 4.48 |
| C (β = 20 kips/in) | 2.54 |
| D (β = 30 kips/in) | 2.06 |
| E (β = 50 kips/in) | 1.49 |

**Table 3.8.5. Column capacity and maximum brace forces for four different brace stiffnesses from DM.**

| Brace stiffness β | Column Capacity | Maximum brace force | |
|---|---|---|---|
| | (kips) | (kips) | %*P* |
| $\beta = \beta_i = 20$ kip/in | 983 | 8.9 | 0.9 |
| $\beta = 1.3\beta_i = 26$ kip/in | 1010 | 9.1 | 0.9 |
| $\beta = 2\beta/\phi = 53$ kip/in | 1040 | 7.1 | 0.7 |
| $\beta = \infty$ | 1060 | 8.3 | 0.8 |

Table 3.8.2 summarizes the results for the column capacity and the maximum brace forces from the Direct Analysis Method and Effective Length Method for all the brace stiffnesses β = 0.8, 5, 10, 20, 30, and 50 kips/inch . The column capacity and maximum brace forces between the Distributed Plasticity Solution and Direct Analysis Solutions are compared in Table 3.8.3. The amplifications of brace point displacements from the DM corresponding to each of the brace stiffness are given in the Table 3.8.4. One can observe from this table that the amplification is excessive for Cases A (β = 0.8 kips/inch), B (β = 5 kips/inch), and C (β = 10 kips/inch).

The column strength versus bracing stiffness curves from the DP, DM and ELM solutions are plotted in Fig. 3.8.1.12. The DM and the ELM give very similar predictions for the column maximum resistance. The Distributed Plasticity solution predicts a slightly smaller column resistance; this is related to the use of a single column curve by AISC. Appendix 6 gives a very conservative prediction of the maximum column resistance for $\beta$ = 20 kips/inch. ($\beta_i = 3.62\frac{\phi_c P_n}{L_b} = 3.62\frac{1000}{180} = 20.1$kips/inch)

Table 3.8.5 shows that the brace stiffness $\beta$ = 20 kips/inch $\cong \beta_i$ develops 93% of the rigidly-braced column capacity and $\beta = 1.3\beta_i$ = 26 kips/inch develops 97 to 98 % of the column capacity when using brace stiffness based on the AISC (2005) Appendix 6 and 95 to 96% of the rigidly-braced column capacity.

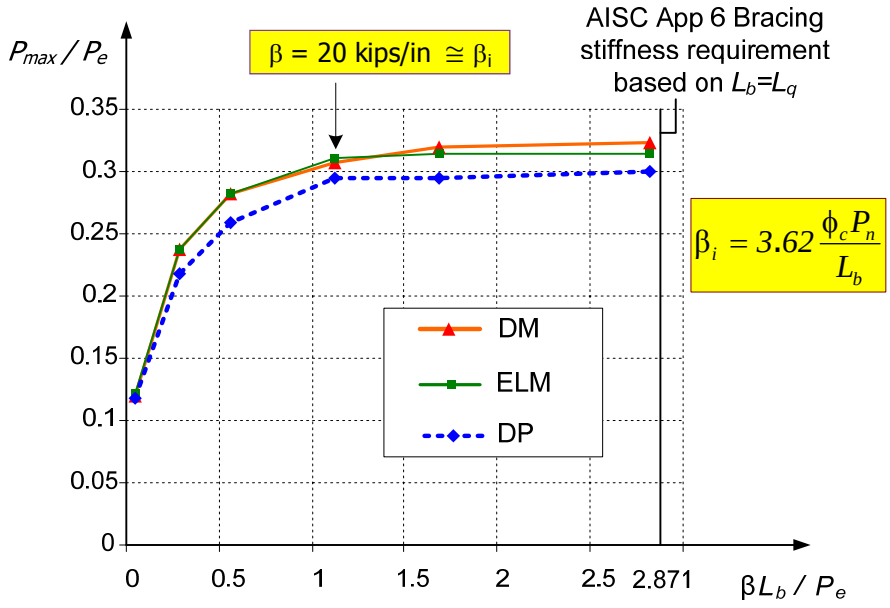


**Fig. 3.8.1.12. Column strength vs. bracing stiffness ELM, DM, and DP.**

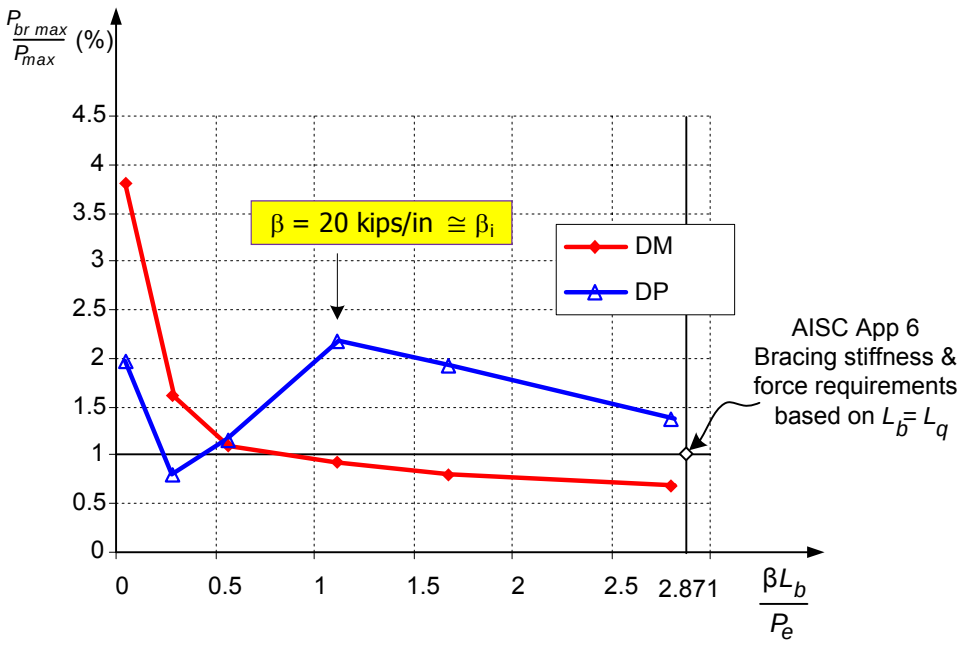


**Fig. 3.8.1.13. Brace force vs. brace stiffness DM and DP.**

Fig. 3.8.1.13 displays the relationship between the brace force and brace stiffness from the DM and DP as well as the brace strength and stiffness requirements based on $L_b = L_q$ from the AISC Appendix 6. One can observe from Fig. 3.8.1.13 that the maximum brace force is larger than $0.02P_{max}$ only for Case A (β = 0.8 kips/inch). The brace stiffness β = 50 kips/inch for Case E is similar to the brace stiffness required by the AISC Appendix 6. For Case E, Appendix 6 requires $P_{br}$ = 10 kips for $P_u$ = 1000 kips whereas the DM gives a maximum brace force of $P_{br}$ = 7.11 kips at a column capacity of 1036 kips. The DM gives smaller brace forces than the AISC Appendix 6 equations at the full bracing limit. The DM indicates that the column performance is adequate for β = 20 kips/inch ($P_{max}$ = 983 kips, $(\Delta_b + \Delta_{bo})/\Delta_{bo} = 2.54$, $P_{br}$ = 8.90 kips). The Distributed Plasticity solution also indicates that the column performance is adequate for β = 20 kips/inch ($P_{max}$ = = 940 kips, $(\Delta_b + \Delta_{bo})/\Delta_{bo}$ = 4.35, $P_{br}$ = 19.3 kips). The larger

displacements and brace forces in the Distributed Plasticity Solution occur only at $P > 0.95P_{max}$.

3.8.1.3 Summary

The column flexural rigidity contributes significantly to the resistance of the brace point deflections (Winter's model, i.e., hinges inserted in the column at the brace points, is appropriate only for full bracing). The appropriate geometric imperfection varies significantly for different levels of partial bracing. These attributes affect the results of bracing force and stiffness in DM and DP, and explain the higher force and stiffness requirements for nodal bracing in AISC Appendix 6. The brace stiffness $\beta = 1.3\ \beta_i$ develops 97 to 98 % of the column capacity compared to the column capacity when using brace stiffness required by the AISC (2005) Appendix 6.

### 3.8.2 Case 1b: Column with Single Nodal Brace

The column with four intermediate nodal braces studied in the previous Section demonstrates that the continuity effects of one brace to the adjacent braces as well as the contribution of column flexural rigidity give more economical bracing designs. The goal of this section is to investigate further the continuity effects on the bracing requirements by considering a structural system with little continuity effects.

Fig. 3.8.2.1 shows a pinned-pinned column with single nodal brace at mid-height. Similar to the column studied in Section 3.8.1, a W14x90 weak-axis flexural buckling with $F_y$ = 50ksi is used in the analysis. A variable brace stiffness $\beta$ is considered based on various requirements. The unbraced length $L_b$ is varied along the complete range of $L_b/r$ from 20 to 140.

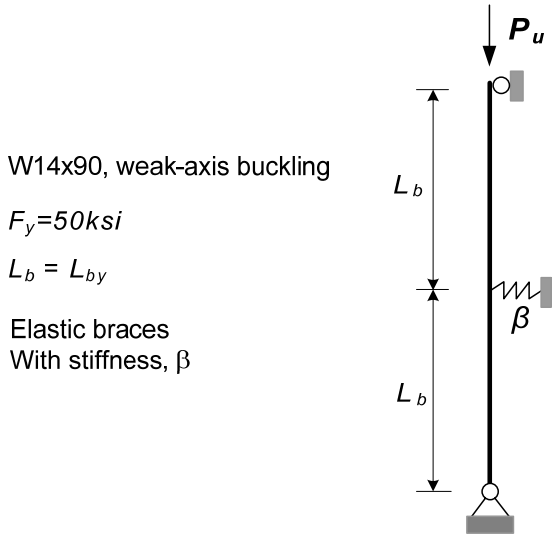


**Fig. 3.8.2.1. Pinned-pinned column with single nodal brace, case 1b.**

Using the Distributed Plasticity Analysis and the Direct Analysis Method determines the brace stiffness requirements necessary to develop 97 to 98 % of the strength of the rigidly braced column and amplification of brace point displacements $\leq 4$ corresponding to brace forces at the maximum load capacity. First, the brace requirements based on the AISC Appendix 6 Commentary are presented in Section 3.8.2.1. Then, the results from the DM and DP are summarized in Section 3.8.2.2.

3.8.2.1 Bracing Requirements based on the AISC Appendix 6 Commentary

From the AISC 2005 Appendix 6 Commentary, the brace stiffness and strength requirements for a single intermediate nodal brace can be calculated as follows. It should be noted that these requirements depend only indirectly on the ratio ($L_b/r$) (via the influence of $L_b/r$ on the maximum possible value of $P_u$)

The ideal brace stiffness: $$\beta_i = 2\frac{P_u}{L_b} \qquad (3.8.1)$$

The required brace stiffness: $\beta = 2\frac{\beta_i}{\phi} = 2.667\beta_i$ (3.8.2)

The required brace force: $P_{br} = 0.01P_u$ (3.8.3)

3.8.2.2 DM and DP Solutions

According to the procedure to determine the critical imperfection discussed in Section 4.2, the critical imperfection for this case is relatively straightforward and is shown in Fig. 3.8.2.2.

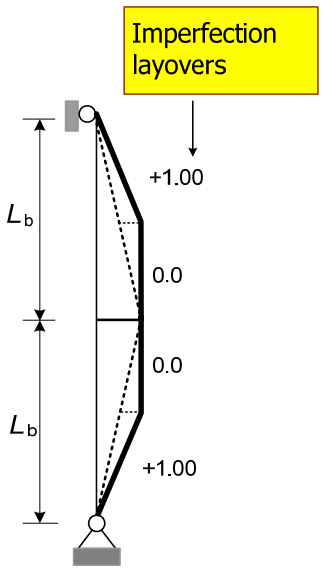


**Fig. 3.8.2.2. Critical imperfection, case 1b.**

The brace stiffnesses are determined based on criteria of developing 98 % of the strength of the rigidly braced column and restricting the amplification of brace point displacements to a value less than 4 are shown in Table 3.8.6.

**Table 3.8.6. Brace stiffnesses from the AISC Appendix 6 and from the DP solutions with column strength is equal to 98% strength of column with the rigid brace.**

| $L_b/r$ | $P_u$ = 98% $P_{rigid}$ (kips) | $\beta_{i(APP6)}$ (kip/in) | $\beta_{DP}$ (kip/in) |
|---|---|---|---|
| 20 | 1137.5 | 29.78 | 38.50 |
| 30 | 1083.63 | 19.35 | 25.00 |
| 40 | 1014.83 | 14.12 | 20.00 |
| 60 | 849.3 | 8.43 | 13.50 |
| 80 | 689.2 | 5.04 | 9.00 |
| 100 | 525.8 | 2.88 | 5.25 |
| 120 | 394.9 | 1.71 | 3.15 |
| 140 | 304.03 | 1.10 | 2.05 |

In Table 3.8.6, $P_{rigid}$ is the strength of column based on the Distributed Plasticity Analysis with a rigid intermediate brace; $P_u$ is the applied force; $\beta_{i(APP6)}$ is the ideal brace stiffness calculated using Eq. (3.8.1); $\beta_{DP}$ is the brace stiffness determined from the Distributed Plasticity Solution to develop the 98% of the strength of the rigidly braced colum. The results are also plotted in Fig. 3.8.2.3. One can observe from Fig. 3.8.2.3 that the recommended brace stiffness depends on the ratio ($L_b/r$). For the short or stocky column, $L_b/r$ = 20 or 30, the required brace stiffness is approximately 1.3 $\beta_i$. For the medium or long column, $L_b/r$ = 80 to 140 the required brace stiffness is around of 1.9 $\beta_i$.

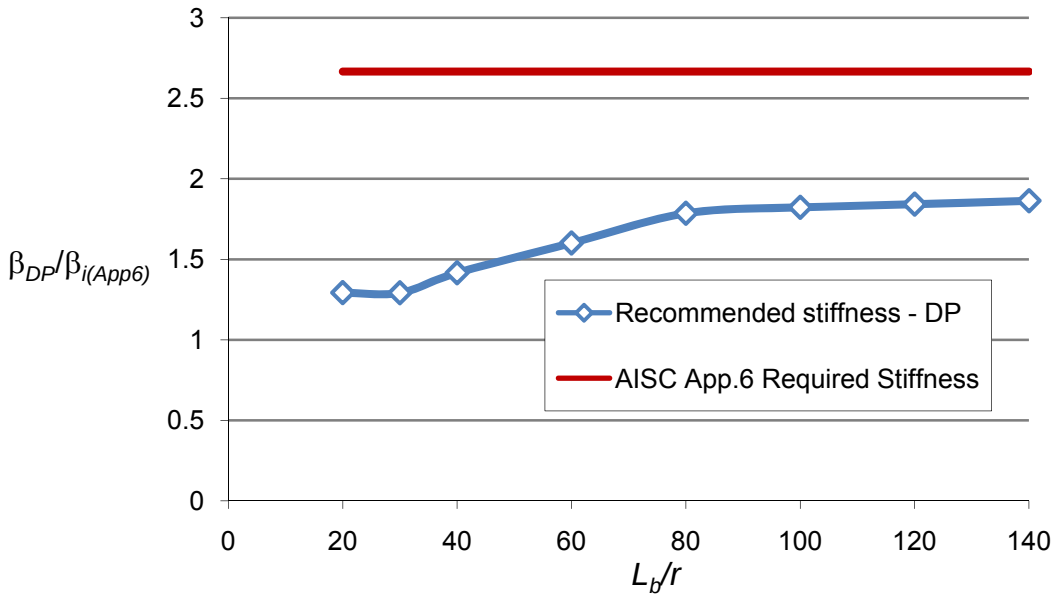


**Fig. 3.8.2.3. Recommended brace stiffness vs. the AISC 2005 Appendix 6 brace stiffness.**

The brace forces corresponding to the recommended stiffness and to the required full bracing stiffness from the AISC Appendix6 are summarized in Tables 3.8.7 and 3.8.8.

**Table 3.8.7. Brace forces with the recommended stiffness from the DP solutions.**

| $L_b/r$ | $\beta_{DP}$ (kip/in) | $P_{br}$ (kips) | $P_{max}$ (kips) | $P_{br}/P_{max}$ |
|---|---|---|---|---|
| 20 | 38.50 | 15.02 | 1138.26 | 1.32% |
| 30 | 25.00 | 26.64 | 1086.00 | 2.45% |
| 40 | 20.00 | 31.80 | 1033.20 | 3.08% |
| 60 | 13.50 | 28.90 | 907.17 | 3.19% |
| 80 | 9.00 | 19.90 | 771.00 | 2.58% |
| 100 | 5.25 | 18.90 | 602.90 | 3.13% |
| 120 | 3.15 | 20.17 | 457.50 | 4.41% |
| 140 | 2.05 | 17.29 | 354.80 | 4.87% |

In Tables 3.8.7 and 3.8.8, $P_{max}$ is the maximum column capacity from the Distributed Plasticity Analysis; $P_{br}$ is the brace force corresponding to the maximum column capacity. The results also are plotted in Fig. 3.8.2.4.

**Table 3.8.8. Brace forces with the AISC Appendix 6 required Stiffness.**

| $L_b/r$ | $\beta_{i(APP6)}$ (kip/in) | $2\beta_{i(APP6)}/\phi$ | $P_{br}$ (kips) | $P_{max}$ (kips) | $P_{br}/P_{max}$ |
|---|---|---|---|---|---|
| 20 | 29.78 | 79.41 | 3.72 | 1054.88 | 0.35% |
| 30 | 19.35 | 51.60 | 21.82 | 1045 | 2.09% |
| 40 | 14.12 | 37.65 | 20.1 | 1106 | 1.82% |
| 60 | 8.43 | 22.48 | 23.19 | 983.8 | 2.36% |
| 80 | 5.04 | 13.44 | 17.33 | 843.3 | 2.06% |
| 100 | 2.88 | 7.68 | 16.93 | 690.9 | 2.45% |
| 120 | 1.71 | 4.56 | 16.95 | 540.9 | 3.13% |
| 140 | 1.10 | 2.93 | 17 | 423.6 | 4.01% |

From these results, one can observe that for the stocky column the ratio of brace force and column capacity ($P_{br}/P_{max}$) corresponding to brace stiffness based on the AISC Appendix 6 ranges from 0.5% to 2.0% while this ratio corresponding to recommended stiffness ranges from 1.4% to 3.1%. For the medium column this ratio is around 2.2% for braces stiffness based on the AISC Appendix 6 and around 3.0% for the recommended stiffness. For the slender column, the ratio of brace force and column capacity can reach to 4.0% corresponding to brace stiffness from the AISC Appendix 6 and 5.0% corresponding to recommended stiffness.

Fig. 3.8.2.4 reveals that the brace forces $(P_{br})$ from the Distributed Plasticity Solution give bigger 2% than the maximum applied load ($P_{max}$) in most cases. The maximum brace force occur for the column with $L_b/r = 140$. The reason is that the Distributed

Plasticity Solution is related to the use of a single column curve by AISC and the large brace forces occur only at $P > 0.95P_{max}$.

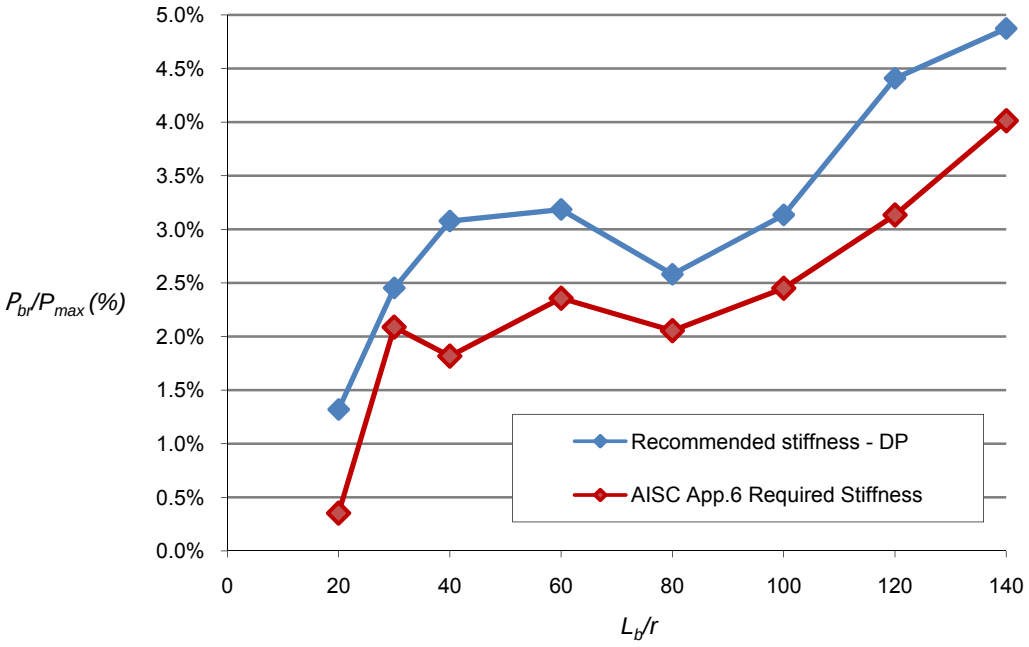


**Fig. 3.8.2.4. Brace forces vs. slenderness ratio for recommended brace stiffness and brace stiffnesses based on the AISC Appendix 6.**

The detailed results from the Direct Analysis and Distributed Plasticity Solutions using the recommended brace stiffness are plotted in Figs. 3.8.2.5 to 3.8.2.9. The brace force ($P_{br}$) in horizontal axis is normalized by the maximum applied load ($P_{max}$) and the applied load ($P_u$) in the vertical axis is normalized by yield load ($P_y$). Also, the maximum column capacity from AISC also is plotted in each figure. From Figs. 3.8.2.5 to 3.8.2.9, it can be observed that the brace forces based on the Direct Analysis Solution are smaller than brace forces based on the Distributed Plasticity Solution at the maximum load limit.

The results from Figs. 3.8.2.5 to 3.8.2.9 show that the brace forces corresponding to the recommended brace stiffness based on the Direct Analysis Solution give smaller than 2% of the applied load. If the applied load is smaller than maximum column capacity

calculated from AISC, both the Direct Analysis and the Distributed Plasticity Solution give the brace forces smaller 2% applied load for recommend brace stiffness.

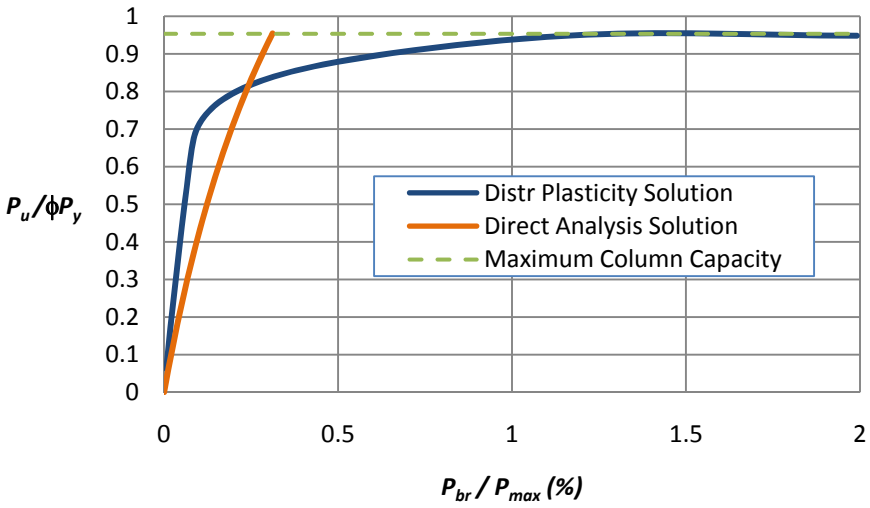


**Fig. 3.8.2.5. Load vs. brace force with $L_b/r$ =20.**

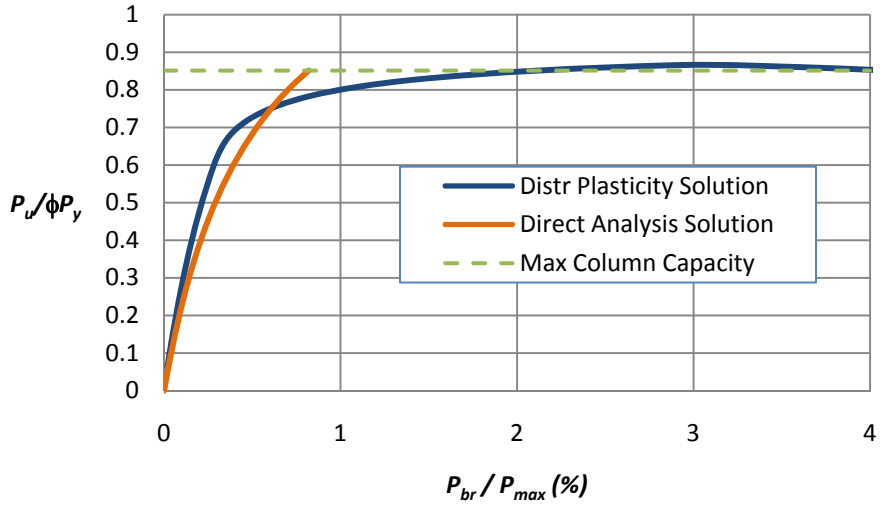


**Fig. 3.8.2.6. Load vs. brace force with $L_b/r$ =40.**

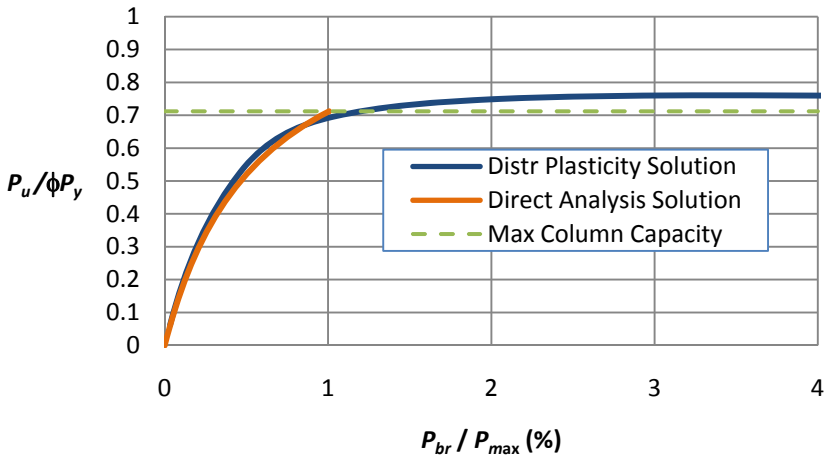


**Fig. 3.8.2.7. Load vs. brace force with $L_b/r$ =60.**

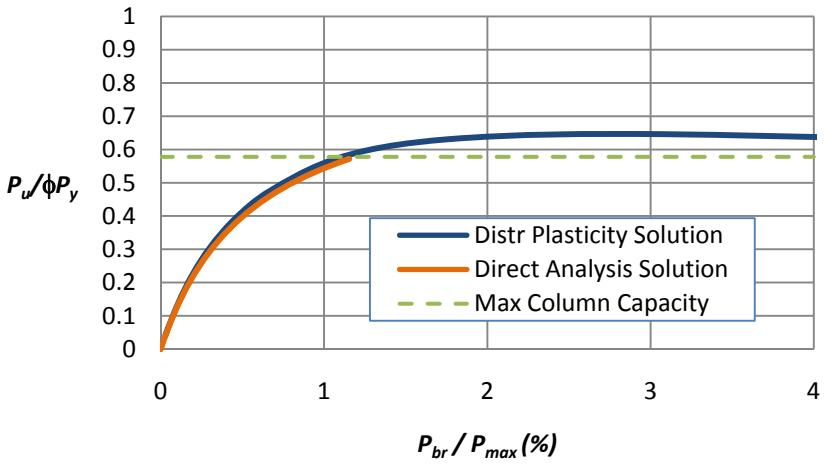


**Fig. 3.8.2.8. Load vs. brace force with $L_b/r$ =80.**

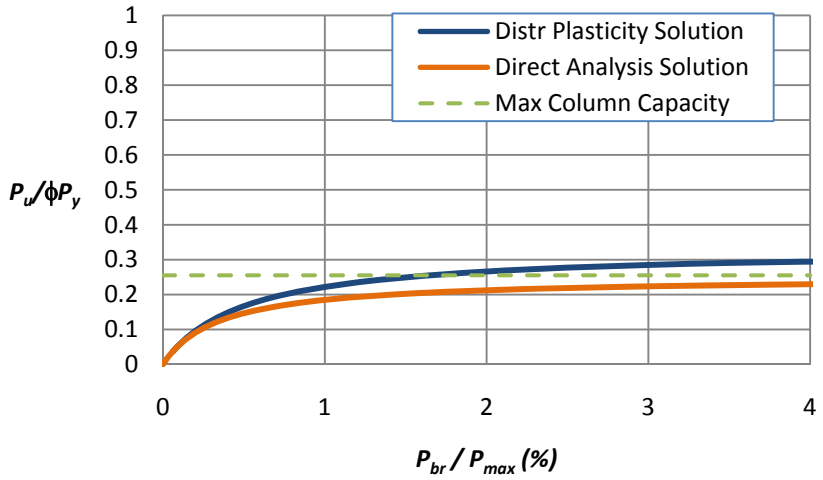


**Fig. 3.8.2.9. Load vs. brace force with $L_b/r$ =140.**

This result is consistent with the results from Li et al. (2002). Li modeled the column considered here in ABAQUS and found that the minimum required brace stiffness in order for column reach the capacity of 95% of the strength of the rigidly braced column ($P_{cr(K=1)}$) is

$$\beta = 2\frac{P_{cr\,(K=1)}}{L_b} \tag{3.8.4}$$

This brace stiffness is equal to the ideal brace stiffness ($\beta_i$) calculated based on equation (3.8.1).

3.8.2.3 Summary

The brace stiffness $\beta = 1.3\ \beta_i$ is sufficient to develop fully-braced column strengths ($K = 1$) in many (but not all) cases and $\beta = 1.9\beta_i$ appears to be sufficient as a worst case. The brace force $P_{br} = 0.02P$ appears to be an appropriate and sufficient approximation with the use of these stiffnesses.

### 3.8.3 Case 2: Column with Flexible End Supports

Shown in Fig. 3.8.3.1 is the same column as in Section 3.8.1: four intermediate nodal braces; equal unbraced lengths $L_b = L_{by} = 15$ ft; equal brace stiffness, β; wide flange W14x90 with yield stress $F_y = 50$ ksi subjected to constant axial load P. However, instead of pinned-pinned column as in Section 3.8.1, the column is restrained by two lateral spring supports at the ends. Assuming that the stiffness of flexible end supports are the same as stiffness of the intermediate braces and the applied load P is equal to the design compressive strength, $\phi_c P_n$, calculated from AISC based on $KL_y = L_{by} = 15$ ft.

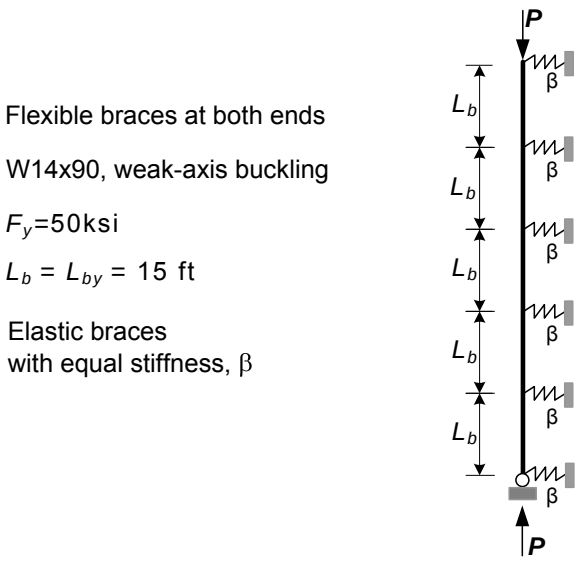


**Fig. 3.8.3.1. Flexible end supports, case 2.**

The solutions of determining the brace stiffness necessary to achieve UC ≤ 1.0 and brace point displacement amplification approximately ≤ 4.0 and corresponding brace forces are as follows.

3.8.3.1 DM Solution

Using a trial and error approach and applying the DM procedure from step 1 to step 6, the brace stiffness necessary to achieve UC $\leq$ 1.0 in this problem is determined as $\beta$ = 25.85 kips/inch $\approx 1.3\beta_i$ . The buckling eigenvalues and mode shapes are shown in Fig. 3.8.3.2.

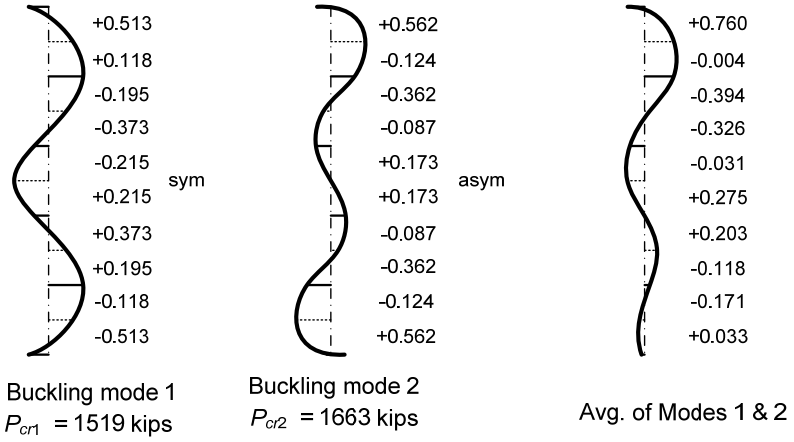


**Fig. 3.8.3.2. Buckling mode shapes, case 2 – DM.**

Because the eigenvalue of mode 2, $P_{cr2}$ = 1663 kips, is only approximately 14% larger than the eigenvalue of mode 1, $P_{cr1}$ = 1519 kips, the combination of these two modes needs to be considered for applying geometric imperfections. Fig. 3.8.3.3 shows the geometric imperfections potentially causing the largest outside brace force. Based on the procedure to determine the critical geometric imperfections in Section 3.3, the imperfection "*3o*" should be the critical one. Likewise, the geometric imperfections potentially causing the largest inside brace force are displayed in Fig. 3.8.3.4 and imperfection "*3i2*" should be the critical one. Finally, the geometric imperfections potentially causing the largest end brace force are demonstrated in Fig. 3.8.3.5 and imperfection "*1s*" should be the critical imperfection. The notation "s" indicates a

geometric imperfection potentially causing maximum force at one of the “end” brace points. The other notations are the same as in Section 3.5.

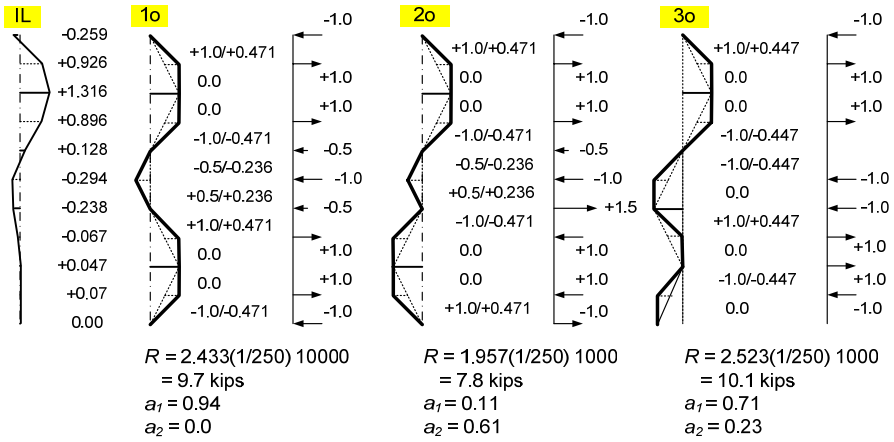


**Fig. 3.8.3.3. Geometric imperfections potentially causing the largest outside brace force, case 2 – DM.**

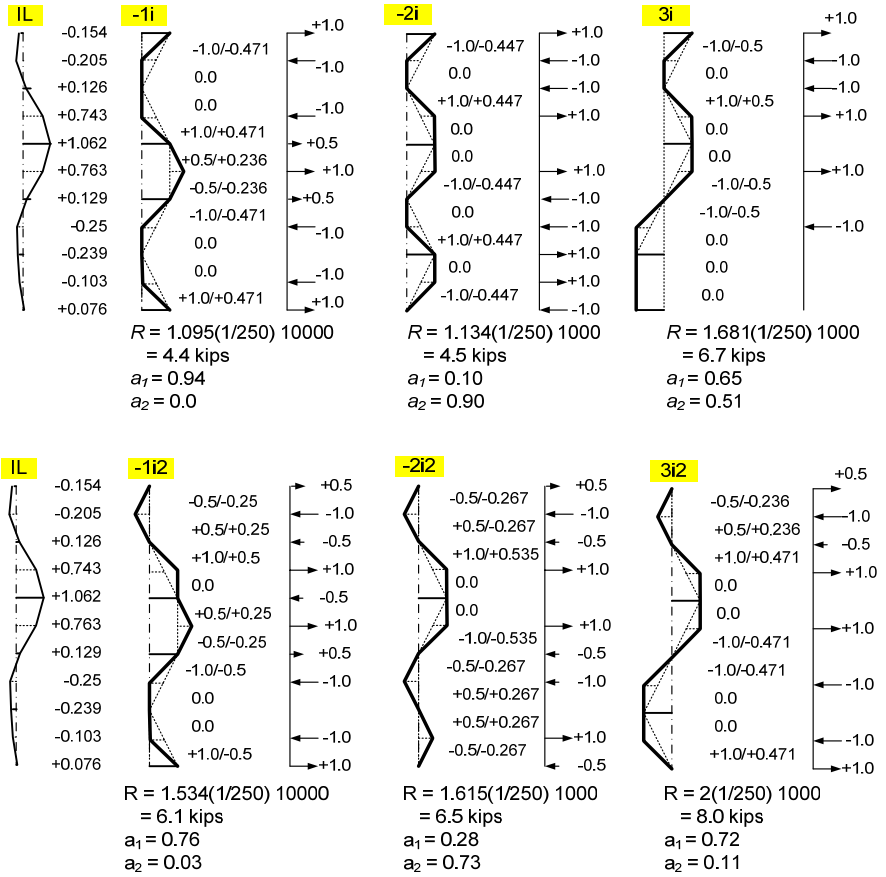


**Fig. 3.8.3.4. Geometric imperfections potentially causing the largest inside brace force, case 2 – DM.**

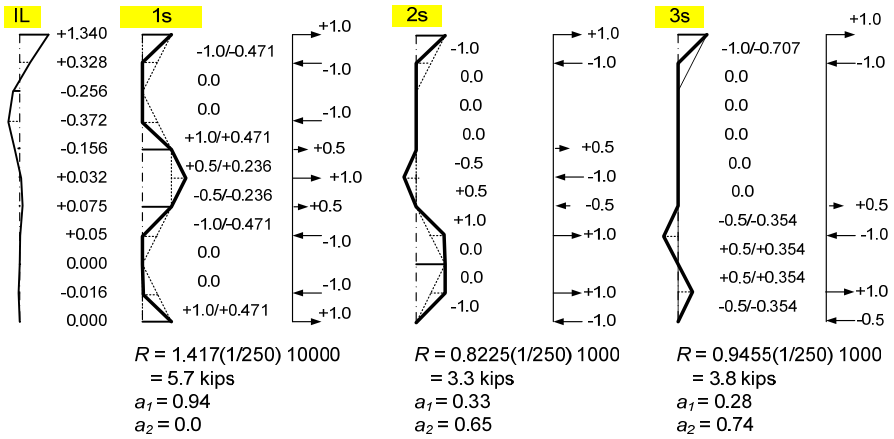


**Fig. 3.8.3.5. Geometric imperfections potentially causing the largest end brace force, case 2 – DM.**

The results from second-order analysis are shown in Table 3.8.9.

**Table 3.8.9. Results from the second-order analysis with β = 25.58 kips/inch and $P_u$ = 1000kips, case 2 – DM.**

| No | Imperfection | *UC* | $P_{out}$ (kips) | $P_{in}$ (kips) | $P_{end}$ (kips) | $\Delta_b$ (in) | $(\Delta_b+\Delta_{bo})/\Delta_{bo}$ |
|---|---|---|---|---|---|---|---|
| 1 | 1o | 1.0004 | 9.73 | 4.39 | 5.34 | 0.4705 | 2.3069 |
| 2 | 2o | 0.9466 | 7.87 | 1.42 | 5.1 | 0.3806 | 2.0572 |
| 3 | 3o | 0.9952 | 10.12 | 4.73 | 5.69 | 0.4894 | 2.3594 |
| 4 | 1i | 1.0004 | 9.73 | 4.39 | 5.34 | 0.4705 | 2.3069 |
| 5 | 2i | 0.9926 | 5.97 | 4.58 | 3.23 | 0.2887 | 1.8019 |
| 6 | 3i | 1.0011 | 7.36 | 6.76 | 3.53 | 0.3559 | 1.9886 |
| 7 | 1i2 | 0.9687 | 9.43 | 6.16 | 5.45 | 0.456 | 2.2667 |
| 8 | 2i2 | 0.9703 | 3.46 | 6.51 | 0.79 | 0.3148 | 1.8744 |
| 9 | 3i2 | 0.9427 | 10.34 | 10.7 | 6.1 | 0.5174 | 2.4372 |
| 10 | 1s | 1.0004 | 9.73 | 4.39 | 5.34 | 0.4705 | 2.3069 |
| 11 | 2s | 0.9525 | 8.54 | 2.69 | 5.19 | 0.413 | 2.1472 |
| 12 | 3s | 0.9451 | 4.69 | 0.66 | 3.97 | 0.2268 | 1.63 |

Table 3.8.9 shows that "*3o*", "*3i2*", and "*1s*" are the critical imperfections causing the largest outside, inside and end brace forces. This demonstrates that the procedure to

determine the critical imperfection gives the consistent results with second-order analysis. Table 3.8.9 also indicates that the imperfection "*1o*", "*1i*", and "*1s*" give the same results. Actually, these imperfections are identical with the exception of a rigid body motion. The maximum of the brace point displacement amplification is 2.44 shown in Table 3.8.9. By using the relative displacement, this amplification is within the acceptable level. The responses at the maximum load for imperfection "*1o*" and "*3i2*" are plotted in Fig. 3.8.4.6.

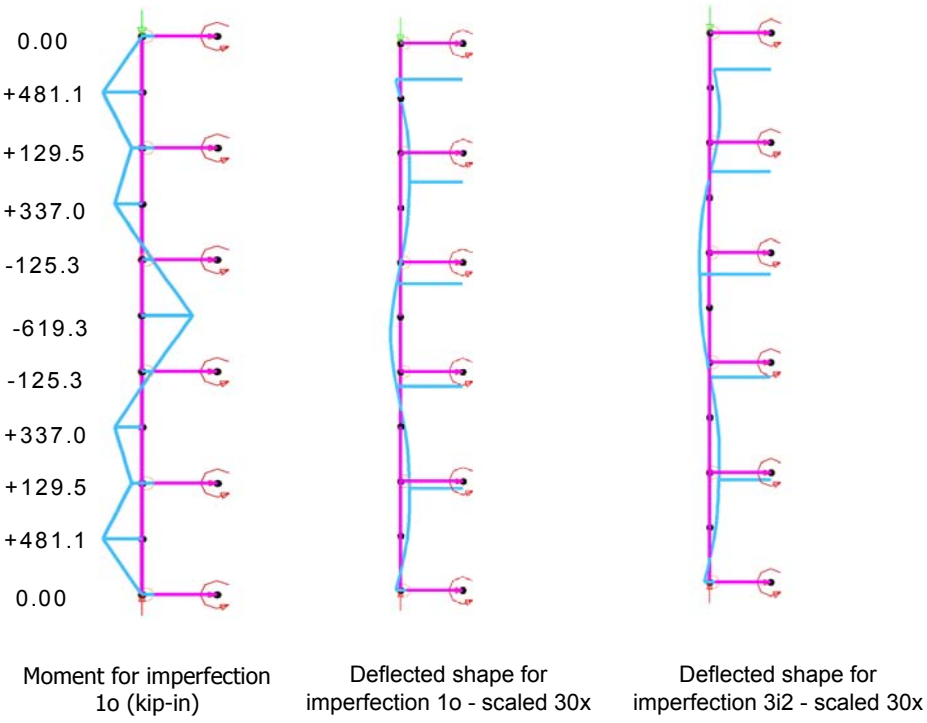


**Fig. 3.8.3.6. Responses at the maximum load, case 2 – DM.**

3.8.3.2 DP Solution

Based on the results from the DM solution, the critical imperfection "*1o*" or "*1i*" = "*1s*" shown in Fig. 3.8.3.7 causing the smallest column axial resistance is selected for a single DP solution.

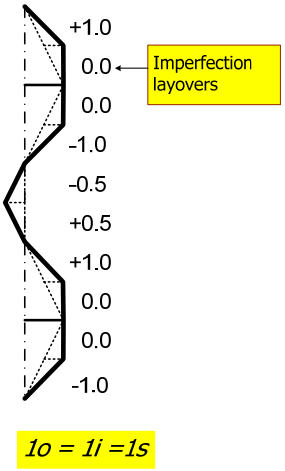


**Fig. 3.8.3.7. Critical imperfections for the DP solution, case 2 – DP.**

The results from the DP are plotted from Figs. 3.8.3.8 to 3.8.3.11. The maximum column capacity is equal to 955.2 kips shown in Fig. 3.8.3.8. The maximum brace force for outside, inside, and end braces is respectively 19.4 kips, 9.8 kips, and 9.5 kips. The smaller column capacity and larger brace forces from the DP Solution comparing to the DM Solution are consistent with the previous section.

The diagrams of moment, equivalent area $A_{eq}$, equivalent elastic section modulus $Q_{eq}$, and the equivalent of moment inertia $I_{eq}$ along the member length at the maximum load due to the spread of plasticity are displayed in Figs. 3.8.3.10 and 3.8.3.11.

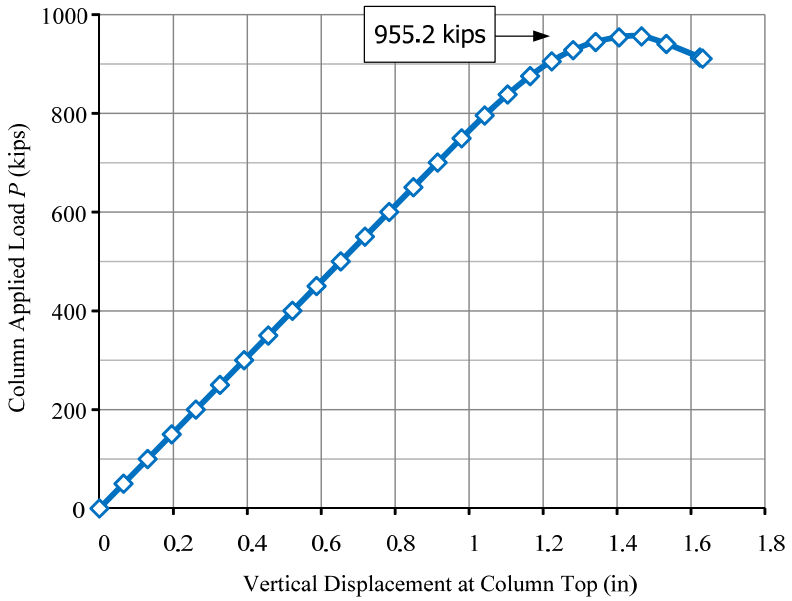


**Fig. 3.8.3.8. Trace for load vs. displacement, case 2 – DP.**

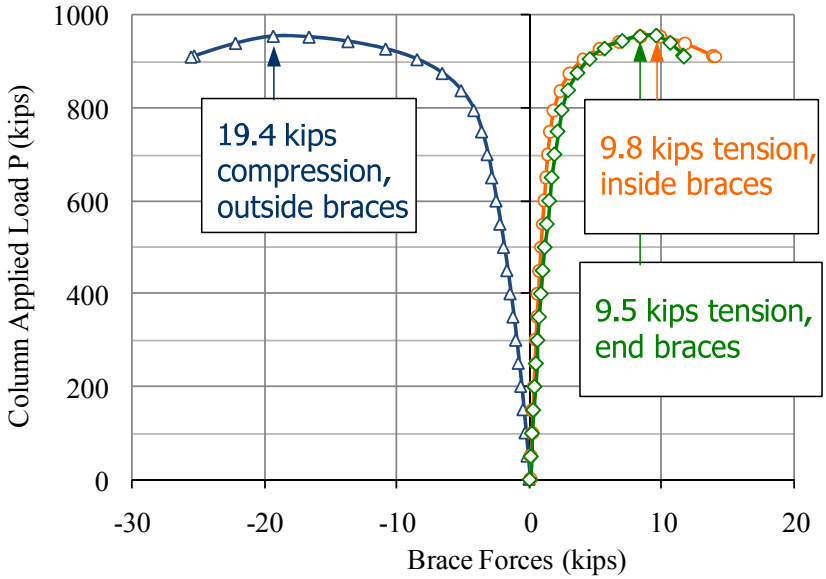


**Fig. 3.8.3.9. Trace for load vs. brace forces, case 2 – DP.**

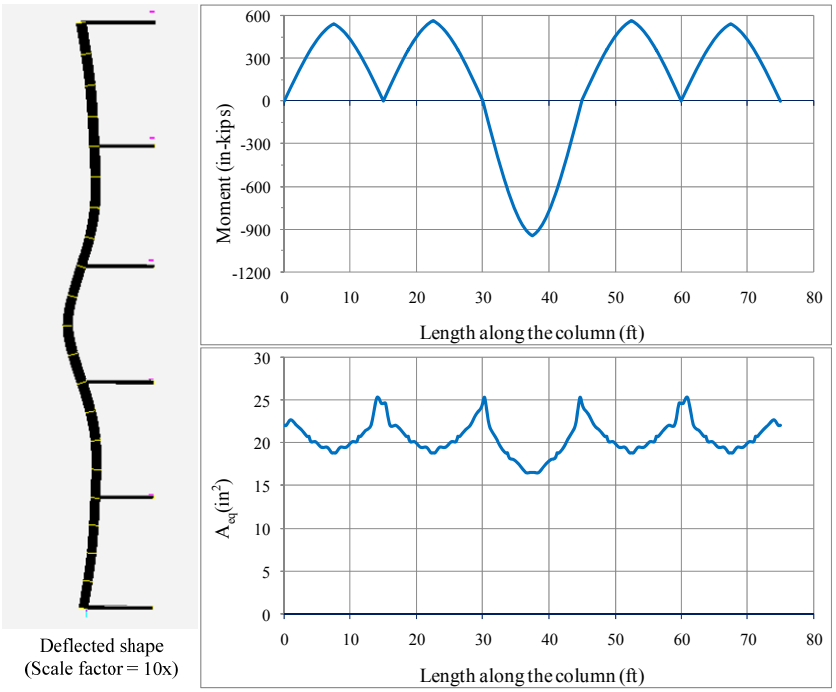


**Fig. 3.8.3.10. Response at the maximum load (1), case 2 – DP.**

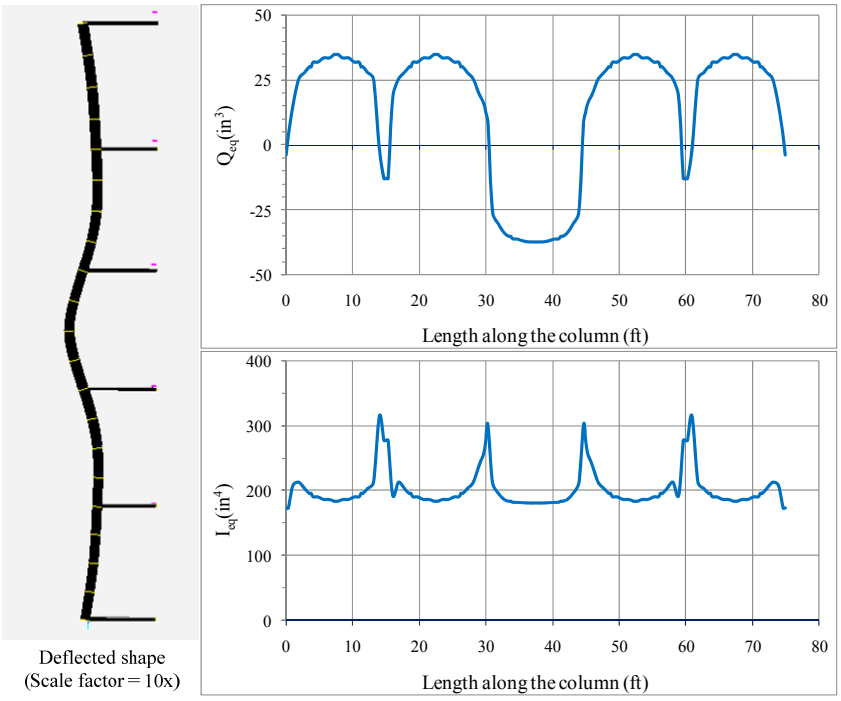


**Fig. 3.8.3.11. Response at the maximum load (2), case 2 – DP.**

3.8.3.3 Summary

The brace stiffness required to develop $P_u$ = 1000 kips (β = 25.85 kips/inch) appears to be about the same as that required for *UC* = 1.0 in the previous DM example of Section 3.5. For β = 25.85 kips/inch, the fundamental buckling mode and the deflected shape in governing DM solutions involves three half-waves. This is similar to the fundamental buckling modes and deflected shapes for β = 20 kips/inch in the DM example. However, there are significant displacements at the end brace points for this problem with β = 25.85 kips/inch.

### 3.8.4 Unequal Brace Spacing

Plaut (1993) has analytically solved the problem of a column with a single brace at any location. Also, Yura (1996) has solved this problem by using Winter's rigid bar model and found that Winter solution gave the identical results with Plaut (1993) only for the load level corresponding to an assumed Euler buckling load controlled by the longest segment.

In this section, two cases studies are considered. The first one focuses on the unequal brace spacing for the multiple intermediate nodal braces namely Case 3, while the second one considers the unequal brace spacing for a single intermediate brace namely Case 3b.

3.8.4.1 Case 3: Unequal Brace Spacing, Multiple Intermediate Nodal Braces

Fig. 3.8.4.1 shows a pinned-pinned W14x90 column with yield stress $F_y$ = 50 ksi with four intermediate nodal braces, equal brace stiffness β, unequally spaced braces. The unbraced length at the middle of column double the other ones, $2L_b$, and $L_b = L_{by}$ = 15 ft. The applied load *P* is equal to the design compressive strength, $\phi_c P_n$, from the longest

unbraced length, $P$ = 596 kips = $\phi_c P_n$ based on $KL_y$ = 30 ft. This problem is investigated by using the Direct Analysis and Distributed Plasticity Solutions.

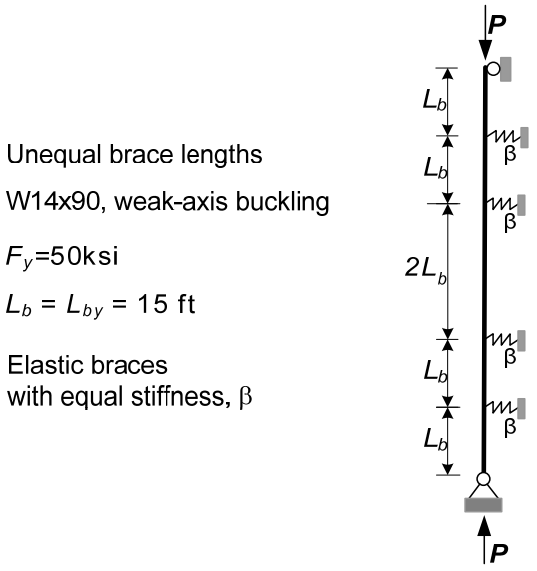


**Fig. 3.8.4.1. Unequal brace spacing – Case 3.**

*3.8.4.1.1 DM Solution*

The brace stiffness necessary to achieve $UC \leq 1.0$ and brace point displacement amplification approximately $\leq 4.0$ by using the DM is β = 3.8 kips/inch. With this braces stiffness, the buckling eigenvalues and mode shapes are displayed in Fig. 3.8.4.2. Based on these buckling modes, the procedure to determine the critical imperfection is performed in Figs. 3.8.4.3 and 3.8.4.4. Fig. 3.8.4.3 indicates the imperfection potentially causing the largest outside brace force while Fig. 3.8.4.4 shows the imperfection potentially causing the largest inside brace force.

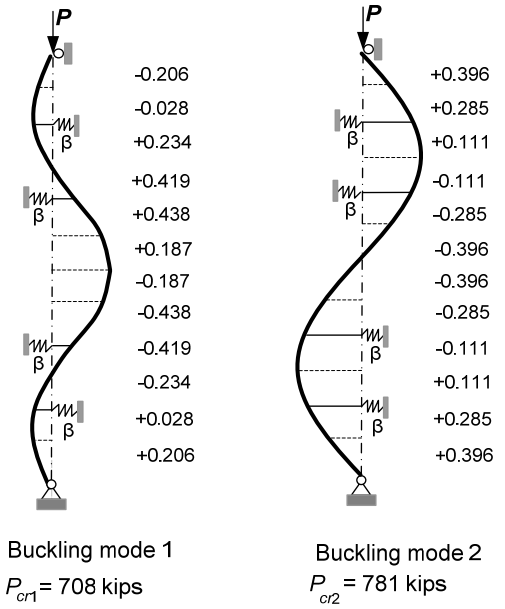


**Fig. 3.8.4.2. Buckling mode shapes, case 3 – DM.**

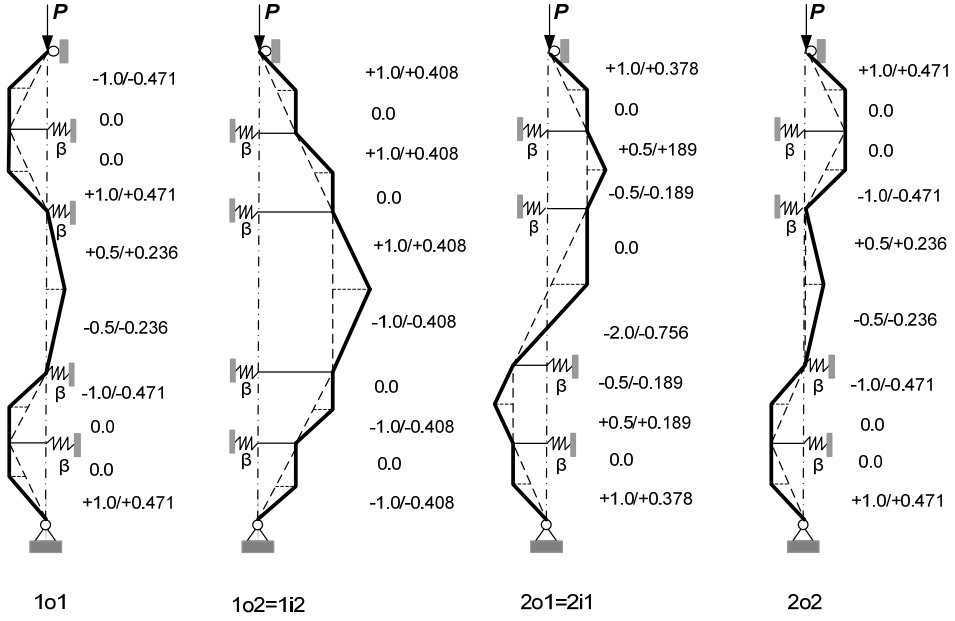


**Fig. 3.8.4.3. Geometric imperfections potentially causing the largest outside brace force, case 3 – DM.**

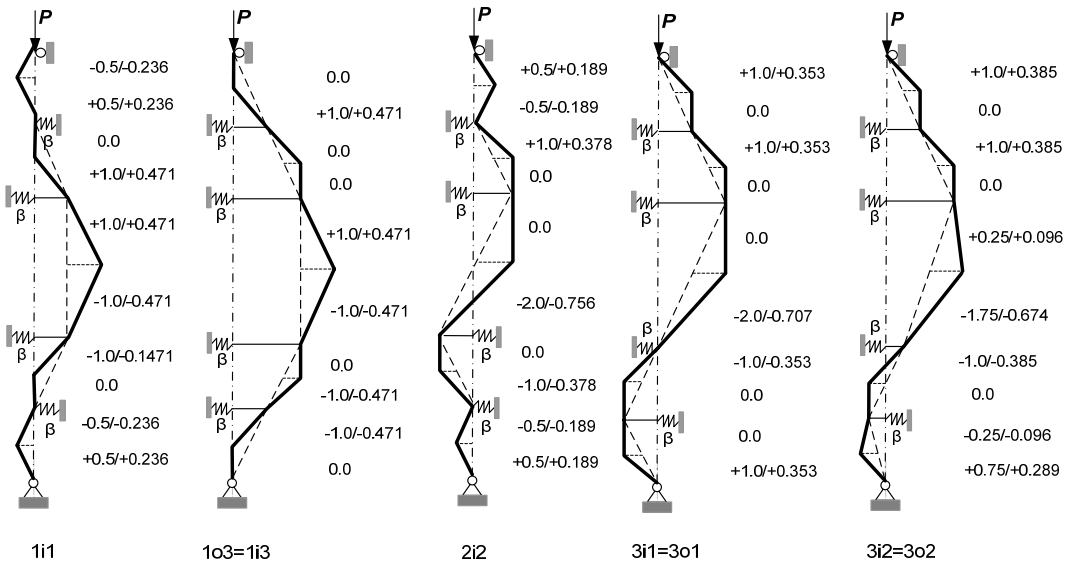


**Fig. 3.8.4.4. Geometric imperfections potentially causing the largest inside brace force, case 3 – DM.**

The results from the second-order analysis are shown in Table 3.8.10.

**Table 3.8.10. Results from the second-order analysis with β = 3.8 kips/inch and $P_u$ = 596 kips, case 3 – DM.**

| No | Imperfection | *UC* | $P_{out}$ (kips) | $P_{in}$ (kips) | $\Delta_b$ (in) | $(\Delta_b+\Delta_{bo})/\Delta_{bo}$ |
|---|---|---|---|---|---|---|
| 1 | 1o1 | 0.8473 | 2.79 | 3.43 | 1.1283 | 2.56 |
| 2 | 1o2=1i2 | 0.6521 | 0.33 | 2.9 | 0.9539 | 2.32 |
| 3 | 2o1=2i1 | 0.6984 | 4.59 | 5.13 | 1.6875 | 3.34 |
| 4 | 2o2 | 0.6509 | 3.37 | 3.23 | 1.1086 | 2.54 |
| 5 | 1i1 | 0.8131 | 1.86 | 3.76 | 1.2368 | 2.71 |
| 6 | 1o3=1i3 | 0.7045 | 0.32 | 3.53 | 1.1612 | 2.61 |
| 7 | 2i2 | 0.6509 | 2.7 | 3.89 | 1.2796 | 2.77 |
| 8 | 3i1=3o1 | 0.754 | 5.21 | 6.94 | 2.2829 | 4.17 |
| 9 | 3i2=3o2 | 0.7069 | 4.03 | 5.91 | 1.9441 | 3.70 |

Table 3.8.10 shows that the imperfection "*1o1*" gives the largest beam-column unity check of 0.85 at $P_u$ = 596 kips and the imperfection "*3i1=3o1*" causes the maximum "outer" and "inner" brace force with $P_{out}$ = 5.21 kips, and $P_{in}$ = 6.94 kips. The maximum brace point displacement amplification is slightly larger than 4. The responses at the maximum load for imperfection "1o" and "*3i1=3o1*" are plotted in Fig. 3.8.4.5.

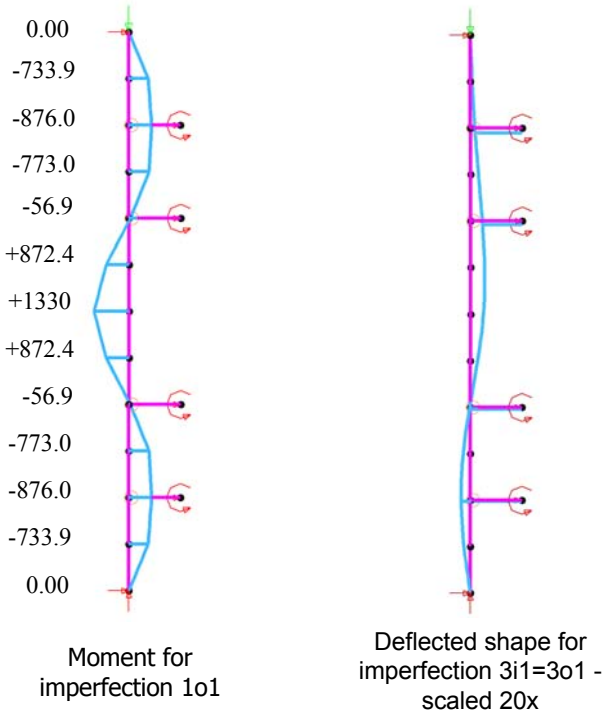


**Fig. 3.8.4.5. Responses at the maximum load, case 3 – DM.**

*3.8.4.1.2 DP Solution*

From the DM results, the imperfection "*3i1=3o1*" that causes the largest outside and inside brace forces is applied in the DP solution as shown in Fig. 3.8.4.6.

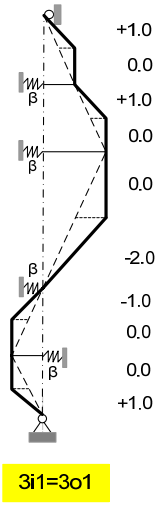


**Fig. 3.8.4.6. Critical imperfection - Case 3 – DP.**

The results from the DP are plotted from Figs. 3.8.4.7 to 3.8.4.10. Fig. 3.8.4.7 shows that the maximum column capacity is equal to 596 kip the same as the DM solution. The maximum outside brace force is 4.6 kips and the maximum inside brace force is 5.4 kips as shown in Fig. 3.8.4.8. The column capacity and brace forces from the DP Solution are slightly smaller than those from the DM since in this case the column still work in the elastic ranges.

The diagrams of moment, equivalent area $A_{eq}$, equivalent elastic section modulus $Q_{eq}$, and the equivalent of moment inertia $I_{eq}$ along the member length at the maximum load due to the spread of plasticity are displayed in Figs. 3.8.4.9 and 3.8.4.10.

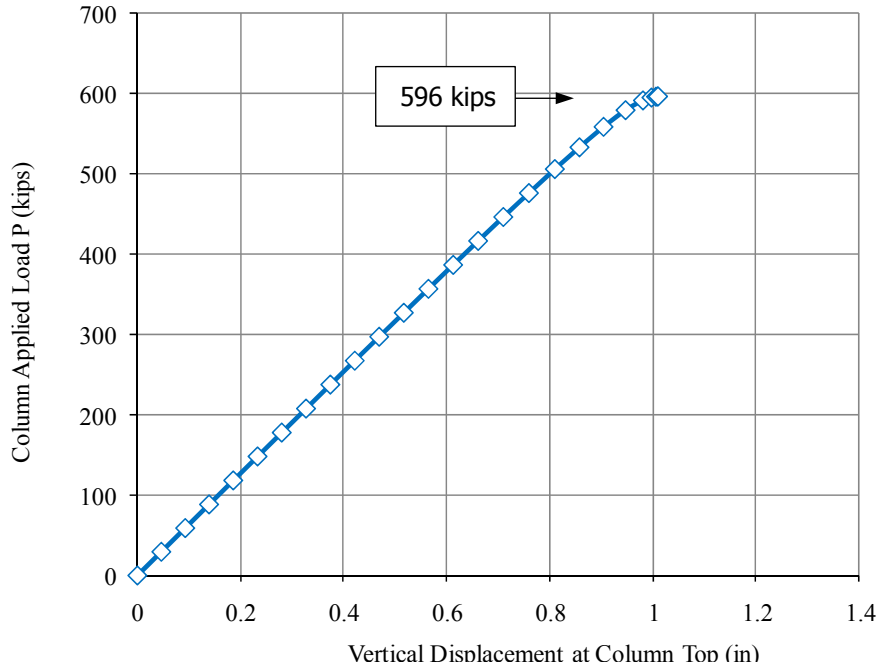


**Fig. 3.8.4.7. Trace for load vs. displacement, case 3 – DP.**

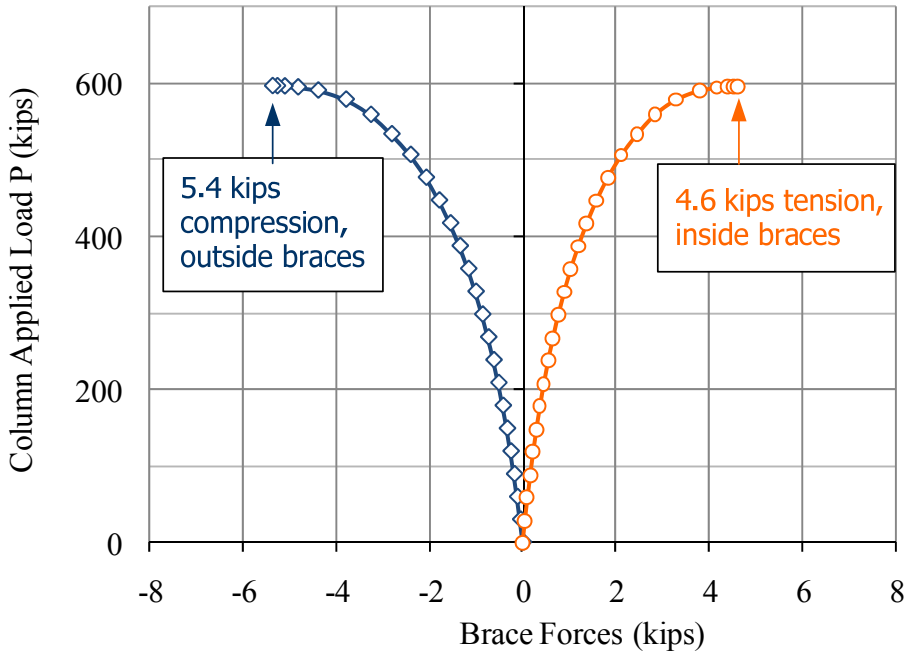


**Fig. 3.8.4.8. Trace for load vs. brace forces, case 3 – DP.**

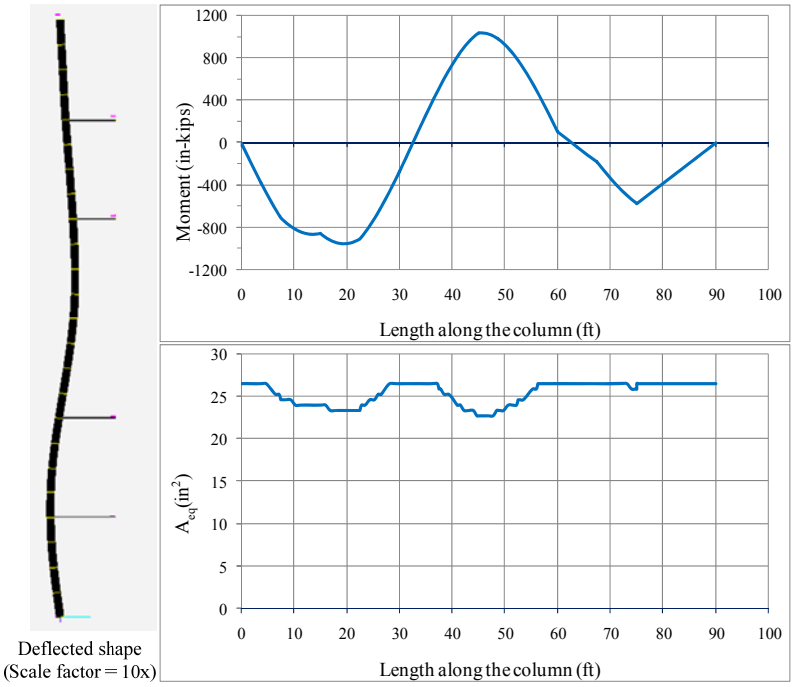


**Fig. 3.8.4.9. Response at the maximum load (1), case 3 – DP.**

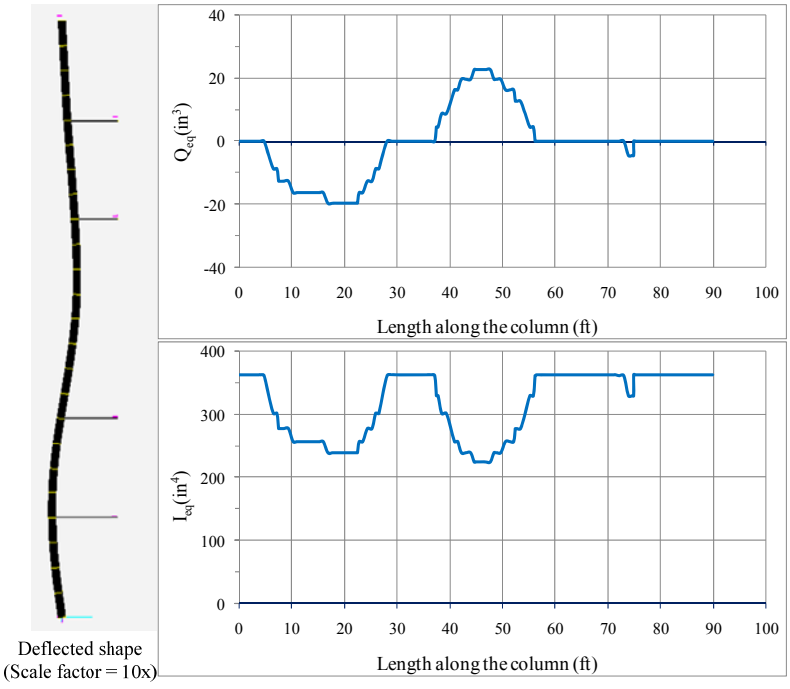


**Fig. 3.8.4.10. Response at the maximum load (2), case 3 – DP.**

*3.8.4.1.3 Summary*

The brace stiffness, β = 3.8 kips/inch, is sufficient to reduce the brace point displacement amplification to approximately 4.0 at $P_u = \phi_c P_n$ = 596 kips ($KL_y$ = 30 ft). However, the unity check is much smaller than 1.0 in this case. At this brace stiffness, significant displacements occur at brace point(s) adjacent to the longer unbraced length. There is no avoiding this unless β is made very large. The applied load $P_u \leq \phi_c P_n$ based on $KL = L_b$ of the longest segment is recommended for the design of columns with unequal unbraced lengths. The recommended β = 3.8 kips/inch, determined using the DM, is substantially smaller than any stiffness value that might be estimated by an ad hoc application of the AISC Appendix 6 equations. The AISC Appendix 6 does not apply to cases with unequal brace spacing. Further discussion about unequal brace spacing by investigating the simply supported column with only one internal brace with unequal unbraced lengths is studied in Section 3.8.4.2.

3.8.4.2 Case 3b: Unequal Brace Spacing, Single Intermediate Nodal Brace

Fig. 3.8.4.11 shows an unequal brace spacing for the column with a single intermediate brace. The W14x90 column, weak-axis flexural buckling with $F_y$ = 50ksi is used in the analysis. The brace stiffness is β. The longer unbraced length is $L_b$ = 555 inches and the shorter unbraced length is $L_b/3$ = 185 inches. The applied load $P$ is equal to 0.8 Euler buckling load for the longer segment, $P_u = 0.8P_{eL} = 0.8(\pi^2 EI/L_b^2) = 269.1$ kips.

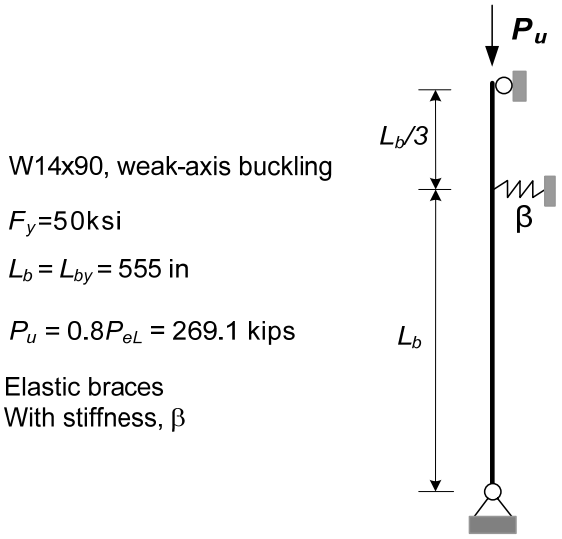


**Fig. 3.8.2.11. Pinned-pinned column with unequal brace spacing, single intermediate nodal brace, case 3b.**

Using the Direct Analysis Method and Distributed Plasticity Method assess the brace stiffness and strength requirements for both pinned model (Winter's model) and the physical continuous model. The organization of this section is as follows. The brace stiffness corresponding to the Euler buckling load for the longer unbraced length is presented in Section 3.8.4.2.1. Then the brace forces based on these brace stiffnesses from the Direct Analysis Method and Distributed Plasticity Method are summarized in Sections 3.8.4.2 and 3.8.4.3 respectively.

*3.8.4.2.1 Brace Stiffness corresponding to the Euler Buckling Load for the Longer Segment*

The minimum brace stiffness required to develop $P_u = 0.8P_{eL}$ in the pinned model is the same as that in the continuous models. These brace stiffnesses are determined as

$$\beta_{iP} = \beta_{iC} = 2.424 \text{kip/inch}$$

This brace stiffness is consistent with the previous results studied by Winter (1958), and Yura (1996). However, the brace force requirements in the pinned and continuous

models have not been discussed in the previous works. The differences of brace forces in pinned and continuous models are presented in Section 3.8.4.2.2.

*3.8.4.2.2 DM Solution: Brace Force corresponding to the Brace stiffness to develop the Euler Buckling Load for the Longer Segment*

According to the previous discussion of geometric imperfections, two imperfections shown in Fig. 3.8.4.12 are used in the DM analysis for this problem.

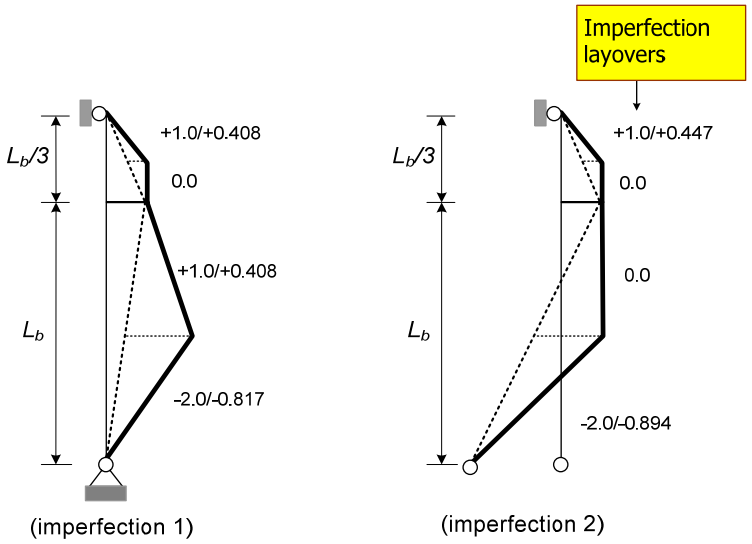


**Fig. 3.8.4.12. Critical imperfections – Case 3b.**

In Fig. 3.8.4.12, notation "+1.0" in the vectors of imperfection layovers corresponds to 1.0($L_b$/1500).

The brace forces for the pinned and continuous models corresponding to the imperfections 1 and 2 are summarized as follows.

**a) For the Pinned Model**

Brace stiffness used in the analysis is

$$\beta_P = 2\frac{\beta_{iP}}{\phi} = 2\frac{2.424}{0.75} = 6.465 \text{ kip/inch}$$

Brace force from DM solution with imperfection 1 is

$P_{br}$ = 1.15 kips corresponding to Unity Check, $UC$ = 3.82

Brace force from DM solution with imperfection 2 is

$P_{br}$ = 1.74 kips corresponding to Unity Check, $UC$ = 3.82

**b) For the continuous model**

Brace stiffness used in the analysis is the same as brace stiffness used in the pinned model.

$$\beta_C = 2\frac{\beta_{iC}}{\phi} = \beta_P = 6.465 \text{ kip/inch}$$

Brace force from DM solution with imperfection 1 is

$P_{br}$ = 3.24 kips corresponding to Unity Check, $UC$ = 0.336

Brace force from DM solution with imperfection 2 is

$P_{br}$ = 3.81 kips corresponding to Unity Check, $UC$ = 0.346

From the above results, one can observe that the pinned model gives the bracing stiffness to develop the Euler buckling load for the longer segment the same as for the continuous model. However, the brace force in the continuous model is mostly larger two times than the brace force in the pinned model.

*3.8.4.2.3 DP Solution: Brace Force corresponding to the Brace stiffness to develop the Euler Buckling Load for the Longer Segment*

Based on the results from the DM solution, the only continuous model with the geometric imperfection 2 shown in Fig. 3.8.4.12 is investigated in this section. The results are summarized from Figs. 3.8.4.13 to 3.8.4.16.

Fig. 3.8.4.13 shows that the maximum column capacity is equal to 269.1 kip the same as the DM solution. The maximum brace force is 3.3 kips as shown in Fig. 3.8.4.14.

The diagrams of moment, equivalent area $A_{eq}$, equivalent elastic section modulus $Q_{eq}$, and the equivalent of moment inertia $I_{eq}$ along the member length at the maximum load due to the spread of plasticity are displayed in Figs. 3.8.4.15 and 3.8.4.16.

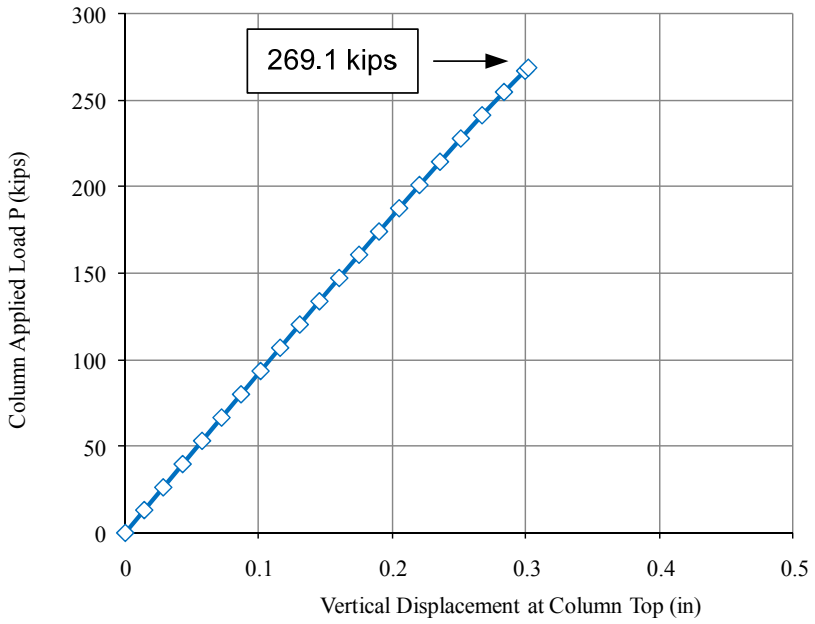


**Fig. 3.8.4.13. Trace for load vs. displacement, Case 3b – DP.**

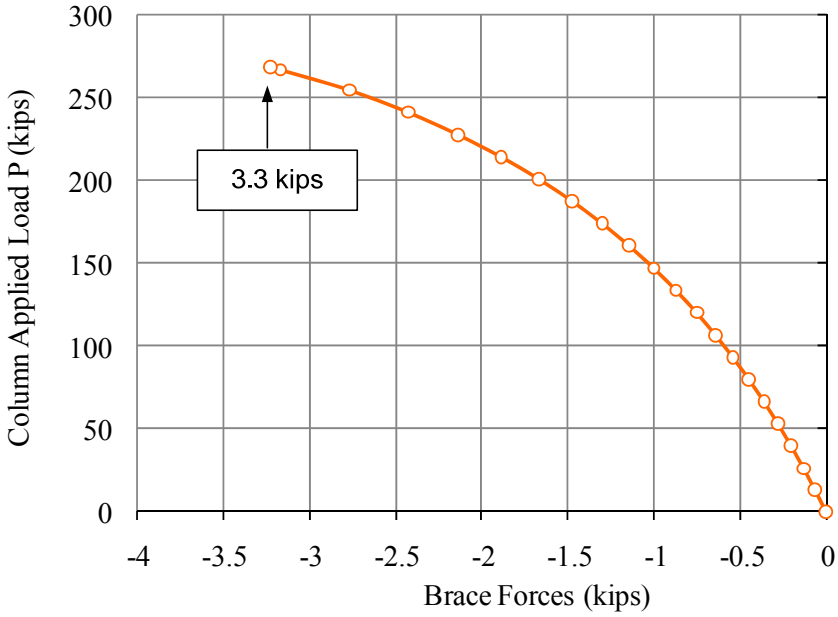


**Fig. 3.8.4.14. Trace for load vs. brace forces, case 3b – DP.**

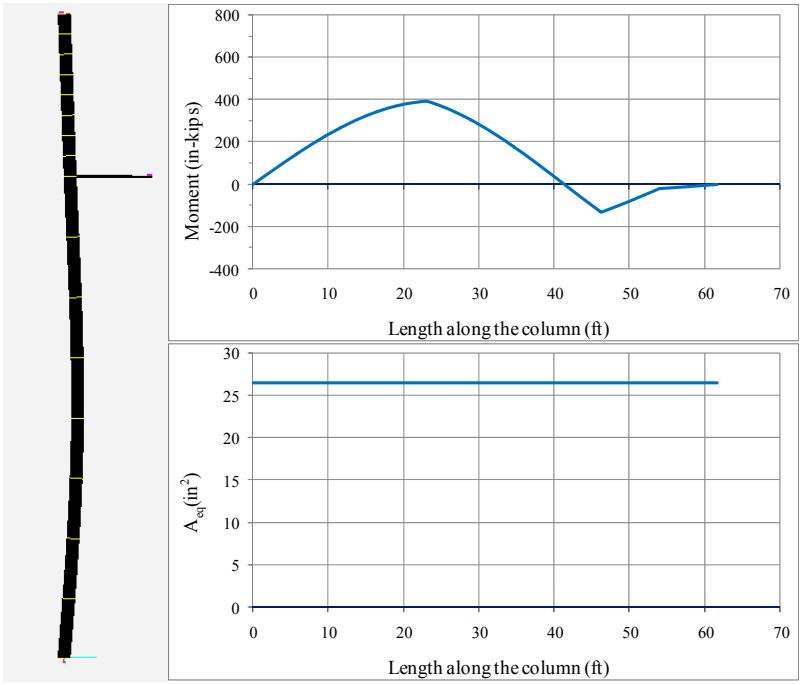


**Fig. 3.8.4.15. Response at the maximum load (1), case 3b – DP.**

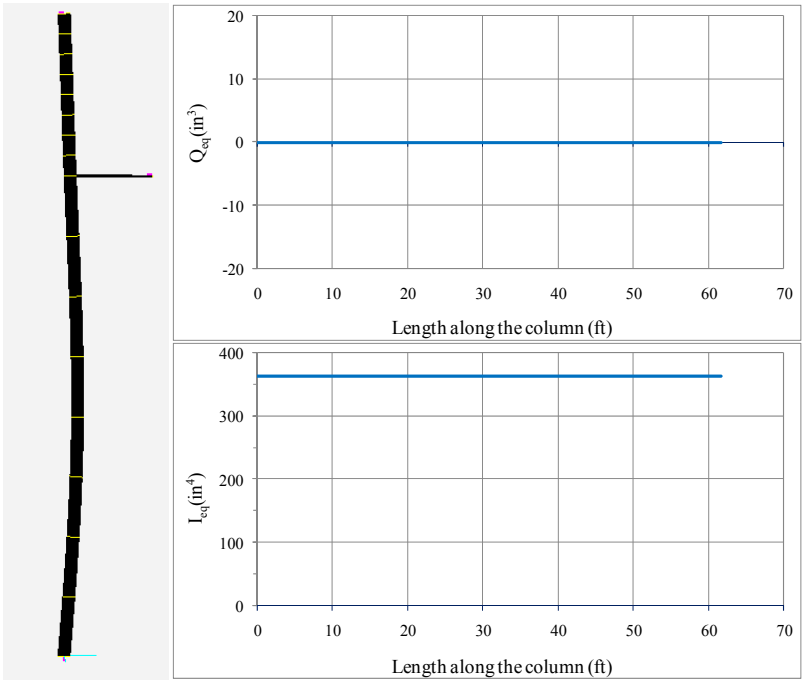


**Fig. 3.8.4.16. Response at the maximum load (2), case 3b – DP.**

### 3.8.5 Case 4: Non-constant Axial Force

Fig. 3.8.5.1 shows the structural layout the same as in Section 3.8.1. The description of the problem is repeated here: a pinned-pinned column with four intermediate nodal braces, equal unbraced lengths $L_b = L_{by} = 15$ ft, and equal brace stiffness, β, wide flange W14x90 with yield stress $F_y = 50$ ksi. However, in this problem the column is subjected non-constant axial force with $P = 1000$ kips.

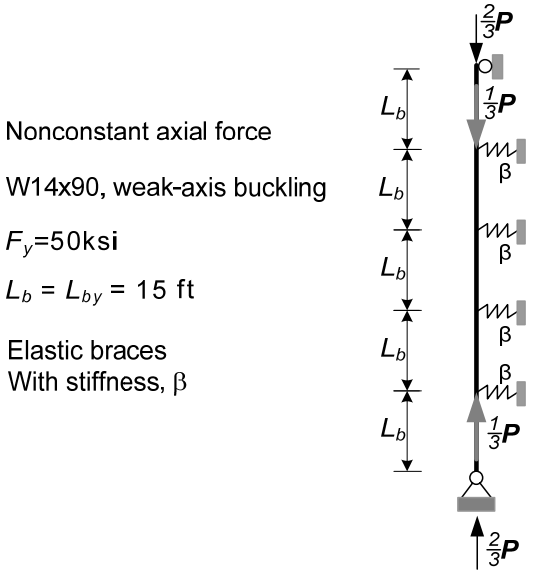


**Fig. 3.8.5.1. Non-constant axial force, case 4.**

The brace stiffness necessary to achieve $UC \leq 1.0$ and brace point displacement amplification approximately $\leq 4.0$ and corresponding brace forces are determined by the DM and DP solutions as follows.

3.8.5.1 DM Solution

Using the trial and error approach and the DM procedure, the brace stiffness necessary to achieve $UC \leq 1.0$ and brace point displacement amplification approximately

$\leq 4.0$ is $\beta = 19.5$ kips/inch. The buckling eigenvalues and mode shapes are plotted in Fig. 3.8.5.2.

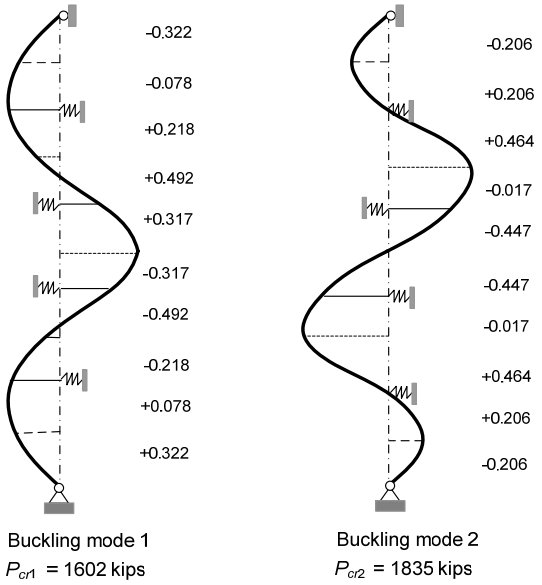


**Fig. 3.8.5.2. Buckling mode shapes, case 4 – DM.**

Based on the buckling mode shapes in Fig. 3.8.5.2, the geometric imperfections tend to become the critical imperfection are displayed in Figs. 3.8.5.3 and 3.8.5.4. As noted above, all notations are defined in Section 3.5. Fig. 3.8.5.3 indicates the imperfection potentially causing the largest outside brace force and Fig. 3.8.5.4 shows the imperfection potentially causing the largest inside brace force.

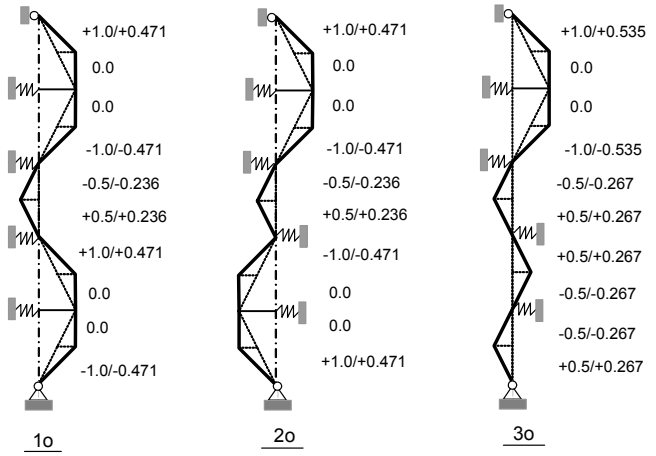


**Fig. 3.8.5.3. Geometric imperfections potentially causing the largest outside Brace force, case 4 – DM.**

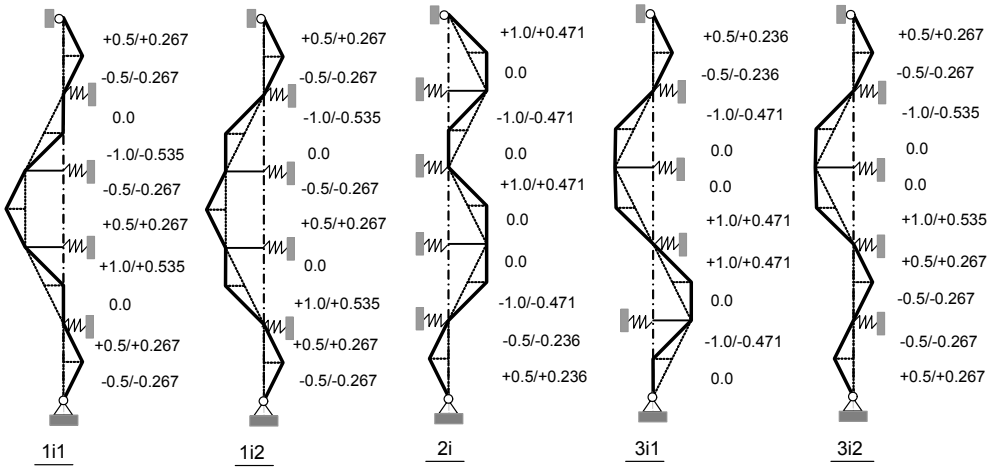


**Fig. 3.8.5.4. Geometric imperfections potentially causing the largest inside brace force, case 4 – DM.**

Table 3.8.11 is summarized the results from the second-order analysis. This table shows that the imperfection "*1o*" gives the maximum outside brace force, $P_{out}$ = 5.98 kips and the imperfection "*3i1*" causes the maximum inside brace force, $P_{in}$ = 6.66 kips. Also, the imperfection "*1o*" gives the largest beam-column unity check of 1.0 at $P_u$ = 1000 kips. The maximum amplification factor is of 2.19 corresponding to the

imperfection "*3i1*". The responses at the maximum load for the imperfection "*1o*" and "*3i1*" are plotted in Fig. 3.8.5.5.

**Table 3.8.11 Results from the second-order analysis with β = 19.5 kips/inch and $P_u$ = 1000 kips, case 4 – DM.**

| No | Imperfection | *UC* | $P_{out}$ (kips) | $P_{in}$ (kips) | $\Delta_b$ (in) | $(\Delta_b+\Delta_{bo})/\Delta_{bo}$ |
|---|---|---|---|---|---|---|
| 1 | 1o | 1.0003 | 5.98 | 4.06 | 0.3833 | 2.06 |
| 2 | 2o | 0.9014 | 4.74 | 1.31 | 0.3038 | 1.84 |
| 3 | 3o | 0.9658 | 5.33 | 2.78 | 0.3417 | 1.95 |
| 4 | 2i | 0.9279 | 0.85 | 4.29 | 0.275 | 1.76 |
| 5 | 1i1 | 0.9839 | 4.54 | 3.98 | 0.291 | 1.81 |
| 6 | 1i2 | 0.9147 | 2.61 | 3.22 | 0.2064 | 1.57 |
| 7 | 3i1 | 0.9582 | 5.82 | 6.66 | 0.4269 | 2.19 |
| 8 | 3i2 | 0.9431 | 2.59 | 5.48 | 0.3513 | 1.98 |

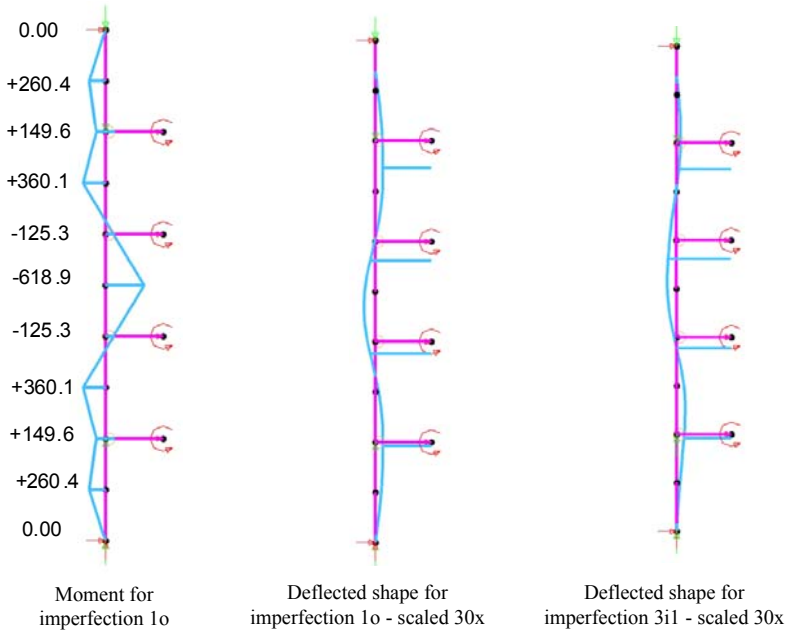


**Fig. 3.8.5.5. Responses at the maximum load, case 4 – DM.**

3.8.5.2 DP Solution

The critical imperfection "*1o*" from the DM solution is used to analyze in the DP solution shown in Fig. 3.8.5.6.

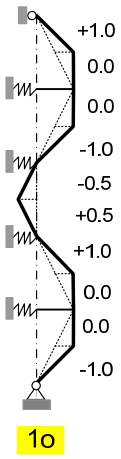


**Fig. 3.8.5.6. Critical imperfection, case 4 – DP.**

The results from the DP are shown in Figs. 3.8.5.7 to 3.8.3.11. Fig. 3.8.5.7 shows that the maximum column capacity is equal to 946.1 kips. The maximum brace force for outside and inside braces is respectively 12.3 kips and 8.6 kips as shown in Fig. 3.8.5.8.

The diagrams of moment, equivalent area $A_{eq}$, equivalent elastic section modulus $Q_{eq}$, and the equivalent of moment inertia $I_{eq}$ along the member length at the maximum load due to the spread of plasticity are displayed in Figs. 3.8.5.9 and 3.8.3.10.

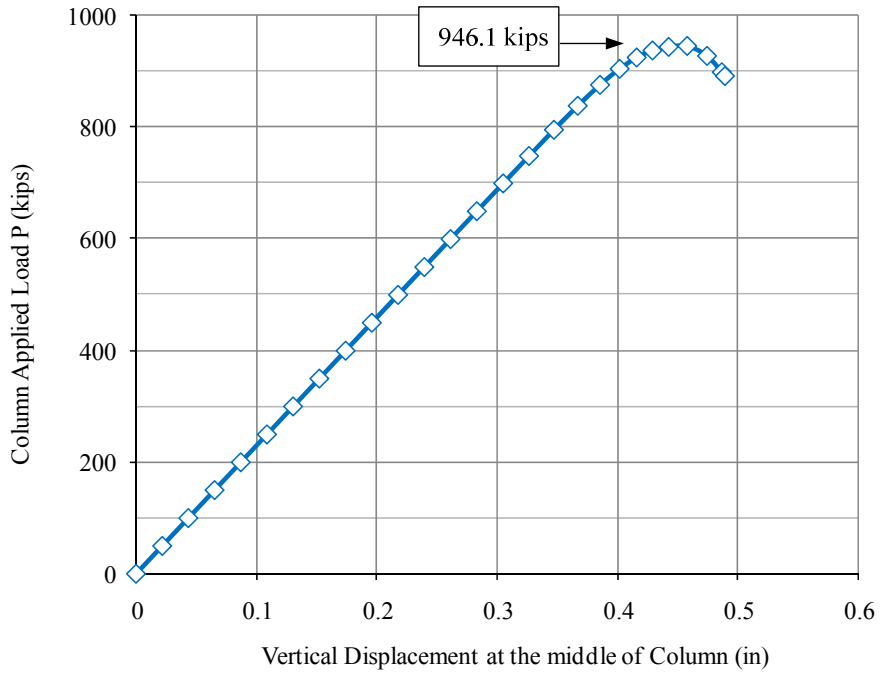


**Fig. 3.8.5.7. Trace for load vs. displacement, case 4 – DP.**

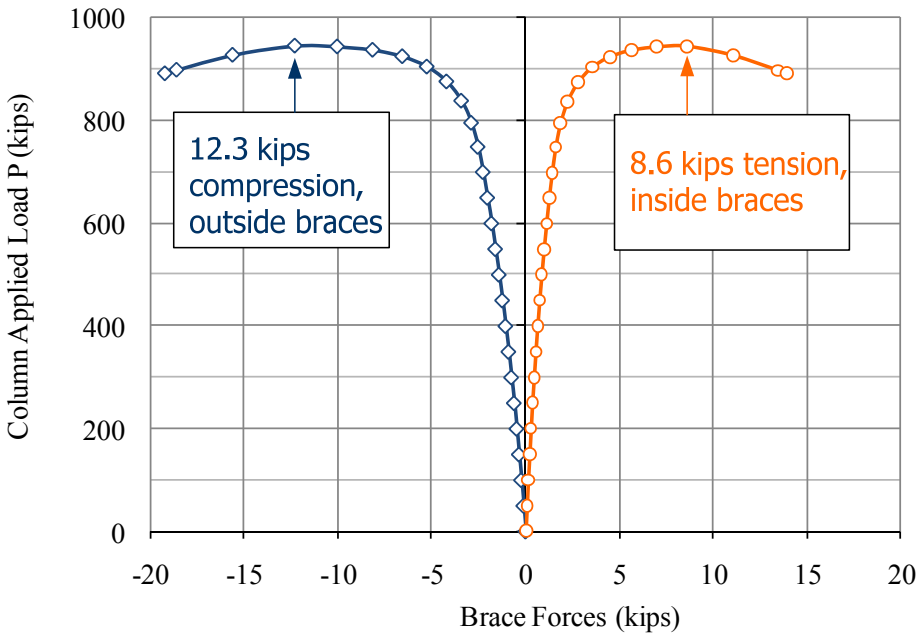


**Fig. 3.8.5.8. Trace for load vs. brace forces, case 4 – DP.**

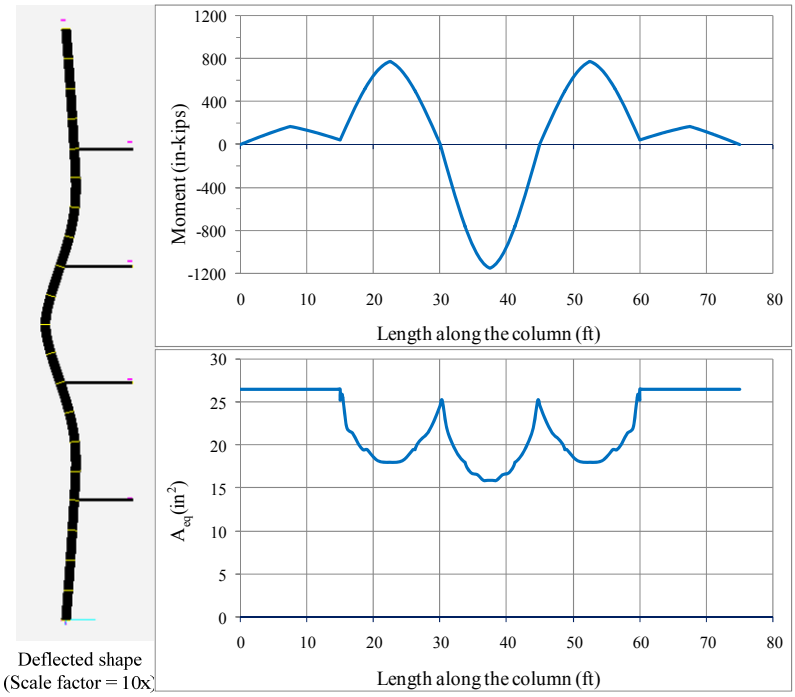


**Fig. 3.8.5.9. Response at the maximum load (1), case 4 – DP.**

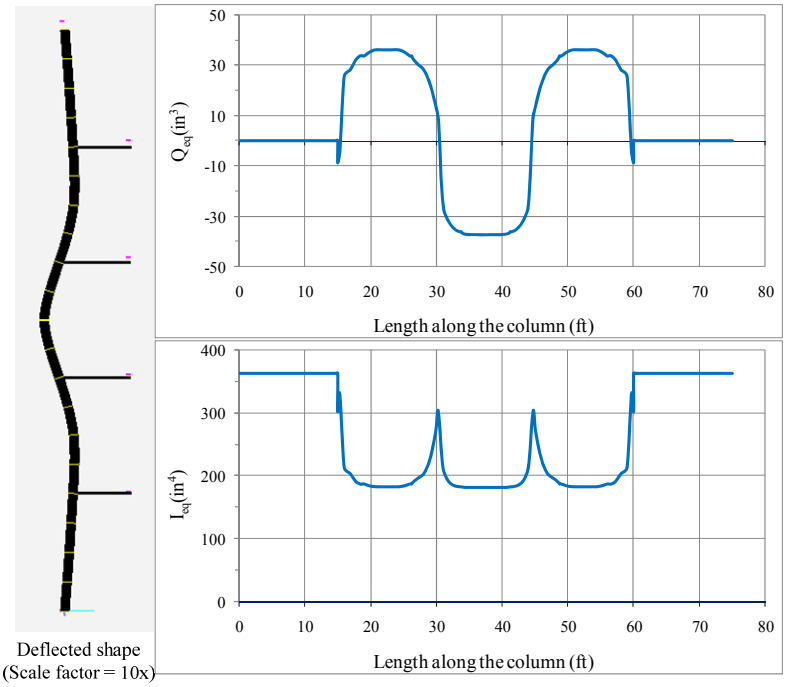


**Fig. 3.8.5.10. Response at the maximum load (2), case 4 – DP.**

3.8.5.3 Summary

The DM example in Section 3.4 and this problem are the same except that the applied load for this case is varied along the height of column. The required brace stiffness, β = 19.5 kips/inch, is similar to the brace stiffness from the DM example, β = 20 kips/inch. The brace forces from the DM example are smaller than brace force in this problem. Also, the largest amplification for the DM example is 2.54 for imperfection "*1o*" while the largest amplification for this problem is 2.19 for imperfection "*3i1*".

### 3.8.6 Case 5: Nonprismatic Geometry

Fig. 3.8.6.1 shows a pinned-pinned column subjected non-constant internal axial load with $P$ = 1000 kips. The column is comprised by stepped cross-section W14x74 ($\phi_c P_n$ = 667 kips) and W14x90 ($\phi_c P_n$ = 1000 kips) based on $KL_y$ = 15 ft with an equal brace stiffness β. The equally unbraced length is $L_b = L_{by}$ = 15 ft.

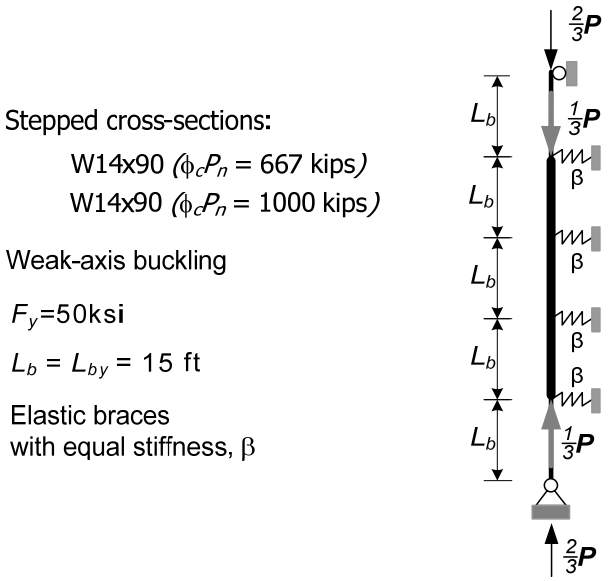


**Fig. 3.8.6.1 Stepped cross-section geometry, case 5.**

Using the DM and DP solutions to determine the brace stiffness necessary to achieve UC $\leq$ 1.0 and brace point displacement amplification approximately $\leq$ 4.0 and corresponding brace forces is presented below.

3.8.6.1 DM Solution

Similar to the above analyses, using the DM procedure the brace stiffness necessary to achieve *UC* $\leq$ 1.0 and brace point displacement amplification approximately $\leq$ 4.0 is $\beta$ = 18.54 kips/inch. With this brace stiffness, the buckling eigenvalues and mode shapes are plotted in Fig. 3.8.6.2.

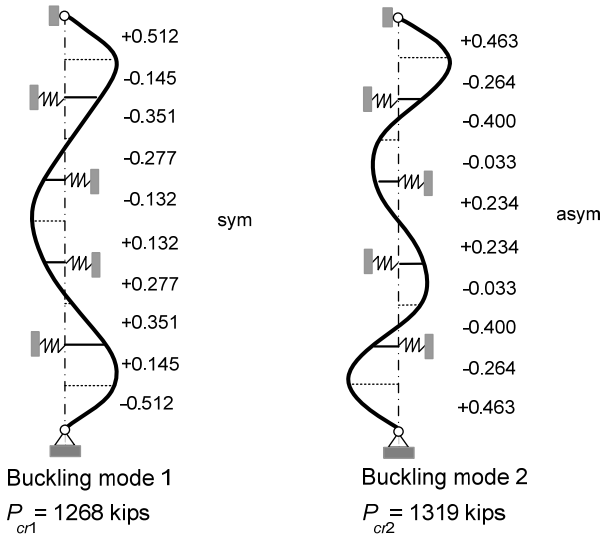


**Fig. 3.8.6.2. Buckling mode shapes, case 5 – DM.**

The geometric imperfections potentially causing the largest outside brace force are displayed in Fig. 3.8.6.3 and the geometric imperfections potentially causing the largest inside brace force are displayed in Fig. 3.8.6.4.

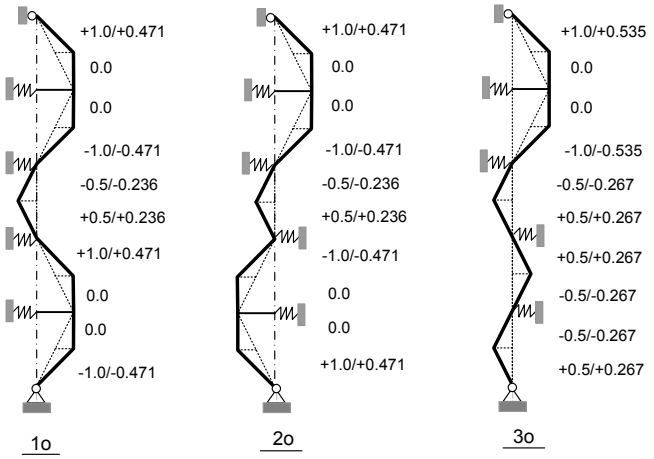


**Fig. 3.8.6.3. Geometric imperfection potentially causing the largest outside brace force, case 5 – DM.**

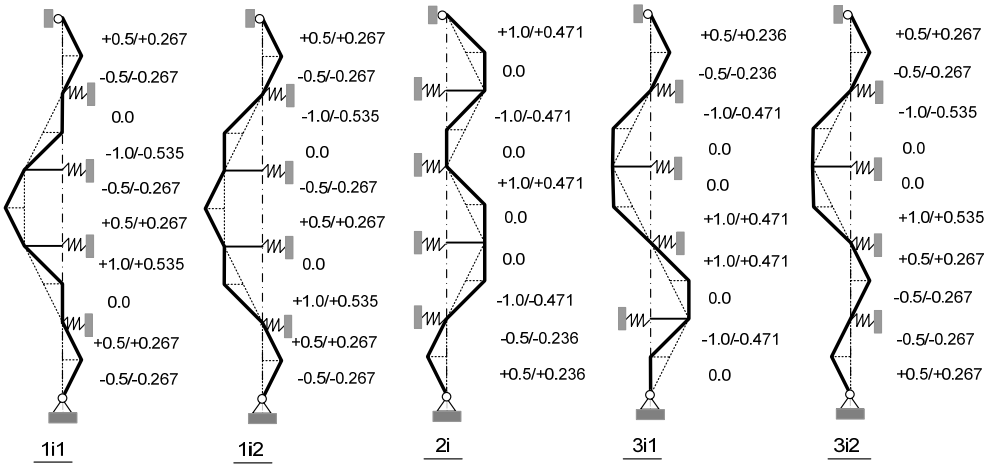


**Fig. 3.8.6.4. Geometric imperfection potentially causing the largest inside brace force, case 5 – DM.**

The results from second-order analysis are shown in Table 3.8.12. One can observe from this table that the imperfection "*1o*" gives the maximum outside brace force $P_{out}$ = 11.61 kips and the imperfection "*3i1*" gives the maximum inside brace force $P_{in}$ = 10.84 kips and maximum unity check. The maximum brace point displacement amplification is 3.6 corresponding to imperfection "*1o*". The responses at the maximum load for imperfection "*1o*" and "*3i1*" are plotted in Fig. 3.8.6.5.

**Table 3.8.12 Results from the second-order analysis with β = 18.54 kips/inch, case 5 – DM**

| No | Imperfection | $P_{u\_end}$ (kips) | $P_{u\_mid}$ (kips) | *UC* | $P_{out}$ (kips) | $P_{in}$ (kips) | $\Delta_b$ (in) | $(\Delta_b+\Delta_{bo})/\Delta_{bo}$ |
|---|---|---|---|---|---|---|---|---|
| 1 | 1o | 667 | 1000 | 0.9325 | 11.610 | 7.784 | 0.9363 | 3.60 |
| 2 | 2o | 667 | 1000 | 0.8527 | 7.308 | 1.684 | 0.5894 | 2.64 |
| 3 | 3o | 667 | 1000 | 0.8983 | 9.070 | 5.194 | 0.7315 | 3.03 |
| 4 | 2i | 667 | 1000 | 0.9645 | 5.175 | 6.996 | 0.5642 | 2.57 |
| 5 | 1i1 | 667 | 1000 | 0.8915 | 9.053 | 6.976 | 0.7301 | 3.03 |
| 6 | 1i2 | 667 | 1000 | 0.9561 | 9.030 | 7.326 | 0.7282 | 3.02 |
| 7 | 3i1 | 667 | 1000 | 1.0001 | 8.104 | 10.840 | 0.8742 | 3.43 |
| 8 | 3i2 | 667 | 1000 | 0.9748 | 6.548 | 8.920 | 0.7194 | 3.00 |

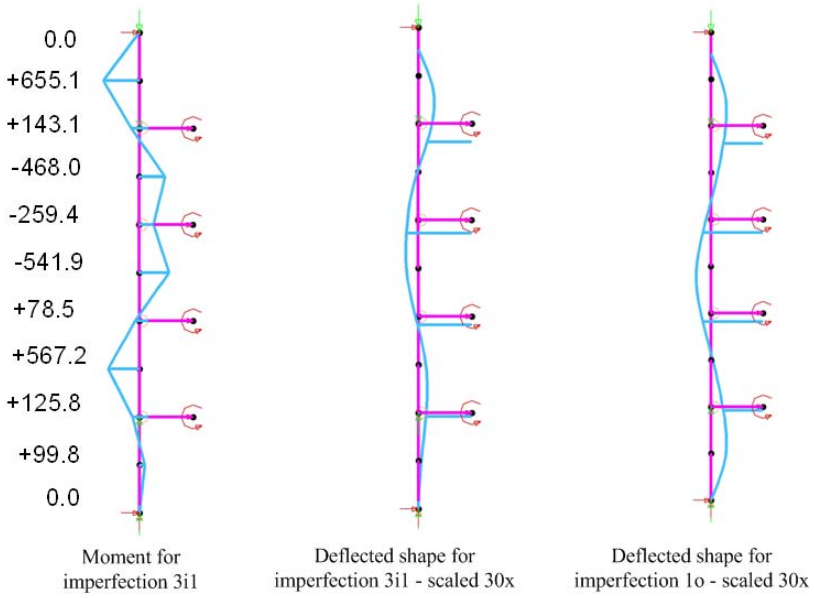


**Fig. 3.8.6.5. Responses at the maximum load, case 5 – DM.**

3.8.6.2 DP solution

From the DM results, the imperfection "*3i1*" as shown in Fig. 3.8.6.6 that causes the largest inside brace forces and the smallest column axial resistance is used in the DP solution.

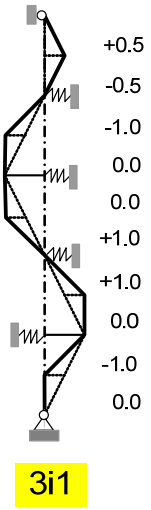


**Fig. 3.8.6.6 Critical imperfection, case 5 – DP.**

The results from the DP are plotted from Figs. 3.8.6.7 to 3.8.6.10. Fig. 3.8.6.7 shows that the maximum column capacity is equal to 894.6kips for cross-section W14x90 and equal to 596.4 kips for cross-section W14x74. The maximum outside brace force is 7.3 kips and inside brace force is 9.5 kips as shown in Fig. 3.8.6.8. The column capacity and brace forces from the DP Solution are slightly smaller than those from the DM.

The diagrams of moment, equivalent area $A_{eq}$, equivalent elastic section modulus $Q_{eq}$, and the equivalent of moment inertia $I_{eq}$ along the member length at the maximum load due to the spread of plasticity are displayed in Figs. 3.8.6.9 and 3.8.6.10.

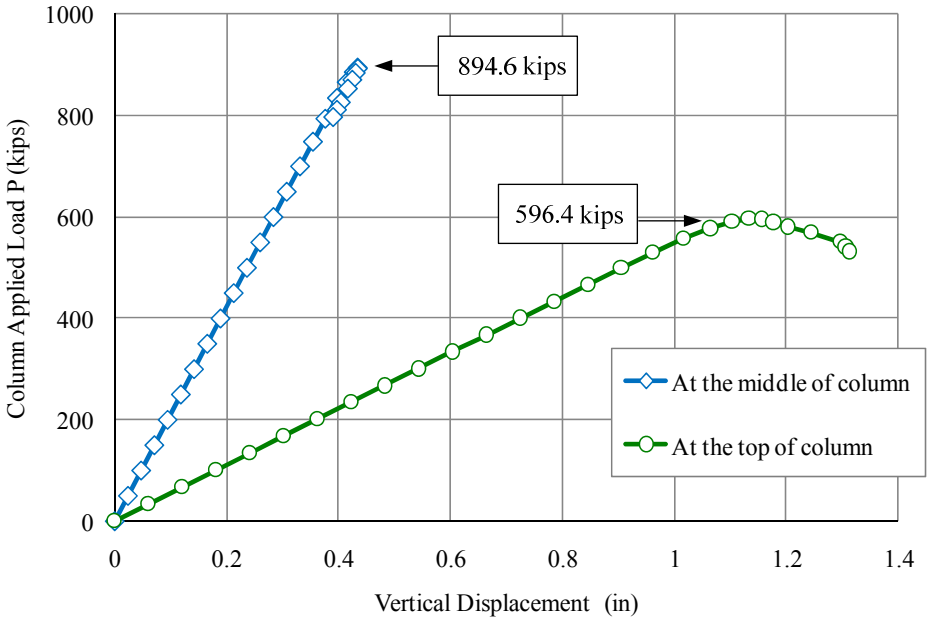


**Fig. 3.8.6.7. Trace for load vs. displacement, case 5 – DP.**

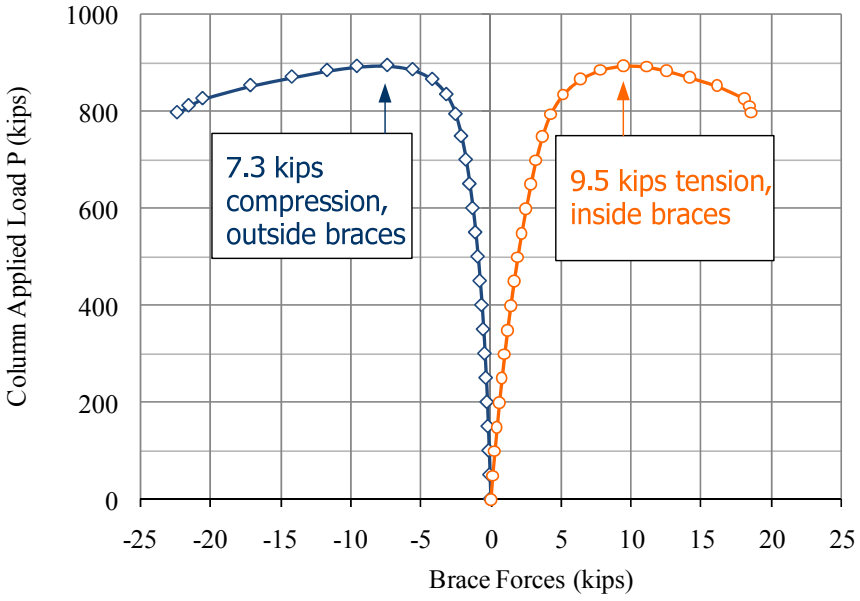


**Fig. 3.8.6.8. Trace for load vs. brace forces, case 5 – DP.**

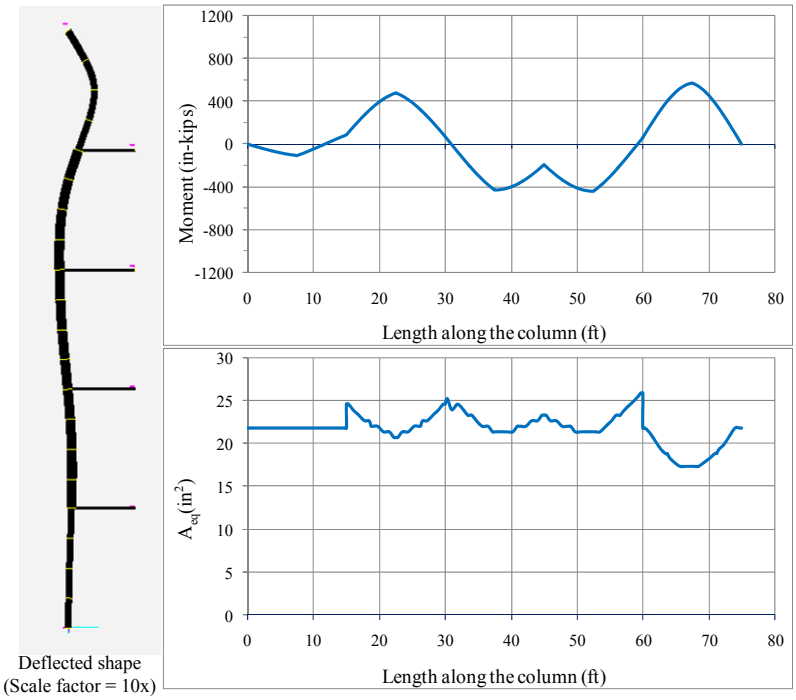


**Fig. 3.8.6.9. Response at the maximum load (1), case 5 – DP.**

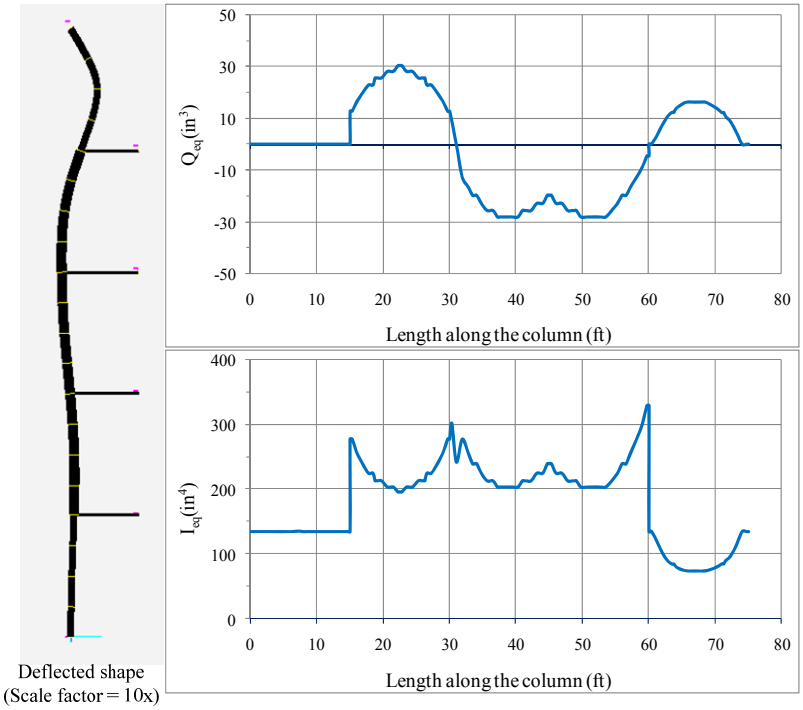


**Fig. 3.8.6.10. Response at the maximum load (2), case 5 – DP.**

3.8.6.3 Summary

The required brace stiffness for this case ($\beta$ = 18.54 kips/inch) is similar to that of case 5 in Section 3.8.5 ($\beta$ = 19.54kips/inch). The end unbraced segment (W14x74) is the critical one. Interestingly, the required brace stiffness from the DM Solution for three case studies: DM example in Section 3.5, Non-constant Axial Force in Section 3.8.5 and Nonprismatic Geometry in this Section are very close. These brace stiffnesses are almost equal to ideal brace stiffness $\beta_i$ calculated from the AISC Appendix 6 and brace forces corresponding these brace stiffnesses are within 2% of applied load.

### 3.8.7 Hybrid Bracing

The column bracing discussed so far was the nodal bracing with wide-ranging considerations. To understand the beam or beam-column bracing as well as the complete framing systems, the combination of relative bracing with nodal bracing or/and lean-on bracing system is effective to study. Fig. 3.2.3 is repeated here as shown in Fig. 3.8.7.1. Figure 3.8.7.1(c) shows the truss system under the concentrated load applied at the joints. For this system, the top chord is in compression with non-constant axial forces and tends to buckle laterally. The lateral braces are required for this chord to increase the strength of the system. This phenomenon is similar to the behavior of a simply supported beam under positive moment that will study in Chapter 4. In this section, problem H1 and H2 illustrated in Fig. 3.8.7.1 (a) and (b) are discussed based on the Direct Analysis and Distributed Plasticity Solutions.

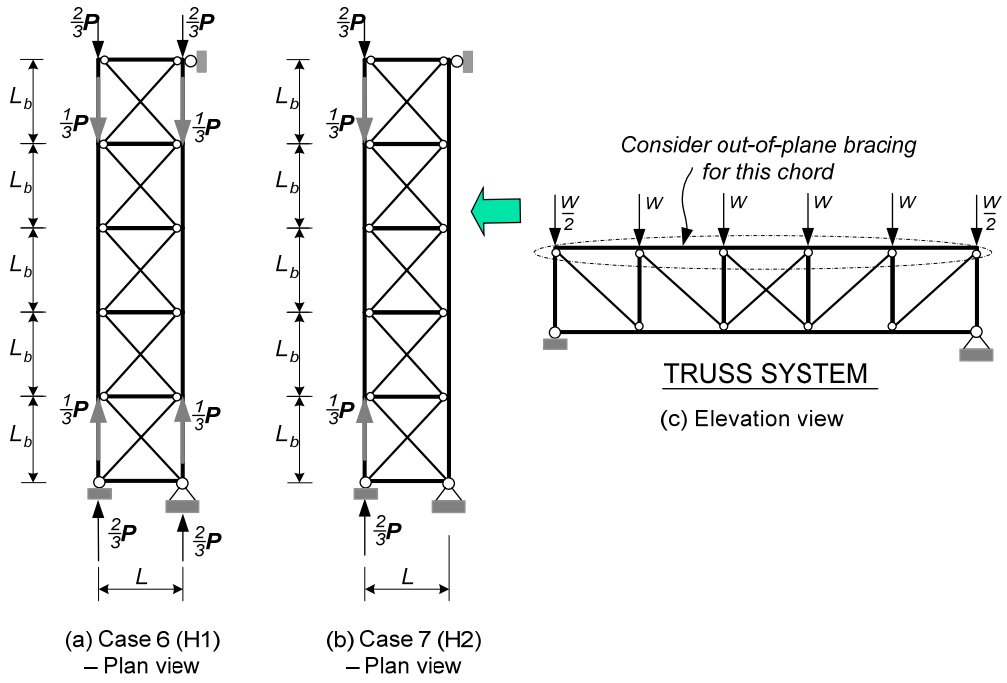


**Fig 3.8.7.1. Hybrid bracing.**

Shown in Figs 3.8.7.1 (a) and (b) are two chords braced with truss system, W14x90 with $F_y$ = 50ksi under the non-constant internal axial load, $P$ = 1000 kips. The unbraced length is $L_b = L_{by} = L$ = 15 ft. The panel shear stiffness is considered as the brace stiffness. Using the DM and DP to determine the brace stiffness necessary to achieve $UC \leq 1.0$ and brace point displacement amplification approximately $\leq 4.0$ and corresponding brace forces is summarized as follows.

3.8.7.1 Case 6 – Hybrid Bracing (Problem H1)

*3.8.7.1.1 DM Solution*

The brace stiffness necessary to satisfy $UC \leq 1.0$ and brace point displacement amplification approximately $\leq 4.0$ is $\beta$ = 14.1 kips/inch. The buckling eigenvalues and mode shapes are shown in Fig. 3.8.7.2.

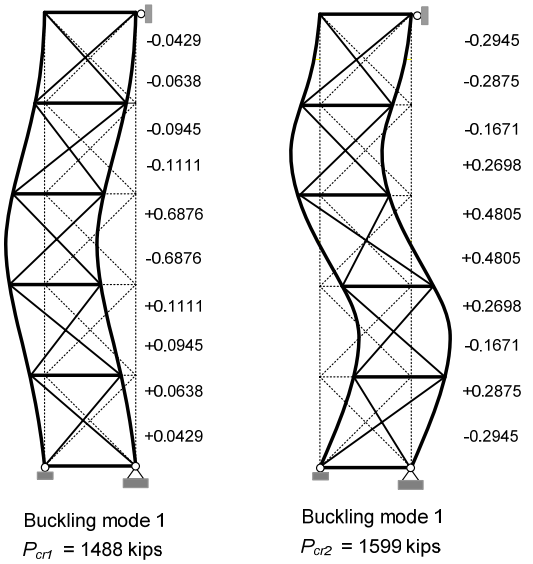


**Fig. 3.8.7.2. Buckling mode shapes, problem H1, case 6 – DM.**

The geometric imperfections potentially causing the largest outside brace force are shown in Fig. 3.8.7.3 and the geometric imperfections potentially causing the largest inside brace force are shown in Fig. 3.8.7.4.

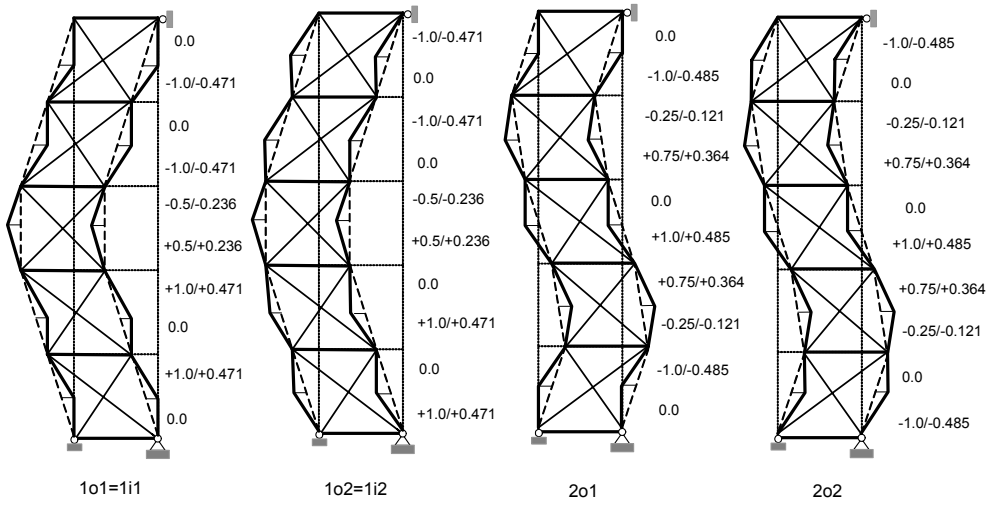


**Fig. 3.8.7.3. Geometric imperfection potentially causing the largest outside brace force, problem H1, case 6 – DM.**

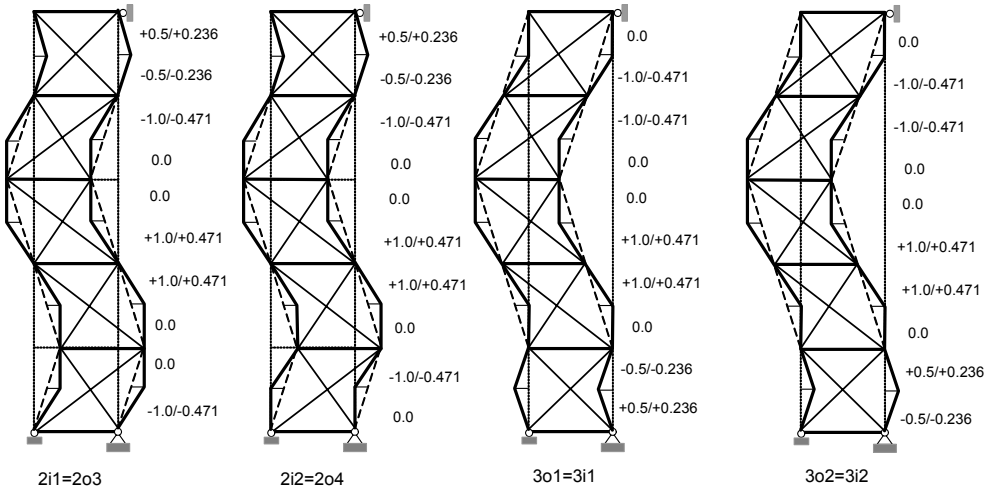


**Fig. 3.8.7.4. Geometric imperfection potentially causing the largest inside brace force, problem H1, case 6 – DM.**

The results from second-order analysis are shown in Table 3.8.13. The notations such as "Panel 1" to "Panel 5" are respectively from the bottom to the top of system. From Table 3.8.13, it is indicated that imperfection "*1o1=1i1*" gives maximum unity check as well as maximum brace forces for panel 2 and 4. Imperfection "*1o2=1i2*" gives maximum brace forces for panel 1; Imperfection "*2o1*" gives maximum brace forces for panel 3; and Imperfection "*3o2=3i2*" gives maximum brace forces for panel 5. Practically speaking, the imperfection "*1o1=1i1*" is the critical imperfection.

**Table 3.8.13. Results from the second-order analysis with β = 14.1 kips/inch, and $P_u$ = 1000 kips, problem H1, case 6 – DM.**

| No | Imperfection | *UC* | Panel shear forces (kips) | | | | |
|---|---|---|---|---|---|---|---|
| | | | Panel 1 | Panel 2 | Panel 3 | Panel 4 | Panel 5 |
| 1 | 1o1=1i1 | 1.0005 | 6.16 | 12.41 | 3.17 | 12.11 | 5.86 |
| 2 | 1o2=1i2 | 0.9344 | 9.70 | 10.39 | 3.30 | 10.03 | 9.33 |
| 3 | 2o1 | 0.9651 | 6.71 | 3.38 | 10.70 | 3.30 | 7.14 |
| 4 | 2o2 | 0.9534 | 7.76 | 4.44 | 10.65 | 3.30 | 8.19 |
| 5 | 2i1=2o3 | 0.9661 | 4.01 | 8.53 | 9.30 | 8.13 | 5.49 |
| 6 | 2i2=2o4 | 0.9604 | 4.91 | 9.78 | 9.27 | 8.32 | 5.64 |
| 7 | 3o1=3i1 | 0.9644 | 2.18 | 10.54 | 9.37 | 10.00 | 10.10 |
| 8 | 3o2=3i2 | 0.9661 | 2.20 | 11.78 | 9.34 | 10.18 | 10.25 |

Based on the result from the second-order analysis, the brace point displacement amplification is calculated below:

$$\Delta_{Tm} = \Delta_{om} + \Delta_m = 2.5*0.36+1.624 = 2.546 \text{ in}$$

$$(\Delta_{om} + \Delta_m)/\Delta_{om} = 2.83$$

Where: $\Delta_{om}$ = the initial displacement at the brace point.

$\Delta_m$ = the displacement from second-order analysis.

$\Delta_{Tm}$ = the total displacement at the brace point

This amplification is within the acceptable level.

If the bracing system is considered as the pure relative bracing, the required brace stiffness based on the AISC Appendix 6 is of 29.6 kips/inch, almost double the brace

stiffness from the DM solution. The results from the DM solutions for this stiffness are shown in Table 3.8.14.

**Table 3.8.14. Results from the second-order analysis with β =29.6 kips/inch, and $P_u$ = 1000 kips, problem H1, case 6 – DM**

| No | Imperfection | *UC* | Panel shear forces (kips) | | | | |
|---|---|---|---|---|---|---|---|
| | | | Panel 1 | Panel 2 | Panel 3 | Panel 4 | Panel 5 |
| 1 | 1o1=1i1 | 0.9446 | 3.68 | 8.62 | 5.52 | 7.78 | 3.68 |
| 2 | 1o2=1i2 | 0.8906 | 6.10 | 6.48 | 5.50 | 6.11 | 5.72 |
| 3 | 2o1 | 0.9274 | 5.14 | 5.52 | 7.95 | 5.50 | 4.86 |
| 4 | 2o2 | 0.9137 | 6.09 | 5.52 | 7.51 | 5.50 | 5.82 |
| 5 | 2i1=2o3 | 0.9315 | 4.03 | 5.91 | 7.37 | 6.77 | 3.67 |
| 6 | 2i2=2o4 | 0.9178 | 4.94 | 7.11 | 7.14 | 6.81 | 3.68 |
| 7 | 3o1=3i1 | 0.9241 | 3.67 | 6.68 | 7.44 | 7.39 | 5.73 |
| 8 | 3o2=3i2 | 0.9164 | 3.67 | 7.88 | 7.23 | 7.43 | 5.78 |

One can observe from Table 3.8.14 that the critical imperfections give smaller values both unity check and brace forces from Table 3.8.14. Also, the brace point displacement amplification is:

$$\Delta_{Tm} = \Delta_{om} + \Delta_m = 2.5*0.36+0.670 = 1.570 \text{ in}$$

$$(\Delta_{om} + \Delta_m)/\Delta_{om} = 1.74$$

When the structure is analyzed with β = 29.6 kips/inch determined from the AISC Appendix 6, the maximum panel shear forces are approximately equal to the AISC relative bracing force requirement. Regardless of whether β = 14.1 kips/inch (DM) or β = 29.6 kips/inch (AISC App 6) is used, the lateral displacements are noticeable at the panel

points in the middle of the truss. The responses at the maximum load for two brace stiffnesses are plotted in Fig. 3.8.7.5.

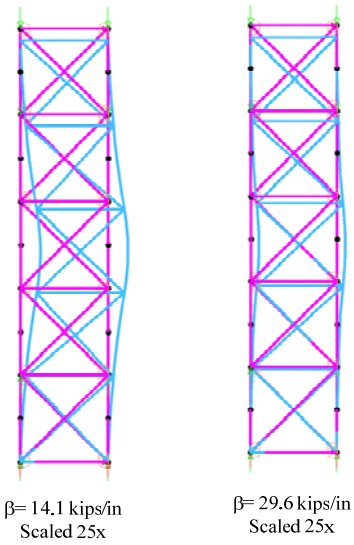


**Fig. 3.8.7.5. Deformation at the maximum load, problem H1, case 6 – DM.**

*3.8.7.1.2 DP Solution*

From the DM Solution, the critical imperfection "*1o1=1i1*" causing the smallest column axial resistance and maximum brace forces at Panel 2 and 4 shown in Fig. 3.8.7.6 is used in the DP Solution.

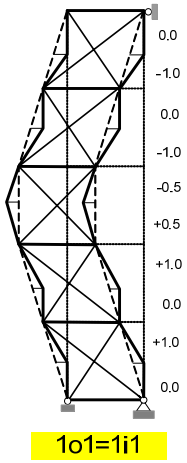


**Fig. 3.8.7.6. Critical imperfections for problem H1, case 6 – DP.**

The results from the DP are shown from Figs. 3.8.7.7 to 3.8.7.8. Fig. 3.8.7.7 shows that the maximum column capacity is equal to 930.1 kips. The maximum brace force for Panel 2 is 20.9 kips as shown in Fig. 3.8.7.8.

The diagrams of moment, equivalent area $A_{eq}$, equivalent elastic section modulus $Q_{eq}$, and the equivalent of moment inertia $I_{eq}$ along the member length at the maximum load due to the spread of plasticity are displayed in Figs. 3.8.7.9 and 3.8.7.10.

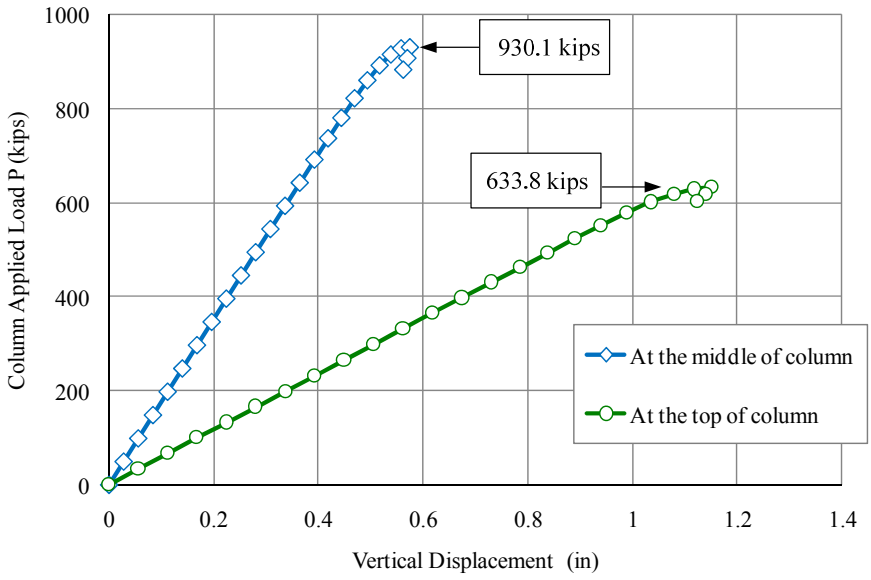


**Fig. 3.8.7.7. Trace for load vs. displacement, problem H1, case 6 – DP.**

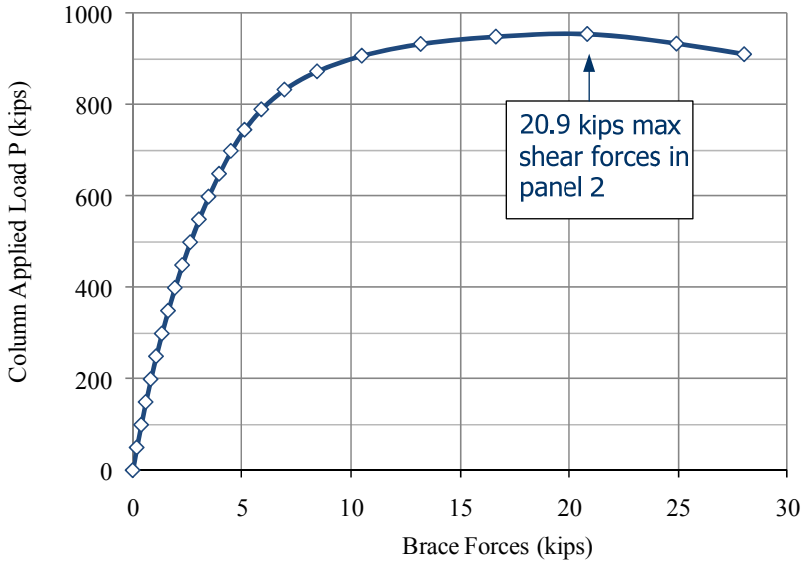


**Fig. 3.8.7.8. Trace for load vs. brace force, problem H1, case 6 – DP.**

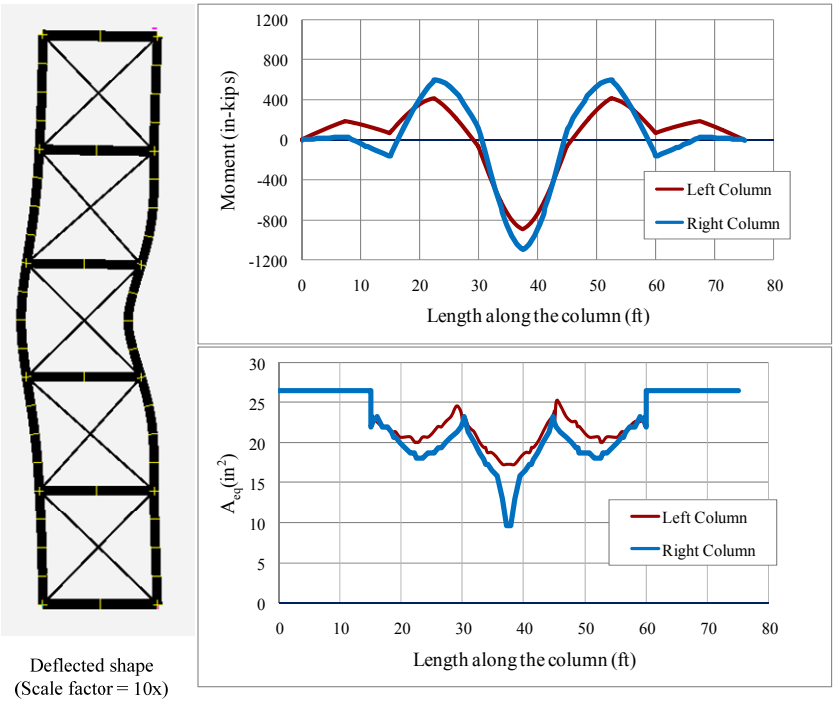


**Fig. 3.8.7.9. Response at the maximum load (1), problem H1, case 6 – DP.**

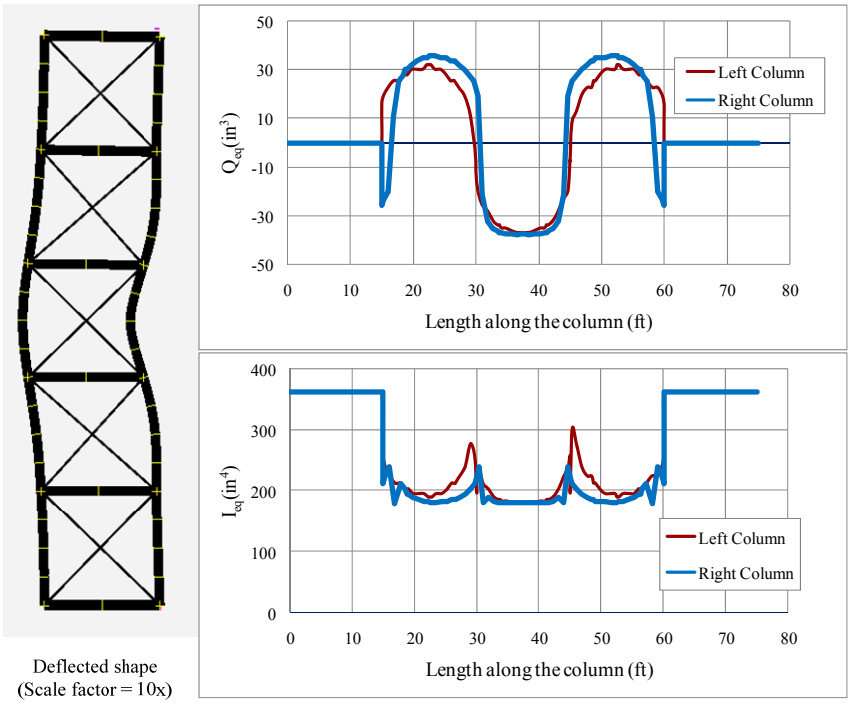


**Fig. 3.8.7.10. Response at the maximum load (2), problem H1, case 6 – DP.**

3.8.7.2 Case 7 – Hybrid Bracing (Problem H2)

*3.8.7.2.1 DM Solution*

The only difference from problem H1 is that the axial force is applied only one of two truss chords. However, the behavior for this problem is more complicated than that of problem H1. It seems that this bracing system is combined relative, nodal and lean-on bracings.

Using the same fashion as in the problem H1, the two brace stiffness: one is based on $UC \leq 1.0$ and brace point displacement amplification approximately $\leq 4.0$ ($\beta = 6.7$ kips/inch) and the second one is based on the relative bracing equations in the AISC Appendix 6 ($\beta = 14.8$ kips/inch) are used to predict the brace forces.

The buckling eigenvalues and mode shapes for brace stiffness $\beta = 6.7$ kips/inch are shown in Fig. 3.8.7.11.

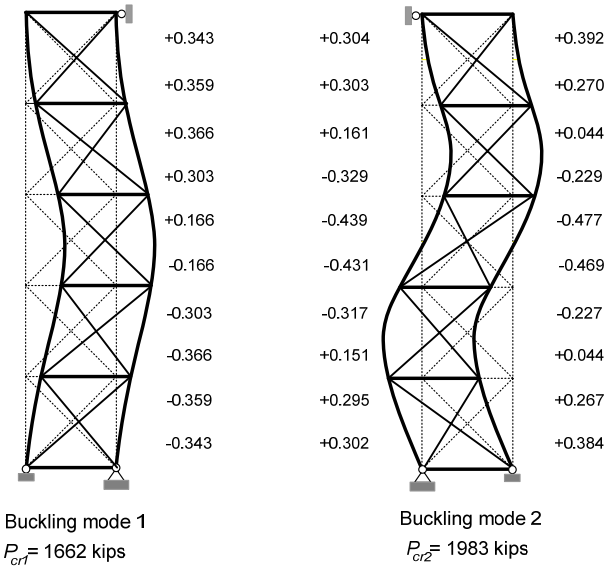


**Fig. 3.8.7.11. Buckling mode shapes, problem H2, case 7 – DM.**

The geometric imperfections potentially causing the largest outside brace force are shown in Fig. 3.8.7.12 and the geometric imperfections potentially causing the largest inside brace force are shown in Fig. 3.8.7.13.

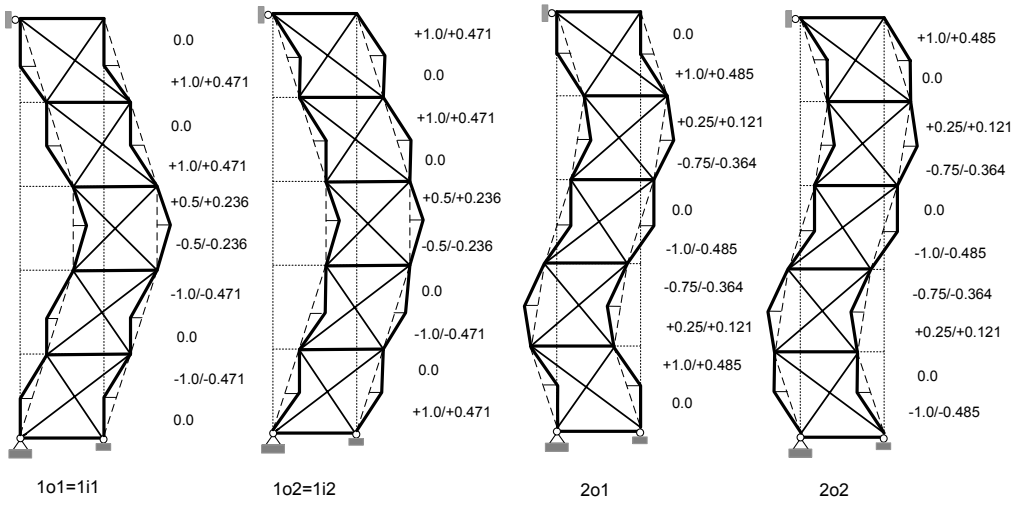


**Fig. 3.8.7.12. Geometric imperfection potentially causing the largest outside brace force, problem H2, case 7 – DM.**

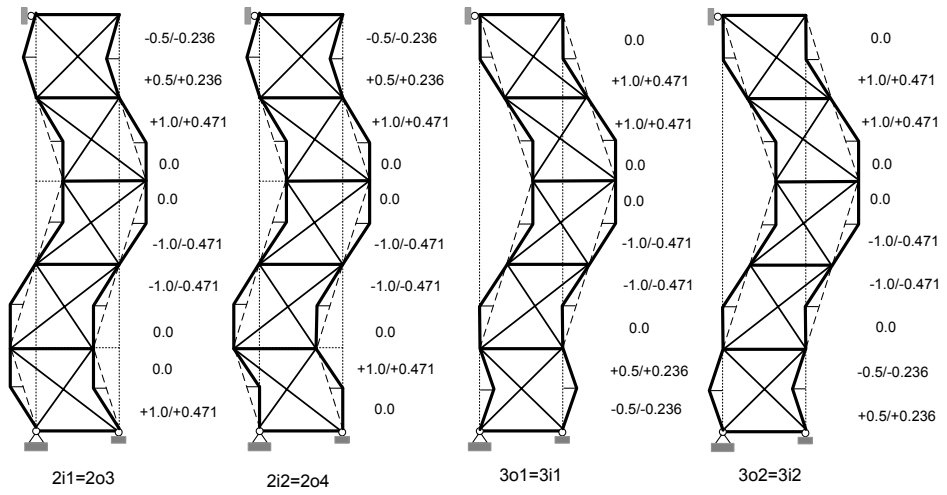


**Fig. 3.8.7.13. Geometric imperfection potentially causing the largest inside brace force, problem H2, case 7 – DM.**

The results from the DM solution for the brace stiffness β = 6.7 kips/inch are shown in Table 3.8.15 and for the brace stiffness β = 14.8 kips/inch are shown in Table 3.8.16.

**Table 3.8.15 Results from second-order analysis with β = 6.7 kips/inch, and $P_u$ = 1000 kips, problem H2, case 7 – DM**

| No | Imperfection | *UC* | Panel shear forces (kips) | | | | |
|---|---|---|---|---|---|---|---|
| | | | Panel 1 | Panel 2 | Panel 3 | Panel 4 | Panel 5 |
| 1 | 1o1=1i1 | 1.0009 | 8.96 | 9.43 | 3.38 | 2.69 | 2.21 |
| 2 | 1o2=1i2 | 0.9540 | 10.31 | 9.28 | 3.39 | 2.54 | 3.56 |
| 3 | 2o1 | 0.9635 | 7.83 | 4.53 | 0.78 | 0.96 | 3.01 |
| 4 | 2o2 | 0.9527 | 8.15 | 4.25 | 0.78 | 0.78 | 3.33 |
| 5 | 2i1=2o3 | 0.9593 | 6.68 | 3.20 | 0.91 | 3.05 | 2.84 |
| 6 | 2i2=2o4 | 0.9470 | 6.97 | 2.91 | 0.86 | 3.05 | 2.88 |
| 7 | 3o1=3i1 | 0.9462 | 4.65 | 2.17 | 0.89 | 4.04 | 4.84 |
| 8 | 3o2=3i2 | 0.9339 | 4.94 | 1.90 | 0.85 | 4.04 | 4.88 |

**Table 3.8.16 Results from second-order analysis with β = 14.8 kips/inch, and $P_u$ = 1000 kips, problem H2, case 7 – DM.**

| No | Imperfection | *UC* | Panel shear forces (kips) | | | | |
|---|---|---|---|---|---|---|---|
| | | | Panel 1 | Panel 2 | Panel 3 | Panel 4 | Panel 5 |
| 1 | 1o1=1i1 | 0.9556 | 9.11 | 10.54 | 5.82 | 1.38 | 2.52 |
| 2 | 1o2=1i2 | 0.9099 | 10.34 | 10.02 | 5.83 | 1.61 | 1.28 |
| 3 | 2o1 | 0.9372 | 9.36 | 6.43 | 2.92 | 4.11 | 6.10 |
| 4 | 2o2 | 0.9252 | 9.71 | 6.07 | 2.93 | 3.75 | 6.43 |
| 5 | 2i1=2o3 | 0.9379 | 8.73 | 5.25 | 3.30 | 6.20 | 5.40 |
| 6 | 2i2=2o4 | 0.9247 | 9.06 | 4.89 | 3.30 | 6.21 | 5.42 |
| 7 | 3o1=3i1 | 0.9315 | 7.20 | 4.74 | 3.28 | 6.68 | 6.89 |
| 8 | 3o2=3i2 | 0.9083 | 7.52 | 4.38 | 3.28 | 6.68 | 6.91 |

The brace point displacement amplification for the brace stiffness β = 6.7 kips/inch is:

$$\Delta_{Tm} = \Delta_{om} + \Delta_m = 2.5*0.36+2.797 = 3.697 \text{ in}$$

$$(\Delta_{om} + \Delta_m)/\Delta_{om} = 2.47$$

The brace point displacement amplification for the brace stiffness β = 14.8 kips/inch is:

$$\Delta_{Tm} = \Delta_{om} + \Delta_m = 2.5*0.36+1.548 = 2.448 \text{ in}$$

$$(\Delta_{om} + \Delta_m)/\Delta_{om} = 1.60$$

Similarly, regardless of whether β = 6.7 kips/inch (DM) or β = 14.8 kips/inch (based on the AISC Appendix 6) is used, the lateral displacements are noticeable at the panel points in the middle of the truss. This behavior is an overall *2nd-order* bending amplification problem. The responses at the maximum load for two brace stiffnesses are plotted in Fig. 3.8.7.14.

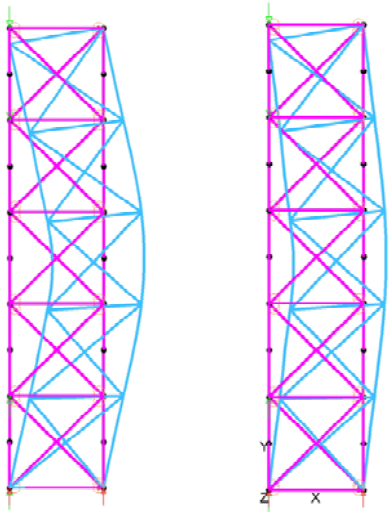


**Fig. 3.8.7.14. Deformation at the maximum load, problem H2, case 7 – DM.**

*3.8.7.2.2 DP Solution*

From the DM Solution, the critical imperfection "*1o1=1i1*" causing the smallest column axial resistance and maximum brace forces at Panel 2 is selected to model in DP Solution. This imperfection is the same as pattern shown in Fig. 3.8.7.6 in Section 3.8.7.1.2.

The results from the DP are shown from Figs. 3.8.7.15 to 3.8.7.18. Fig. 3.8.7.15 indicates that the maximum column capacity is equal to 993.5 kips. The maximum brace force for panel 2 is 13.1 kips as shown in Fig. 3.8.7.16.

The diagrams of moment, equivalent area $A_{eq}$, equivalent elastic section modulus $Q_{eq}$, and the equivalent of moment inertia $I_{eq}$ along the member length at the maximum load due to the spread of plasticity are displayed in Figs. 3.8.7.17 and 3.8.7.18.

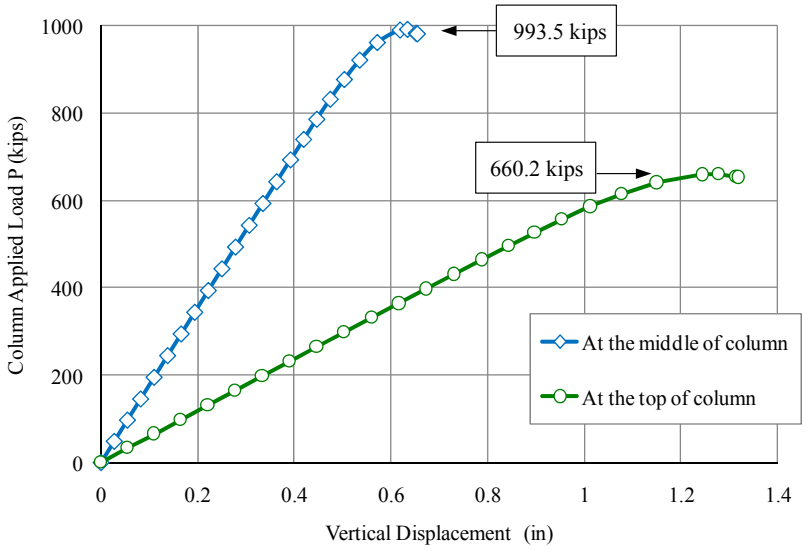


**Fig. 3.8.7.15. Trace for load vs. displacement, problem H2, case 7 – DP.**

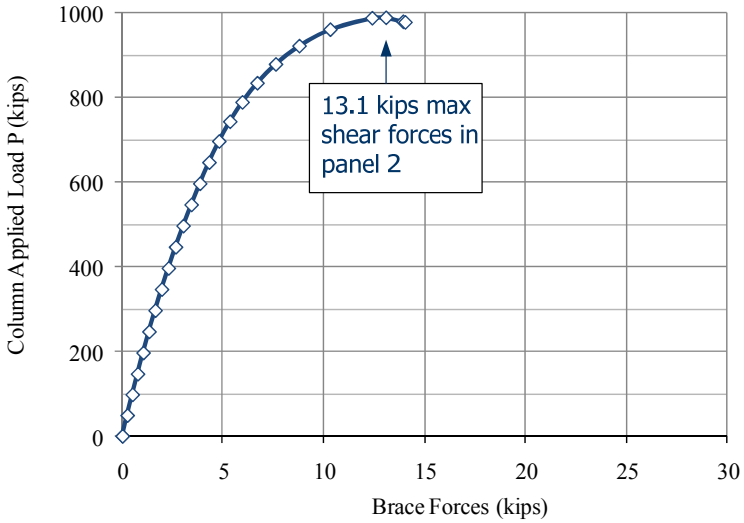


**Fig. 3.8.7.16. Trace for load vs. brace forces, problem H2, case 7 – DP.**

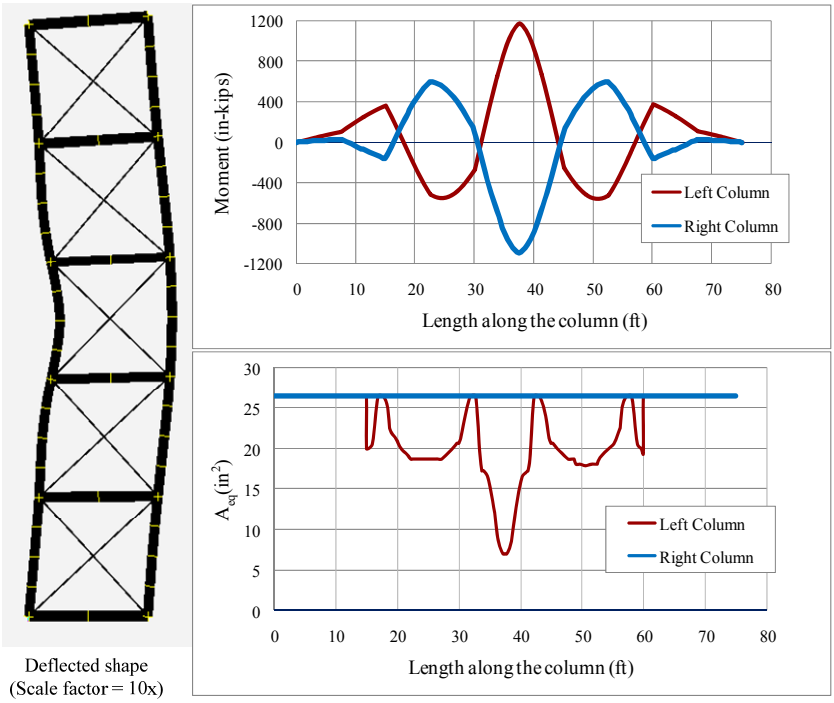


**Fig. 3.8.7.17. Response at the maximum load (1), problem H2, case 7 – DP.**

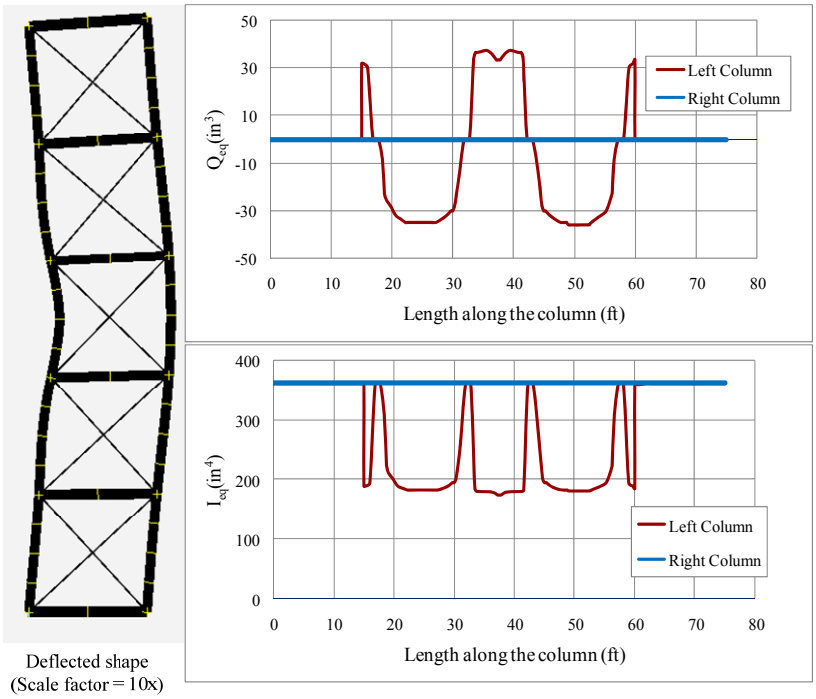


**Fig. 3.8.7.18. Response at the maximum load (2), problem H2, case 7 – DP.**

3.8.7.3 Summary

The required sizes of the diagonal members to satisfy $UC = 1.0$ on the truss chords by the DM is significantly smaller than that required by the AISC Appendix 6 relative bracing equations. The panel shear forces computed by the DM are approximately from 0.6% to 1.1% of the total internal axial load. The improvement in the DM solution is due to the contribution of the flexural rigidity of the truss chords.

## 3.9 Summary and Conclusions for Column Bracing

Based on the results from the above analyses, the summary and conclusion for column bracing are:

1) The nodal bracing stiffness needed to develop the column flexural buckling strength is dramatically smaller than the Appendix 6 base value of $2\beta_i/0.75 = 2.67\beta_i$ for cases involving substantial continuity or end restraint effects, i.e.,
    - Members with two or more intermediate braces, and/or
    - Members with end rotational restraint.
2) Nodal bracing stiffnesses as low as $1.3\beta_i$ work well for members with multiple internal braces.
3) An upper bound nodal bracing stiffness of $1.9\beta_i$ works well for cases with little continuity and end restraint effects, i.e., simply-supported columns with just one intermediate brace.
4) The Appendix 6 *relative* bracing equations do not account for any contribution of the column flexural rigidity ($EI$) to the resistance of the brace point displacements.

Significant benefits can be gained by including the column continuity and the corresponding contributions from the flexural rigidity ($EI$) in the analysis.

5) Substantial contributions from the member flexural rigidity can occur even for cases such as truss chords that are typically considered as just relatively braced. The above benefits are demonstrated by several hybrid bracing models of parallel truss chords and of a representative two-story braced frame. These benefits can be quantified reliably for column bracing problems by using the Direct Analysis Method. Quantifying these benefits for general structures using simplified design equations is difficult; improved design equations can be developed for some specific cases.

6) The use of $L_q$ in the Appendix 6 nodal bracing provisions effectively reduces $P_n/\Omega$ to $P_a$ (ASD), or $\phi P_n$ to $P_u$ (LRFD). As such, there is conceptually no ability of the bracing system to accommodate combined bending and axial compression. That is $\Omega P_a/P_n$ or $P_u/\phi P_n$ is conceptually equal to 1.0 when the bracing is designed using $L_q$; thus, for example, $P_u/2\phi P_n + M_u/\phi M_n$ is greater than 1.0 for any $M_u$.

7) The use of $L_q$ in the Appendix 6 nodal bracing provisions accounts in a practical way for partial bracing, but is conservative relative to analytical solutions for the strength of partially braced columns. This is particularly true for cases with multiple intermediate braces.

8) The Direct Analysis Method (DM) is able to predict bracing demands and column strengths with good accuracy; however:

    - For all but the simplest of problems, the DM requires an elaborate assessment of (1) buckling modes; (2) brace force influence lines and (3) lateral loads

equivalent to the $\Delta_o$ (out-of-plumbness) and $\delta_o$ (out-of-straightness) geometric imperfections within the Code of Standard Practice tolerances.

- Several candidate critical geometric imperfections can typically be identified by inspection, given a high-level conceptual understanding of the factors that influence the brace forces. That is, given an understanding of the above fundamental factors that influence the brace forces, one can usually establish by inspection a few likely imperfections that may cause the largest bracing force demands.
- The DM represents a useful advance in the ability to predict bracing force and stiffness demands, but the above imperfection modeling considerations can be tedious.
- As a result, in the context of predicting brace force and brace stiffness demands, the DM is possibly most useful primarily for research studies and specialized design problems.

9) The Distributed Plasticity Method is a good resolution in predicting bracing stiffness and force demands

- For columns that fail by inelastic flexural buckling, Distributed Plasticity Analysis (DP) tends to predict somewhat larger brace forces than the DM in the vicinity of the column limit load; the differences between the DP and DM solutions in the vicinity of the column limit load are greatest for close spacing of braces (short column unbraced lengths)
- It should be noted that use of the Distributed Plasticity Method does not imply inelastic design. Rather, this approach provides the capability of conducting

high resolution *virtual experimental tests* accounting in detail for the influence of residual stresses and the spread of yielding in the physical members as their *inelastic buckling* strength limit state is approached.

10) The Appendix 6 bracing force equations provide a reasonable but coarse approximation of the actual bracing force demands at the column strength limit state *in the cases to which these equations are applicable*:

- Generally, the brace force versus column force curves are very flat in the vicinity of the column maximum strength. That is, the brace force tends to vary significantly with small changes in the column load at load levels close to the column strength limit.
- Reductions in the bracing stiffness typically result in increases in the bracing force demands.
- With the use of nodal brace stiffnesses between 1.3 and $1.9\beta_i$, the largest bracing force demands at the column strength limit are in the vicinity of 2 % of the column force. These results are consistent with prior studies by Li.
- As the brace stiffnesses are reduced below the above values, the brace force demands can increase dramatically. However, for inelastic columns with multiple intermediate nodal braces, the force demands at the maximum strength stillcan be less than 1 % of the column force, in some cases, even with $\beta < \beta_i$ .
- Brace point displacement amplifications larger than about 4.0 generally should be discouraged; at these levels of amplification, the system response

becomes very sensitive to minor changes in the loading and stiffness characteristics of the structure.

- Bracing forces increase dramatically in the post-peak range of the column response. Therefore, if it is desired to develop large inelastic deformation capacities of components, the bracing force and stiffness demands can be substantially higher.

11) In some cases, the design of the bracing for a target force demand of 2% of the relevant member force results in excessive amplification at the maximum load level. Therefore, the use of a 2% force requirement alone is generally not sufficient. It is necessary to also provide a certain minimum stiffness. The minimum stiffness that ensures that the brace force demands are not excessive is not a constant but is a function of a wide range of system characteristics and parameters. Unfortunately, equations do not exist at present that capture all the factors that influence this minimum requirement.

12) Self-supported systems that effectively "cantilever" above the foundation of the structure tend to have uniform out-of-plumbness of $L/500$ as their critical imperfection pattern for overall strength.

13) Application of Winter's model to columns with unequal brace spacing:

    - As noted by Yura (1996), the bracing stiffness requirements can be determined by assuming hinges at each of the brace point locations
    - However, this type of model can underestimate the actual brace force demands at $P_u = \phi P_{n(K=1)}$ ; in this case, the brace force demands are accentuated (i.e., increased) by the column continuity effects.

- The above findings are consistent with the findings by Plaut (1993) and by Stanway et al. (1992a & b).

# CHAPTER 4

# ASSESSMENT OF BEAM BRACING REQUIREMENTS BY SECOND-ORDER ELASTIC ANALYSIS

## 4.1 Introduction

This chapter focuses on beam lateral bracing, torsional bracing, and combined lateral and torsional bracing behavior and design. The main objectives are to:

1. Investigate and demonstrate the application of second-order elastic analysis for the solution of beam bracing problems,
2. Determine refined estimates of the coupled bracing stiffness and force requirements for selected example cases, and
3. Assess the qualities and limitations of practical design expressions, such as those in Appendix 6 of the 2005 AISC Specification.

The background for this study and the research approach taken in this work are presented in Section 4.2. Section 4.3 then focuses on general aspects of the analysis models and Section 4.4 discusses specific considerations in defining the geometric imperfections for beam load-deflection analysis solutions. Next, elastic eigenvalue buckling analyses are applied to determine brace stiffness requirements for a range of benchmark problems previously studied by Yura (2001). The results from these analyses are presented in Section 4.5. This is followed in Section 4.6 by the use of second-order elastic load-deflection analyses to estimate the brace strength requirements for the above problems. To the knowledge of the author, this is first time that refined elastic load-deflection analyses of these fundamental benchmark problems have been presented in the literature. The brace forces at the member strength limit are compared to the corresponding results from AISC

Appendix 6. Finally, the brace stiffness and strength requirements are evaluated for a number of combined lateral and torsional bracing problems in Section 4.7. SAP 2000 Version 11 (CSI 2008) is utilized to generate all of the analysis solutions presented in this chapter.

## 4.2 Background and Research Approach

The applicability of the DM to the bracing of columns against flexural buckling is relatively clear and straightforward. A wide range of example solutions have been demonstrated in Chapter 3. Similar concepts can be applied for the assessment of beam and beam-column bracing. However, beam and beam-column bracing considerations are generally more complex. This is because these types of problems can involve:

- Lateral bracing, torsional bracing and/or combined lateral and torsional bracing,
- Moment gradient (or flange stress gradient) effects,
- Transverse load height effects, and
- Web distortional flexibility effects.

Of the above effects, the influence of the web distortional flexibility can be very important for torsionally braced beams.

This chapter focuses on elastic eigenvalue buckling and second-order elastic load-deflection analyses of I-section beams using models in which the flanges are considered as "equivalent columns" and in which the web is considered as a generalized structural component. One may view this approach as being similar to the analysis of a shear wall with adjacent boundary and/or framing elements in an overall structural system analysis. The DM concept, extended in this way, has the potential to address the analysis of column, beam, beam-column, and frame bracing problems having any degree of complexity. However,

based on the column studies completed in Chapter 3, and based on an assessment of the overall AISC beam design procedures, there are a few issues that need to be resolved before the above types of analysis can be used for design. These problems are explained in the following subsections.

**a) Beam Elastic Buckling Behavior for Long Unbraced Lengths**

For I-beams governed by the elastic lateral torsional buckling (LTB) limit state, the nominal AISC LTB resistance is taken as the theoretical elastic LTB buckling moment $M_{cr}$. The design resistance of these types of members is $\phi_b M_n = 0.9 M_{cr}$ (in AISC LRFD). As a result, if one uses a stiffness reduction factor of $SRF = 0.8$ ($\cong 0.877\ \phi_b = 0.877(0.9)$ where 0.877 is the strength reduction applied to the theoretical elastic column buckling load) to obtain the nominal column elastic buckling resistance, the second-order elastic analysis model will likely not support the required load. The value $SRF = 1.0\ \phi_b = 1.0(0.9)$ is required for consistency with the AISC elastic LTB design strength. This is also the consistent value for the application of distributed plasticity analysis. As shown above, there are two contributors to the value $SRF = 0.8$ in the AISC DM:

(1) The resistance factor $\phi_c = \phi_b = 0.9$.

(2) The factor 0.877. This factor accounts for:

(a) Geometric imperfection and distributed yielding effects within the member length for columns of all lengths, as well as,

(b) The traditional higher AISC margin of safety for long columns.

It can be argued that a value similar to the 0.877 factor used in column design should be applied for the calculation of beam LTB resistances. In refined inelastic analysis solutions of I-beams in which the strength limit state is in the elastic LTB range, the beams typically

cannot reach their theoretical elastic LTB resistances. This is due to the second-order amplification of initial lateral sweep and twist, plus the onset of partial yielding. For beams with large $d/b_f$, there is evidence that the reductions below $M_{cr}$ can be substantial (Kim and White 2008). It should be noted that Eurocode 3 applies a substantial reduction to the theoretical elastic LTB resistance for these types of beams. However, the current AISC Specification does not apply any reduction to its nominal beam elastic LTB resistance. The AISC Specification takes the moment at the theoretical out-of-plane bifurcation of the perfectly straight elastic member as the elastic LTB strength. When combined with the ASCE 7 load models, the target reliability index of $\beta = 2.7$ is achieved (White and Jung 2008; White and Kim 2008). Nevertheless, if the AISC equations are applied to cases where the member end conditions are defined "exactly," there is no doubt that the mean LTB resistances within the elastic buckling range will be smaller than the theoretical elastic LTB load.

**b) Inelastic Buckling Behavior for Short Unbraced Lengths**

For beams that have very short unbraced lengths, such that their strengths are associated with the development of substantial yielding, some type of inelastic stiffness reduction needs to be applied. Otherwise, a DM model with an elastic stiffness reduction of just 0.8 (or 0.9) will tend to grossly underpredict the brace force demands at the member strength limit. Application of an inelastic stiffness reduction factor for the assessment of beam LTB is more difficult than application of such a factor for assessment of column flexural buckling. One option is to apply the stiffness reduction factor $\tau_b$ individually to the beam flanges, considering the flanges as equivalent columns.

**c) Other Considerations**

If the prior column-type DM solutions are to be applied for beam bracing assessment, one needs to perform a member strength interaction check for combined major-axis bending, minor-axis bending and flange warping. AASHTO (American Association of State Highway and Transportation Officials) provides such an equation for checking of I-girders, but most engineers are not accustomed to these design checks for ordinary assessment of beams in building design.

Due to the above complexities, all the analyses in this chapter are conducted as "elastic virtual test simulations" using *2nd-order elastic* analysis models. This means that the analysis model simply uses the elastic nominal stiffness for all the members. Running these types of models as "elastic virtual tests" (no yielding considered) is consistent with prior solutions for assessment of stability bracing demands developed by Yura (1993), Helwig (1993), Wang and Helwig (2005), Helwig and Yura (2008a & b) and others. A fundamental assumption employed in this approach is that the ratio of the true brace stiffness or brace force to the member inelastic strength is approximately the same as the ratio of the brace stiffness or brace force to $M_{cr}$ based on a second-order elastic analysis of the beam and its bracing system. Alternative inelastic virtual test simulations (shell plastic zone analyses) are presented in Chapter 5.

## 4.3 Analysis Models

The analysis models considered in this chapter capture the following essential attributes of the beam stability bracing behavior:

- Various types of bracing including lateral bracing, torsional bracing, and/or combined lateral and torsional bracing.

- Complex two- and three-dimensional structural characteristics including moment gradient effects, load height effects, and cross-section distortional flexibility.

In the following, three analysis models are investigated that capture these attributes at different levels of refinement. These models are referred to as the equivalent truss model, the simplified model, and the refined model. Fig. 4.3.1 shows a representation of each of these analysis models. The models differ mainly in the idealization they use for the web. The web plate of an *I*-beam may be modeled as an equivalent truss system, a simplified plate model using shell elements that span the entire depth of the web, and as a refined web plate model composed of a larger number of shell elements. The flanges are modeled by beam elements in all of these solutions.

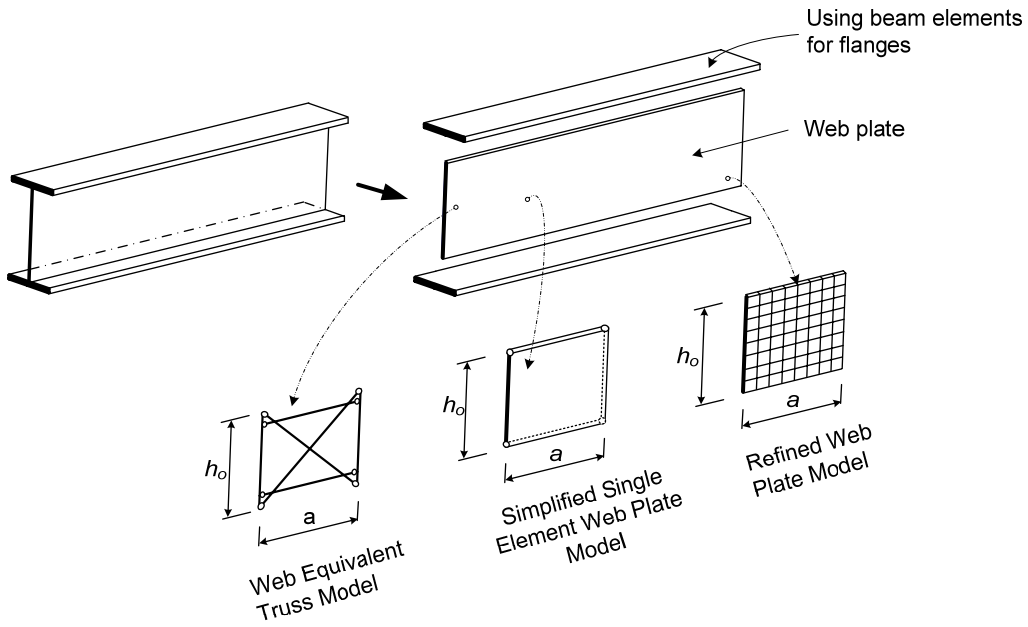


**Fig. 4.3.1. Analysis models.**

### 4.3.1 Equivalent Truss Model

The development of the equivalent truss model is based on matching the plane stress stiffness of the web in a member segment of length *a*. The process of matching the web

plate and equivalent truss system stiffnesses is illustrated in Figs. 4.3.2 to 4.3.5. The truss system is comprised of two flexurally-rigid axially-deformable vertical bars with area $A_h$ and length $h$, two horizontal truss bars with area $A_a$ and length $a$, located at a depth determined based on matching the in-plane flexural stiffness of the web, and two diagonal truss bars with area $A_d$ and length $L_d$.

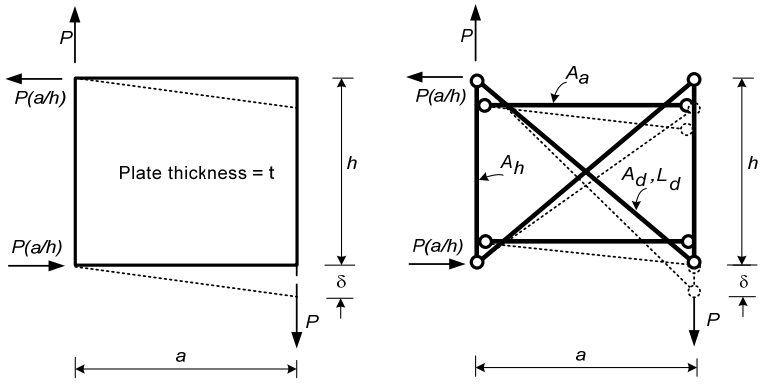


**Fig. 4.3.2. Models for calculation of equivalent shear stiffness.**

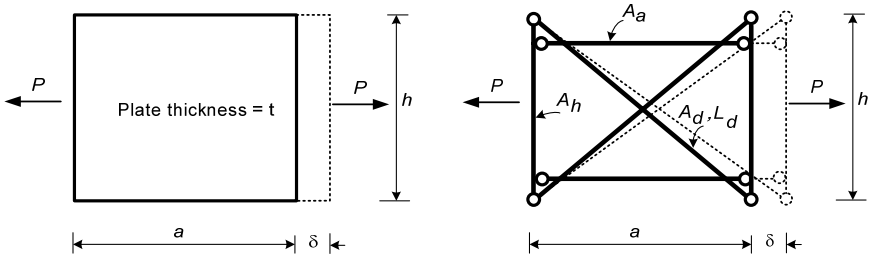


**Fig. 4.3.3. Models for calculation of equivalent axial stiffness in x-direction.**

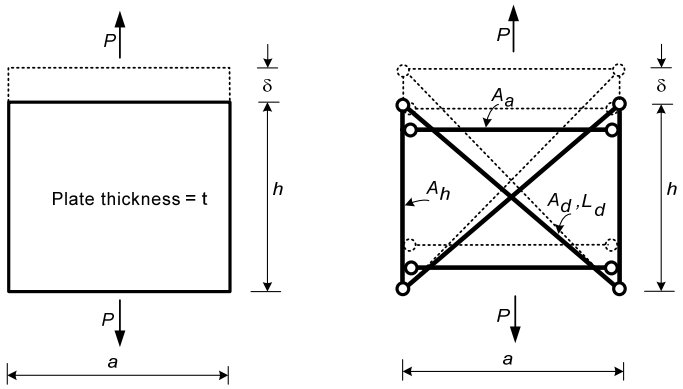


**Fig. 4.3.4. Models for calculation of equivalent axial stiffness in y-direction.**

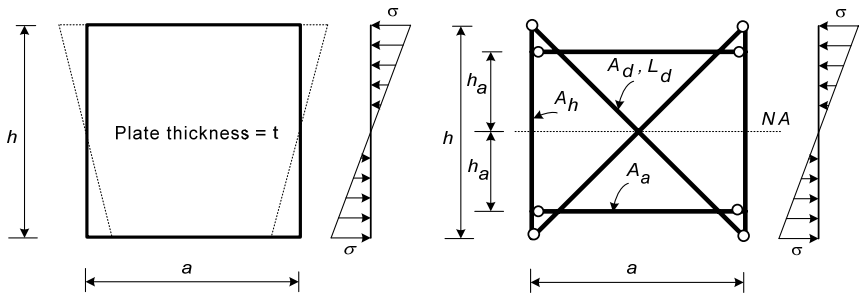


**Fig. 4.3.5. Models for calculation of equivalent flexural stiffness.**

In Fig. 4.3.2, $P$ is a load applied at the right edge of the plate to produce a vertical shearing displacement δ at the right-hand edge, with all of the other displacement degrees of freedom held fixed. To obtain the same load in the truss system subjected to the same statical loading pattern and displacements, the area for the diagonal bars must be

$$A_d = \frac{1}{4(1+\nu)} \frac{L_d^3}{h} \frac{t}{a} \tag{4-1}$$

where: $t$ = the thickness of plate.

ν = the Passion's ratio.

Similarly, to achieve the same axial stiffness for the plate and truss system in both the horizontal and vertical directions, the areas of the horizontal and vertical bars must be

$$A_a = \frac{ht}{2} \frac{1}{(1-\nu^2)} - A_d \frac{a^3}{L_d^3} \tag{4-2}$$

$$A_h = \frac{at}{2} \frac{1}{(1-\nu^2)} - A_d \frac{h^3}{L_d^3} \tag{4-3}$$

where $A_a$ is the area of the horizontal bars and $A_h$ is the area of the vertical bars.

Fig. 4.3.5 shows how the equivalent flexural stiffness between the web plate and truss system is obtained. To match the plane stress stiffness of the web plate in bending, the distance, $h_a$, from the horizontal bars to the neutral axis must be

$$h_a = 0.342h. \quad (4\text{-}4)$$

The Equivalent Truss Model provides an accurate characterization of the plane stress behavior of the web, essentially equivalent to that of the Simplified Single-Plate Element Model discussed below. In programs such as SAP2000, the engineer can use the above areas with second-order truss elements to approximate the second-order effects associated with the 3D displacements of the web.

Unfortunately, the modeling of the various components of the Equivalent Truss Model is elaborate and tedious. The Single-Element Web Plate Model captures the same effects and is much simpler. As a result, the Equivalent Truss Model is not considered any further in this research.

### 4.3.2 Simplified Single-Element Web Plate Model

The Single-Element Web Plate Model uses one shell element through the depth of the web. To account for the web distortional flexibility, the rotational continuity is released between the flanges and the web at the web-flange juncture, as shown in Fig. 4.3.6(a). Without releasing these rotations, the web distortional stiffness is generally overpredicted by the single shell element. The transverse bending stiffness of the web is modeled by using transverse beam elements of dimension $1.5h_o \times t_w$ at the brace points as illustrated in Fig. 4.3.6(b), where $h_o$ is the distance between flange centroids and $t_w$ is the web thickness. This gives an approximation similar to that associated with the representation of the web distortional stiffness in the torsional bracing equations of the AISC Specification Appendix 6. The number of shell elements along the length of the member is selected such that the aspect ratio $(a/h_o)$ of the web shell elements is approximately equal to 1.0 in this model.

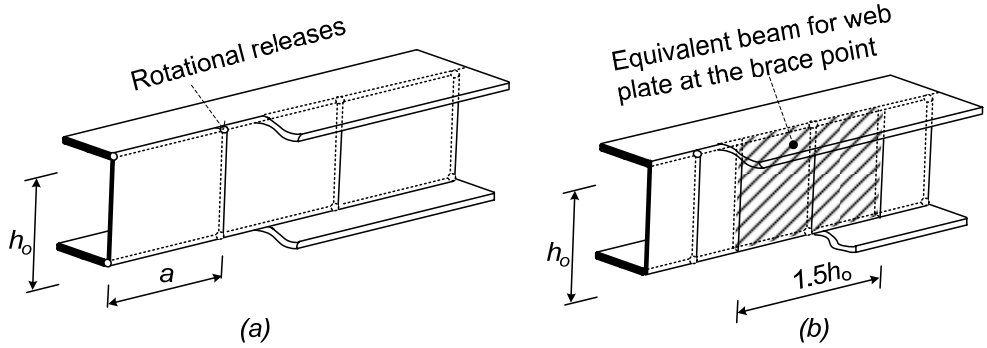


**Fig. 4.3.6. Single-element web plate model.**

### 4.3.3 Refined Web Plate Model

To fully capture the behavior of a physical I-section member and its bracing system, the refined model discussed in this section needs to be used. For typical I-section members, the use of eight shell elements through the depth of beam and element aspect ratios approximately equal to 1.0, as illustrated in Fig. 4.3.7, gives converged finite element analysis solutions for all practical purposes. In this case, no artificial rotational releases are placed in the model. The shell representation of the web captures the web distortional flexibility.

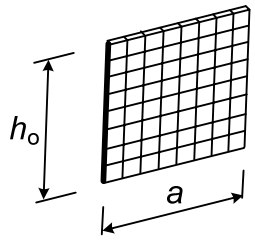


**Fig. 4.3.7. Refined web plate model.**

### 4.3.4 Finite Element Idealization (SAP 2000)

The two-node frame element from the SAP 2000 element library is selected to model the flanges of the beams, and the beam transverse stiffeners and bearing stiffeners in this

research. This element is based on a three-dimensional, beam-column formulation that includes the effects of biaxial bending, torsion, axial deformation, and biaxial shear deformations. This element has six degrees of freedom at its end nodes.

The four node shell element shown in Fig. 4.3.8 is used to model the I-section web in the simplified and refined web plate models. This element utilizes separate membrane and plate bending formulations. The membrane behavior is based on an isoparametric formulation that includes translational degrees of freedom (dofs) along the "in-plane" axes 1 and 2 in Fig. 4.3.8 and a rotational dof about the axis normal to the element reference plane. The plate bending behavior is modeled by two rotational dofs about the 1 and 2 axes and a translational dof along the 3 axis.

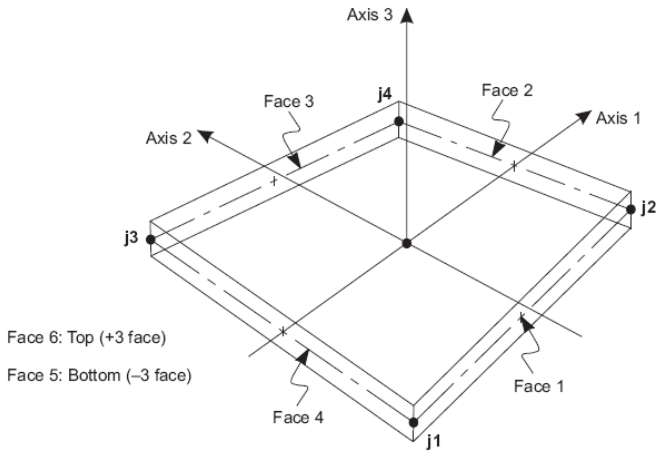


**Fig. 4.3.8. Four-node quadrilateral shell element (CSI 2007).**

### 4.3.5 Cantilever Beam Benchmark Tests

This section presents benchmark solutions of the simplified and refined models described above. Fig. 4.3.9 shows a wide flange W16x26 cantilever beam with a yield stress of $F_y$ = 50 ksi. The distance between flange centroids of this section is $h_o$ = 15.355 inches.

The length of beam is $L = 6h_o = 92.13$inches. A transverse stiffener of dimension $b_f$ x $t_f$ is used to restrain cross-section distortion at the free end of the beam.

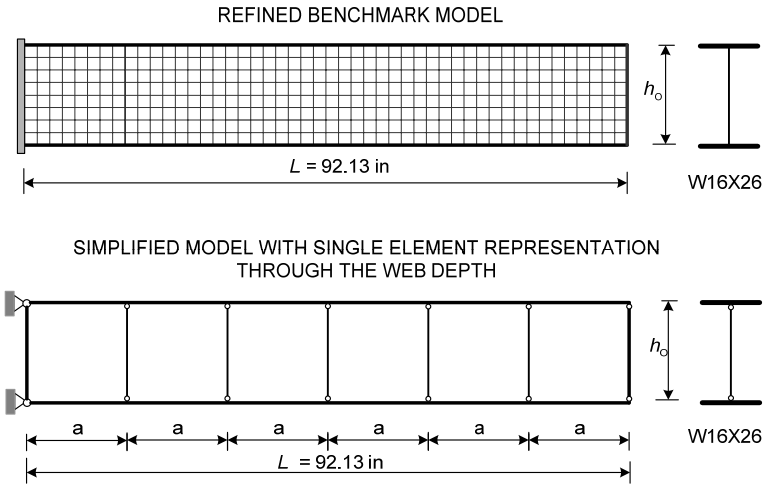


**Fig. 4.3.9. Cantilever beam benchmark test.**

It should be noted that the properties of section W16x26 are calculated based on the built-up sections. This means that the fillet areas between the flanges and web do not count in the calculation. For example, the cross-section area is equal to $A = 7.5474$ in$^2$, the moment of inertia about the major axis bending is $I_x = 294.1834$ in$^4$. The warping restraint from the end transverse stiffener is negligible. As noted above, frame elements are used to model the flanges of the beam and four-node shell elements are used to model the web of beam. Fig. 4.3.10 illustrates six types of loading considered in these tests: axial tension, in-plane shear and bending, out-of-plane shear and bending, twist, in-plane moment, and out-of-plane moment.

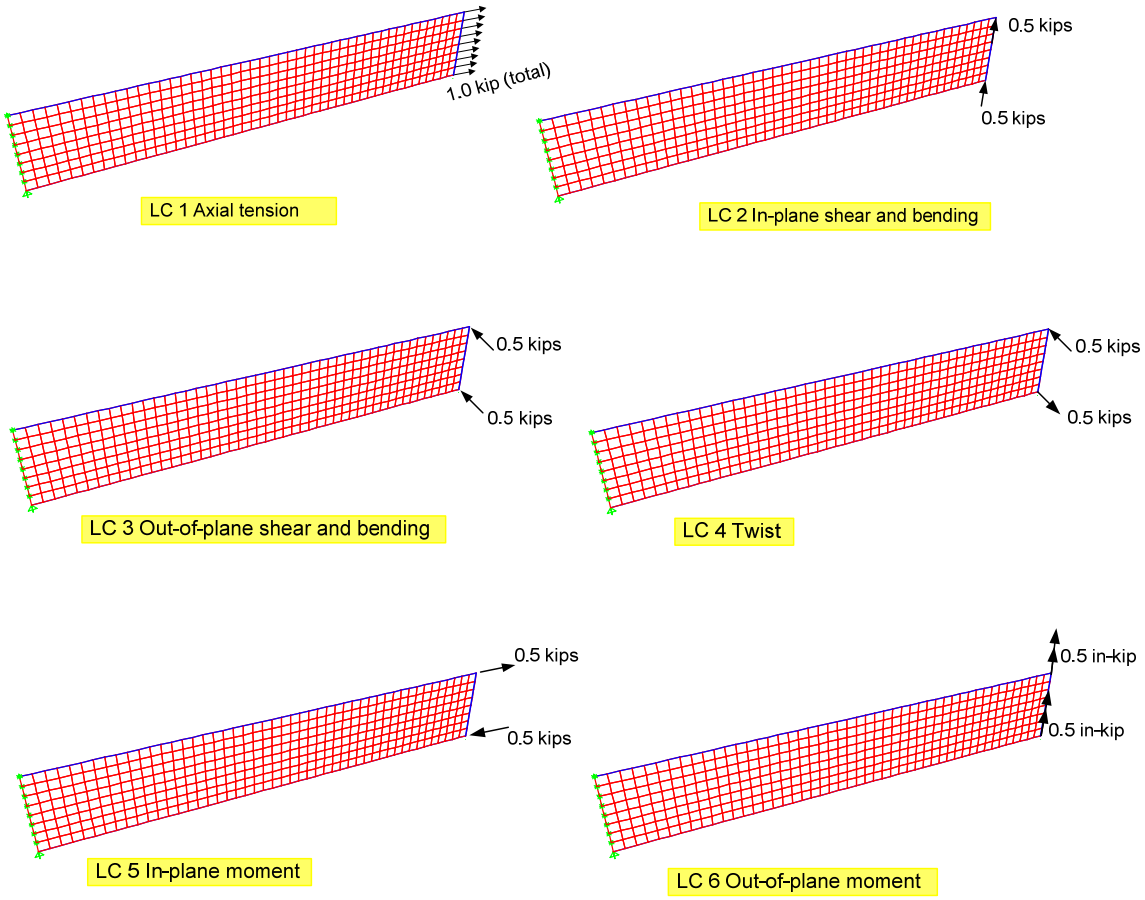


**Fig. 4.3.10. Loading cases for cantilever beam benchmark test.**

The refined model is displayed in Fig. 4.3.11 and the simplified model is shown in Fig. 4.3.12. The refined model uses a 48x8 grid of shell elements and 48 beam elements along the length of the flanges, whereas the simplified model uses only a 6x1 grid of shell elements with six beam elements along the length of the flanges.

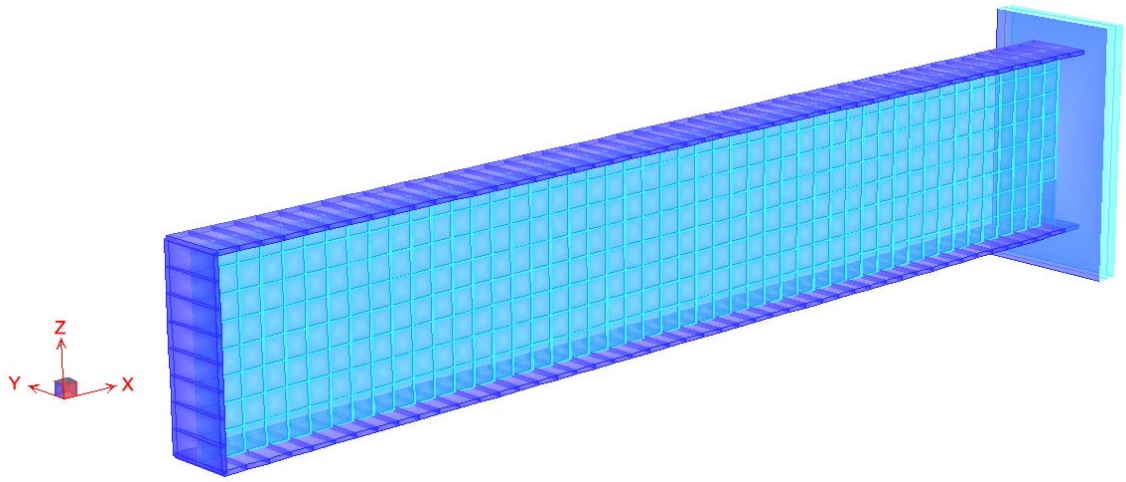


**Fig. 4.3.11. Cantilever beam benchmark test – Refined model.**

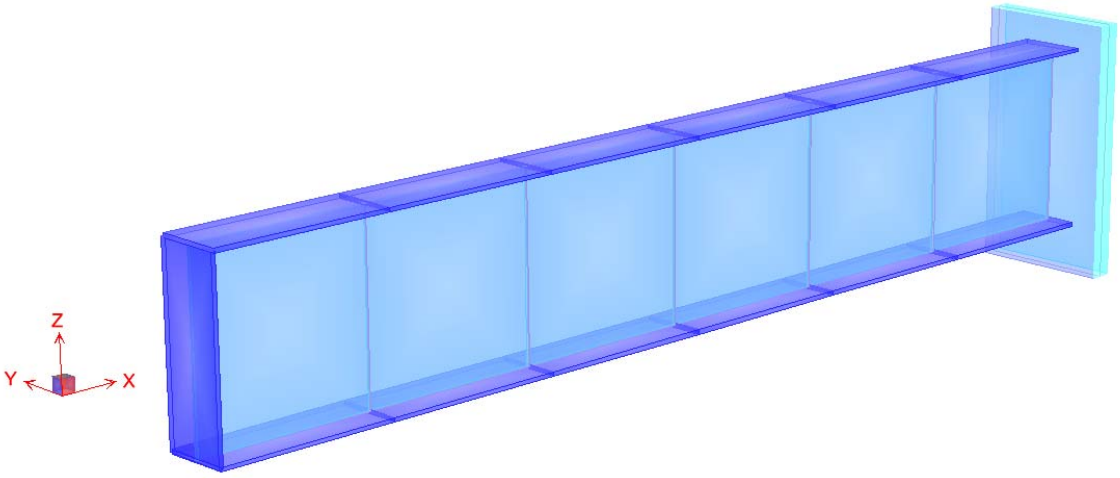


**Fig. 4.3.12. Cantilever beam benchmark test – Simplified model.**

The linear elastic analysis results for these models are summarized in Table 4.1. The values $U_x$, $U_y$, and $U_z$ shown in the table are the displacements in the global XYZ coordinate system shown in Figs. 4.3.11 and 4.3.12. The beam theory results are calculated including the flexural and shear deformations for load cases LC2 and LC3. Table 4.1 shows that the results from the simplified and the refined models are both very close to the beam theory

solution. It is noted that the tiny overlapped areas between the web and flanges causes a slight difference of results between the beam theory and analysis models.

**Table 4.1. Cantilever beam benchmark tests – Comparison of results.**

| End Loading Type | Output Parameters | (1) Beam theory (in) | (2) Refined Model (in) | (3) Simplified Model (in) | (2)/(1) | (3)/(1) |
|---|---|---|---|---|---|---|
| LC 1 Axial Extension | Average $U_x$ at flanges | 4.2092E-04 | 4.1620E-04 | 4.1620E-04 | 0.9888 | 0.9888 |
| LC 2 In-plane shear and bending | Average of $U_z$ at flanges | 3.2981E-02 | 3.2514E-02 | 3.1950E-02 | 0.9858 | 0.9687 |
| LC 3 Out-of-plane shear and bending | Average of $U_y$ at flanges | 9.4008E-01 | 9.4020E-01 | 9.2021E-01 | 1.0001 | 0.9789 |
| LC 4 Twist | Average of $U_y$ at flanges | 6.2018E-01 | 6.0250E-01 | 6.2170E-01 | 0.9715 | 1.0024 |
| LC 5 In-plane moment | Average of $U_z$ at flanges | 3.8192E-03 | 3.7500E-03 | 3.7300E-03 | 0.9819 | 0.9766 |
| LC 6 Out-of-plane moment | Average of $U_y$ at flanges | 1.5266E-02 | 1.5270E-02 | 1.5270E-02 | 1.0002 | 1.0002 |

It should be emphasized that the simplified model (i.e., coarse mesh) results can vary substantially among different structural analysis software packages. Similar benchmarks should be conducted if it is desired to use any software other than SAP 2000 Version 11, or when changing to any newly released versions of a software package.

## 4.4 Geometric Imperfections

The approach for determining the critical geometric imperfections discussed for columns in Chapter 3 can be applied for all types of bracing problems. Similar to the column bracing studies, the geometric imperfections for beam bracing should be based on the following:

- Satisfaction of the base Code of Standard Practice limits on the out-of-plumbness and the out-of-straightness in each unbraced length, but in this case, the out-of-plumbness and out-of-straightness of the compression flange.

- Affinity with the low eigenvalue buckling modes. As discussed in Section 3.3.5, it is important to note that for cases involving full bracing, the lowest eigenvalue buckling mode often involves zero brace displacement, and hence, is not the important one for the calculation of brace forces. The second lowest eigenvalue buckling mode is typically the more important mode for the bracing analysis.
- Affinity of lateral loads that are equivalent to the geometric imperfections with second-order analysis based influence lines for the brace forces. As discussed in Chapter 3, the second-order analysis based influence lines capture the important attributes pertaining to the affinity of the imperfections with the important buckling modes, while also allowing the engineer to directly consider the limits on the maximum relative deflections within each unbraced length.

Additional rules can be useful for beam type problems. Since beam lateral torsional buckling involves both a lateral deflection as well as a twist of the cross-section, it is not clear at first to what extent the cross-section should be deflected laterally or twisted to form the critical geometric imperfections.

For beam bracing problems, Wang and Helwig (2005) have considered a number of problems in which the beam was fully braced and subjected to single-curvature bending. They concluded that the most critical imperfection, assuming a maximum initial twist of $(L_b/500)/h_o$ and a maximum initial sweep of the compression flange of $L_b/500$, is the one in which the tension flange is kept straight and the section is twisted to impose the imperfect geometry on the compression flange. Cases with a maximum compression flange sweep of $L_b/500$ but with a twist imperfection smaller than $(L_b/500)/h_o$ had substantially smaller brace forces. Cases with the maximum twist of $(L_b/500)/h_o$ but with a compression flange sweep

slightly smaller than $L_b/500$ had slightly smaller brace forces. This is consistent with the results obtained by applying the approach presented in Chapter 3 to the beam cases studied by Wang and Helwig (2005). The beam buckling modes tend to involve relatively small lateral displacements of the tension flange. Also, when the brace stiffnesses are close to the values required for full bracing, cases with both the relative twist and the relative compression flange lateral deflection set to the maximum limits within the unbraced lengths adjacent to the brace under consideration tend to produce the largest forces in this brace.

The imperfection patterns shown in Fig. 4.4.1 are used to analyze the beams and beam bracing considered in this chapter. All the members have two unbraced segments and mid-span intermediate bracing. In this chapter, imperfection pattern 2 is comparable to the column out-of-plumb and out-of-straight imperfections utilized in Section 3.3.4. Imperfection 1 involves only an "out-of-plumbness" in each unbraced length. As discussed in Section 3.8.2, the imperfection "2" is more critical than imperfection "1" for column bracing. However, the beam bracing system is much more complex than the column bracing system due to the web distortional flexibility, load height and moment gradient effects. Therefore, both imperfections "1" and "2" are used in the analyses in this chapter. Appropriate geometric imperfections for cases with more than one intermediate brace are considered in Chapter 5.

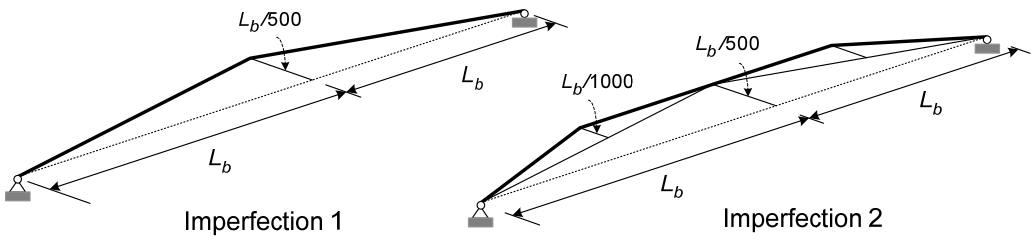


**Figure 4.4.1. Geometric imperfections considered in this research for the beam benchmarks having two unbraced segments.**

It is important to note that out-of-straightness within the unbraced length can have an important effect on the brace forces.

In the current research, the section is twisted about the bottom web-flange juncture to impose the imperfections on the compression flange for beams with single curvature. The maximum twist angle of the beam shown in Fig. 4.4.2 (a) is $L_b/500h_o$ for the refined model, where $h_o$ is the distance between flange centroids. Since the rotational continuity is released between the flanges and the web at the web-flange juncture in the simplified model, the geometric imperfections for the simplified model are generated as shown in Fig. 4.4.2(b).

For beams subjected to double-curvature bending, the section is twisted about its centroid in the studies conducted in this research, since both flanges are subjected to compression. The maximum twist angle of the beam shown in Fig. 4.4.3(a) then becomes $L_b/250h_o$ for the refined model. Likewise, the geometric imperfections for the simplified model are applied as shown in Fig. 4.4.3(b), i.e, the web in this cross-section is subjected to the same twist rotations but the flanges are modeled as untwisted. Some engineers may consider that the above value of $L_b/250h_o$ for the cross-section twist is excessive. As such, imperfections equal to $L_b/1000$ are also considered for each flange in the subsequent solutions, giving a total twist of $L_b/500h_o$.

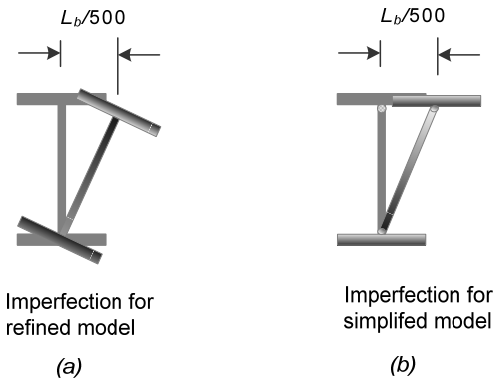


**Fig. 4.4.2. Cross-section view of geometric imperfections at the brace location for a beam subjected to single curvature bending.**

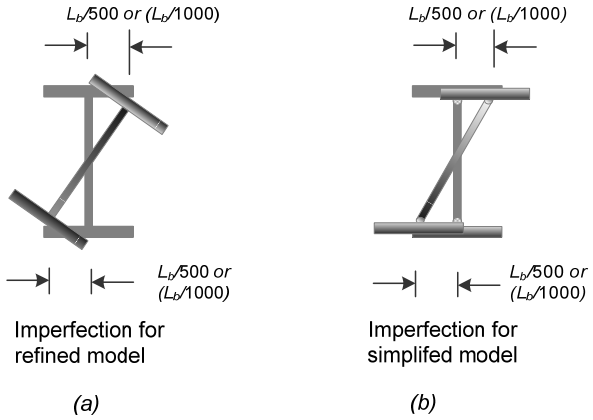


**Fig. 4.4.3. Cross-section view of geometric imperfections at the brace location for a beam subjected to double curvature bending.**

### 4.5 Calculation of Brace Stiffness Requirements by Eigenvalue Buckling Analysis

This section focuses on the use of the eigenvalue buckling analysis capabilities in SAP 2000 to estimate required beam bracing stiffnesses. As noted previously, sufficient bracing stiffness is generally essential to the stability of the structural system. Inadequate bracing stiffness can lead to large displacements or rotations in the structure; this in turn may cause large brace forces or even failure of the structure. Yura (1995) recommended that bracing stiffness values equal to two times the ideal stiffness be used to limit the brace point

displacements and the brace forces. The effect of brace stiffness on the brace forces and displacements is studied in Section 4.6.

In this research, the ideal *full* bracing stiffness is defined as the smallest brace stiffness for which the buckling strength of the ideal member is developed based on $KL_b = = L_b$ ($K$ = 1). This stiffness is denoted by the symbol $\beta_{iF}$. This may be contrasted with the general ideal stiffness, $\beta_i$, which includes $\beta_{iF}$, as well as various stiffness values for partial bracing, where the bracing is sufficient to develop a particular buckling load level smaller than that associated with the fully braced member.

In general, there are many different ideal brace stiffnesses corresponding to different degrees of partial bracing. However, in cases involving partial bracing, the bracing stiffness is not sufficient to develop the member buckling strength associated with $K = 1$. In addition, in some situations, member buckling loads larger than that associated with $K = 1$ (i.e., buckling loads associated with $K < 1$) may be developed by providing braces with a stiffness larger than $\beta_{iF}$.

In many cases, $\beta_{iF}$ is a well defined value. For all stiffnesses larger than this value, the buckling strength is a constant maximum value and the buckling displacement at the brace point(s) is zero. For stiffnesses smaller than this value, the buckling strength is reduced and the displacement at the brace point(s) is non-zero. However, for other problems, the member buckling strength approaches the maximum strength only asymptotically with increasing brace stiffness. For these types of problems, the brace displacements also are often non-zero in the governing buckling mode. In these situations, $\beta_{iF}$ should be determined as a stiffness such as the value at which, for instance, 98% of the strength corresponding to a rigid brace is achieved.

The following sub-sections demonstrate the calculation of the ideal bracing stiffnesses from the simplified and refined models, discussed in Sections 4.3.2 and 4.3.3 using the eigenvalue buckling analysis capabilities in SAP 2000. A range of benchmark problems from the prior research by Yura (2001) are investigated, including both lateral and torsional beam bracing.

### 4.5.1 Beam Lateral Bracing Benchmarks

The purpose of beam lateral bracing is not only to restrain lateral displacement but also to prevent twist of the section. There are several factors that affect the ability of the bracing to control member twisting, such as the location of braces through the section depth, the load height, and whether the beam is bent in single or double curvature. The four benchmark studies presented below illustrate the relative effectiveness of various types of beam bracing considering these factors.

#### 4.5.1.1 Benchmark Study LB1

Fig. 4.5.1 shows a simply supported W16x26 beam subjected to uniform bending moment. A single lateral brace of stiffness β is attached at the mid-span either at the top flange or at the cross-section centroid. The unbraced length is $L_b$ = 10 ft. The following bracing cases are considered:

1. Top flange brace, no stiffener.
2. Centroidal brace, no stiffener.
3. Centroidal brace with a 4x1/4 stiffener (total width, two-sided).

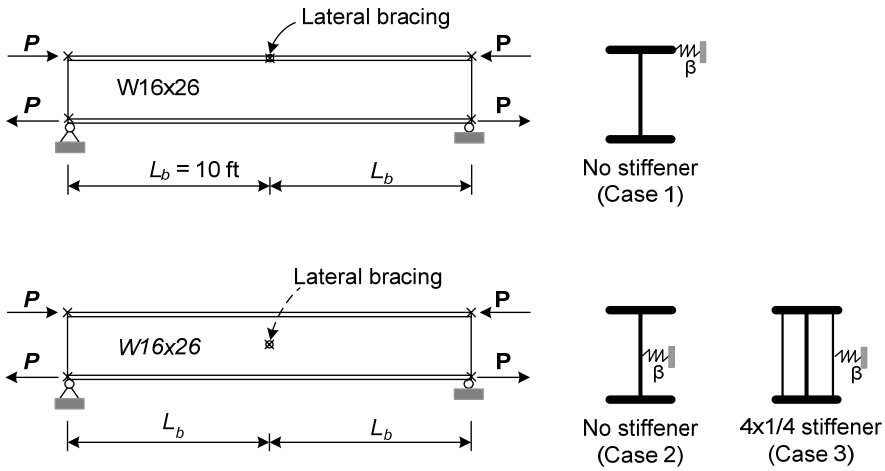


**Fig. 4.5.1. Benchmark Study LB1 – Problem description.**

The buckling modes at $\beta = \beta_{iF}$ for Case 1 are plotted in Figs. 4.5.2 and 4.5.3 for the refined and simplified models respectively. The $\beta_{iF}$ value in this case is determined as 1.58 kips/inch using the refined model and 1.51 kips/inch using the simplified model. The critical moment is $M_{cr}$ = 1616 kip-inch for the refined model and $M_{cr}$ = 1508 kip-inch for the simplified model. The $M_{cr}$ value determined from the AISC Specification LTB equation (Eq. F2-4) is $M_{cr}$ = 1617 kip-inch. The refined model matches the AISC equation very closely. This should not be surprising since AISC Eq. (F2-4) gives the exact analytical solution for this situation.

If the brace stiffness is smaller than $\beta_{iF}$ = 1.58 kips/inch in the refined model or $\beta_{iF}$ = 1.51 kips/inch in the simplified model, the beam will buckle in a shape having a single wave. If the brace stiffness is larger than these values, the beam buckles into an *S* shape and the buckling capacity does not increase if the bracing stiffness is increased further.

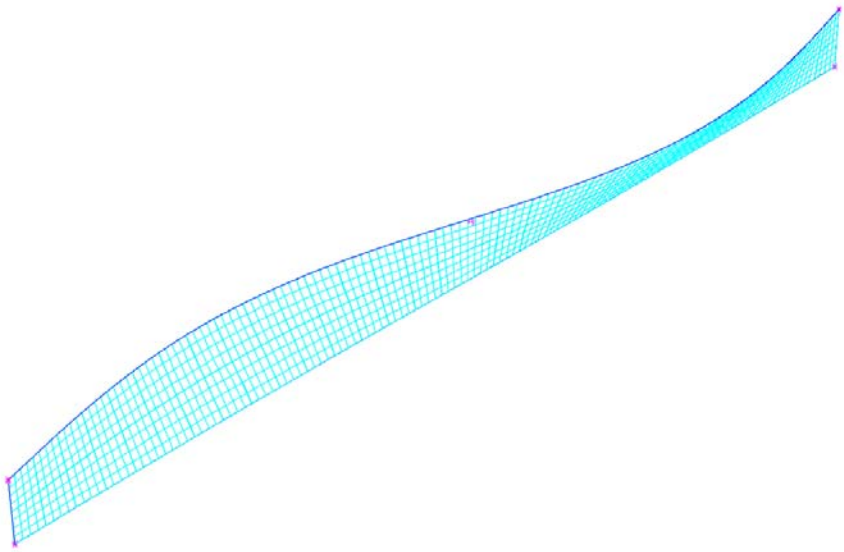

**Fig. 4.5.2. Benchmark Study LB1, Case 1 – Buckling mode at $\beta = \beta_{iF}$, refined model.**

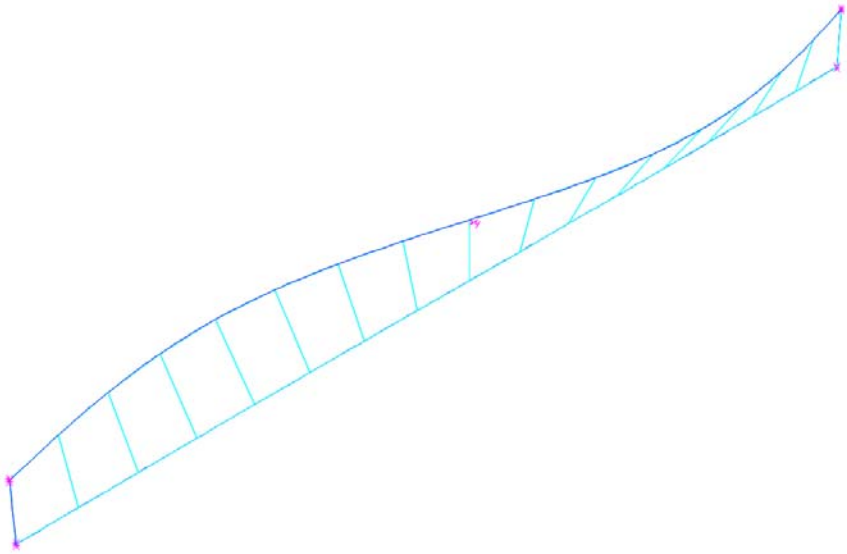

**Fig. 4.5.3. Benchmark Study LB1, Case 1 – Buckling mode at $\beta = \beta_{iF}$, simplified model.**

The normalized eigenvalue buckling moment from the refined analysis model is plotted versus the lateral brace stiffness in Fig. 4.5.4. The eigenvalue buckling result is normalized by the AISC critical moment for the case with no intermediate brace, $M_{cro}$. The $\beta_{iF}$ for a centroidal brace is 10.8 kips/inch when a 4x1/4 stiffener is employed and 50.8 kips/inch without a stiffener. That is, a much stiffer brace is needed when a transverse stiffener is not

employed. This is due to the distortion of the web in the vicinity of the centroidal lateral brace in Case 2. The refined analysis results in Fig. 4.5.4 are practically identical to those originally presented by Yura (2001).

One can observe from Fig. 4.5.4 that the top flange brace is much more effective than the centroidal brace. Also, the $\beta_{iF}$ value for the centroidal brace is substantially different depending on whether a transverse stiffener is used or not. As observed by Yura (2001), when a lateral brace is attached at the top flange, there is no cross section distortion; thus no stiffener is required at the brace point.

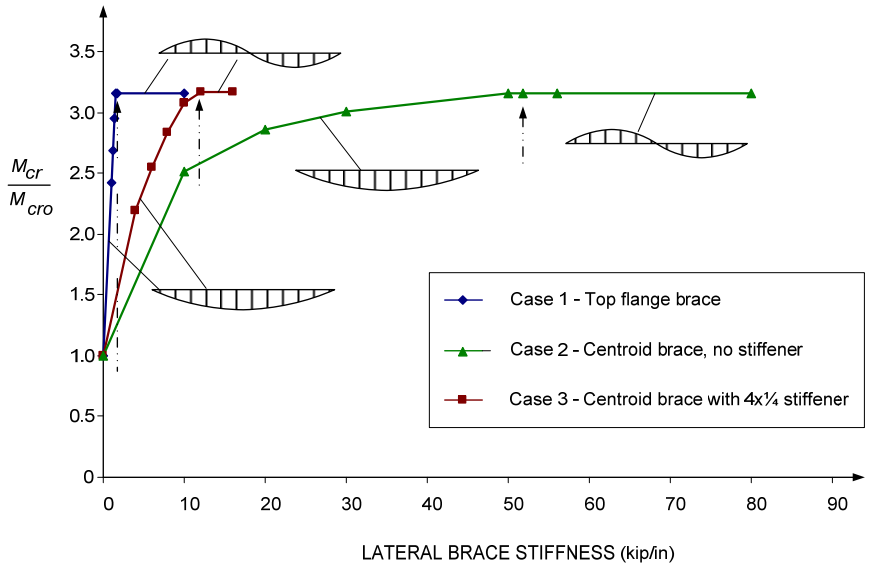


**Fig. 4.5.4. Benchmark Study LB1 – Eigenvalue buckling results, refined model.**

Fig. 4.5.5 compares the results between the refined and simplified models for Benchmark Study LB1. The simplified analysis models give $M_{cr}$ values of 90 to 93 % of the critical moment from the refined models over the complete range of β values. The simplified analysis models give $\beta_{iF}$ values of 96 to 103 % of the corresponding refined analysis $\beta_{iF}$ values.

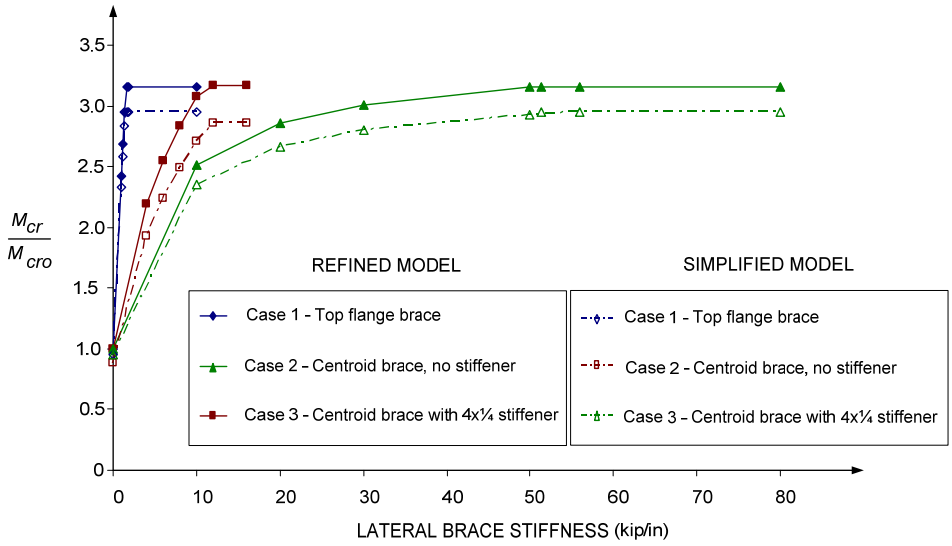


**Fig. 4.5.5. Benchmark Study LB1 – Comparison of eigenvalue buckling results between the refined and simplified models.**

4.5.1.2 Benchmark Study LB2

The Benchmark Study LB1 shows that for a simply supported beam subjected to positive uniform bending moment, a top flange lateral brace is the most effective. In this section, the same beam is considered; however, instead of applying uniform bending moment, the beam is subjected to moment gradient. A concentrated vertical load is applied to the cross-section centroid at the mid-span as shown in Fig. 4.5.6.

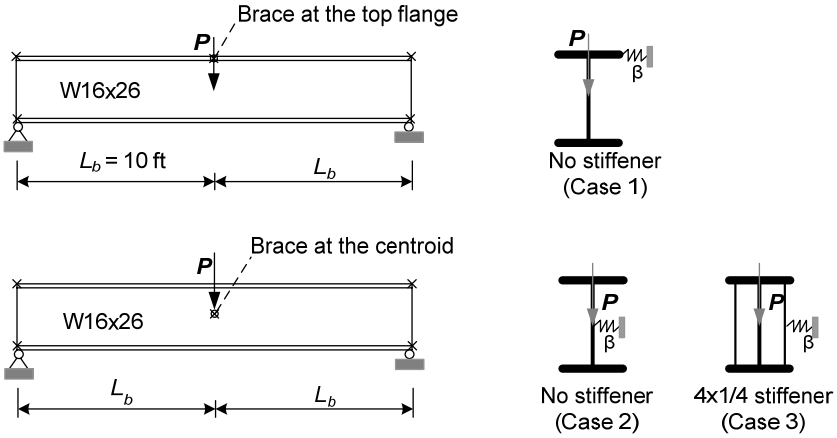


**Fig. 4.5.6. Benchmark Study LB2 – Problem description.**

The buckling modes at $\beta = \beta_{iF}$ for the top flange brace case (Case 1) are plotted in Figs. 4.5.7 and 4.5.8 for the refined and simplified models respectively. The ideal brace stiffness for full bracing in this case is determined as $\beta_{iF} = 3.7$ kips/inch using the refined model and $\beta_{iF} = 3.3$ kips/inch using the simplified model. The critical moment is $M_{cr} =$ = 2868 kip-inch for the refined model and is $M_{cr} = 2825$ kip-inch for the simplified model. The elastic critical moment calculated from the AISC Specification LTB equation (Eq. F2-4) is $M_{cr} =$ 2829 kip-inch using the approximate moment gradient modifier $C_b = 1.75$ (AISC Eq. C-F1-1). The refined model gives an eigenvalue buckling load very close to this AISC solution.

The normalized eigenvalue buckling moment from the refined analysis model is plotted versus the lateral brace stiffness in Fig. 4.5.9. The $\beta_{iF}$ value for a centroidal brace is 110 kips/inch with a 4x1/4 stiffener (Case 3) and 140 kips/in without a stiffener (Case 2). However, the buckling load versus brace stiffness curves for these two cases are very flat at these stiffness values. There is actually little difference between the curves for Cases 2 and 3. The refined analysis results in Fig. 4.5.9 are practically identical to those originally presented by Yura (2001).

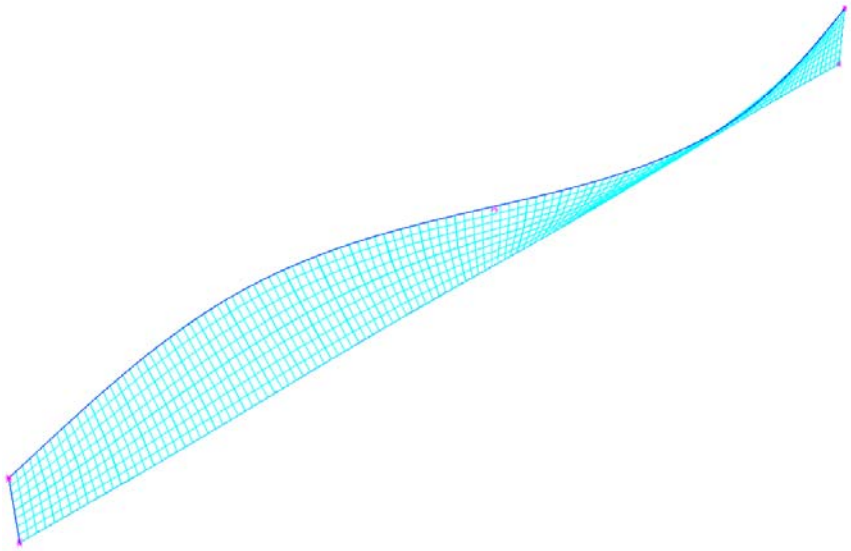

**Fig. 4.5.7. Benchmark Study LB2, Case 1 – Buckling mode at $\beta = \beta_{iF}$, refined model.**

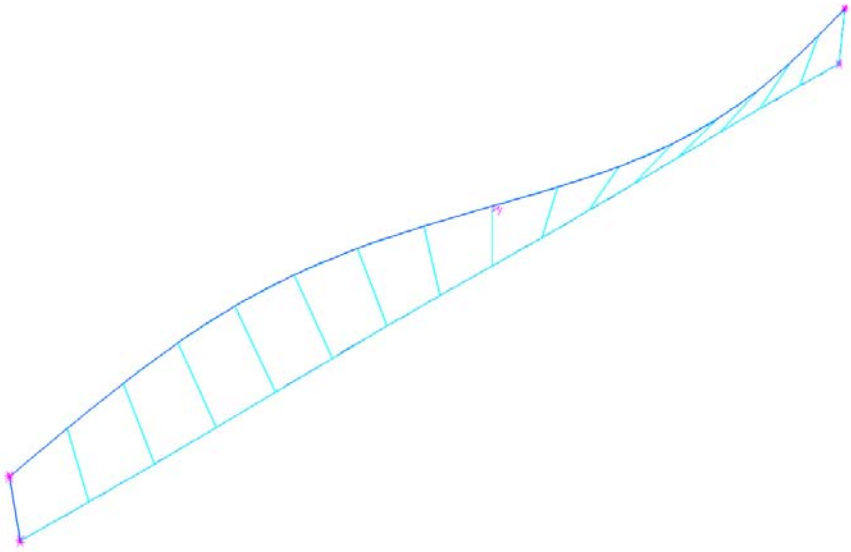

**Fig. 4.5.8. Benchmark Study LB2, Case 1 – Buckling mode at $\beta = \beta_{iF}$, simplified model.**

One can observe from Fig. 4.5.9 that the top flange brace is much more effective than the centroidal brace. Also, the eigenvalue buckling results for the case of the centroidal

brace are similar with or without a transverse stiffener for this loading. This indicates that cross-section distortion has a minor effect in this problem.

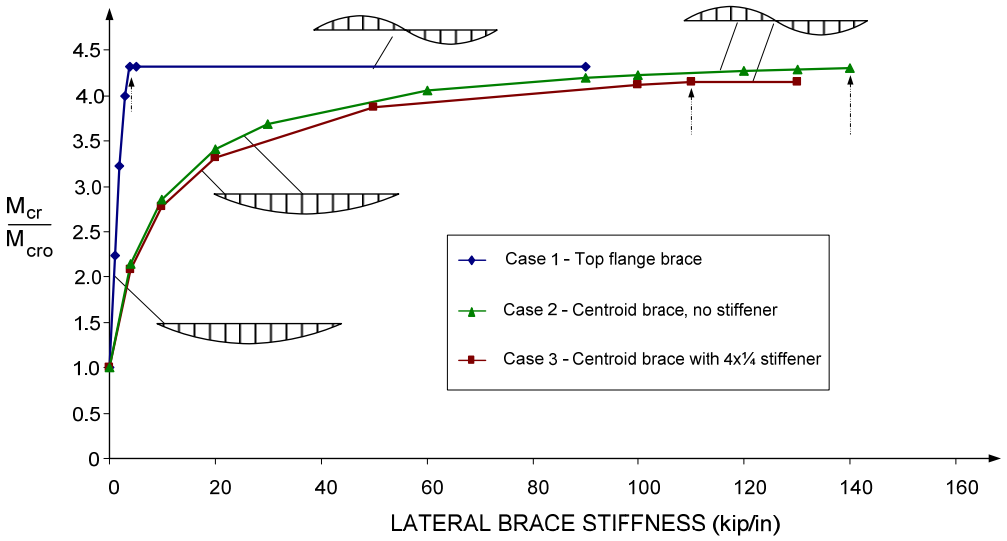


**Fig. 4.5.9. Benchmark Study LB2 – Eigenvalue buckling results, refined model.**

Comparisons of the eigenvalue buckling results from the refined and simplified models are shown in Fig. 4.5.10. The simplified analysis models give $M_{cr}$ values of 98 to 108 % of the critical moment from the refined models over the complete range of β values. The simplified analysis models give $\beta_{iF}$ values of 42 to 89 % of the corresponding refined analysis $\beta_{iF}$ values. The large errors in the simplified model $\beta_{iF}$ occur in the centroidal brace case. One of the reasons to explain this phenomenon is that the brace is attached in the centroid of cross-section. Due to the effects of web flexibility, the full bracing strength is approached very gradually when the brace stiffness is increased. The accuracy of the simplified model in predicting $P_{cr}$ for a given lateral brace stiffness is reasonably good.

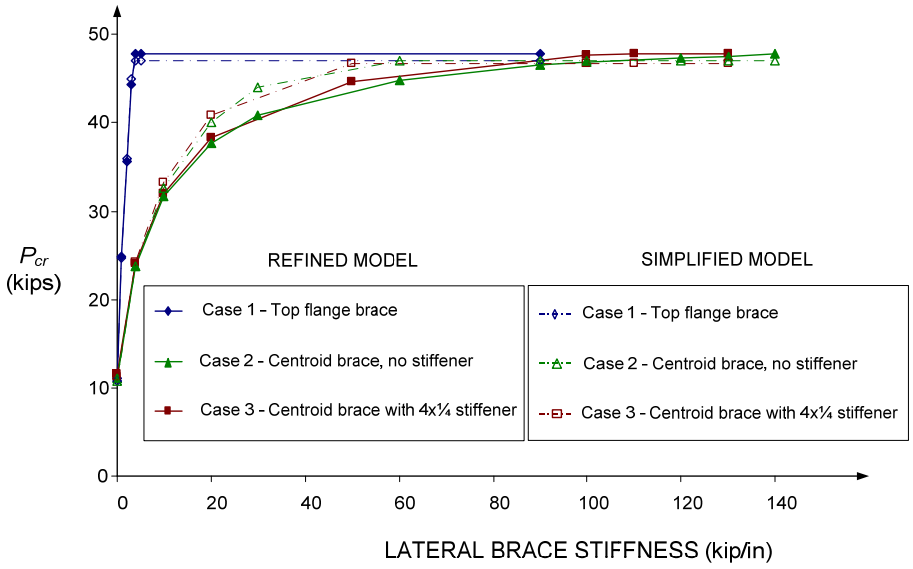


**Fig. 4.5.10 Benchmark Study LB2 – Comparison of eigenvalue buckling results between the refined and simplified models.**

4.5.1.3 Benchmark Study LB3

The effects of brace position and moment gradient on the elastic buckling capacity of a simply supported beam are studied in Benchmark Studies LB1 and LB2. In this section, the load height effect on the beam bracing behavior is illustrated.

Fig. 4.5.11 shows the same simply supported W16x26 beam as in the previous studies, with a single lateral brace attached to mid-span either at the top flange or at the cross-section centroid. The unbraced length is again $L_b$ = 10 ft. A two-sided 4x1/4 stiffener is used at the brace point to prevent cross-section distortion in all of the following cases. The concentrated load is applied at the centroid or at the top flange to investigate the load height effect. Three loading and/or bracing cases are considered:

1. Top flange brace, load at top flange.
2. Top flange brace, load at centroid.
3. Centroidal brace, load at top flange.

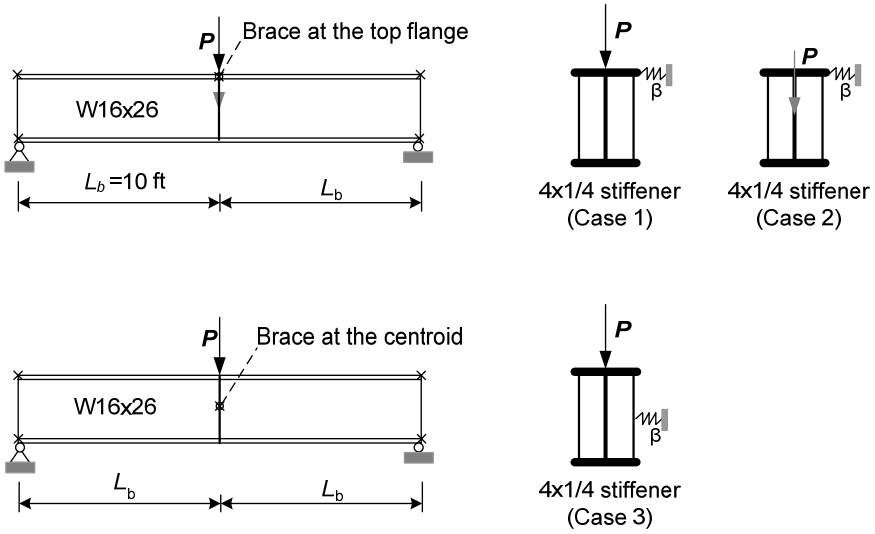


**Fig. 4.5.11. Benchmark Study LB3 – Problem description.**

The buckling modes at the $\beta_{iF}$ value for the top flange brace (Case 1) from the refined and simplified models are shown in Figs. 4.5.12 and 4.5.13. For the refined model, the $\beta_{iF}$ value is determined as 6.1 kips/inch and the critical moment is $M_{cr}$ = 2872 kip-inch. For the simplified model, the $\beta_{iF}$ value is determined as 5.5 kips/inch and the critical moment is $M_{cr}$ = 2820 kip-inch. The elastic critical moment determined from the AISC Specification LTB equation (Eq. F2-4) is $M_{cr}$ = 2829 kip-inch.

The normalized eigenvalue buckling moment versus the lateral brace stiffness for the refined analysis model are plotted in Fig. 4.5.14. The $\beta_{iF}$ value for the case with a top flange brace and the load at the centroid (Case 2) is approximately 2.5 kips/inch. As noted by Yura (2001), the top flange loading causes the center of twist of the cross section to be close to the cross-section mid-depth. This dramatically reduces the effectiveness of the centroidal brace.

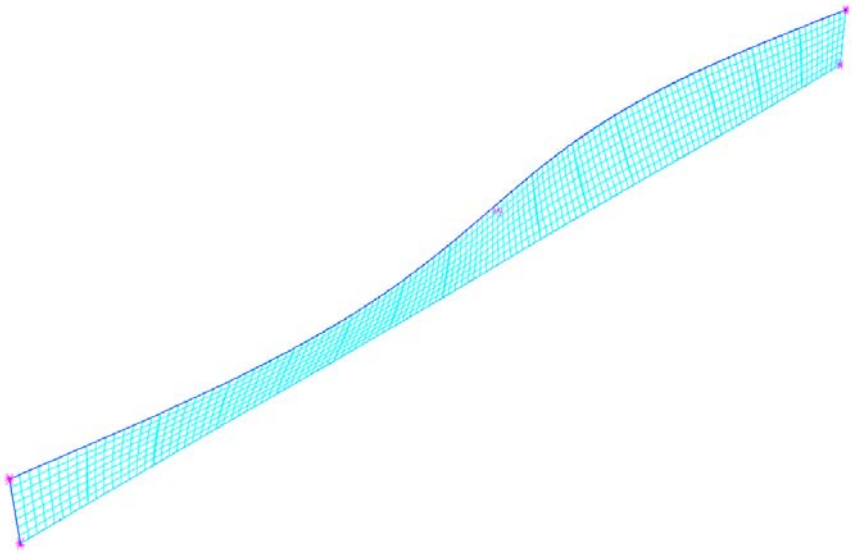

**Fig. 4.5.12. Benchmark Study LB3, Case 1 – Buckling mode at $\beta = \beta_{iF}$, refined model.**

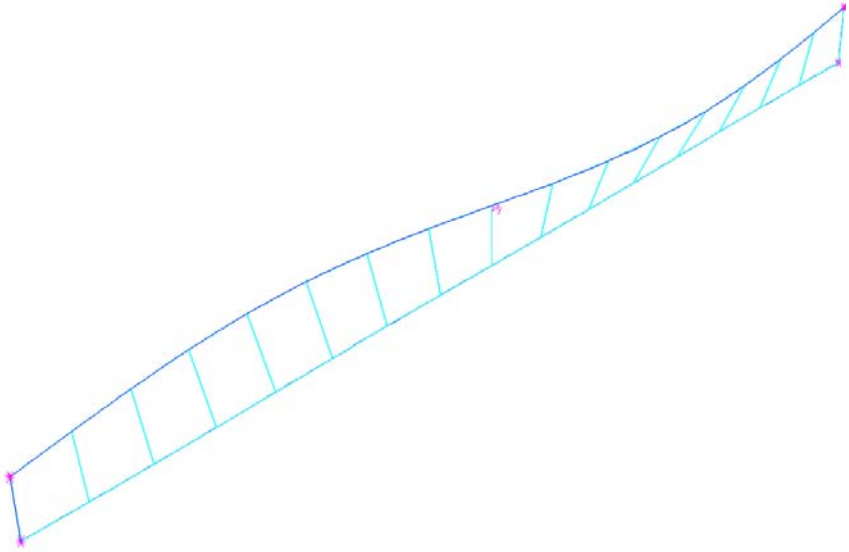

**Fig. 4.5.13. Benchmark Study LB3, Case 1 – Buckling mode at $\beta = \beta_{iF}$, simplified model.**

The refined analysis results in Fig. 4.5.14 are practically identical to those originally presented by Yura (2001). Fig. 4.5.14 shows that the load position significantly affects the brace stiffness required to reach full bracing. For the load at the centroid (Case 2), the ideal

brace stiffness for full bracing is approximately 2.5 kips/inch while for the load at the top flange (Cases 1 and 3), the ideal brace stiffness for full bracing is approximately 6.1 kips/inch. It should be noted that the centroidal brace is quite ineffective when the load is applied at the top flange. This benchmark study shows that the brace stiffness demand is quite sensitive to the load height.

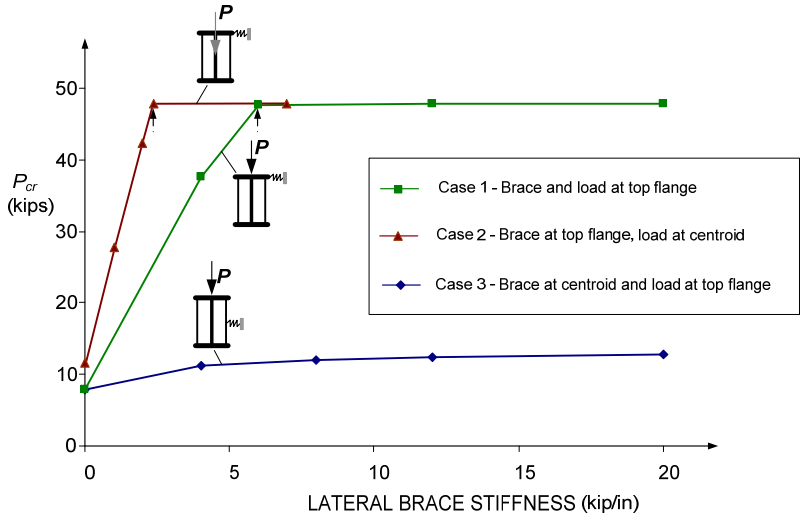


**Fig. 4.5.14. Benchmark Study LB3 – Eigenvalue buckling results, refined model.**

Fig. 4.5.15 compares the results from the refined and simplified analysis models. This figure shows that the simplified analysis models give $M_{cr}$ values of 97 to 102 % of the critical moment from the refined models over the complete range of β values. For the cases with the brace at the top flange, the simplified analysis models give $\beta_{iF}$ values of approximately 90% of the corresponding refined analysis $\beta_{iF}$ values.

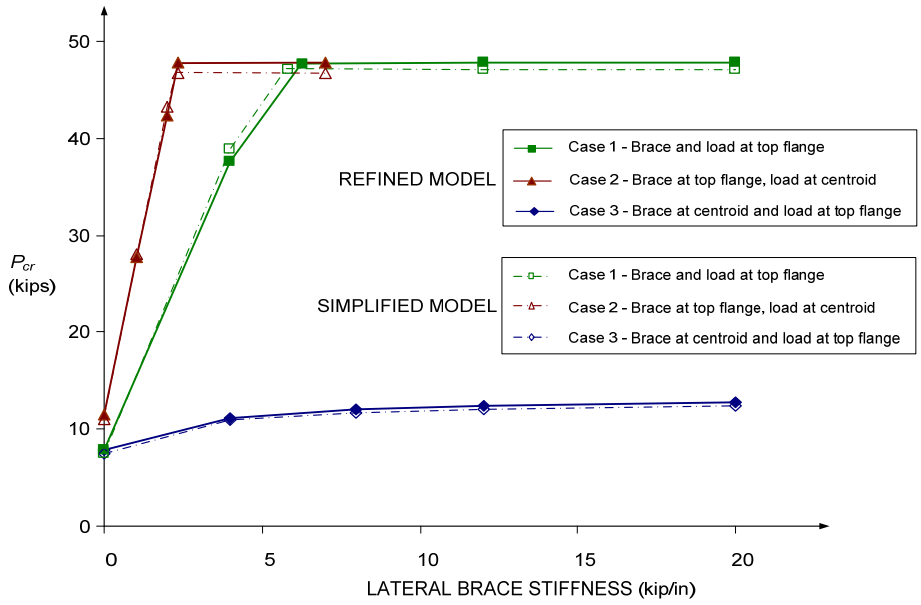


**Fig. 4.5.15. Benchmark Study LB3 – Comparison of eigenvalue buckling results between the refined and simplified models.**

4.5.1.4 Benchmark Study LB4

Benchmark studies LB1 to LB3 address the beam bracing behavior for segments subjected to single curvature. In this section, the beam bracing behavior is discussed for a loading producing fully reversed-curvature bending. Fig. 4.5.16 shows a simply supported W16x26 beam (same cross section and unbraced lengths as in the previous cases) subjected to equal end moments. No stiffener is provided at the intermediate brace point. The unbraced length is again $L_b$ = 10 ft. Two cases are considered:

1. Only the top flange laterally braced.
2. Top and bottom flanges laterally braced.

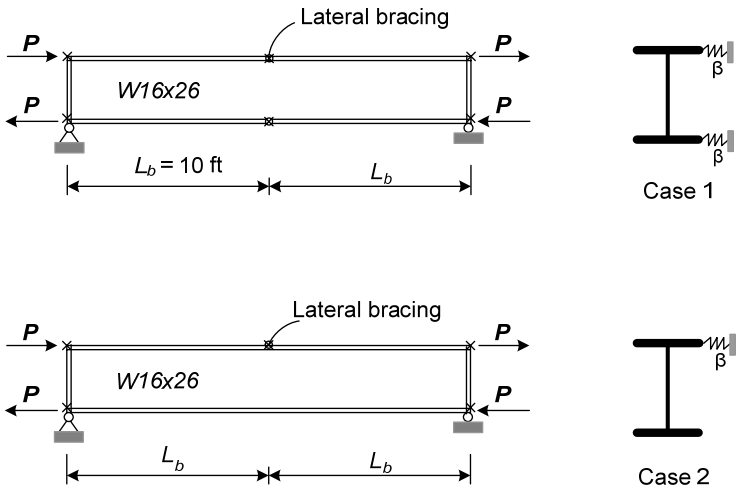


**Fig. 4.5.16. Benchmark Study LB4 – Problem description.**

The buckling modes at $\beta = \beta_{iF}$ with bracing at both the top and bottom flanges (Case 2) are plotted in Figs. 4.5.17 and 4.5.18 for the refined and simplified models respectively. The ideal brace stiffness for full bracing in this case is determined as approximately $\beta_{iF} = 19$ kips/inch for the refined model and $\beta_{iF} = 22$ kips/inch for the simplified model. The corresponding critical moment is $M_{cr} = 3391$ kip-inch for the refined model and $M_{cr} = 3417$ kip-inch for the simplified model. The critical moment from the AISC Specification LTB equation (Eq. F2-4) is $M_{cr} = 2829$ kip-inch. The reason for the significantly larger buckling moments in the finite element analyses compared to the AISC equation is due to the warping continuity across the brace at the mid-span. The $M_{cr}$ in the refined and simplified models is approximately 20% larger than that determined from the AISC LTB equation using $K = 1$.

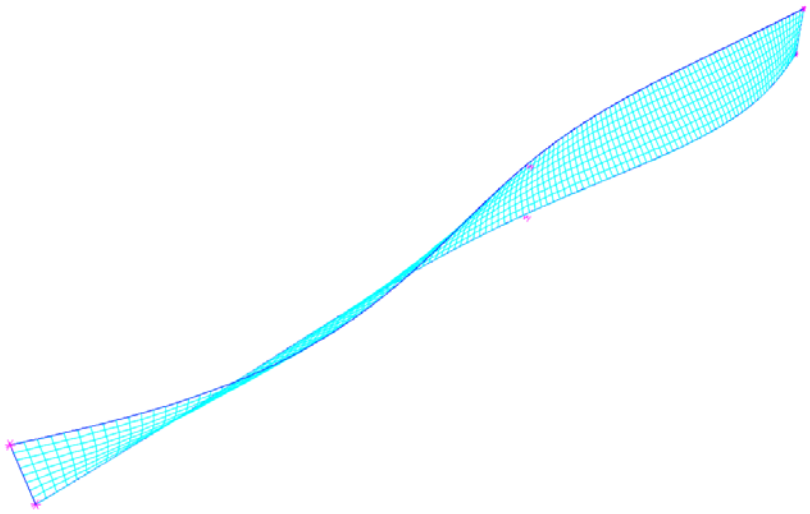

**Fig. 4.5.17. Benchmark Study LB4, Case 2 – Buckling mode at $\beta = \beta_{iF}$ for full bracing, refined model.**

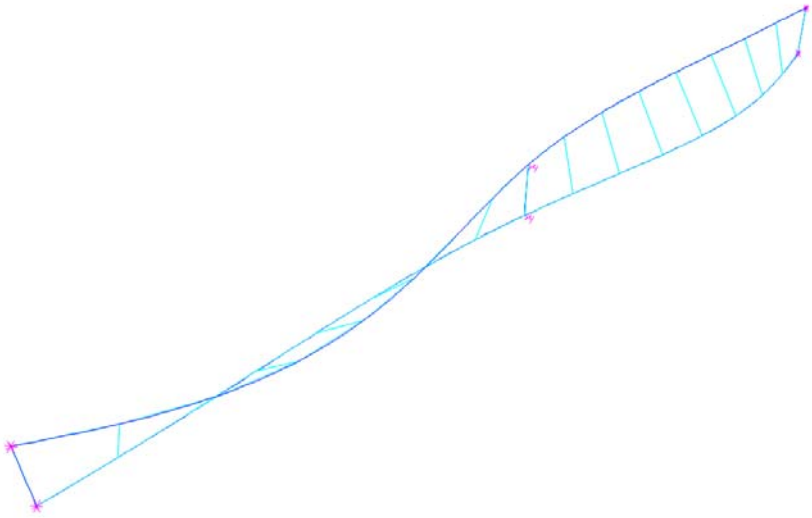

**Fig. 4.5.18 Benchmark Study LB4, Case 2 – Buckling mode at $\beta = \beta_{iF}$ for full bracing, simplified model.**

The eigenvalue buckling moments from the refined analysis model are plotted versus the lateral brace stiffness in Fig. 4.5.19. One can observe from Fig. 4.5.19 that providing a brace only at the top flange is not effective. This is because the twist of the cross-section at the brace point is not prevented. For beams subjected to double-curvature bending, the

inflection point cannot be considered as a brace point because twist occurs at that point. This confirms the discussion of this issue in references such as (Galambos,1998).

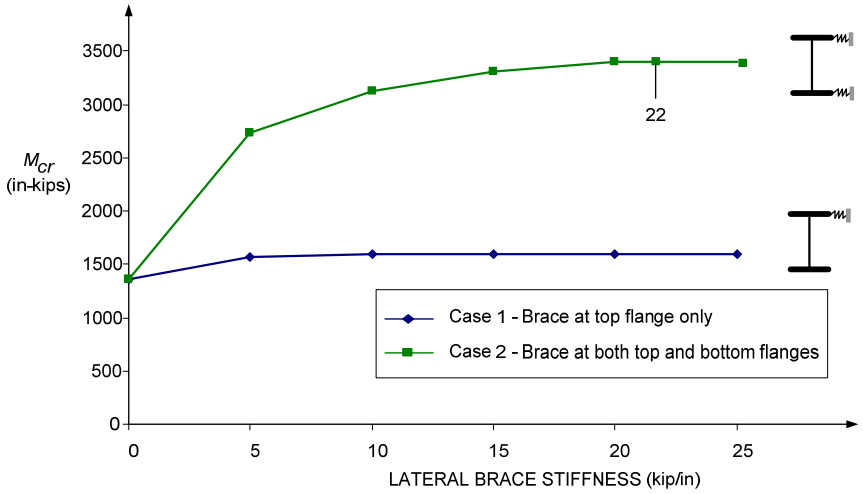


**Fig. 4.5.19. Benchmark Study LB4 – Eigenvalue buckling results, refined model.**

The above results show that lateral braces should be provided at both the top and the bottom flanges for the bracing to be effective near inflection point locations.

Fig. 4.5.20 compares the results between the refined and simplified analysis models for Benchmark Problem LB4. The refined analysis results in Fig. 4.5.19 are practically identical to those originally presented by Yura (2001). The simplified analysis models give $M_{cr}$ values of 86 to 101 % of the critical moment from the refined models over the complete range of β values and load-displacement boundary conditions considered. For this case, the behavior is asymptotic as the brace point stiffnesses are increased. Therefore, the $\beta_{iF}$ values are sensitive to minor changes in the models.

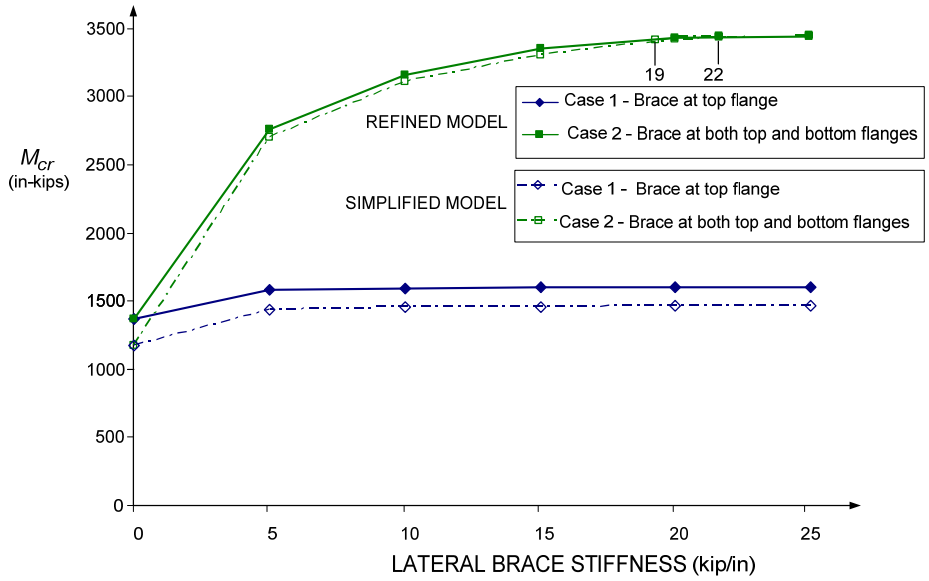


**Fig. 4.5.20. Benchmark Study LB4 – Comparison of eigenvalue buckling results between the refined and simplified models.**

### 4.5.2 Torsional Beam Bracing Benchmarks

The purpose of any beam bracing is to prevent lateral displacement and twist of the section. However, with lateral bracing, the lateral displacement of the compression flange (or some other location on the cross-section) is prevented directly while the twist of the section is not directly prevented (unless there are multiple lateral braces). That is, considering Cases 1 and 2 of Benchmark Problem LB3 for example, the lateral brace does not provide any explicit restraint against cross-section twisting at the brace location. Conversely, with torsional bracing, the twist of the cross section is restrained directly whereas the lateral displacement is restrained indirectly. In this section, two torsional bracing case studies that illustrate the effects of moment gradient, load height effect, and cross section distortion are investigated.

4.5.2.1 Benchmark Study TB1

Fig. 4.5.1 shows the simply supported W16x26 beam subjected to uniform bending moment. A single torsional brace is attached to the top flange at the mid-span. The unbraced length is $L_b$ = 10 ft and the stiffness is β. Three bracing cases are considered:

1. 4x1/4 stiffener
2. 2.67x1/4 stiffener
3. No stiffener

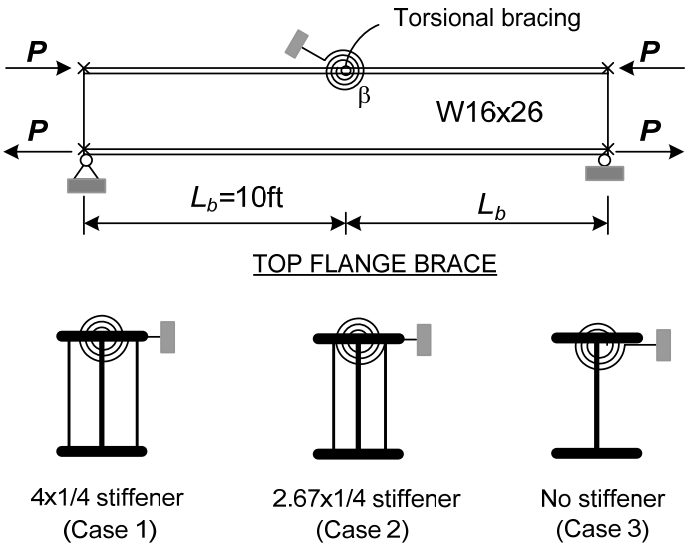


**Fig. 4.5.21. Benchmark Study TB1 – Problem description.**

The buckling modes at $\beta = \beta_{iF}$ for Case 1 are plotted in Figs. 4.5.22 and 4.5.23 from the refined and simplified models respectively. The $\beta_{iF}$ in this case is determined as 1799 kip-inch/rad using the refined model and 1550 kip-inch/rad using the simplified model. The critical moment is $M_{cr}$ = 1616 kip-inch from the refined model and $M_{cr}$ = 1500 kip-inch from the simplified model. As noted previously, the $M_{cr}$ determined from the AISC Eq. F2-4 is 1617 kip-inch.

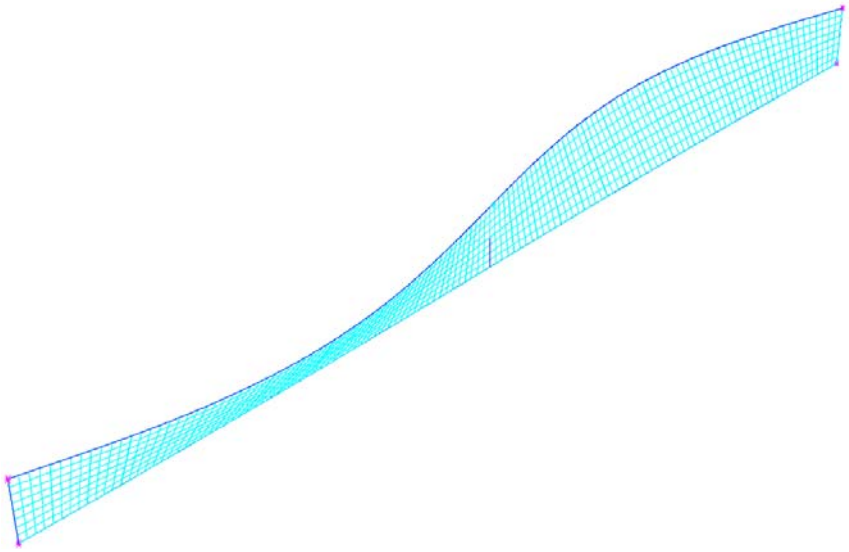

**Fig. 4.5.22. Benchmark Study TB1, Case 1 – Buckling mode at $\beta = \beta_{iF}$, refined model.**

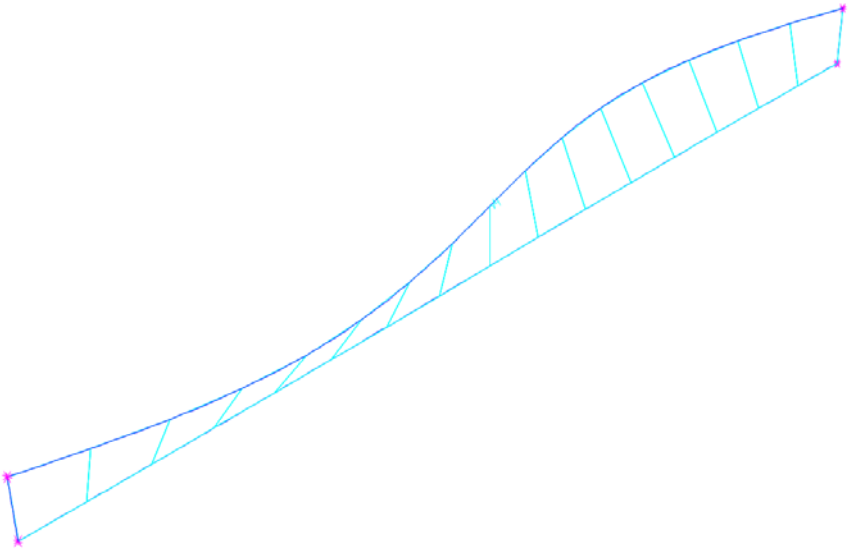

**Fig. 4.5.23 Benchmark Study TB1, Case 1 – Buckling mode at $\beta = \beta_{iF}$, simplified model.**

The eigenvalue buckling results versus the torsional brace stiffness for the refined analysis model are plotted in Fig. 4.5.24. These results are practically identical to those originally presented by Yura (2001). The $\beta_{iF}$ value is approximately 3650 kip-inch/rad with a 2.67x1/4 stiffener (Case 2). One can observe from Fig. 4.5.24 that the cross section

distortion at the brace point is an important factor affecting the torsional bracing effectiveness. The buckling capacity of the beam with a torsional brace attached to the top flange but no stiffener at the brace point can be increased only 1.5 times compared to the buckling moment for the unbraced beam. However, when the transverse stiffeners are used, the buckling capacity of the braced beam can be increased approximately 3.3 times compared to the unbraced beam. This example shows that a discrete torsional brace attached to the compression flange does not work very well unless a transverse stiffener is provided.

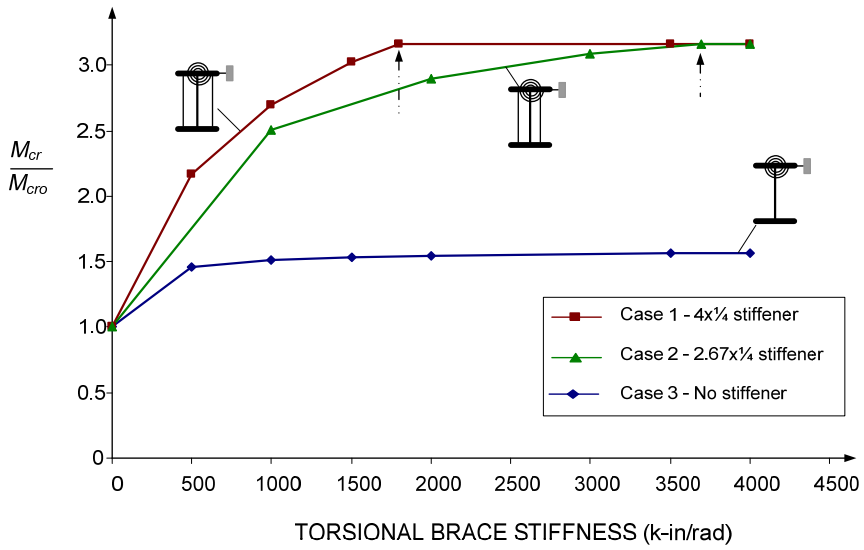


**Fig. 4.5.24. Benchmark Study TB1 – Eigenvalue buckling results, refined model.**

Fig. 4.5.25 compares the results between the refined and simplified analysis models. The simplified analysis models give $M_{cr}$ values of 92 to 98 % of the critical moment from the refined analysis models over the complete range of β values. For the cases with the transverse stiffeners, the simplified analysis models give $\beta_{iF}$ values of approximately 83 to 86 % of the corresponding refined analysis $\beta_{iF}$ values.

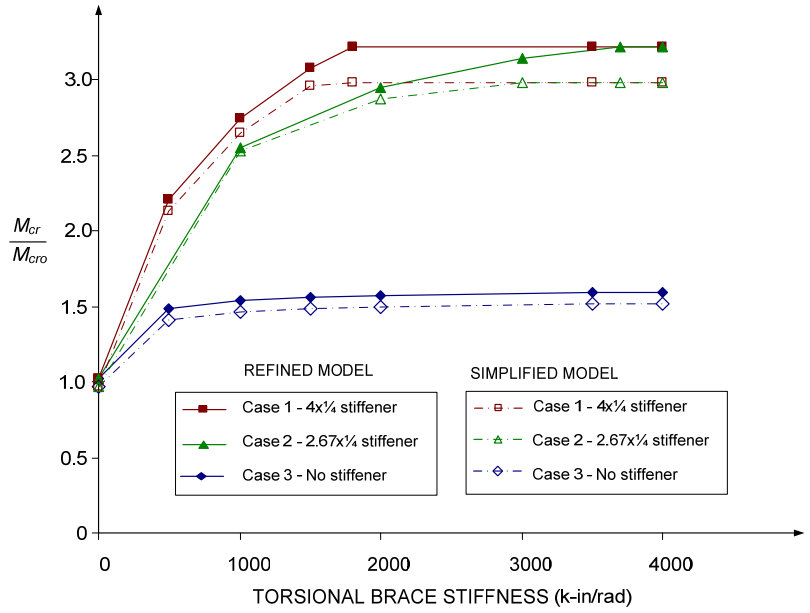


**Fig. 4.5.25 Benchmark Study TB1 – Comparison of eigenvalue buckling results between the refined and simplified models.**

4.5.2.2 Benchmark Study TB2

This study considers the beam shown as Case 1 from Benchmark Study TB1. However, instead of applying uniform moment, the transverse load *P* is applied at the midspan of beam as shown in Fig. 4.5.26. This problem focuses on the effect of load height and moment gradient on the torsional bracing stiffness requirements.

The two loading cases are considered as follows:

1. Concentrated vertical load applied at the top flange.
2. Concentrated vertical load applied at the centroid.

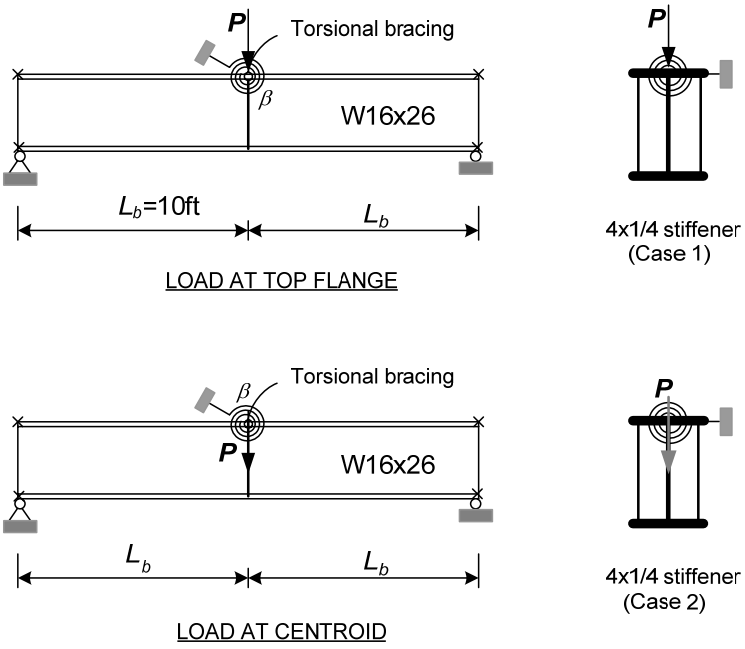


**Fig. 4.5.26. Benchmark Study TB2 – Problem description.**

The buckling modes at $\beta = \beta_{iF}$ for the case of the concentrated vertical load applied at the top flange (Case 1) are shown in Figs. 4.5.27 and 4.5.28 for the refined and simplified models respectively. The ideal brace stiffness for $\beta = \beta_{iF}$ in this case is determined as 4000 kips/inch for the refined model and 3800 kips/inch for the simplified model. The critical moment is $M_{cr}$ = 2872 kip-inch for the refined model and is $M_{cr}$ = 2820 kip-inch for the simplified model. The elastic critical moment determined from the AISC Specification LTB equation (F2-4) is $M_{cr}$ = 2830 kip-inch.

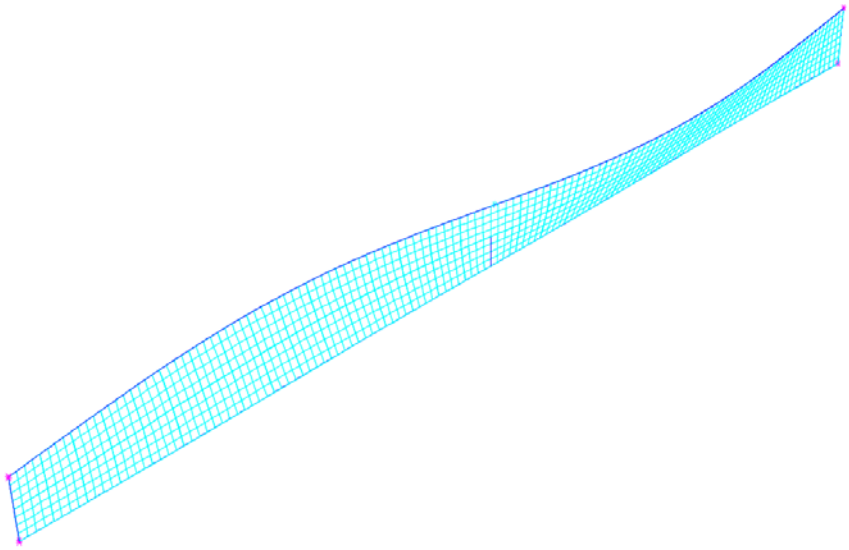

**Fig. 4.5.27. Benchmark Study TB2, Case 1 – Buckling mode at $\beta = \beta_{iF}$, refined model.**

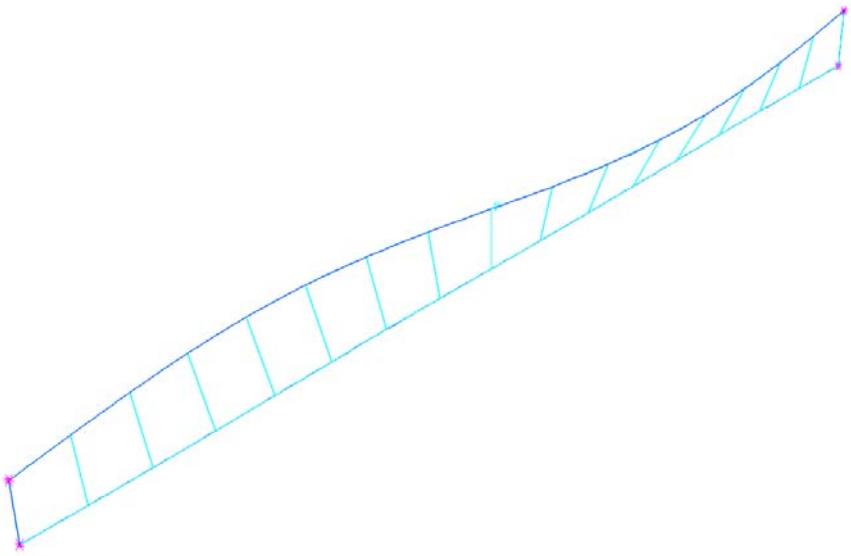

**Fig. 4.5.28. Benchmark Study TB2, Case 1 – Buckling mode at $\beta = \beta_{iF}$, simplified model.**

The refined analysis results, shown in Fig. 4.5.29, are practically identical to those originally presented by Yura (2001). The $\beta_{iF}$ value for the case of load applied at the centroid (Case 2) is approximately 3500 kip-inch/rad. Fig. 4.5.29 indicates that the load

height effect does not have a significant influence on the torsional bracing response for this problem. The $\beta_{iF}$ value for the case with the load applied at the top flange is approximately 1.1 times larger than that for the case with the load applied at the centroid. On the other hand, for Benchmark Study LB3 in Section 4.5.1.3, the $\beta_{iF}$ value with the load applied at the top flange is approximately 2.4 times that with the load applied at the centroid (6.1 kips/inch vs. 2.5 kips/inch).

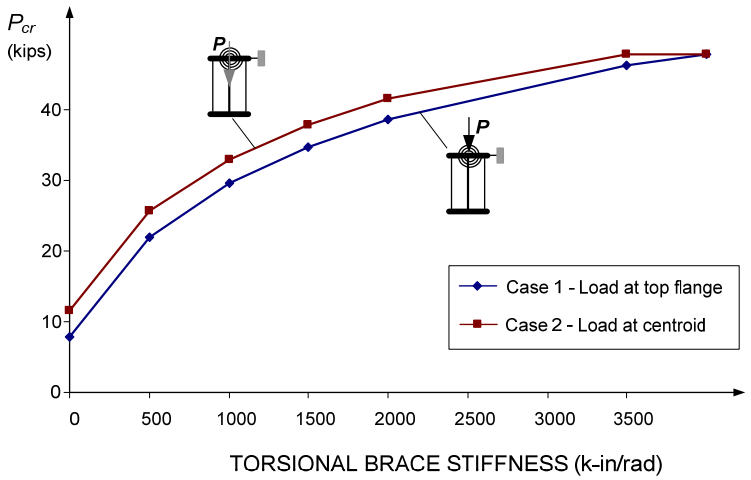


**Fig. 4.5.29. Benchmark Study TB2 – Eigenvalue buckling results, refined model.**

Fig. 4.5.30 compares the results between the refined and simplified models. The simplified analysis models give $M_{cr}$ values of 98 to 100 % of the critical moment obtained from the refined model over the complete range of β values. The simplified analysis models give $\beta_{iF}$ values that are very close to the refined analysis $\beta_{iF}$ values.

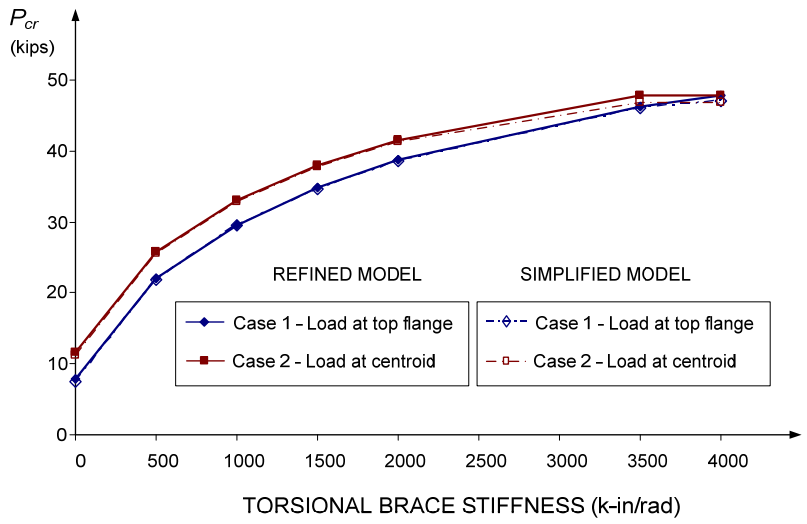


**Fig. 4.5.30. Benchmark Study TB2 – Comparion of eigenvalue buckling results between the refined and simplified models.**

## 4.6 Calculation of Brace Force Requirements by Second-Order Elastic Load-Deflection Analysis

The eigenvalue buckling analyses discussed in Section 4.5 can be used only to determine the brace stiffness requirements. These analyses provide no information about the required brace strengths. In order to fundamentally assess the brace strength requirements, a second-order load-deflection analysis of the geometrically imperfect beam must be used. In this section, second-order elastic load-deflection analyses are conducted to determine the brace forces for both lateral and torsional bracing. The results are compared to the strength requirements from AISC Appendix 6. One should note that the selection of the critical initial imperfections influences the lateral displacement and twist of the beam, and thus influences the brace forces. The critical imperfections for the following analyses are determined as discussed in Section 4.4.

### 4.6.1 Beam Lateral Bracing

The most efficient bracing configurations from Benchmark Studies LB1 to LB4 are analyzed in this section. For each of the benchmark problems, two brace stiffnesses are considered. First, the brace stiffness is estimated based on the AISC Appendix 6, that is, $\beta = 2\beta_{iF}/\phi \approx 2.67\ \beta_{iF}$. The second brace stiffness is used based on the reduced stiffness value, i.e., $\beta = 1.9\beta_{iF}$ ($\beta_{iF}$ determined in this section using the AISC Appendix 6 equations). This reduced stiffness is found by studying the column bracing problems with only a single intermediate brace (see Section 3.8.2). The requirements from the most refined versions of the AISC Appendix 6 equations are provided and compared to the above values for each of the benchmark problems.

#### 4.6.1.1 Benchmark Study LB1

Fig. 4.6.1 shows a simply supported W16x26 beam with a top flange brace and no transfer stiffener subjected to the uniform bending (Case 1 of the Benchmark Study LB1). The results from the eigenvalue buckling analyses showed that the ideal brace stiffness is $\beta_{iF(SAP)} = 1.58$ kips/inch using the refined model and $\beta_{iF(SAP)} = 1.51$ kips/inch using the simplified model.

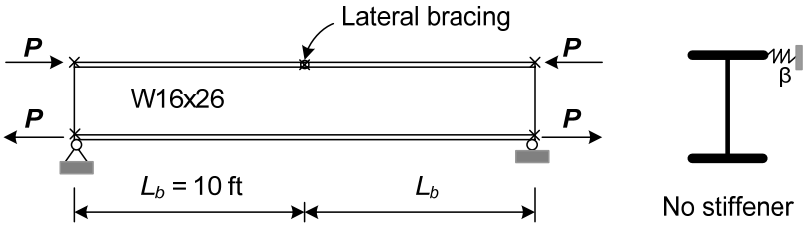


**Fig. 4.6.1. Load-deflection analysis, Benchmark Study LB1, Case 1 – Problem description.**

*4.6.1.1.1 Brace Requirements based on the AISC 2005 Appendix 6 Commentary*

According to the equations from the Commentary of AISC Appendix 6, the brace stiffness and strength requirements can be calculated as follows:

- Brace stiffness requirement ($\beta_{br}$):

$$\beta_{br} = \frac{2\beta_{iF(App\ 6)}}{\phi} \tag{4.6-1}$$

where $\beta_{iF(App\ 6)}$ is the Appendix 6 estimate of the ideal brace stiffness for full bracing

$$\beta_{iF(App\ 6)} = \frac{N_i C_b P_f}{L_b} C_d C_t \tag{4.6-2}$$

- Brace strength requirement ($P_{br}$):

$$P_{br} = \frac{(0.01) M_{cr}}{h_o} C_d C_t \tag{4.6-3}$$

where

$N_i = 4 - \frac{2}{n}$

$n$ = number of intermediate braces

$C_b$ = moment modifier

$C_d$ = double curvature factor

$C_d$ = 1.0 for single curvature

$C_d$ = 2.0 for double curavature

$C_t$ = accounts for top flange loading; $C_t$ = 1+ (1.2*/n)*

$C_t$ = 1.0 for centroidal loading

$P_f$ = beam compressive flange force; $P_f = \frac{\pi^2 E I_{yc}}{L_b^2}$

$I_{yc}$ = out-of-plane moment of inertia of the compression flange; $I_{yc}=I_y/2$ for doubly-symmetric cross sections.

For this problem, $n = 1$ (single brace). Therefore, $N_i = 2$. Also, $C_b = 1$, because of the uniform bending moment, $C_d = 1.0$, $C_t = 1.0$, $L_b = 120$ inch, and

$$P_f = \frac{\pi^2 EI_{yc}}{L_b^2} = \frac{\pi^2 (29000)(9.59/2)}{120^2} = 95.3 \text{ kips}$$

By combining the above results, the ideal full bracing stiffness is obtained as

$$\beta_{iF(App\ 6)} = \frac{N_i C_b P_f}{L_b} C_d C_t = \frac{2(1)(95.3)}{120} 1(1) = 1.59 \text{ kips/inch}$$

and the required brace stiffness is obtained as

$$\beta_{br} = \frac{2\beta_{iF(App\ 6)}}{\phi} = \frac{2(1.59)}{0.75} = 4.24 \text{ kips/inch}$$

In addition, the required brace strength (at $M = M_{cr}$) is

$$P_{br} = \frac{(0.01)M_{cr}}{h_o} C_d C_t = \frac{(0.01)(1617)}{15.355} 1(1) = 1.05 \text{ kips} = 0.01\frac{M_{cr}}{h_o}$$

*4.6.1.1.2 Load-Deflection Results using $\beta = 2\beta_{iF(SAP)}/\phi$*

Fig. 4.6.2 shows the load-deflection analysis results from SAP 2000 using the brace stiffness

$$\beta_{br(SAP)} = \frac{2\beta_{iF(SAP)}}{\phi} = \frac{2(1.58)}{0.75} = 4.21 \text{ kips/inch}$$

from the refined FEA model. The figure shows the normalized applied moment $M / M_{cr}$ versus the normalized bracing force $P_{br} /(M_{cr} /h_o)$. The critical moment $M_{cr}$ used in normalizing the results is calculated using the AISC elastic LTB equation (Eq. F2-4). It should be noted that the imperfection 1 involves only an "out-of-plumbness" in each

unbraced length. And imperfection 2 involves both an "out-of-plumbness" and an "out-of-straightness" in each unbraced length.

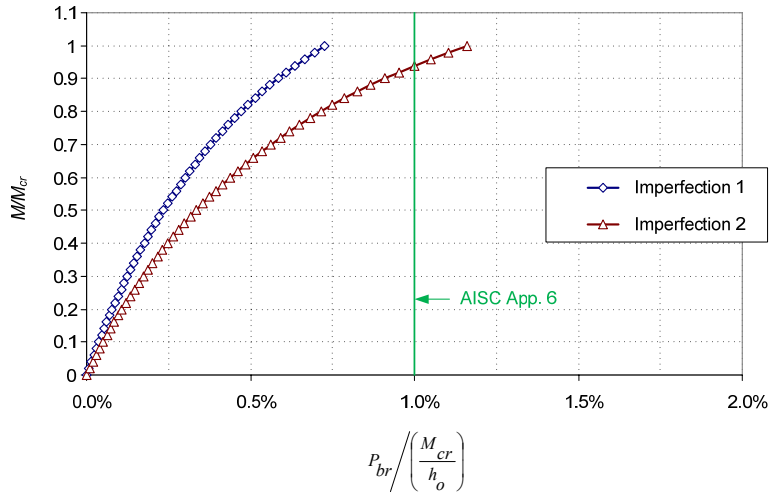


**Fig. 4.6.2. Benchmark Study LB1, Case 1 – Load vs. brace forces using $\beta = 2\beta_{iF\ (SAP)}/\phi$, refined model.**

The brace stiffness used in the simplified model is

$$\beta_{br(SAP)} = \frac{2\beta_{iF(SAP)}}{\phi} = \frac{2(1.51)}{0.75} = 4.03 \text{ kips/inch}$$

In the same fashion, Fig. 4.6.3 plots the results from SAP 2000 for the simplified model.

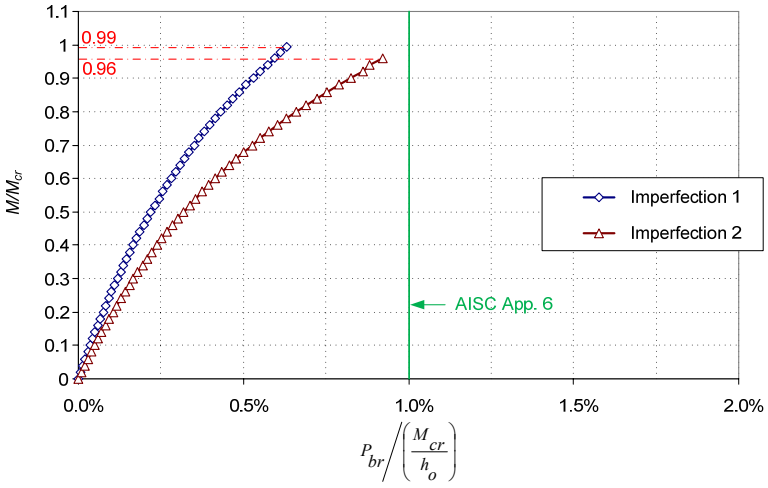


**Fig. 4.6.3. Benchmark Study LB1, Case 1 – Load vs. brace forces using $\beta = 2\beta_{iF\ (SAP)}/\phi$, simplified model.**

*4.6.1.1.3 Load-Deflection Results using $\beta = 1.9\beta_{iF\ (APP\ 6)}$*

Figs. 4.6.4 and 4.6.5 show the load-deflection analysis results from SAP 2000 using the brace stiffness $\beta = 1.9\beta_{iF\ (APP\ 6)} = 3.02$ kips/inch and using the refined and simplified models respectively.

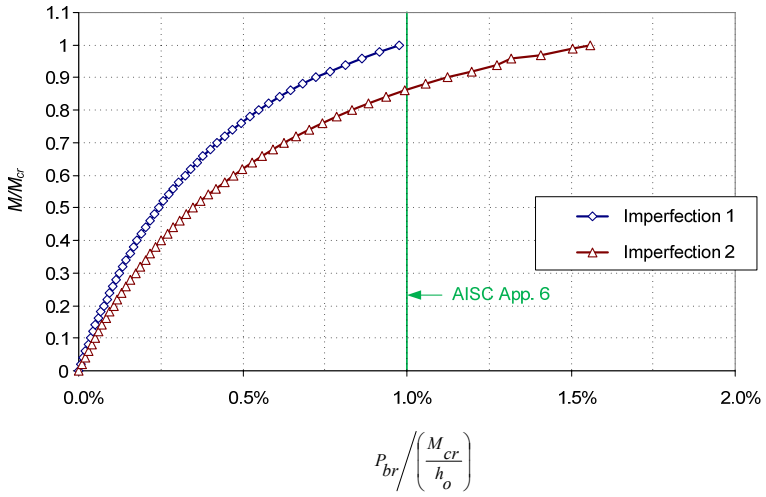


**Fig. 4.6.4. Benchmark Study LB1, Case 1 – Load vs. brace forces using $\beta = 1.9\beta_{iF\ (APP\ 6)}$, refined model.**

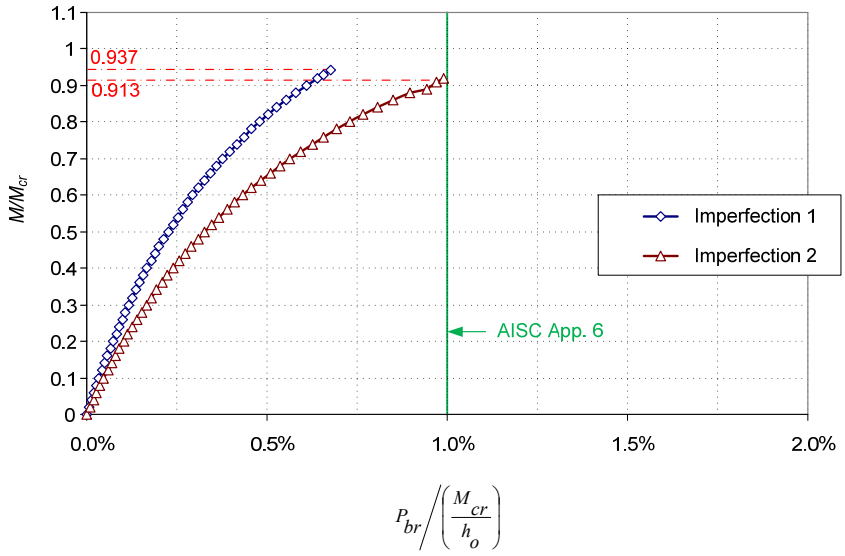


**Fig. 4.6.5. Benchmark Study LB1, Case 1 – Load vs. brace forces using $\beta = 1.9\beta_{iF\ (APP\ 6)}$, simplified model.**

*4.6.1.1.4 Discussion of Results*

The following observations can be made from the above Benchmark Study LB1 solutions:

- Both the Appendix 6 equations and the simplified analysis model give accurate approximations of the refined analysis ideal full bracing stiffness $\beta_{iF}$ for this problem.
- Imperfection 2, which includes both out-of-plumbness and out-of-straightness, is more critical than imperfection 1, which includes only out-of-plumbness.
- For the solutions based on a brace stiffness of $2\beta_{iF\ (SAP)}/\phi$, Appendix 6 overpredicts the refined analysis brace forces associated with imperfection 1 by 36 % and underpredicts brace forces associated with imperfection 2 by 14 %.
- The simplified model fails to converge slightly before reaching $M_{cr}$ for both imperfections and for both brace stiffnesses. Up until the point where the solution fails, the simplified model underpredicts the refined analysis brace forces by up to 15 % for the solutions based on a brace stiffness of $2\beta_{iF\ (SAP)}/\phi$. It underpredicts the refined analysis brace forces by up to approximately 50 % for the smaller brace stiffness.
- Although there are significant increases in the brace forces for $\beta = 1.9\beta_{iF\ (App\ 6)}$, the refined analysis brace forces are still less than 2 % of the corresponding beam flange force. For the solutions based on a brace stiffness of $1.9\beta_{iF\ (App\ 6)}$, the refined analysis maximum brace force for the beam with imperfection 1 is almost equal to the brace force requirement from Appendix 6. However, the brace force for the beam with imperfection 2 is nearly equal to 1.5% of $M_{cr}/h_o$.
- The applied load versus brace force curve for a brace stiffness of $1.9\beta_{i\ (App\ 6)}$ is noticeably more nonlinear than that for a brace stiffness of $2\beta_{i(SAP)}/\phi = 2.67\beta_{i(SAP)}$. This is an

indication that the brace forces will increase at a much greater rate if one were to decrease the brace stiffness further from $1.9\beta_{i\ (App\ 6)}$.

4.6.1.2 Benchmark Study LB2

Fig. 4.6.6 shows the simply supported W16x26 beam with a top flange brace and with no transfer stiffener subjected to the concentrated vertical load applied at mid-span and at the section mid-depth (Case 1 in the Benchmark Study LB2). The results from the eigenvalue buckling analysis show that the ideal full bracing stiffness is $\beta_{iF(SAP)} = 3.7$ kips/inch for the refined model and $\beta_{iF(SAP)} = 3.3$ kips/inch for the simplified model. This study is important to ascertain if the trends observed in the prior column solutions apply for beam cases with a significant moment gradient.

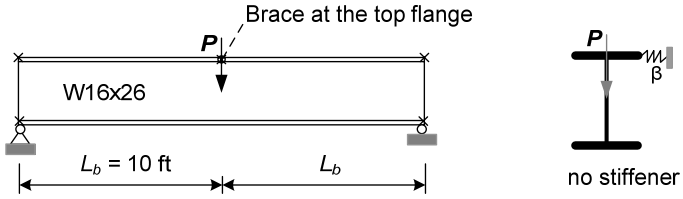


**Fig. 4.6.6. Load-deflection analysis Benchmark Study LB2, Case 1 – Problem description.**

*4.6.1.2.1 Brace Requirements based on the AISC (2005) Appendix 6 Commentary*

Based on Eqs. (4.6-1), (4.6-2), and (4.6-3) (see Section 4.6.1.1.1), the brace stiffness and brace strength requirements are calculated as follows:

For this problem: $n$ =1 (single brace), $N_i = 2$

$C_b = 1.75$ based on AISC Eq. (C-F1-1)

$C_d$ =1.0 (because of single curvature)

$C_t = 1.0$ (because of centroidal loading)

$L_b$ = 120 inch

$M_{cr}$ = 2830 kip-inches (AISC Eq. F2-4, using $C_b$=1.75)

$$P_f = \frac{\pi^2 EI_{yc}}{L_b^2} = \frac{\pi^2 (29000)(9.59/2)}{120^2} = 95.3 \text{ kips}$$

- Ideal full bracing stiffness:

$$\beta_{iF(App\ 6)} = \frac{N_i C_b P_f}{L_b} C_d C_t = \frac{2(1.75)(95.3)}{120} 1(1) = 2.78 \text{ kips/inch}$$

- Required brace stiffness:

$$\beta_{br} = \frac{2\beta_i}{\phi} = \frac{2(2.78)}{0.75} = 7.41 \text{ kips/inch}$$

- Required brace strength (at $M = M_{cr}$):

$$P_{br} = \frac{(0.01)M_{cr}}{h_o} C_d C_t = \frac{(0.01)(2830)}{15.355} 1(1) = 1.84 \text{ kips} = 0.01\frac{M_{cr}}{h_o}$$

*4.6.1.2.2 Load-Deflection Results using $\beta = 2\beta_{i\,(SAP)}/\phi$*

Fig. 4.6.7 shows the load-deflection analysis results from SAP 2000 with brace stiffness

$$\beta_{br(SAP)} = \frac{2\beta_{iF(SAP)}}{\phi} = \frac{2(3.7)}{0.75} = 9.87 \text{ kips/inch}$$

from the refined FEA model. Similar to Fig. 4.6.2, this figure shows the normalized maximum internal moment $M/M_{cr}$ versus the normalized bracing force $P_{br}/(M_{cr}/h_o)$. The critical moment $M_{cr}$ utilized in normalizing the results is calculated using Eq. (F2-4) from the AISC Specification with $C_b$ = 1.75 from AISC Eq. (C-F1-1).

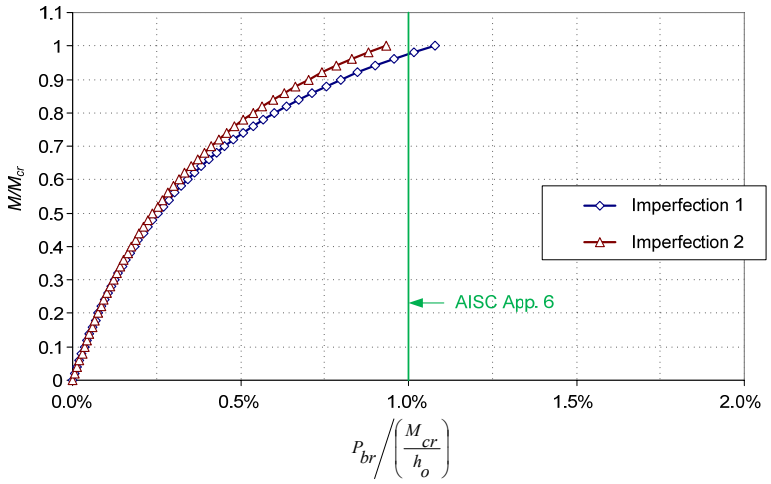


**Fig. 4.6.7. Benchmark Study LB2, Case 1 – Load vs. brace forces using $\beta = 2\beta_{iF(SAP)}/\phi$, refined model.**

The brace stiffness used in the simplified model is

$$\beta_{br(SAP)} = \frac{2\beta_{iF(SAP)}}{\phi} = \frac{2(3.3)}{0.75} = 8.80 \text{ kips/inch}$$

The load-deflection analysis results from SAP 2000 with brace stiffness $\beta = 2\beta_{iF(SAP)}/\phi$ for the simplified model are plotted in Fig. 4.6.8.

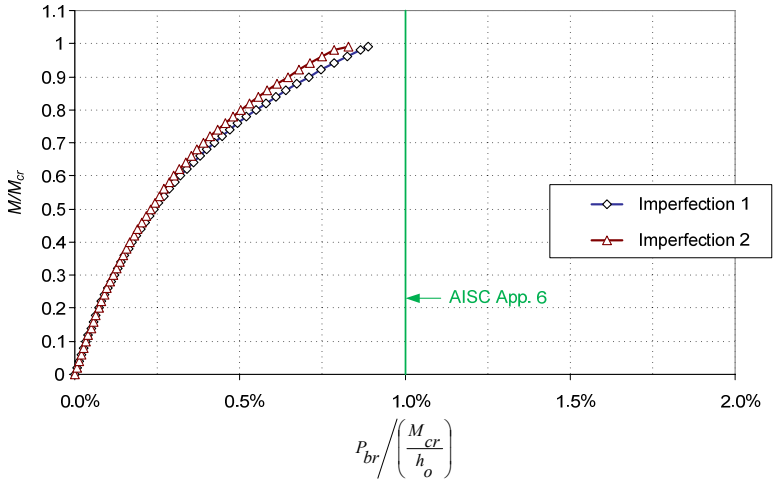


**Fig. 4.6.8. Benchmark Study LB2, Case 1 – Load vs. brace forces using $\beta = 2\beta_{iF\ (SAP)}/\phi$, simplified model.**

*4.6.1.2.3 Load-Deflection Results using $\beta = 1.9\beta_{iF(App\ 6)}$*

Figs. 4.6.9 and 4.6.10 show the load-deflection analysis results from SAP 2000 with brace stiffness $\beta = 1.9\beta_{i\ (App\ 6)} = 5.28$ kips/inch for the refined and simplified models.

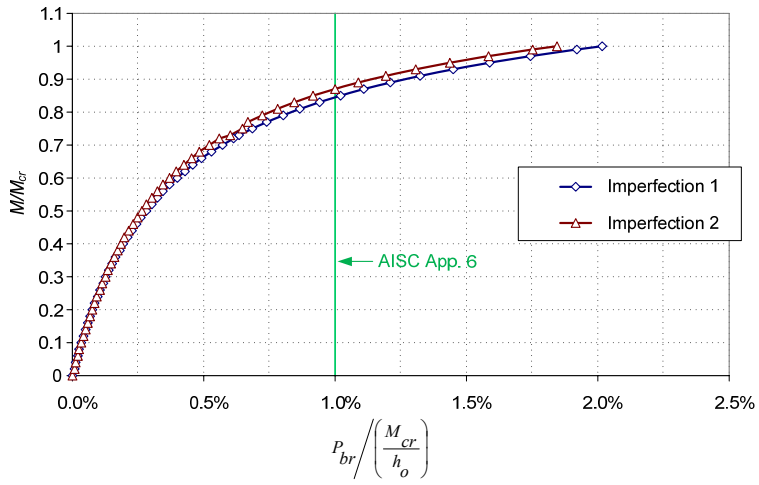


**Fig. 4.6.9. Benchmark Study LB2, Case 1 – Load vs. brace forces using $\beta = 1.9\beta_{iF\ (App\ 6)}$, refined model.**

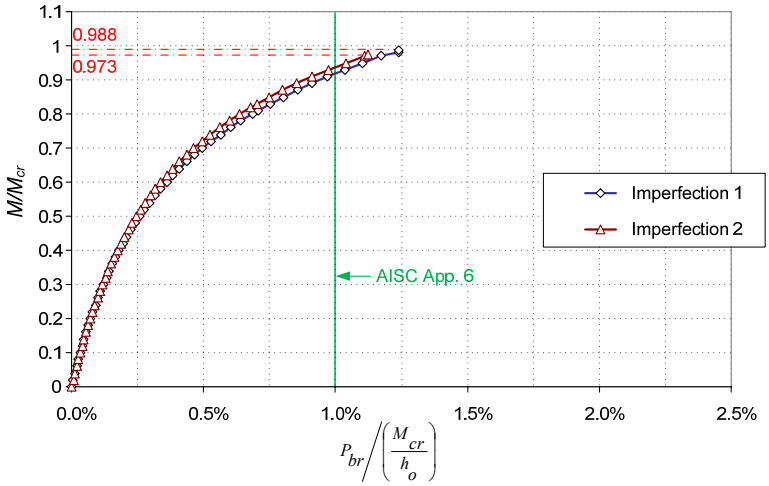


**Fig. 4.6.10. Benchmark Study LB2, Case 1 – Load vs. brace forces using $\beta = 1.9\beta_{iF\ (App\ 6)}$, simplified model.**

*4.6.1.2.4 Discussion of Results*

The following observations can be made from the above Benchmark Study LB2 solutions:

- Appendix 6 underpredicts the refined analysis $\beta_{iF}$ value by 24 % whereas the simplified model underestimates the refined analysis $\beta_{iF}$ value by 11 %.
- Interestingly, imperfection 1 gives slightly higher brace forces than imperfection 2 for both of the brace stiffnesses considered for this problem using either the refined or the simplified analysis models.
- For the solutions based on a brace stiffness of $2\beta_{iF\ (SAP)}/\phi$, Appendix 6 underpredicts the refined analysis brace forces associated with imperfection 1 by 8 % and overpredicts the corresponding brace forces associated with imperfection 2 by 7 %.
- The simplified model gives converged solutions at $M = M_{cr}$ for the beams with a brace stiffness of $2\beta_{iF\ (SAP)}/\phi$ in this problem, but underestimates the refined analysis brace forces by up to 19 %. For the beams with a brace stiffness of $1.9\beta_{iF\ (App\ 6)}$, the simplified model fails to converge before reaching $M = M_{cr}$ and underpredicts the brace force by up to approximately 40 %.
- Similar to Benchmark Study LB1, the brace with a stiffness of $1.9\beta_{iF\ (App\ 6)}$ exhibits good performance for this problem. Although there are significant increases in the brace forces for $\beta = 1.9\beta_{iF\ (App\ 6)}$, the refined analysis brace forces are still approximately only 2 % of the corresponding beam flange force. The influence of out-of-straightness appears to be relatively minor in this problem, and in fact tends to reduce the required brace force. The refined analysis maximum brace force (for imperfection 1) is increased from

1.1% *of* $M_{cr}/h_o$ using the previous $\beta$ = 9.87 kips/inch = 3.55$\beta_{iF\ (App\ 6)}$ = 2.67$\beta_{iF\ (SAP)}$ to 2.0 % of $M_{cr}/h_o$ using $\beta$ = 1.9$\beta_{iF\ (App\ 6)}$ = 5.28 kips/inch.

- The Applied Load versus Brace Force curve with a brace stiffness 1.9$\beta_{iF\ (App\ 6)}$ is noticeably more nonlinear than with a brace stiffness 2$\beta_{iF\ (SAP)}/\phi$ = 2.67$\beta_{iF\ (SAP)}$ as well as the reduced stiffness LB2 solution. This is an indication that the brace forces will increase at a much greater rate if one were to decrease the brace stiffness further from 1.9$\beta_{iF\ (App\ 6)}$. The larger brace force and the more significant nonlinearity in this problem relative to Benchmark Study LB1 is likely due in part to the underestimation of $\beta_{iF\ (SAP)}$ by $\beta_{iF\ (App\ 6)}$.

4.6.1.3 Benchmark Study LB3

Fig. 4.6.11 shows the Case 1 of the Benchmark Study LB3. This problem is the simply supported beam W16x26 with a top flange brace and a 4x1/4 transverse stiffener subjected to a concentrated vertical load applied to the top flange at its mid-span. The results from eigenvalue buckling analysis show that the ideal full bracing stiffness is $\beta_{iF(SAP)}$ = 6.1 kips/inch for refined model and $\beta_{iF(SAP)}$ = 5.5 kips/inch for simplified model.

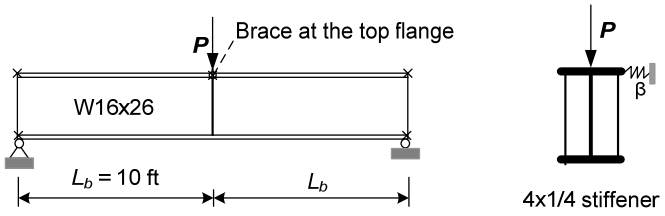


**Fig. 4.6.11. Load-deflection analysis Benchmark Study LB3, Case 1 – Problem description.**

*4.6.1.3.1 Brace Requirements based on the AISC (2005) Appendix 6 Commentary*

Based on Eqs. (4.6-1), (4.6-2), and (4.6-3) (see Section 4.6.1.1.1), the brace stiffness and brace strength requirements are calculated as follows:

For this problem: $n$ =1 (single brace), $N_i$ = 2

$C_b$ = 1.75 based on AISC Eq. (C-F1-1)

$C_d$ =1.0 (because of single curvature)

$C_t$ = 1+1.2/1=2.2 (because of top flange loading)

$L_b$ = 120 inch

$M_{cr}$ = 2830 kip-inches (AISC Eq. F2-4, using $C_b$=1.75)

$$P_f = \frac{\pi^2 EI_{yc}}{L_b^2} = \frac{\pi^2 (29000)(9.59/2)}{120^2} = 95.3 \text{ kips}$$

- Ideal full bracing stiffness:

$$\beta_{i(App6)} = \frac{N_i C_b P_f}{L_b} C_d C_t = \frac{2(1.75)(95.3)}{120} 1(2.2) = 6.12 \text{ kips/inch}$$

- Required brace stiffness:

$$\beta_{br} = \frac{2\beta_i}{\phi} = \frac{2(6.12)}{0.75} = 16.3 \text{kips/inch}$$

- Required brace strength (at $M = M_{cr}$):

$$P_{br} = \frac{(0.01)M_{cr}}{h_o} C_d C_t = \frac{(0.01)(2830)}{15.355} 1(2.2) = 4.05 \text{ kips} = 0.022 \frac{M_{cr}}{h_o}$$

*4.6.1.3.2 Load-Deflection Results using $\beta = 2\beta_{i\,(SAP)}/\phi$*

Fig. 4.6.12 shows the load-deflection analysis results from SAP 2000 using brace stiffness

$$\beta_{br(SAP)} = \frac{2\beta_{i(SAP)}}{\phi} = \frac{2(6.1)}{0.75} = 16.27 \text{ kips/inch}$$

from the refined FEA model. Similar to Fig. 4.6.2 and 4.6.7, this figure shows the normalized maximum internal moment $M/M_{cr}$ versus the normalized bracing force $P_{br}/(M_{cr}/h_o)$. The critical moment $M_{cr}$ utilized in normalizing the results is calculated using Eq. (F2-4) from the AISC Specification with $C_b = 1.75$ from AISC Eq. (C-F1-1).

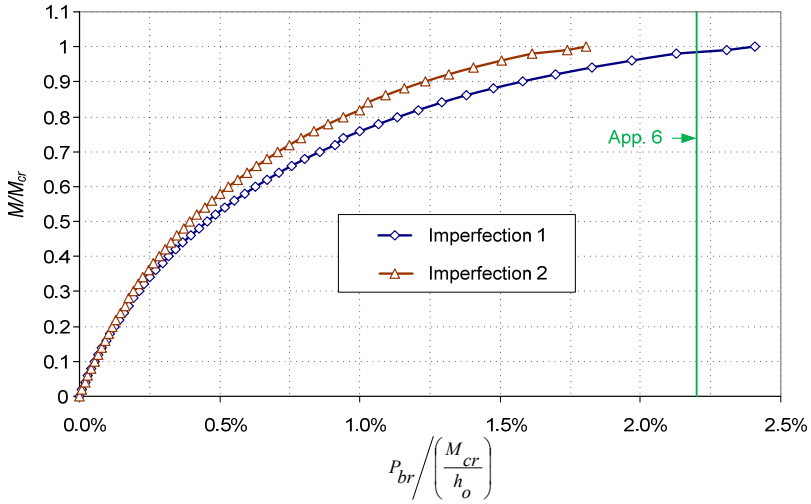


**Fig. 4.6.12. Benchmark Study LB3, Case 1 – Load vs. brace forces using $\beta = 2\beta_{i\,(SAP)}/\phi$, refined model.**

The brace stiffness used in the simplified model is

$$\beta_{br(SAP)} = \frac{2\beta_{iF(SAP)}}{\phi} = \frac{2(5.5)}{0.75} = 14.67 \text{ kips/inch}$$

The load-deflection analysis results from SAP 2000 using the brace stiffness $\beta = 2\beta_{iF(SAP)}/\phi$ for the simplified model are plotted in Fig. 4.6.13.

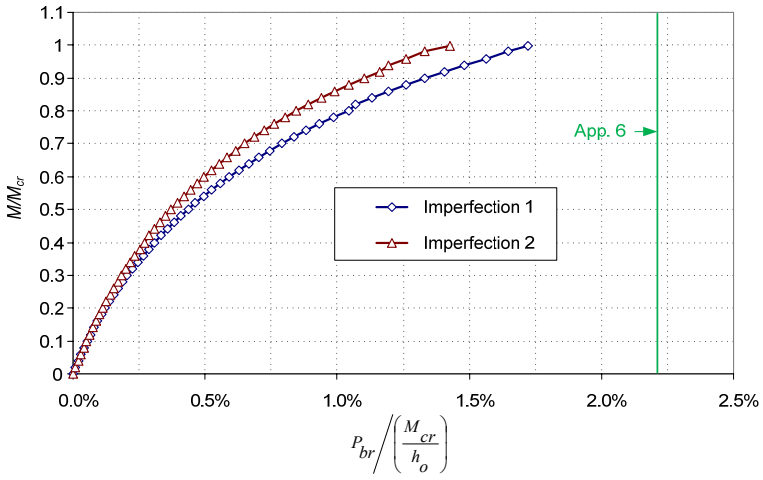


**Fig. 4.6.13. Benchmark Study LB3, Case 1 – Load vs. brace forces using $\beta = (2\beta_{iF\ (SAP)})/\phi$, simplified model.**

*4.6.1.3.3 Load-Deflection Results using $\beta = 1.9\beta_{i\ F(App\ 6)}$*

Figs. 4.6.14 and 4.6.15 show the load-deflection analysis results from SAP 2000 with brace stiffness $\beta = 1.9\beta_{i\ (App\ 6)} = 11.6$ kips/inch for the refined and simplified models.

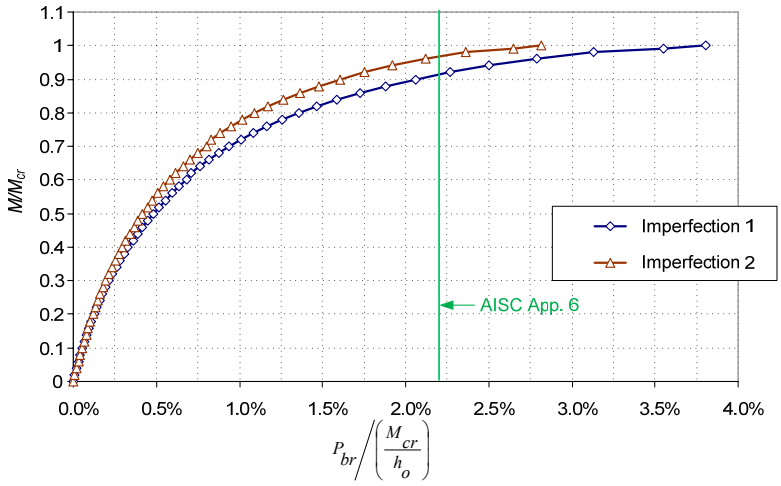


**Fig. 4.6.14. Benchmark Study LB3, Case 1 – Load vs. brace forces using $\beta = 1.9\beta_{iF(App.6)}$, refined model.**

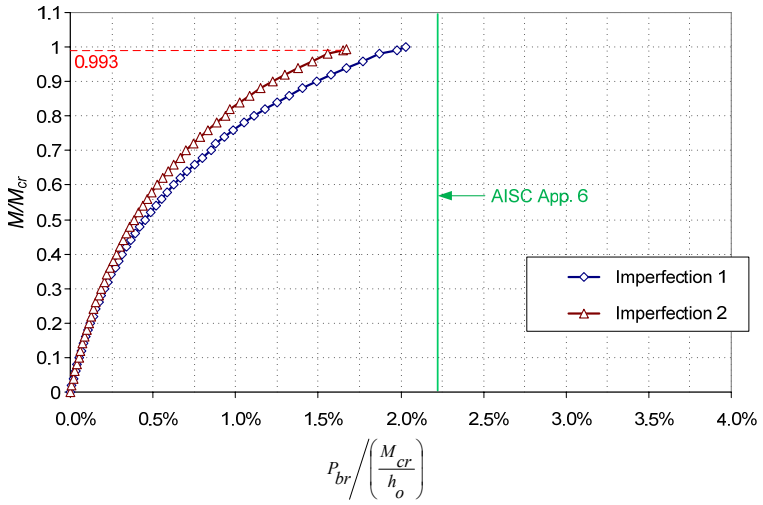


**Fig. 4.6.15. Benchmark Study LB3, Case 1 – Load vs. brace forces using $\beta = 1.9\beta_{iF\ (App.6)}$, simplified model.**

*4.6.1.3.4 Discussion of Results*

The following observations can be made from the above Benchmark Study LB2 solutions:

- For the solutions based on a brace stiffness of $2\beta_{iF\ (SAP)}/\phi$, Appendix 6 underpredicts the brace forces associated with imperfection 1 by 9 % and overpredicts the brace forces associated with imperfection 2 by 22 %.
- The simplified model underpredicts the refined analysis ideal brace stiffness by 10 % and underpredicts the refined analysis brace forces by 9 to 21% and both imperfections 1 and 2 give the brace force smaller than the brace force requirement from the AISC Appendix 6.
- For the refined model, the brace with a stiffness of $1.9\beta_{iF\ (App\ 6)}$ experiences somewhat larger forces than may be desired. Both imperfections 1 and 2 give larger brace force than strength requirement from the Appendix 6. The maximum brace force (with imperfection 1) is increased from 2.4 % of $M_{cr}/h_o$ using the previous $\beta$ = 16.3 kips/inch

$= 2.67\beta_{i(App\ 6)} = 2.67\beta_{i(SAP)}$ to 3.8 % of $M_{cr}/h_o$ using $\beta = 1.9\beta_{i(App\ 6)} = 11.6$ kips/inch. However, the brace forces overpredict when the applied load approaches to the critical load $(M_{cr})$ because the moment gradient and load height effects cause greater nonlinearity at the maximum applied load. For the simplified model, the analysis fails to converge slightly before reaching $M_{cr}$.

- The applied load versus brace force curve is noticeably more nonlinear than in the prior case studies LB1 and LB2. The curve is nearly flat at $M_{cr}$. The more significant nonlinearity in this benchmark study indicates that more than $1.9\beta_{i(SAP)}$ is needed when the load is applied at the top flange level (assuming no significant tipping restraint). Since the maximum brace force (with Imperfection 1) is already larger than 2 % using $\beta = 2.67\beta_{i(App\ 6)}$ in this analysis , it would appear that the Appendix 6 requirement should not be relaxed for this case (unless the additional forces are reduced by the effects of tipping restraint). This tipping restraint effect is presented in the Benchmark Study LB3* below and discussed more in detail in Section 5.3.2.

4.6.1.4 Benchmark Study LB3*

This problem is an extension of Benchmark Study LB3 by providing that includes a torsional brace at the brace point with a stiffness $\beta_T$ as shown in Fig. 4.6.16. The aim of attaching this torsional brace is to restrain the rotation of compression flange.

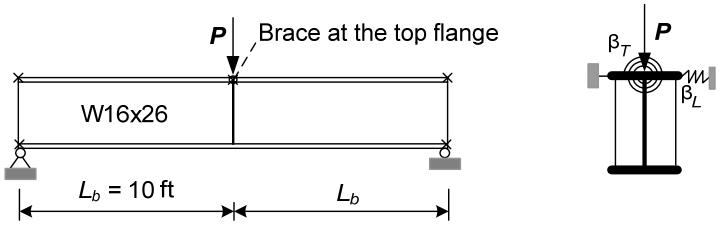


**Fig. 4.6.16. Load-deflection analysis, Benchmark Study LB3* – Problem description**

Based on the results of Benchmark Study LB3, only the refined model with imperfection 1 is considered in this section. In this problem, the torsional brace stiffness $\beta_T$ is determined based on reducing the lateral brace force to 2% of $M_{cr}/h_o$ when using the lateral brace stiffness $\beta_L = 1.9\beta_{i\ (App\ 6)} = 1.9(6.12) = 11.6$ kips/inch. The results for several brace stiffnesses are plotted in Figs 4.6.17 and 4.6.18.

Fig. 4.6.17 shows the lateral brace force versus the applied load for four different torsional brace stiffnesses. They are

- $\beta_T$ = 0.0 kip-inch/rad (the same as Benchmark Study LB3)
- $\beta_T$ = 100 kip-inch/rad
- $\beta_T$ = 200 kip-inch/rad
- $\beta_T$ = 300 kip-inch/rad.

One can observe from Fig. 4.6.7 that by providing a small torsional brace stiffness, the lateral brace forces reduce significantly. The maximum brace forces using imperfection 1 with a stiffness of $1.9\beta_{i\ (App\ 6)}$ including the small torsional spring stiffness ($\beta_T$ = from 100 to 300 kip-inch/rad) are estimated as 2.0% to 2.4% of $M_{cr}/h_o$.

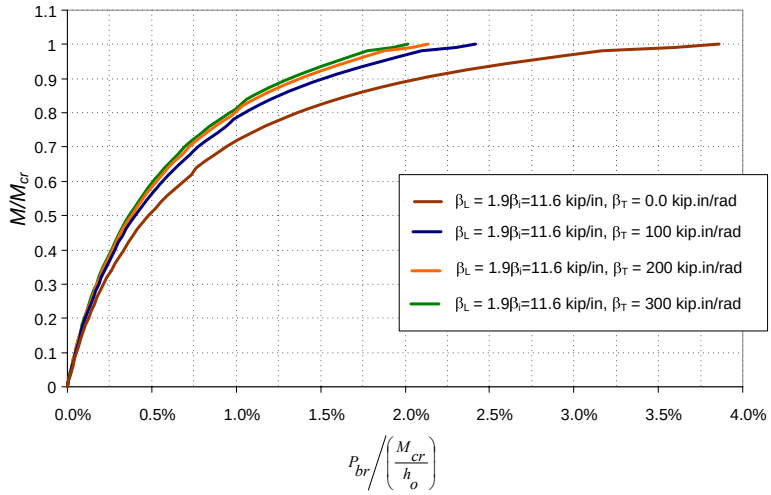


**Fig. 4.6.17. Benchmark Study LB3* – Applied load vs. lateral brace forces.**

Likewise, Fig. 4.6.18 shows the torsional brace forces versus the applied load. This figure indicates that the torsional brace force $(M_{br})$ is very small compared to the critical moment $(M_{cr})$, $M_{br}/M_{cr} < 0.25\%$.

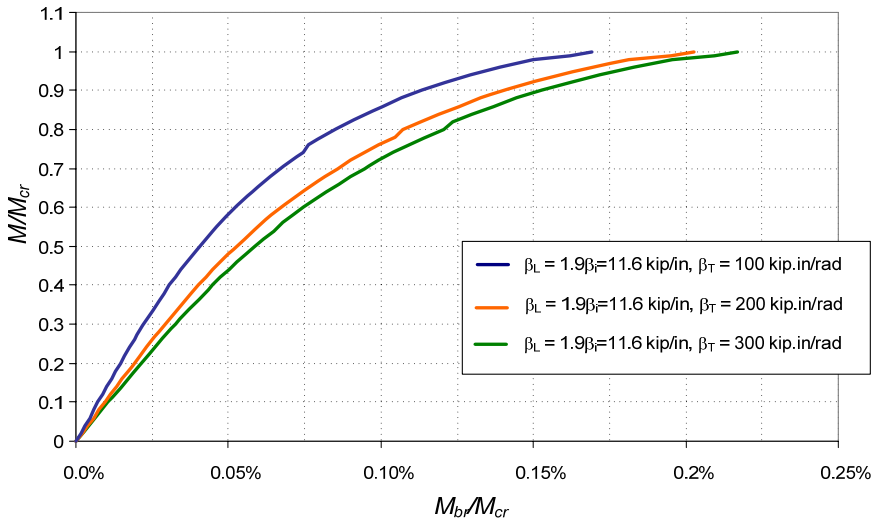


**Fig. 4.6.18. Benchmark Study LB3* – Applied load vs. torsional brace forces.**

It should be noted that web sidesway buckling occurs in Benchmark Studies LB3 and LB3* if the torsional brace stiffness is not large enough to restrain the rotation of the compression flange.

4.6.1.5 Benchmark Study LB4

Fig. 4.6.19 shows the simply supported W16x26 beam with a top flange brace and no transverse stiffener subjected to full reversed-curvature bending (Case 2 of Benchmark Problem LB4). The results from the eigenvalue buckling analysis showed that the ideal brace stiffness for full bracing is approximately $\beta_{i(SAP)} = 19$ kips/inch for the refined model and approximately $\beta_{i(SAP)} = 22$ kips/inch for the simplified model.

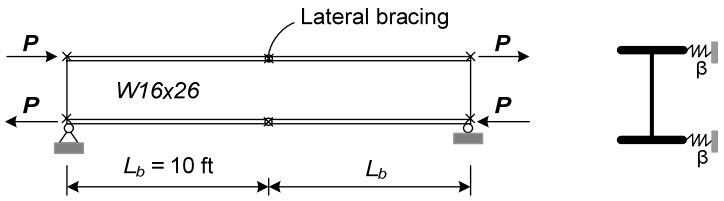


**Fig. 4.6.19. Load-deflection analysis, Benchmark Study LB4, Case 2 – Problem description.**

In this section, two types of geometric imperfections with magnitude of $L_b$/500 and $L_b$/1000 discussed in Section 4.4 are used to predict the brace forces.

*4.6.1.5.1 Brace Requirements based on the AISC 2005 Appendix 6 Commentary*

Based on Eqs. (4.6-1), (4.6-2), and (4.6-3) (see Section 4.6.1.1.1), the brace stiffness and brace strength requirements are calculated as follows:

For this problem: $n$ =1 (single brace), $N_i$ = 2

$C_b$ = 1.75 using AISC Eq. (C-F1-1)

$C_d$ =2.0 (because of double curvature)

$C_t$ = 1.0 (because of centroidal loading)

$L_b$ = 120 inch

$M_{cr}$ = 2830 kip-inches (AISC Eq. F2-4, using $C_b$=1.75)

$$P_f = \frac{\pi^2 EI_{yc}}{L_b^2} = \frac{\pi^2 (29000)(9.59/2)}{120^2} = 95.3 \text{ kips}$$

- Ideal full bracing stiffness:

$$\beta_{iF(App6)} = \frac{N_i C_b P_f}{L_b} C_d C_t = \frac{2(1.75)(95.3)}{120} 2(1) = 5.56 \text{ kips/inch}$$

- Required brace stiffness:

$$\beta_{br} = \frac{2\beta_i}{\phi} = \frac{2(5.56)}{0.75} = 14.82 \text{kips/inch}$$

- Required brace strength (at $M = M_{cr}$):

$$P_{br} = \frac{(0.01)M_{cr}}{h_o} C_d C_t = \frac{(0.01)(2830)}{15.355} 2(1) = 3.68 \text{ kips} = 0.02\frac{M_{cr}}{h_o}$$

*4.6.1.5.2 Load-Deflection Results using $\beta = 2\beta_{i\,F(SAP)}/\phi$ and $\Delta_o = L_b/500$*

Fig. 4.6.20 shows the load-deflection analysis results from SAP 2000 using brace stiffness

$$\beta_{br(SAP)} = \frac{2\beta_{iF(SAP)}}{\phi} = \frac{2(19)}{0.75} = 50.7 \text{ kip/in}$$

from the refined FEA model. Similar to Fig. 4.6.2, this figure shows the normalized maximum internal moment $M/M_{cr}$ versus the normalized bracing force $P_{br}/(M_{cr}/h_o)$. The critical moment $M_{cr}$ utilized in normalizing the results is calculated using AISC Eq. (F2-4).

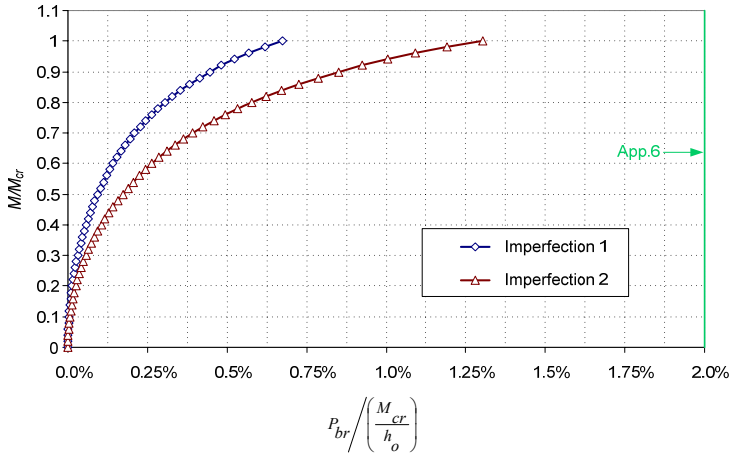


**Fig. 4.6.20. Benchmark Study LB4, Case 2 – Load vs. brace forces, using $\beta = 2\beta_{iF\,(SAP)}/\phi$, refined model.**

The brace stiffness used in the simplified model is

$$\beta_{br(SAP)} = \frac{2\beta_{iF(SAP)}}{\phi} = \frac{2(22)}{0.75} = 58.7 \text{ kips/inch}$$

The load-deflection analysis results from SAP 2000 with brace stiffness $\beta = 2\beta_{iF(SAP)}/\phi$ for the simplified model are plotted in Fig. 4.6.21.

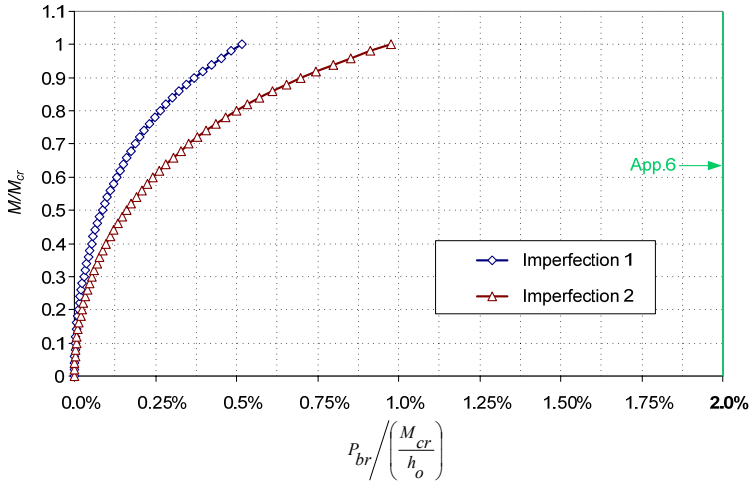


**Fig. 4.6.21. Benchmark Study LB4, Case 2 – Load vs. brace forces, using $\beta = 2\beta_{iF\ (SAP)}/\phi$, simplified model.**

*4.6.1.5.3 Load-Deflection Results using $\beta = 2\beta_{i\ (APP6)}/\phi$ and $\beta = 1.9\beta_{i(APP6)}$*

Figs. 4.6.22 and 4.6.23 show the load-deflection analysis results from SAP 2000 for imperfections 1 and 2 with sweep amplitude of $L_b/500$ for the refined model.

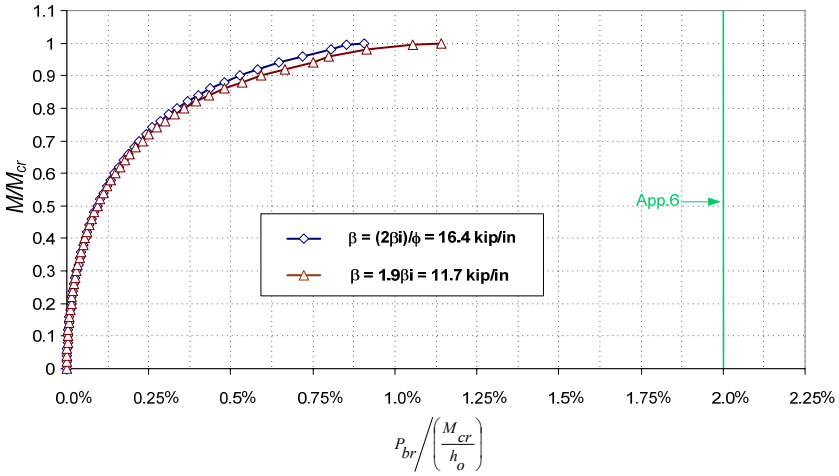


**Fig. 4.6.22. Benchmark Study LB4, Case 2 – Load vs. brace forces for imperfection 1 with $\Delta_o = L_b/500$.**

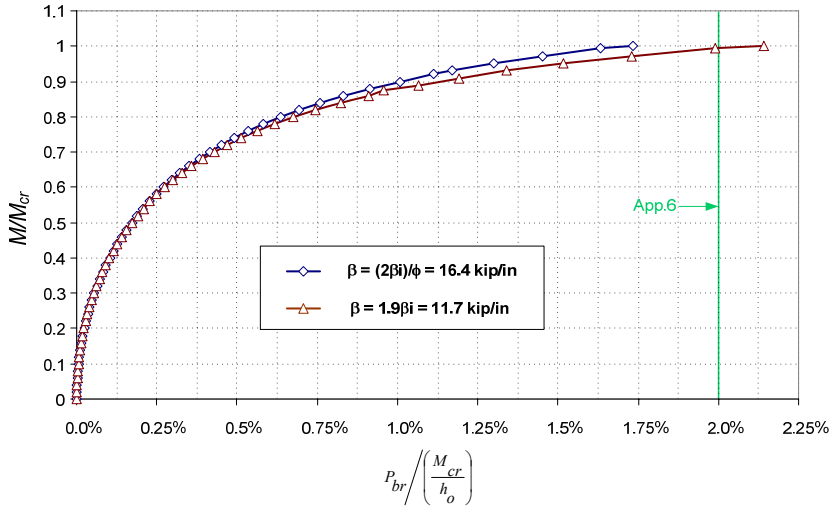


**Fig. 4.6.23. Benchmark Study LB4, Case 2 – Load vs. brace forces for imperfection 2 with $\Delta_o = L_b/500$.**

Figs. 4.6.24 and 4.6.25 show the load-deflection analysis results from SAP 2000 for imperfections 1 and 2 with sweep amplitude of $L_b/1000$ for the refined models.

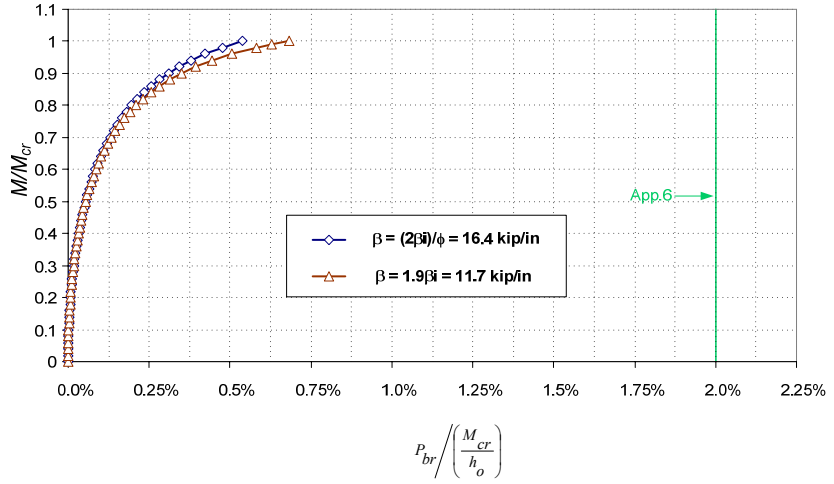


**Fig. 4.6.24. Benchmark Study LB4, Case 2 – Load vs. brace forces for imperfection 1 with $\Delta_o = L_b/1000$.**

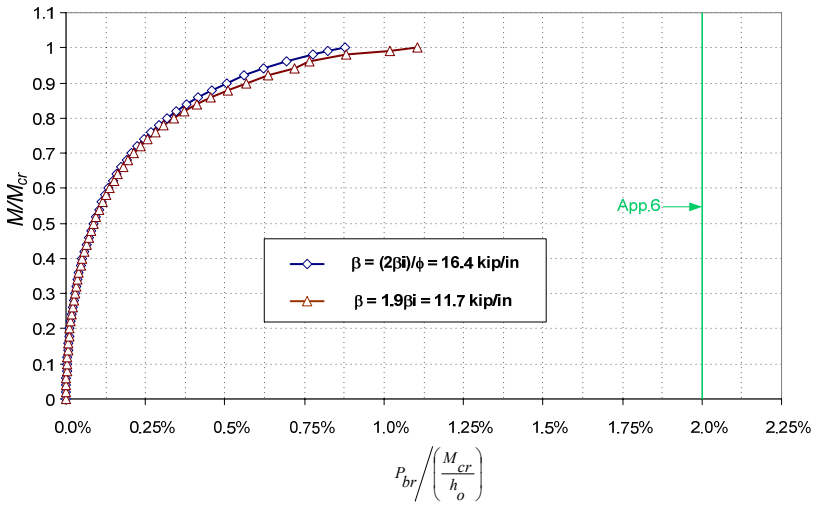


**Fig. 4.6.25. Benchmark Study LB4, Case 2 – Load vs. brace forces for imperfection 2 with $\Delta_o = L_b/1000$.**

*4.6.1.5.4 Discussion of Results*

The following observations can be made from the Benchmark Study LB4 solutions:

- For the solutions based on a brace stiffness of $2\beta_{iF\ (SAP)/}\phi$ and $\Delta_o = L_b/500$**,** imperfections 1 and 2 give the brace force smaller than the brace force requirement from the AISC Appendix 6 for both the refined and simplified models.
- For the solutions based on a brace stiffness of $2\beta_{iF\ (App6)/}\phi$ and $\beta = 1.9\beta_{i(APP6)}$ with imperfection $\Delta_o = L_b/500$, the brace forces are smaller than brace force requirement from the AISC Appendix 6.
- Brace forces reduce half for the geometric imperfections with magnitude of $L_b/1000$ compared to the geometric imperfections with magnitude of $L_b/500$ or cutting the amplitude of the initial imperfections in half reduces the brace forces by approximately a factor of two.
- The applied load versus brace force curves are very similar to one another for brace stiffnesses of $1.9\beta_{i\ (App\ 6)}$ and $2\beta_{i(App\ 6)}/0.75$.

### 4.6.2 Torsional Beam Bracing

In this section, the load-deflection analyses are used to estimate the brace forces for the torsional beam bracing for Benchmark Study TB1 and TB2. The results from SAP 2000 are compared to the results from the AISC Appendix 6 Commentary Equations as well as the refined equations published by Yura and Phillips (1992).

#### 4.6.2.1 Benchmark Study TB1

Fig. 4.6.26 shows the simply supported beam W16x26 ($t_w$ = 0.25 inch, $h_o$= 15.355 inch) with the torsional brace at the top flange, a 4x1/4 transverse stiffener ($t_s$ = 0.25 inch and $b_s$= 4 inch) subjected to uniform bending moment (Case 1 in the Benchmark Study TB1). ). The results from the eigenvalue buckling analysis show that the ideal full bracing stiffness is $\beta_{iF(SAP)}$ = 1799 kip-inch/rad for the refined model and $\beta_{iF(SAP)}$ = 1550 kip-inch/rad for the simplified model.

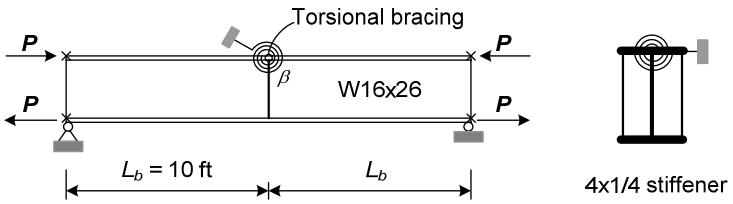


**Fig. 4.6.26. Load-deflection analysis, Benchmark Study TB1- Case 1 – Problem description**

*4.6.2.1.1 Brace Requirements based on the AISC 2005 Appendix 6 Commentary*

Based on AISC Eq. (F2-4), the critical moment *($M_{cr}$)* with $L_b$ = 120 inches is determined as $M_{cr}$ = 1617 kip-inch and the beam capacity assuming no bracing is $M_o$= 502.2 kip-inch.

According to Eq. (2-36) through Eq. (2-39) in Chapter 2 and discussion in the AISC 2005 Appendix 6 Commentary, the brace stiffness and strength requirements can be calculated as follows:

- The brace stiffness excluding web distortion is

$$\beta_T = \frac{1}{\phi}\left(\frac{2.0LM_{cr}^2}{nEI_yC_b^2}\right)$$

$$\beta_T = \frac{1}{0.75}\left(\frac{2.0(240)(1617)^2}{1(29000)(9.59)(1^2)}\right) = 6017\ \text{kip} - \text{in/rad}$$

- The web distortional stiffness is

$$\beta_{sec} = \frac{3.3E}{h_o}\left(\frac{1.5h_ot_w^3}{12} + \frac{t_sb_s^3}{12}\right)$$

$$\beta_{sec} = \frac{3.3(29000)}{15.355}\left(\frac{1.5(15.355)0.25^3}{12} + \frac{(0.25)4^3}{12}\right) = 8497\ \text{kip - in/rad}$$

- Required brace stiffness:

$$\beta_{Tb} = \frac{\beta_T}{\left(1 - \frac{\beta_T}{\beta_{sec}}\right)}$$

$$\beta_{Tb} = \frac{6017}{\left(1 - \frac{6017}{8497}\right)} = 20617\ \text{kip} - \text{in/rad}$$

- Required brace strength (at $M = M_{cr}$):

$$M_{br} = \frac{0.02M_{cr}L}{nC_bL_b}$$

$$M_{br} = \frac{0.02(1617)(240)}{1(1)(120)} = 64.7\,\text{kip - in}$$

*4.6.2.1.2 Brace Requirements based on the Refined Equations from Yura and Phillips (1992)*

According to Eq. (2-31) through Eq. (2-35) in Chapter 2, the bracing requirements are as follows:

- The ideal discrete torsional brace stiffness is

$$\beta_{Ti} = (M_{cr}{}^2 - C_{bu}^2 M_o^2)\frac{C_T}{C_{bb}^2 EI_{eff}}\frac{0.75L}{n}$$

$$\beta_{Ti} = (1617^2 - 1^2(502.2)^2)\frac{1}{1^2.(29000)(9.59)}\frac{(0.75)240}{1} = 1529 \text{ kip - in/rad}$$

- The brace stiffness excluding web distortion is

$$\beta_T = \frac{2\beta_{Ti}}{\phi} = 4077 \text{ kip - in/rad}$$

- The web distortional stiffness is

$$\beta_{sec} = \frac{3.3E}{h_o}\left(\frac{1.5h_o t_w^3}{12} + \frac{t_s b_s^3}{12}\right)$$

$$\beta_{sec} = \frac{3.3(29000)}{15.355}\left(\frac{1.5(15.355)0.25^3}{12} + \frac{(0.25)4^3}{12}\right) = 8497 \text{ kip - in/rad}$$

- Required brace stiffness:

$$\beta_{Tb} = \frac{\beta_T}{\left(1 - \frac{\beta_T}{\beta_{sec}}\right)}$$

$$\beta_{Tb} = \frac{4077}{\left(1 - \frac{4077}{8497}\right)} = 7840 \text{ kip - in/rad}$$

It should be noted that this formula gives the brace stiffness substantially smaller than the formula based on the AISC 2005 Appendix 6 Commentary (7840 kip-in/rad versus 20617 kip-in/rad)

- Required brace strength (at $M = M_{cr}$):

$$M_{br} = \beta_T \theta_o = \beta_T \frac{L_b}{500h_o}$$

$$M_{br} = (4077)\frac{120}{500(15.355)} = 63.7\,\text{kip - in}$$

*4.5.2.1.3 Load-Deflection Results using $\beta = 2\beta_{iF(SAP)}/\phi$*

Fig.4.6.27 shows the load-deflection analysis results from SAP 2000 using the brace stiffness

$$\beta_{br(SAP)} = \frac{2\beta_{iF(SAP)}}{\phi} = \frac{2(1799)}{0.75} = 4797 \text{ kip - in/rad}$$

from the refined FEA model. Interestingly, this brace stiffness is much smaller than the brace stiffness estimated based on the AISC 2005 Appendix 6 Commentary as well as based on the refined equations from Yura and Phillips (1992).

The figure shows the normalized applied moment $M/M_{cr}$ versus the normalized bracing force $M_{br}/M_{cr}$. The critical moment $M_{cr}$ used in normalizing the results is calculated using the AISC elastic LTB equation (Eq. F2-4).

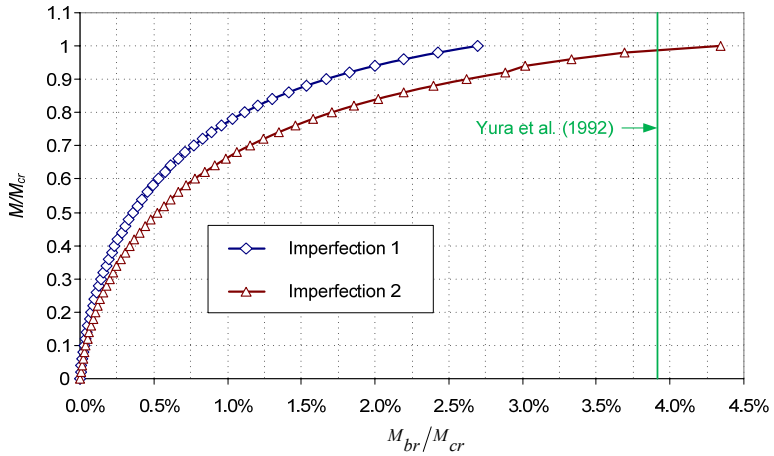


**Fig. 4.6.27. Benchmark Study TB1 – Load vs. brace forces using $\beta = 2\beta_{iF\,(SAP)}/\phi$, refined model.**

The brace stiffness used in the simplified model is

$$\beta_{br(SAP)} = \frac{2\beta_{i(SAP)}}{\phi} = \frac{2(1550)}{0.75} = 4133 \text{ kip - in/rad}$$

Fig. 4.6.28 plots the results from SAP 2000 for the simplified model.

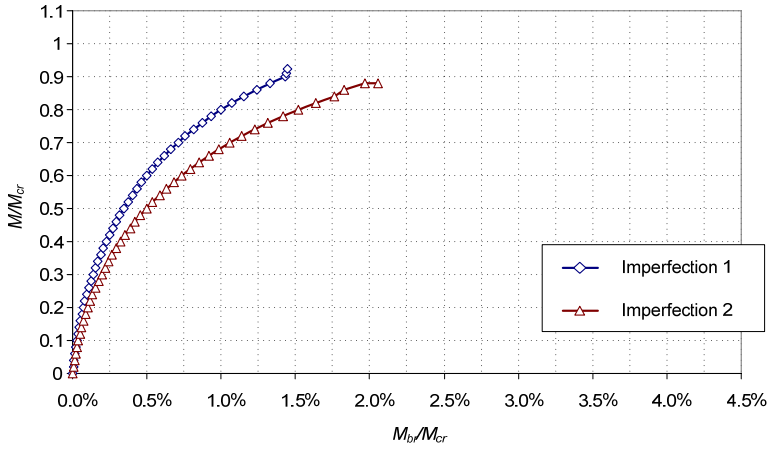


**Fig. 4.6.28. Benchmark Study TB1 – Load vs. brace forces using $\beta = 2\beta_{iF\ (SAP)}/\phi$, simplified model.**

*4.6.2.1.4 Discussion of Results*

The following observations can be made from the above Benchmark Study TB1 solutions:

- Imperfection 2 gives higher brace forces than imperfection 1. Yura and Phillips (1992) equations give approximately 47 % larger than the required brace force for imperfection 1 and 10 % smaller for imperfection 2.
- The simplified model fails to converge slightly before reaching $M_{cr}$ for both imperfections 1 and 2.
- The Appendix 6 Commentary equations give a required brace force similar to the Yura and Phillips (1992). However, the required brace stiffness based on the Appendix 6 Commentary equations is substantially larger than the required brace stiffness based on the Yura and Phillips (1992).

- The Appendix 6 Commentary equations give a required brace stiffness of 5 times the required bracing stiffness of $2\beta_i/0.75$ obtained from the refined model. The Yura and Phillips (1992) equations give a required brace stiffness of 1.64 times the required bracing stiffness of $2\beta_i/0.75$ obtained from the refined model.
- The nonlinearity in the $M_{cr}$ v.s. $M_{br}$ curves is significant given the stiffnesses selected for the load-deflection analyses presented above. The authors believe it would be unwise to reduce the torsional bracing stiffness any further than the values considered here, since this would likely lead to excessive torsional brace forces. The simplified analysis model failed to converge before reaching $M_{cr}$ in this analysis

4.6.2.2 Benchmark Study TB2

Fig. 4.6.29 shows the simply supported beam W16x26 ($t_w$ = 0.25 inch, $h_o$= 15.355 inch) with a torsional brace at the top flange and a 4x1/4 transverse stiffener ($t_s$ = 0.25 inch and $b_s$= 4 inch) subjected to concentrated load at the mid-span and top flange (Case 1 in Benchmark Study TB2). The results from the eigenvalue buckling analysis show that the ideal full bracing stiffness is $\beta_{iF(SAP)}$ = 4000 kip-inch/rad for the refined model and $\beta_{iF(SAP)}$ = 3800 kip-inch/rad for the simplified model.

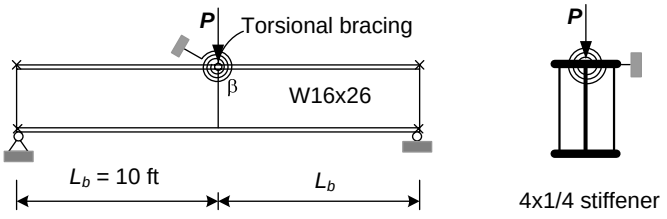


**Fig. 4.6.29. Load-deflection analysis Benchmark Study TB2 – Case 1 - Problem description.**

*4.6.2.2.1 Brace Requirements based on the AISC 2005 Appendix 6 Commentary*

Based on AISC Eq. (F2-4), the critical moment *($M_{cr}$)* with $L_b$= 120 inches is determined as $M_{cr}$ = 2830 kip-inch and the beam capacity assuming no bracing is $M_o$= 502.2 kip-inch.

According to Eq. (2-36) through Eq. (2-39) in Chapter 2 and discussion in the AISC 2005 Appendix 6 Commentary, the brace stiffness and strength requirements can be calculated as follows:

- The brace stiffness excluding web distortion is

$$\beta_T = \frac{1}{\phi}\left(\frac{2.4LM_{cr}^2}{nEI_yC_b^2}\right)$$

$$\beta_T = \frac{1}{0.75}\left(\frac{2.4(240)(2\,830)^2}{1(29000)(9\,.59)(1.75^2)}\right) = 7220 \text{ kip} - \text{in/rad}$$

- The web distortional stiffness is

$$\beta_{sec} = \frac{3.3E}{h_o}\left(\frac{1.5h_ot_w^3}{12} + \frac{t_sb_s^3}{12}\right)$$

$$\beta_{sec} = \frac{3.3(29000)}{15.355}\left(\frac{1.5(15.355)0.25^3}{12} + \frac{(0.25)4^3}{12}\right) = 8497 \text{ kip - in/rad}$$

- Required brace stiffness:

$$\beta_{Tb} = \frac{\beta_T}{\left(1 - \frac{\beta_T}{\beta_{sec}}\right)}$$

$$\beta_{Tb} = \frac{7220}{\left(1 - \frac{7220}{8497}\right)} = 48000 \text{ kip} - \text{in/rad}$$

- Required brace strength (at $M = M_{cr}$):

$$M_{br} = \frac{0.024 M_{cr} L}{n C_b L_b}$$

$$M_{br} = \frac{0.024(2830)(240)}{1(1.75)(120)} = 77.6 \text{ kip - in}$$

*4.6.2.2.2 Brace Requirements based on the Refined Equations from Yura and Phillips (1992)*

According to Eq. (2-31) through Eq. (2-35) in Chapter 2, the bracing requirements are as follows:

- The ideal discrete torsional brace stiffness is

$$\beta_{Ti} = (M_{cr}{}^2 - C_{bu}^2 M_o^2) \frac{C_T}{C_{bb}^2 E I_{eff}} \frac{L}{n}$$

$$\beta_{Ti} = (2830^2 - 1.35^2 (502.2)^2) \frac{1.2}{1.75^2.(29000)(9.59)} \frac{240}{1} = 2552 \text{ kip - in/rad}$$

- The brace stiffness excluding web distortion is

$$\beta_T = \frac{2\beta_{Ti}}{\phi} = 6806 \text{ kip - in/rad}$$

- The web distortional stiffness, including the effect of web transverse stiffeners is

$$\beta_{sec} = \frac{3.3E}{h_o}\left(\frac{1.5 h_o t_w^3}{12} + \frac{t_s b_s^3}{12}\right)$$

$$\beta_{sec} = \frac{3.3(29000)}{15.355}\left(\frac{1.5(15.355)0.25^3}{12} + \frac{(0.25)4^3}{12}\right) = 8497 \text{ kip - in/rad}$$

- Required brace stiffness:

$$\beta_{Tb} = \frac{\beta_T}{\left(1 - \frac{\beta_T}{\beta_{sec}}\right)}$$

$$\beta_{Tb} = \frac{6806}{\left(1 - \frac{6806}{8497}\right)} = 34200 \text{ kip - in/rad}$$

One can observe that this brace stiffness (34200 kip-in/rad) is smaller than brace stiffness (48000 kip-in/rad) calculated based on the AISC 2005 Appendix 6 Commentary.

- Required brace strength (at $M = M_{cr}$):

$$M_{br} = \beta_T \theta_o = \beta_T \frac{L_b}{500 h_o}$$

$$M_{br} = (6806)\frac{120}{500(15.355)} = 107 \text{ kip - in}$$

*4.6.2.2.3 Load-Deflection Results using $\beta = 2\beta_{iF(SAP)}/\phi$*

Fig. 4.6.30 shows the load-deflection analysis results from SAP 2000 using the brace stiffness

$$\beta_{br(SAP)} = \frac{2\beta_{i(SAP)}}{\phi} = \frac{2(4000)}{0.75} = 10667 \text{ kip - in/rad}$$

from the refined FEA model. Similar to the Benchmark Study TB1, this brace stiffness is much smaller than the brace stiffness estimated based on the AISC 2005 Appendix 6 Commentary as well as based on the refined equations from Yura and Phillips (1992).

Fig. 4.6.30 shows the normalized applied moment $M/M_{cr}$ versus the normalized bracing force $M_{br}/M_{cr}$ . The critical moment $M_{cr}$ used in normalizing the results is calculated using the AISC elastic LTB equation (Eq. F2-4).

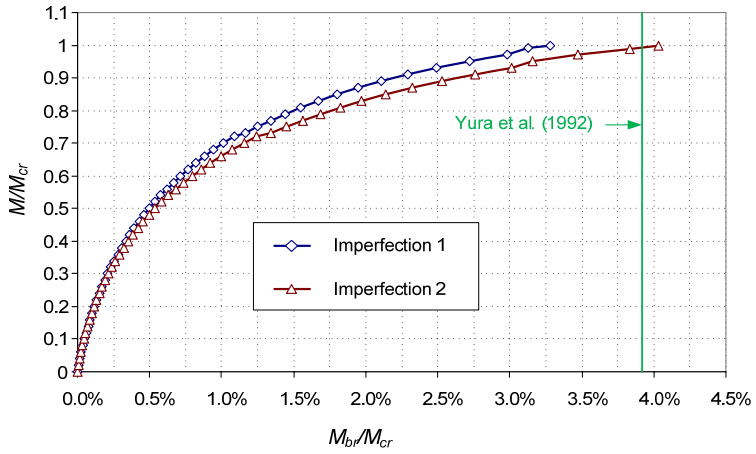


**Fig. 4.6.30. Benchmark Study TB2, Case 1 – Load vs. brace forces using $\beta = 2\beta_{i\,(SAP)}/\phi$, refined model.**

The brace stiffness used in simplified model is

$$\beta_{br(SAP)} = \frac{2\beta_{i(SAP)}}{\phi} = \frac{2(3800)}{0.75} = 10133 \text{ kip - in/rad}$$

The load-deflection analysis results from SAP 2000 using this brace stiffness from the simplified model is plotted Fig. 4.6.31.


**Fig. 4.6.31. Benchmark Study TB2, Case 1 – Load vs. brace forces using $\beta = 2\beta_{i\,(SAP)}/\phi$, simplified model.**

*4.6.2.2.4 Discussion of Results*

The following observations can be made from the Benchmark Study TB2 solutions:

- Imperfection 2 gives higher brace forces than imperfection 1. Yura and Phillips (1992) equations give a required brace force 15% larger than the required brace force from the refined model for imperfection 1 and 6% smaller than the required brace force from the refined model for imperfection 2.
- The simplified model fails to converge slightly before reaching $M_{cr}$ for both imperfections 1 and 2.
- The simplified analysis model underpredicts the refined analysis required stiffness by 5%. The simplified analysis model underpredicts the refined analysis brace forces by 2 to 7%.
- The Appendix 6 Commentary equations give a required brace stiffness of 4.5 times the required bracing stiffness of $2\beta_i/0.75$ obtained from the refined model. The Yura and Phillips (1992) equations give a required brace stiffness of 3.2 times the required bracing stiffness of $2\beta_i/0.75$ obtained from the refined model.
- The Appendix 6 Commentary equations give a required brace force 16% smaller than the required brace force from the refined model for imperfection 1. The Appendix 6 Commentary equations give a required brace force 32% smaller than the required brace force from the refined model for imperfection 2.
- The nonlinearity in the $M_{cr}$ versus $M_{br}$ curves is significant given the stiffnesses selected for the load-deflection analyses presented above. Similar to Benchmark Study TB1, the author believes it would be unwise to reduce the torsional bracing

stiffness any further than the values considered here, since this would likely lead to excessive torsional brace forces.

## 4.7 Combined Lateral and Torsional Bracing

The Benchmark Study LB3* in Section 4.6.1.4 shows that combined lateral and torsional bracing is more effective than only using torsional or lateral bracing. Prior studies have shown that bracing that controls both lateral movement and twist is more effective than lateral or torsional braces acting alone (Tong and Chen 1988; Yura and Phillips 1992). The lateral stiffness may be developed by diaphragm and/or rod/cable bracing stiffness, or it may come from incidental lean-on action against adjacent frames that are less critically loaded. In a metal building, a small incidental lateral stiffness contribution at the purlins or girts can provide a significant reduction in the torsional bracing requirements. The procedure to calculate the torsional and lateral bracing stiffness from the girt and purlin in the metal frame is discussed in this part. This procedure is developed from initial recommendations by Thomas (2007).

### 4.7.1 Calculation of Torsional Bracing Stiffness

Torsional braces prevent relative lateral displacement of the beam flange. The girt/purlin-flange brace assembly stiffness is primarily a function of the supporting girt/purlin flexural stiffness and the area and the angle of inclination of the flange brace. The stiffness for any of the components may be determined by taking the inverse of the deflection caused by a unit load.

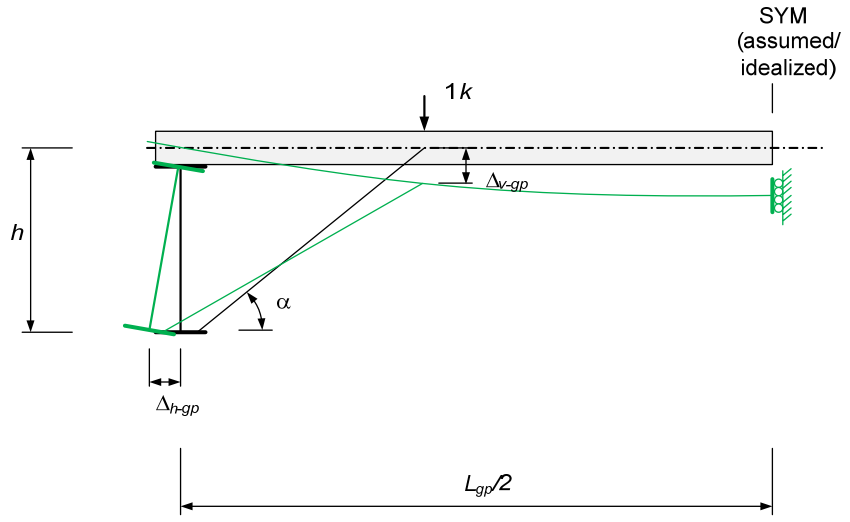


**Fig. 4.7.1. Vertical stiffness of a simply supported girt/purlin.**

The vertical stiffness of a simply supported girt/ purlin can be calculated by application of a unit load at the brace connection location as illustrated in Fig. 4.7.1. The assumption of the symmetry boundary condition is necessary for this calculation since adjacent frames may buckle in the same or opposite directions. Also, it is assumed that the axial deformation of flange brace is neglected; only the flexural deformation of the girt or purlin is considered. From these assumptions, the unit load applied at the juncture between the flange brace and purlin cause a vertical displacement $\Delta_{v\text{-}gp}$ and a horizontal displacement $\Delta_{h\text{-}gp}$. The vertical stiffness of a simply-supported girt/ purlin is

$$\beta_{v\text{-}gp} = \frac{1}{\Delta_{v-gp}} \qquad (4.7\text{-}1)$$

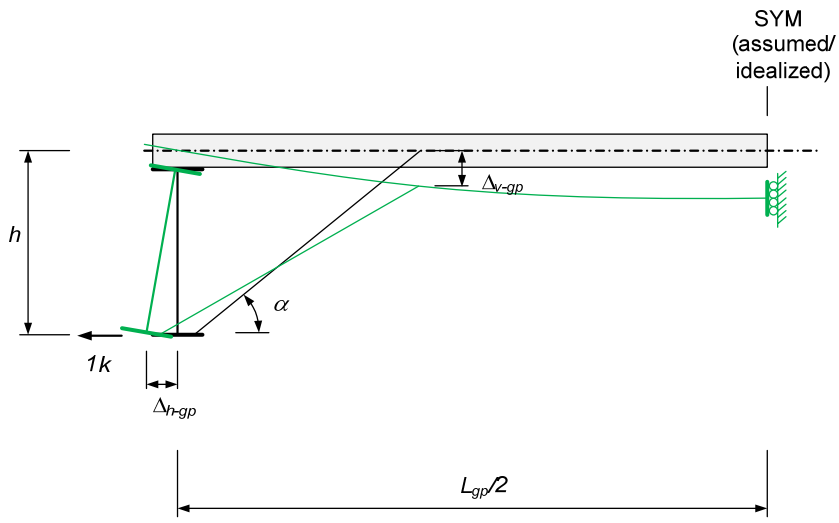


**Fig. 4.7.2. Lateral stiffness provided by a simply supported girt/purlin.**

Fig. 4.7.2 shows the deformation of the connection under the unit load applied in lateral direction at the bottom flange. The lateral stiffness provided by a simply supported girt/purlin is approximately converted to the vertical stiffness.

$$\beta_{h\text{-}gp} = \frac{\beta_{v\text{-}gp}}{\tan^2\alpha} \qquad (4.7\text{-}2)$$

If one considers the axial deformations of flange braces, the brace stiffness is reduced. For this case the flexural deformation of the girt/purlin is not included and only the axial deformation of the flange brace is considered. The lateral stiffness provided by flange brace can be determined from Fig. 4.7.3.

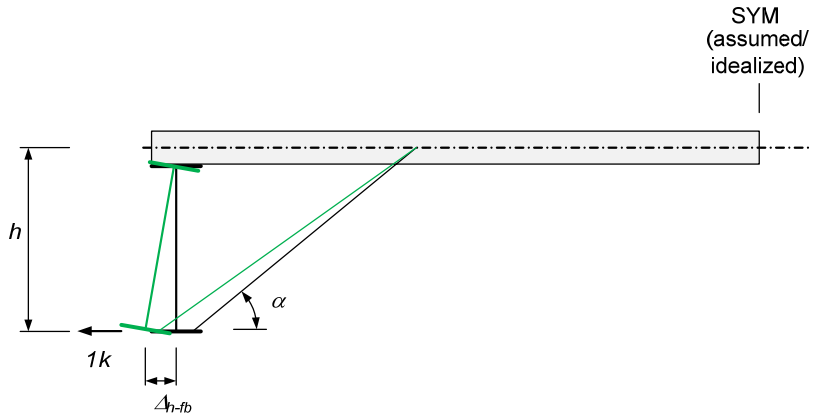


**Fig. 4.7.3. Lateral stiffness provided by flange brace.**

The equivalent lateral stiffness provided by a simply-supported girt/purlin is

$$\beta_{h\text{-}gp} = \frac{1}{\Delta_{h\text{-}fb}} = \frac{A_{fb} E \cos^2 \alpha}{L_{fb}} \tag{4.7-3}$$

The net lateral stiffness from girt/purlin-flange braces assembly

$$\beta_h = \frac{1}{\frac{1}{\beta_{h-gp}} + \frac{1}{\beta_{h-fb}}} \tag{4.7-4}$$

Fig. 4.7.4 shows the web distortional deformations. The stiffness of web due to connection of flange brace to the web can be determined based on Yura (2001). It is assumed that neglect these deformations if connection is directly to flange; otherwise connect as close as possible to the inside flange.

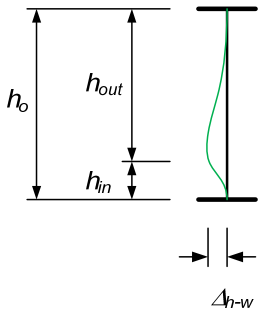


**Fig. 4.7.4 Web distortional deformation.**

The stiffnesses of web accounting for web distortion can be calculated as follows:

$$\beta_{out,in} = \frac{3.3E}{h_i}\left(\frac{h_o}{h_i}\right)^2\left(\frac{1.5h_i t_w^3}{12}\right) \tag{4.7-5}$$

where $h_i = h_{out}$ or $h_{in}$

$$\beta_{sec} = \frac{1}{\frac{1}{\beta_{out}} + \frac{1}{\beta_{in}}} \tag{4.7-6}$$

From the above discussions, the equivalent torsional spring stiffness can be determined by below expression

$$\beta_T = \frac{1}{\frac{1}{\beta_h h^2} + \frac{1}{\beta_{sec}}} \tag{4.7-7}$$

The potential sources of girt/purlin-flange brace deformations (not considered in the above developments) should be considered including:

- Local deformations in bends in the flange brace at its attachment to the member being braced,
- Slip of flange brace fasteners in the attachment to the member being braced and/or to the girt/purlin,
- Slip of fasteners between the girt/purlin and the outside flange of the member being braced,
- Flange torsional deformations due to eccentricity between the attachment of the flange brace and the web-flange juncture of the member being braced,
- Continuous purlins are handled in the same fashion as the above development for simply-supported purlins, but we have a contribution from both sides. The outside flange of the member is assumed to be pin connected to the girt/purlin at the

girt/purlin centroidal (without stiffening of the cross-section, the direct torsional resistance provided by the girt/purlin to the outside flange is negligible),

- Symmetry b.c. are assumed at the mid-span of the girt/purlin on either side, since the adjacent frames may buckle in opposite directions (this assumes continuity over all of the frames),
- If the assembly is not symmetric about the member being braced, include the entire assembly (both sides) in one model. Continuity of the girt/purlin over the outside flange may be considered.

### 4.7.2 Calculation of Lateral Bracing Stiffness

The lateral bracing stiffness contribution at various locations along the length of the members depends on:

- Shear diaphragm stiffness from roof/wall panels,
- Shear stiffness from diagonal bracing systems (it is typically assumed that the shear flexibilities dominate over the bending flexibilities from the "truss chords" in these systems),
- Lateral bending stiffness from other less-critically loaded frames and lean-on action (depends on the axial stiffness of the girts/purlins if developed over long purlin lengths, as well as slip resistance of the fasteners between the girts/purlins and the various frames.)

It is envisioned that lower-bound constant lateral stiffness contributions might be estimated for various specific systems and then used as part of the stability bracing assessment.

### 4.7.3 Eigenvalue Buckling Analysis

In this section, two combined lateral and torsional bracing namely Case Studies CB1 and CB2 are presented. Similar to the order of the lateral or torsional bracing studies, first an eigenvalue buckling analysis is used to determine the brace stiffness. Then, the load-deflection analyses are conducted to estimate the brace forces corresponding to the brace stiffnesses.

#### 4.7.3.1 Benchmark Study CB1

Fig. 4.7.5 shows a simply-supported W16x26 beam with the combined lateral and torsional braces at mid-span, $L_b$ = 10 ft, under the uniform *positive* bending moment. The torsional and lateral springs represent a purlin and flange diagonal bracing. These springs are located at the purlin mid-depth. They are connected to two rigid links. The brace point is located at 2 inches above the top flange (assuming a 4 inch purlin or girt with this 16 inch deep beam). One rigid link is pin connected to the top flange at the web-flange juncture and one is pin connected to the bottom flange at the web-flange juncture. The web is otherwise free to deform out of its plane at the brace point.

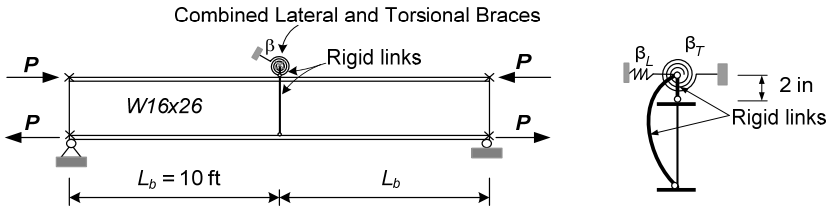


**Fig. 4.7.5. Benchmark Study CB1 – Problem description.**

The results of the eigenvalue buckling analyses below illustrate the effectiveness of using combined lateral and torsional bracing. The ideal brace stiffnesses ($\beta_{iF}$) corresponding

to full bracing at different fractions of torsional and lateral bracing are discussed. The results of using combined lateral and torsional braces are compared to the results for lateral and torsional bracing alone.

The buckling mode at $\beta = \beta_{iF}$ when only a lateral brace is used is plotted in Fig. 4.7.6. The lateral brace stiffness from SAP 2000 is determined as $\beta_{LiF} = 1.31$ kips/inch. This differs from $\beta_{iF} = 1.58$ kips/inch in Benchmark Study LB1 since the brace is attached at 2 inches above the top flange of beam.

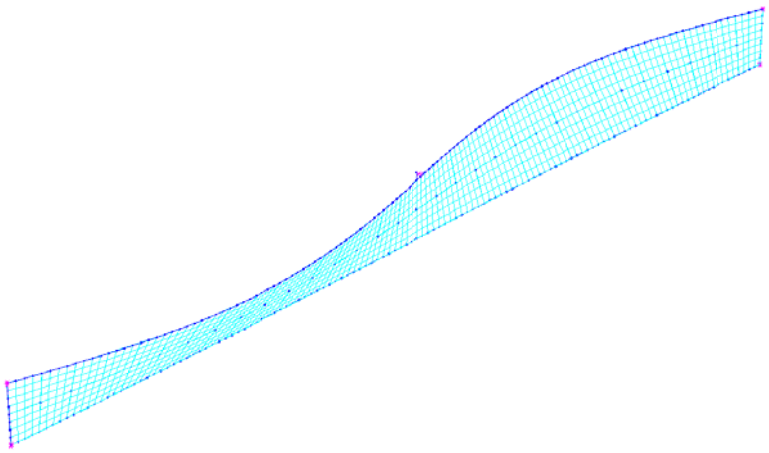

**Fig. 4.7.6. Benchmark Study CB1 – Buckling mode at $\beta = \beta_{LiF}$ for full bracing, lateral brace only.**

Similarly, the buckling mode at the brace stiffness for full bracing for torsional bracing only is displayed in Fig. 4.7.7. The torsional brace stiffness determined from SAP 2000 for this case is $\beta_{TiF} = 1461$ kip-inch/rad. This compares to $\beta_{TiF} = 1799$ kip-inch/rad in Benchmark Study TB1.

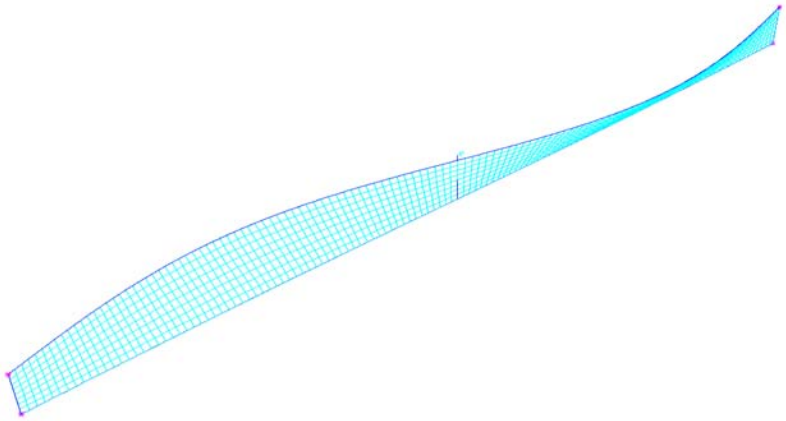

**Fig. 4.7.7. Benchmark Study CB1 – Buckling mode at $\beta = \beta_{TiF}$ for full bracing, torsional brace only.**

Fig. 4.7.8 shows the buckling mode at the brace stiffness for full bracing using one of several cases considered in valuing combined lateral and torsional braces ($\beta_{CLiF}$ = 0.3 kips/inch & $\beta_{CTiF}$ = 781.0 kip-inch/rad).

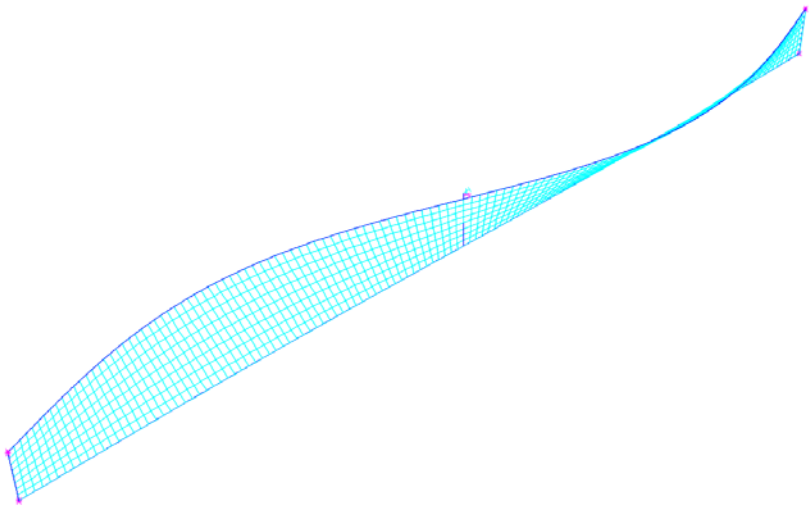

**Fig. 4.7.8. Benchmark Study CB1 – Buckling mode for full bracing using combined lateral and torsional braces with $\beta_{CLiF}$ = 0.3 kips/inch and $\beta_{CTiF}$ = 781.0 kip-inch/rad**

The interaction between lateral and torsional bracing is complex. Using the trial and error method, the interaction curve for a full range of lateral and torsional brace combinations is plotted in Fig. 4.7.9.

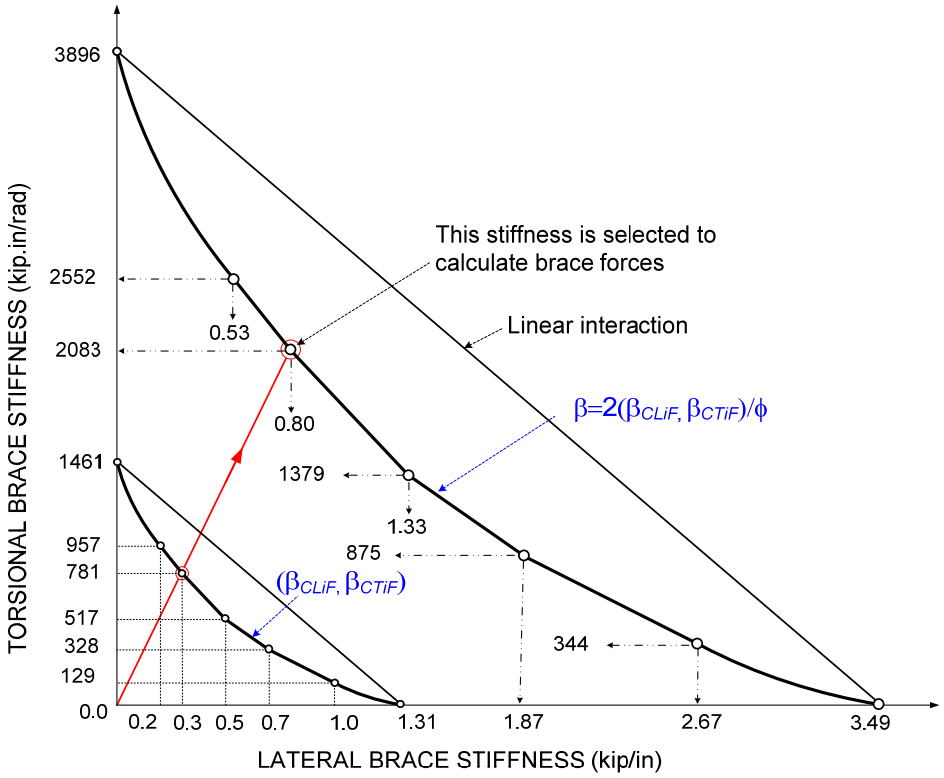


**Fig. 4.7.9. Benchmark study CB1 – Interaction between lateral and torsional bracing stiffness.**

One can observe from Fig. 4.7.9 that combined lateral and torsional bracing is more effective than torsional or lateral bracing alone. In the above example values, the lateral bracing stiffness of $\beta_{CLiF}$ = 0.3 kips/inch (only 23% of $\beta_{LiF}$ = 1.31 kips/inch), illustrated by the radial line in this plot, is sufficient to reduce the corresponding torsional bracing stiffness requirement by 47% ($\beta_{CTiF}$ = 781 kip-in/rad is equal to 47% of $\beta_{TiF}$ = 1461 kip-in/rad).

4.7.3.2 Benchmark Study CB2

Fig. 4.7.10 shows the same structural layout as Benchmark Study CB1 except the moment in this case causes compression on the bottom flange.

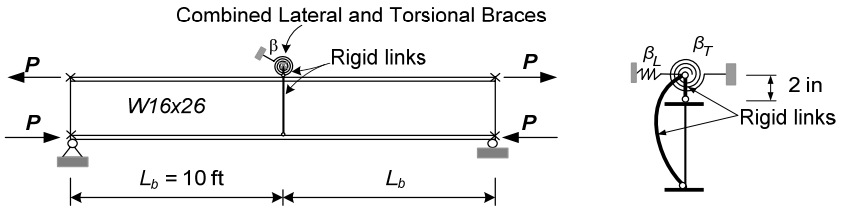


**Fig. 4.7.10. Benchmark Study CB2 – Problem description.**

The buckling mode at the brace stiffness for full bracing for torsional brace only is plotted in Fig. 4.7.11. The torsional brace stiffness for full bracing is determined as $\beta_{TiF}$ = 1461 kip-inch/rad. That is, the $\beta_{TiF}$ requirement is unchanged from that of problem CB1.

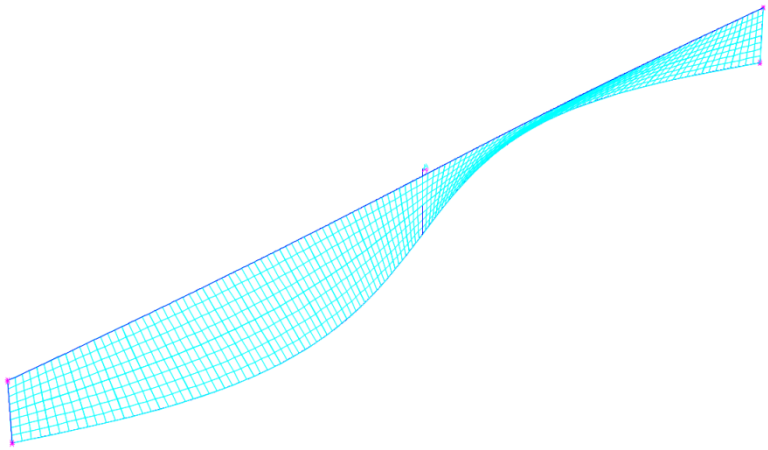

**Fig. 4.7.11. Benchmark Study CB2 – Buckling mode at $\beta = \beta_{TiF}$ for full bracing, torsional brace only.**

Fig. 4.7.12 shows the buckling mode at the brace stiffness for full bracing using one of several cases considered in valuing combined lateral and torsional braces ($\beta_{LiF}$ = 0.3 kips/inch & $\beta_{TiF}$ = 1165 kip-inch/rad)

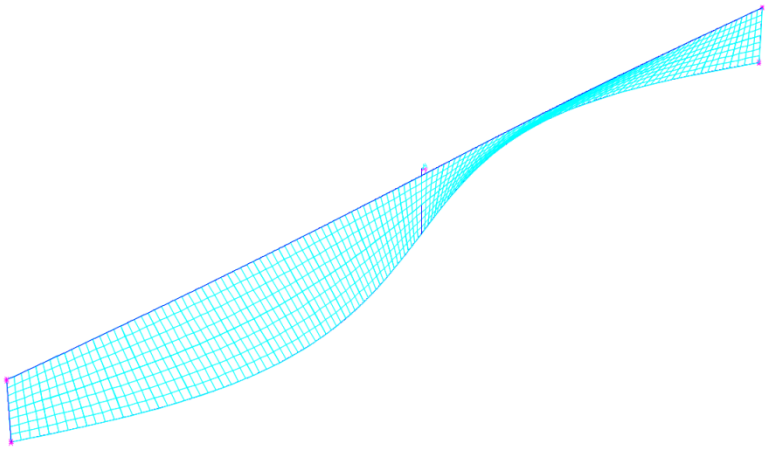

**Fig. 4.7.12. Benchmark Study CB2 – Buckling mode at $\beta = \beta_i$ for full bracing, combined lateral and torsional braces.**

One can note that the lateral brace stiffness requirement is approximately 1.5 times larger than that of Benchmark Study CB1. This is because the lateral brace is located on the tension side of the beam in this problem.

Similar to the Benchmark Study CB1, the interaction curve for a full range of lateral and torsional brace combinations is plotted in Fig. 4.7.13.

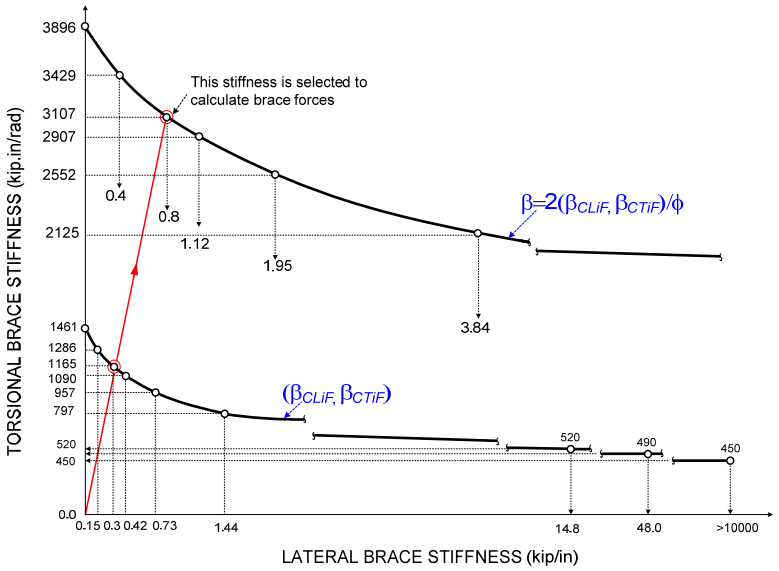


**Fig. 4.7.13. Benchmark Study CB2 – Interaction between lateral and torsional bracing stiffness.**

Fig. 4.7.13 indicates that lateral bracing alone at the tension flange has essentially no effect. The smallest torsional brace stiffness that can provide full bracing (with the lateral brace stiffness at the tension flange approaching infinity) is around 450 kip-inch/rad.

Using the same lateral bracing stiffness as considered previously for Benchmark Study CB1, the required torsional bracing stiffness is reduced by 20 % relative to the torsional bracing stiffness requirement for torsional bracing alone. This percentage decrease in the torsional brace stiffness requirement is roughly one-half of that attained in Benchmark Study CB1 for the selected lateral brace stiffness.

### 4.7.4 Load-Deflection Analysis Results

Load-deflection analysis is used in this section to estimate the required torsional and lateral bracing forces for a range of brace stiffnesses from ($\beta_{CLiF,}$ $\beta_{CTiF}$) to *2*($\beta_{CLiF,}$ $\beta_{CTiF}$)/$\phi$. The brace forces with the combined lateral and torsional braces are compared to the results for lateral bracing alone and for torsional bracing alone.

#### 4.7.4.1 Benchmark Study CB1

Since the interaction between lateral and torsional braces in the combined lateral and torsional bracing is very complicated, determining the lateral bracing stiffness and torsional bracing stiffness need more judgment. This decision requires understanding the physical behavior of a specific structural system. For example, for a system that provide more lateral brace stiffness than torsional brace stiffness, the designer should consider a larger combined lateral brace to torsional brace in stiffness. In this section, several combined brace stiffnesses along the line (ABCD) in Fig. 4.7.14 are selected to calculate the brace forces. First, the brace forces are determined using the brace stiffness $\beta = 2\beta_{LiF(SAP)}/\phi$ for the only

lateral brace or $\beta = 2\beta_{TiF(SAP)}/\phi$ for the only torsional brace. Then, these brace forces are compared to the brace forces using the brace stiffness $\beta_L = 2\beta_{CLiF}/\phi$ and $\beta_T = 2\beta_{CTiF}/\phi$ for combined lateral and torsional braces. Finally, the brace forces are estimated by the range of brace stiffness from 1.0 to $2/\phi$ of the ideal full bracing values $\beta_{CLiF}$, $\beta_{CTiF}$. The results are summarized as follows.

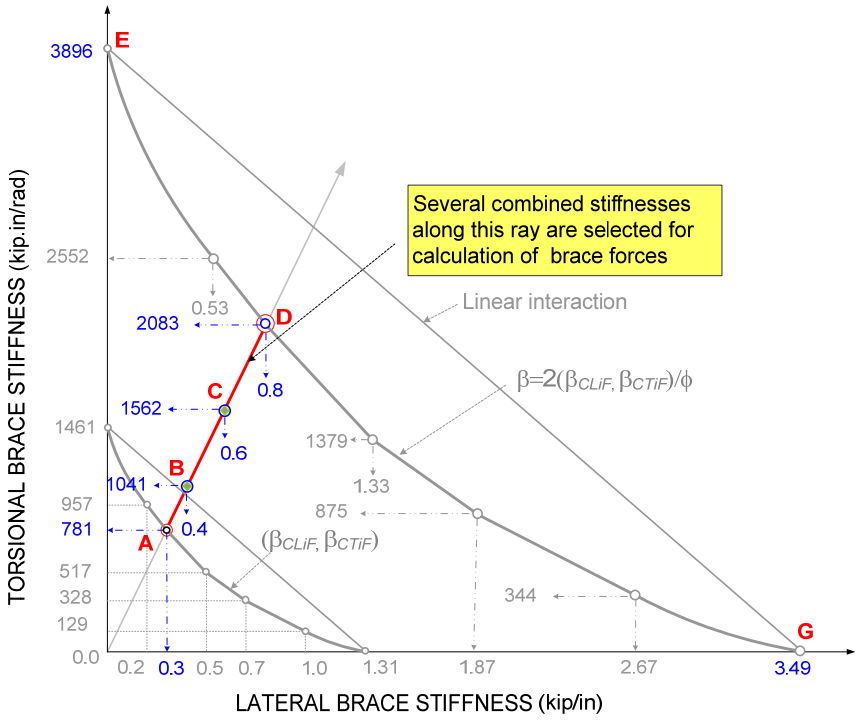


**Fig. 4.7.14. Benchmark Study CB1 – Variation of brace stiffnesses between 1.0 to $2/\phi$ of the ideal full bracing values.**

*4.7.4.1.1 Load-Deflection Results using Stiffness Equal to $2/\phi$ of the Ideal Full Bracing Values*

The brace stiffnesses used to determine the brace forces are as follows:

- For the case where $2/\phi$ of the ideal full bracing value using the lateral brace alone.

$\beta_L = 2\beta_{LiF}/\phi = 3.49$ kips/inch and $\beta_T = 0$ (point G in Fig. 4.7.14)

- For the case where 2/ϕ of the ideal full bracing value using the torsional brace alone.

  $\beta_L$= 0 and $\beta_T$=2$\beta_{TiF}$ /ϕ = 3896 kip-inch/rad (point E in Fig. 4.7.14)

- For the case where 2/ϕ of the ideal full bracing value using combined lateral and torsional brace

  $\beta_L$ = 2$\beta_{CLiF}$/ϕ = 0.8 kips/inch and $\beta_T$=2$\beta_{CTiF}$ /ϕ = 2083 kip-in/rad

  (point D in Fig.4.7.14)

Figs. 4.7.15 and 4.7.16 compare the lateral brace forces for lateral bracing only and for combined lateral and torsional bracing using imperfections 1 and 2. The brace force *($P_{br}$)* in the horizontal axis is normalized by the compressive flange force at the critical load level *($M_{cr}$)*. The applied moment in the vertical axis is normalized by the critical moment *($M_{cr}$)*. The critical moment *($M_{cr}$)* is calculated using AISC Eq. (F2-4). One can observe from Figs. 4.7.15 and 4.7.16 that the brace for combined lateral and torsional bracing are significantly smaller than those from the lateral brace only using imperfections 1 and 2.

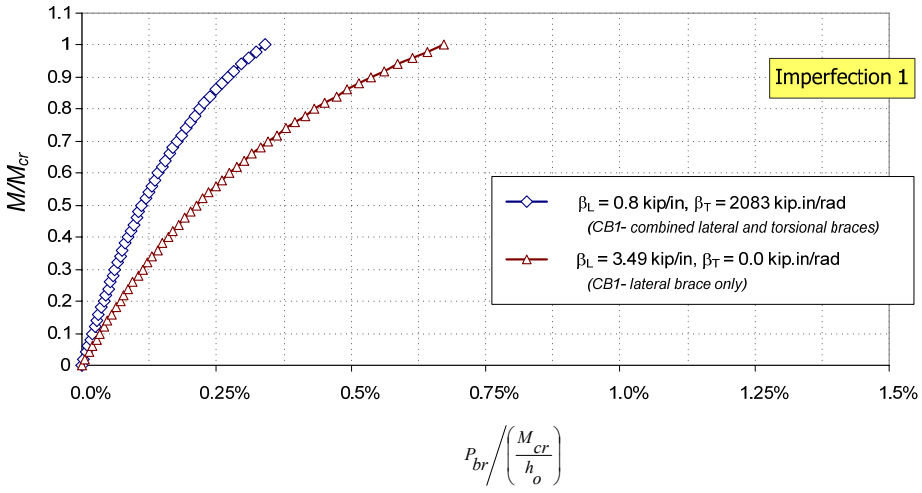


**Fig. 4.7.15. Benchmark Study CB1 – Lateral brace forces, imperfection 1.**

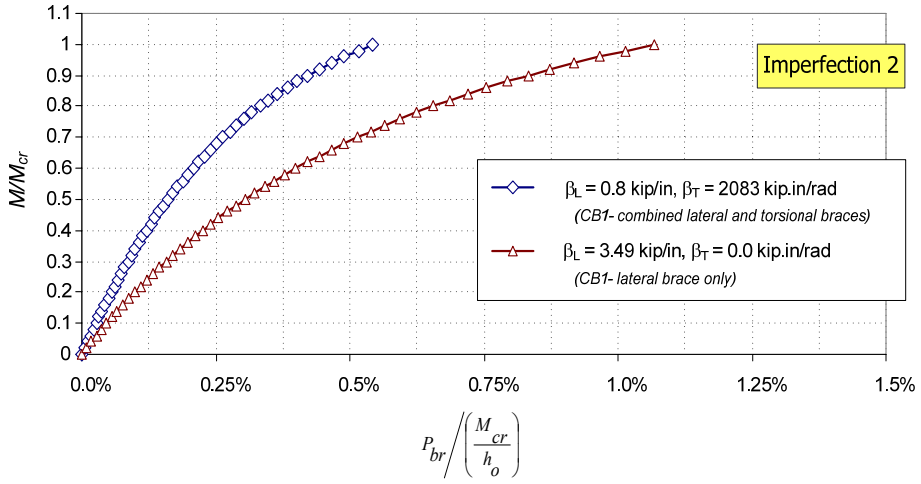


**Fig. 4.7.16. Benchmark Study CB1 – Lateral brace forces, imperfection 2.**

Similarly, Figs. 4.7.17 and 4.7.18 compare the results between the torsional brace forces for torsional bracing only and for combined lateral and torsional bracing using imperfections 1 and 2. Figs. 4.7.17 and 4.7.18 indicate that the brace forces *($M_{br}$)* for combined lateral and torsional braces are significantly smaller than the brace forces for torsional bracing only for both imperfections 1 and 2.

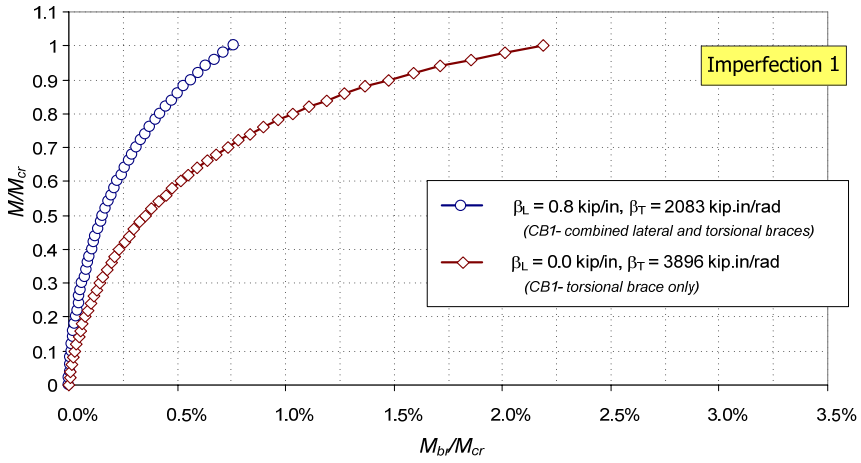


**Fig. 4.7.17. Benchmark Study CB1 – Torsional brace forces, imperfection 1.**

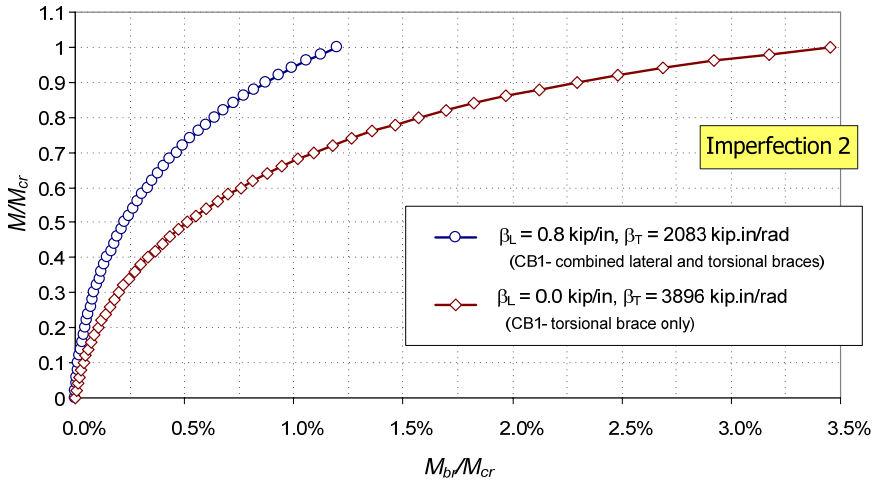


**Fig. 4.7.18. Benchmark Study CB1 – Torsional brace forces, imperfection 2.**

*4.7.4.1.2 Load-Deflection Results using Several Brace Stiffnesses between 1.0 to 2/ϕ of the Ideal Full Bracing Values*

The following four different pairs of brace stiffness are considered in this section:

- $\beta_L = \beta_{CLiF} = 0.3$ kips/inch & $\beta_T = \beta_{CTiF} = 781$ kip-inch/rad (point A in Fig. 4.7.14)
- $\beta_L = \beta_{CLiF}/\phi = 0.4$ kips/inch & $\beta_T = \beta_{CTiF}/\phi = 1041$ kip-inch/rad (point B in Fig. 4.7.14)
- $\beta_L = 1.5\beta_{CLiF}/\phi = 0.6$ kips/inch & $\beta_T = 1.5\beta_{CTiF}/\phi = 1562$ kip-inch/rad (point C in Fig. 4.7.14)
- $\beta_L = 2\beta_{CLiF}/\phi = 0.8$ kips/inch & $\beta_T = 2\beta_{CTiF}/\phi = 2083$ kip-inch/rad (point D in Fig. 4.7.14), this brace stiffnesses are the same as in Section 4.7.1.1

The results of lateral brace forces using imperfections 1 and 2 are shown in Fig. 4.7.19 to 4.7.20. Interestingly, the brace stiffnesses from 1.0 to 2/ϕ of the ideal full bracing values forces do not affect much on the brace forces. For example, for imperfection 1, for brace stiffness based on $\beta_L = \beta_{CLiF} = 0.3$ kips/inch & $\beta_T = \beta_{CTiF} = 781$ kip-inch/rad, the maximum lateral brace force is equal approximately to 0.45% of $M_{cr}/h_o$ while for brace stiffness based

on $\beta_L = 2\beta_{CLiF}/\phi = 0.8$ kips/inch & $\beta_T = 2\beta_{CTiF}/\phi = 2083$ kip-inch/rad, the maximum lateral brace force is equal approximately to 0.35% of $M_{cr}/h_o$.

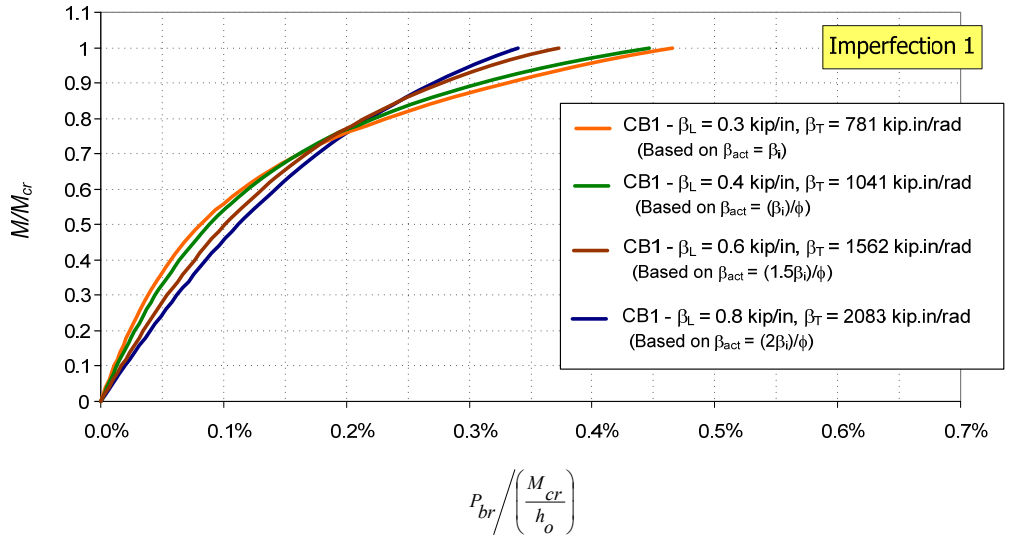


**Fig. 4.7.19. Benchmark Study CB1 – Lateral brace forces using several brace stiffnesses between 1.0 to 2/ϕ of the ideal full bracing values, imperfection 1.**

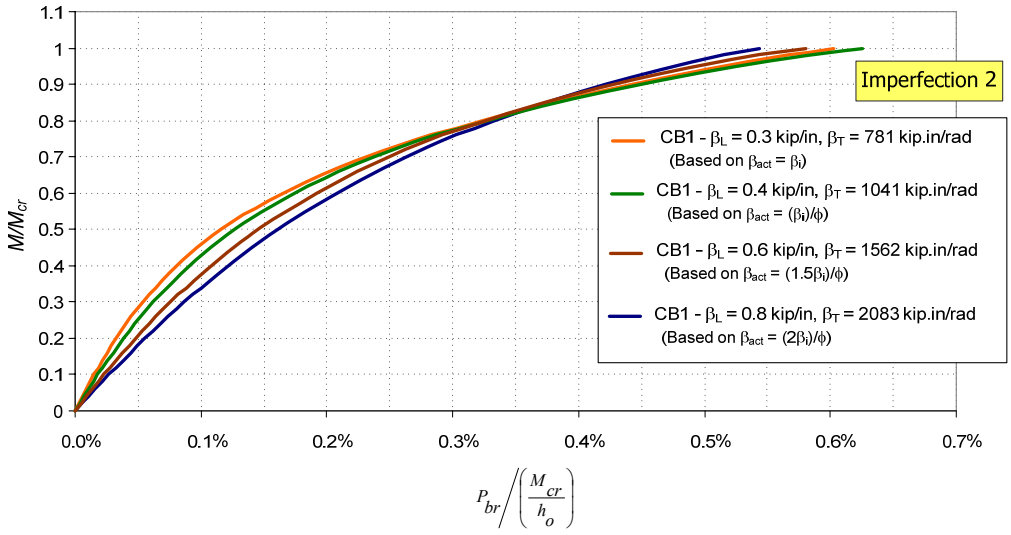


**Fig. 4.7.20. Benchmark Study CB1 – Lateral brace forces using several brace stiffnesses between 1.0 to 2/ϕ of the ideal full bracing values, imperfection 2.**

Figs. 4.7.21 to 4.7.22 show the torsional brace forces using imperfections 1 and 2 with four different pairs of brace stiffness varied from 1.0 to 2/ϕ of the ideal full bracing values. The brace forces are smaller than 2% of critical load $M_{cr}$ in all cases. For example, for imperfection 1, for brace stiffness based on $\beta_L = \beta_{CLiF} = 0.3$ kips/inch & $\beta_T = \beta_{CTiF} = 781$ kip-inch/rad, the maximum torsional brace force is equal approximately to 1.5% of $M_{cr}$ while for brace stiffness based on $\beta_L = 2\beta_{CLiF}/\phi = 0.8$ kips/inch & $\beta_T = 2\beta_{CTiF}/\phi = 2083$ kip-inch/rad, the maximum torsional brace force is equal approximately to 0.75% of $M_{cr}$.

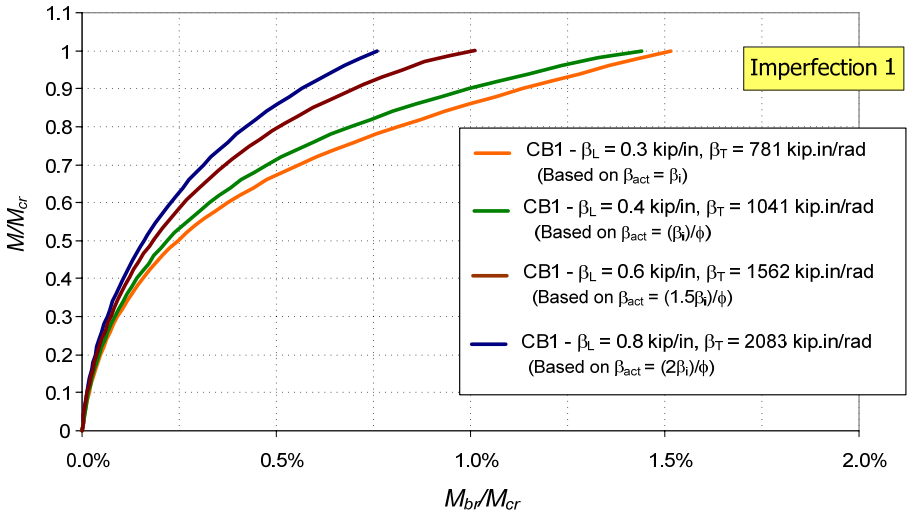


**Fig. 4.7.21 Benchmark Study CB1 – Torsional brace forces using several brace stiffnesses between 1.0 to 2/ϕ of the ideal full bracing values, imperfection 1.**

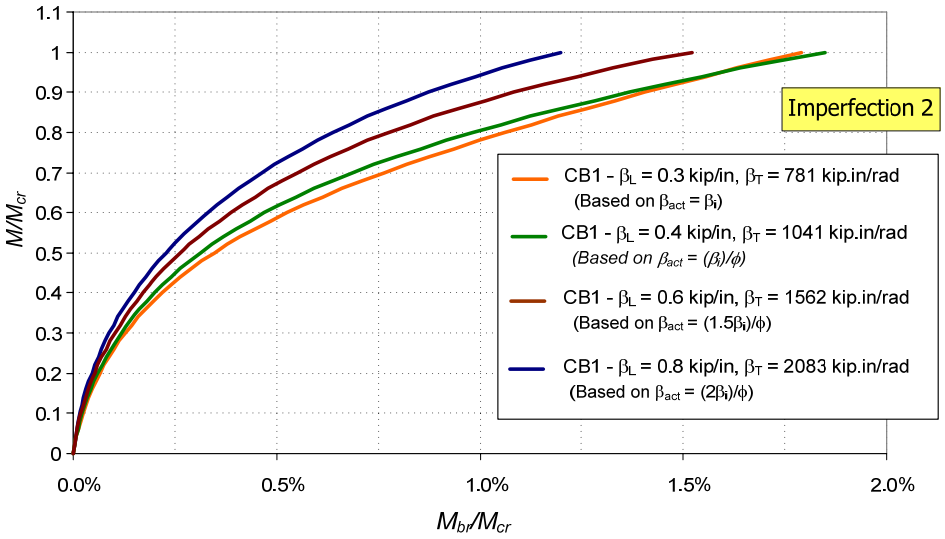


**Fig. 4.7.22 Benchmark Study CB1 – Torsional brace forces using several brace stiffnesses between 1.0 to 2/ϕ of the ideal full bracing values, imperfection 2.**

*4.7.4.1.3 Discussion of Results*

The brace forces for the cases with combined lateral and torsional bracing (with lateral bracing stiffness of approximately 23% $\beta_{LiF}$) are substantially smaller than those associated with lateral or torsional bracing alone. Changes in the brace stiffnesses from 2.0/0.75 to 1.5/0.75 to 1.0/0.75 to 1.0 of the ideal full bracing values have a relatively small influence on the brace forces.

In all the cases considered, the lateral brace force is never larger than 0.63 %. The torsional brace moment increases when the bracing stiffnesses are scaled from 2.0/0.75 to 1.0 of the ideal full bracing stiffnesses from 1.2% to 1.7% of $M_{cr}$ (for imperfection 2).

4.6.4.2 Benchmark Study CB2

From the results of the eigenvalue buckling analysis in Section 4.7.3.2, one can observe that it is not worthy to consider the lateral bracing alone.

In this section, several combined brace stiffnesses along the line (ABCD) in Fig. 4.7.23 are selected to calculate the brace forces. First, the brace forces are determined using the brace stiffness $\beta = 2\beta_{TiF(SAP)}/\phi$ for the only torsional brace. Then, these brace forces are compared to the brace forces using the brace stiffness $\beta_L = 2\beta_{CLiF}/\phi$ and $\beta_T = 2\beta_{CTiF}/\phi$ for combined lateral and torsional braces. Finally, the brace forces are estimated by the range of brace stiffness from 1.0 to $2/\phi$ of the ideal full bracing values $\beta_{CLiF}$, $\beta_{CTiF}$. The results are summarized as follows.

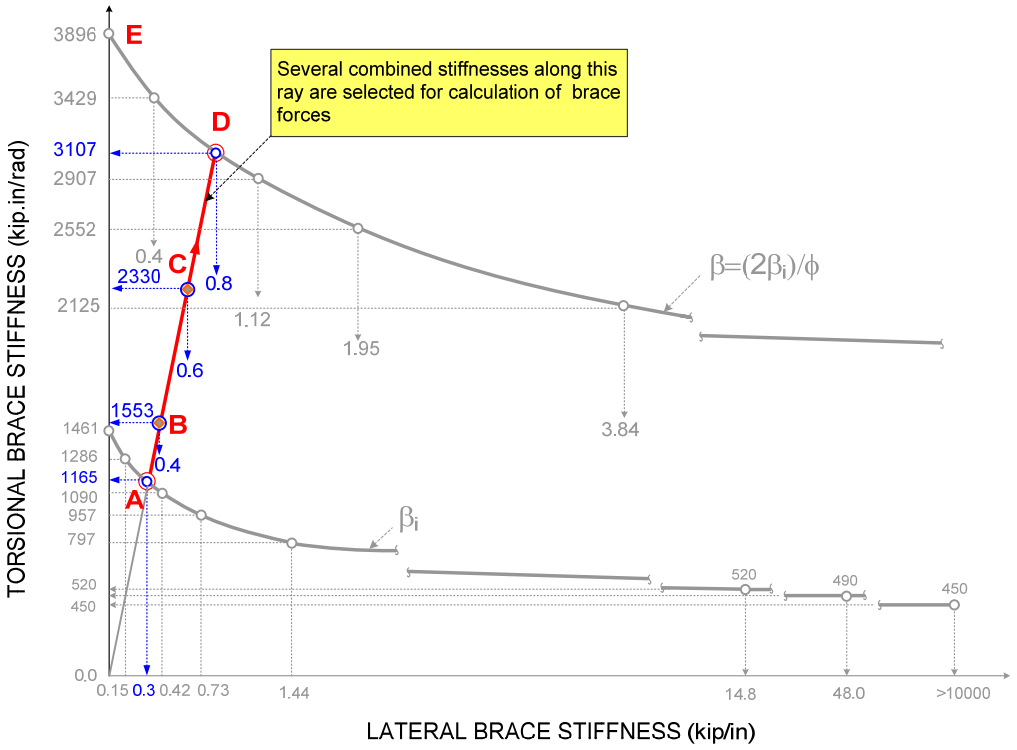


**Fig. 4.7.23 Benchmark Study CB2 – Variation of brace stiffnesses between 1.0 to $2/\phi$ of the ideal full bracing values.**

*4.7.4.2.1 Load-Deflection Results using Stiffness Equal to $2/\phi$ of the Ideal Full Bracing Values*

The brace stiffnesses used to determine the brace forces are as follows:

- For the case where $2/\phi$ of the ideal full bracing value using the torsional brace alone.

$\beta_L$= 0 and $\beta_T$=2$\beta_{TiF}$ /$\phi$ = 3896 kip-inch/rad (point E in Fig. 4.7.23)

- For the case where 2/$\phi$ of the ideal full bracing value using combined lateral and torsional brace

  $\beta_L$ = 2$\beta_{CLiF}$/$\phi$ = 0.8 kips/inch and $\beta_T$=2$\beta_{CTiF}$ /$\phi$ = 3107 kip-in/rad

  (point D in Fig.4.7.23)

Figs. 4.7.24 and 4.7.25 18 compare the results between the torsional brace forces for torsional bracing only and for combined lateral and torsional bracing using imperfections 1 and 2. The plots are normalized by the critical load $M_{cr}$ from AISC. The critical moment $(M_{cr})$ is calculated using AISC Eq. (F2-4).

Similar to Benchmark Study CB1, Figs. 4.7.24 and 4.7.25 indicate that the brace forces $(M_{br})$ from the combined lateral and torsional braces are significantly smaller than the brace forces from the torsional bracing only for both imperfections 1 and 2.

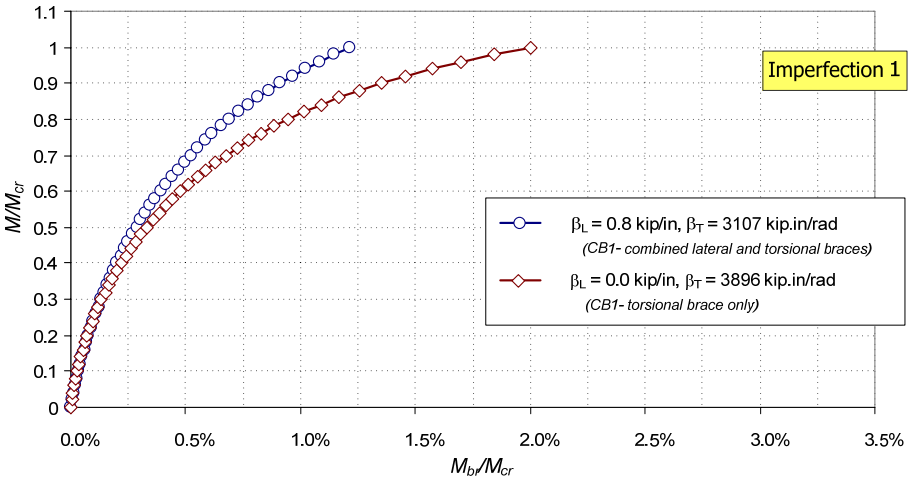


**Fig. 4.7.24. Benchmark Study CB2 – Torsional brace forces, imperfection 1.**

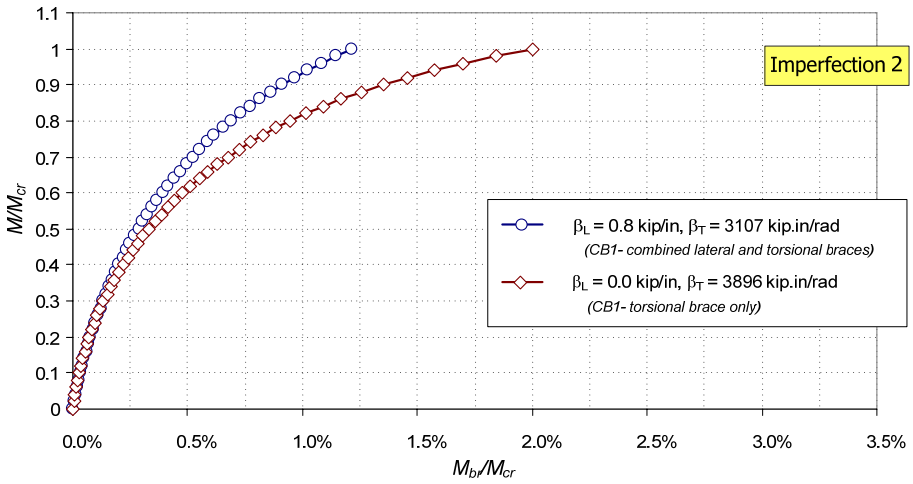


**Fig. 4.7.25. Benchmark Study CB2 – Torsional brace forces, imperfection 2.**

*4.7.4.2.2 Load-Deflection Results using Several Brace Stiffnesses between 1.0 to 2/ϕ of the Ideal Full Bracing Values*

The following four different pairs of brace stiffness are considered in this section:

- $\beta_L = \beta_{CLiF} = 0.3$ kips/inch & $\beta_T = \beta_{CTiF} = 1165$ kip-inch/rad (point A in Fig. 4.7.23)
- $\beta_L = \beta_{CLiF}/\phi = 0.4$ kips/inch & $\beta_T = \beta_{CTiF}/\phi = 1553$ kip-inch/rad (point B in Fig. 4.7.23)
- $\beta_L = 1.5\beta_{CLiF}/\phi = 0.6$ kips/inch & $\beta_T = 1.5\beta_{CTiF}/\phi = 2330$ kip-inch/rad (point C in Fig. 4.7.23)
- $\beta_L = 2\beta_{CLiF}/\phi = 0.8$ kips/inch & $\beta_T = 2\beta_{CTiF}/\phi = 3107$ kip-inch/rad (point D in Fig. 4.7.23), this brace stiffnesses are the same as in Section 4.7.2.1

The results of lateral brace forces using imperfections 1 and 2 are shown in Fig. 4.7.26 to 4.7.27. One can observe that the brace forces do not change much when the brace stiffnesses scaled from 1.0 to 2/ϕ of the ideal full bracing values. For example, for imperfection 1, for brace stiffness based on $\beta_L = \beta_{CLiF} = 0.3$ kips/inch & $\beta_T = \beta_{CTiF} = 1165$ kip-inch/rad, the maximum lateral brace force is equal approximately to 0.33% of $M_{cr}/h_o$

while for brace stiffness based on $\beta_L = 2\beta_{CLiF}/\phi = 0.8$ kips/inch & $\beta_T = 2\beta_{CTiF}/\phi = 3107$ kip-inch/rad, the maximum lateral brace force is equal approximately to 0.28% of $M_{cr}/h_o$.

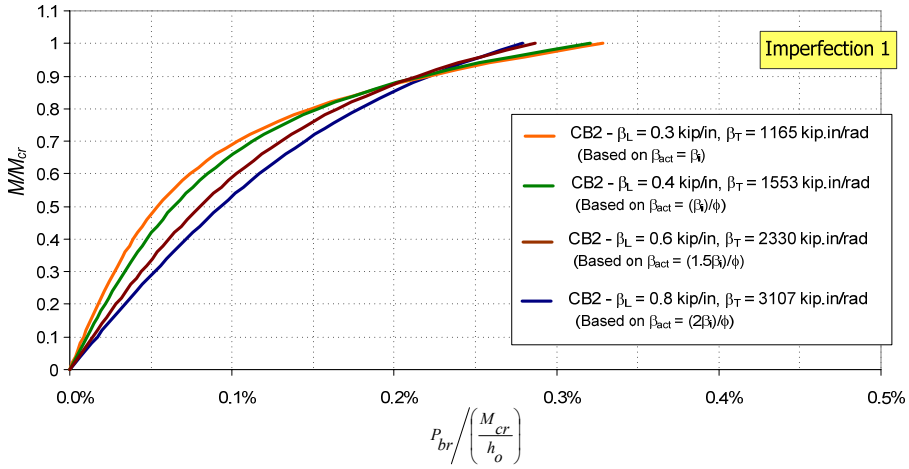


**Fig. 4.7.26. Benchmark Study CB2 – Lateral brace forces using several brace stiffnesses between 1.0 to 2/ϕ of the ideal full bracing values, imperfection 1.**

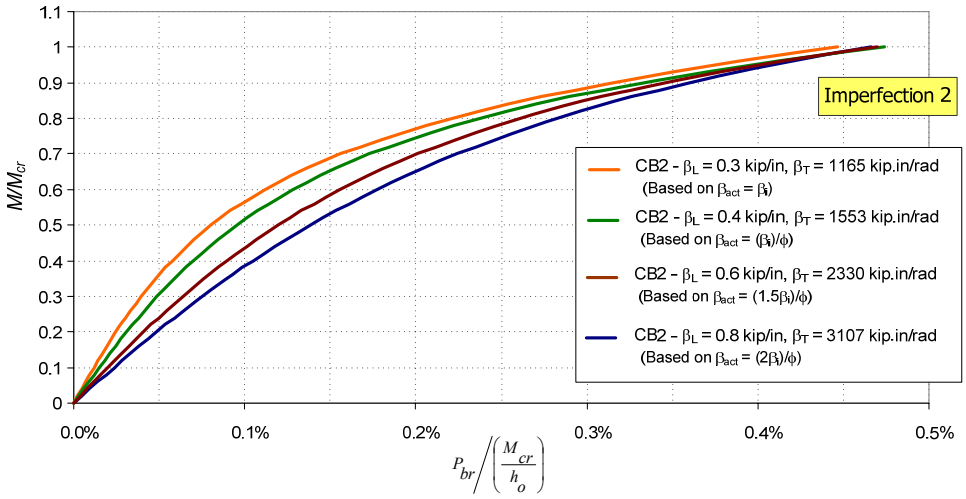


**Fig. 4.7.27. Benchmark Study CB2 – Lateral brace forces using several brace stiffnesses between 1.0 to 2/ϕ of the ideal full bracing values, imperfection 2.**

Figs. 4.7.28 to 4.7.29 show the torsional brace forces using imperfections 1 and 2 with four different pairs of brace stiffness varied from 1.0 to 2/ϕ of the ideal full bracing values. The brace forces are smaller than 3% of critical load $M_{cr}$ in all cases. For example, for

imperfection 1, for brace stiffness based on $\beta_L = \beta_{CLiF} = 0.3$ kips/inch & $\beta_T = \beta_{CTiF} = 1165$ kip-inch/rad, the maximum torsional brace force is equal approximately to 2.2% of $M_{cr}$ whereas for brace stiffness based on $\beta_L = 2\beta_{CLiF}/\phi = 0.8$ kips/inch & $\beta_T = 2\beta_{CTiF}/\phi = 3107$ kip-inch/rad, the maximum torsional brace force is equal approximately to 1.2% of $M_{cr}$

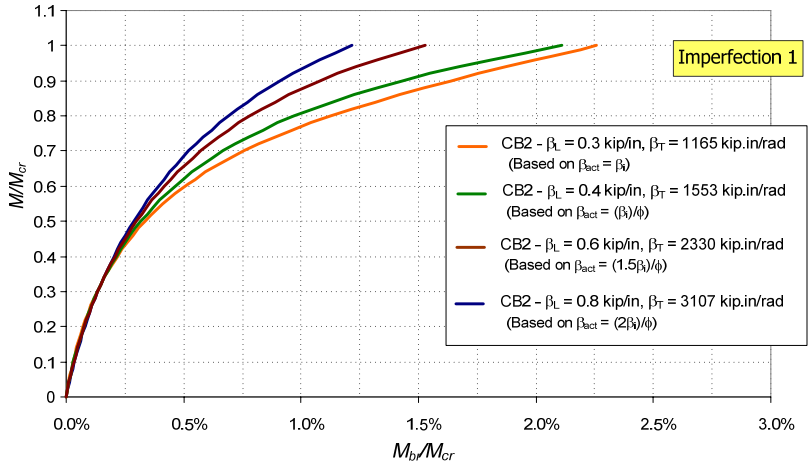


**Fig. 4.7.28. Benchmark Study CB2 – Torsional brace forces using several brace stiffnesses between 1.0 to 2/ϕ of the ideal full bracing values, imperfection 1.**

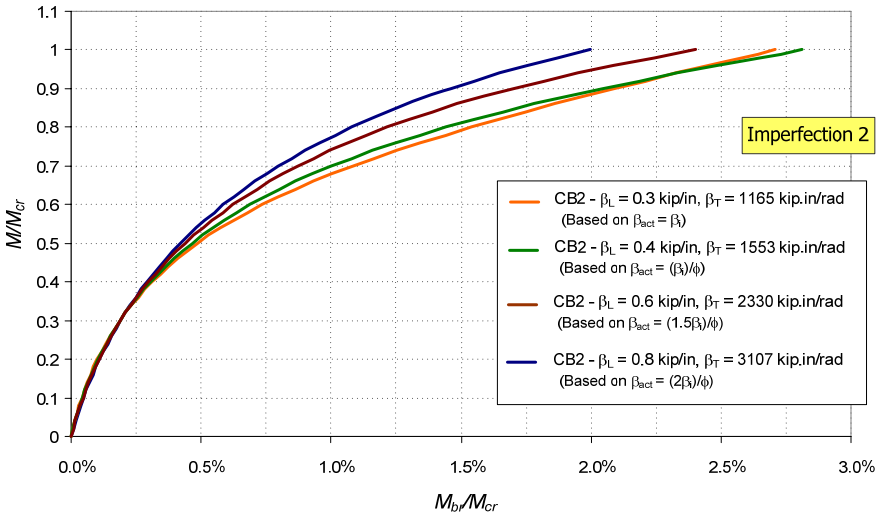


**Fig. 4.7.29. Benchmark Study CB2 – Torsional brace forces using several brace stiffnesses between 1.0 to 2/ϕ of the ideal full bracing values, imperfection 2.**

*4.7.4.2.3 Discussion of Results*

The brace forces for the cases with combined lateral and torsional bracing are substantially smaller than those associated with torsional bracing alone. Changes in the brace stiffnesses from 2.0/0.75 to 1.5/0.75 to 1.0/0.75 to 1.0 of the ideal full bracing stiffnesses have a relatively small influence on the brace forces

In all the cases considered, the lateral brace force is never larger than 0.47 %. The torsional brace moment increases when the bracing stiffnesses are scaled from 2.0/0.75 to 1.0 of the ideal full bracing values from 2.0% to 2.7% of $M_{cr}$ (for imperfection 2).

# CHAPTER 5

# ASSESSMENT OF BEAM BRACING REQUIREMENTS BY PLASTIC ZONE ANALYSIS

## 5.1 Introduction

This chapter presents several plastic zone analysis solutions using the Finite Element Analysis program ABAQUS version 6.7. In Chapter 4, the requirements for beam bracing were determined by second-order elastic solutions up to the elastic critical load level $M_{cr}$ and applying the perfect material without the influence of residual stresses. In this chapter, three types of the beam bracing in Chapter 4 - lateral, torsional, and combined lateral and torsional bracing are investigated accounting for the effects of geometric imperfections, residual stresses as well as the effects of material yielding including. All problems are analyzed up to the nominal strength of the beam $M_n$ instead of the elastic critical moment $M_{cr}$.

The primary attributes of finite element analysis modeling are discussed in Section 5.2 including the finite element discretization, boundary conditions, material stress-strain characteristics, the residual stress distribution, and geometric imperfections. The results from the Plastic Zone Solution for the lateral bracing Study LB3, torsional Study TB1, and the combined lateral and torsional bracing Study CB1 are presented in Section 5.3. This section also discusses the hypothetical application of lateral, torsional or combined lateral and torsional bracing in Richter's (1998) Test No.6. Finally, the torsional bracing for tapered beam is studied briefly in Section 5.3.8. All the analyses are investigated by considering the spread of plasticity through the volume of the members and all potential stability limit states. The results are normalized by $M_{max}$ at the beam inelastic Lateral Torsional Buckling limit load in the FEA model.

## 5.2 Finite Element Modeling

The Finite Element Analysis program ABAQUS version 6.7 is used to study the behavior of the beam bracing system in this chapter. There are several factors affecting the accuracy of the results in Finite Element Model such as: structural discretization, element properties, and boundary conditions.

### 5.2.1 Finite Element Discretization

S4R element in the ABAQUS element library is chosen to model the web and flanges and transverse stiffeners. S4R element is also used to model the bearing stiffener in Benchmark Study LB3. The beam element B31 is used to model the bearing stiffeners in the Benchmark Studies TB1 and CB1. The S4R element is a 4-node general purpose shell, with reduced integration, hourglass control, and finite strains. The S4R element can be used in thick shell and thin shell formulations. The element has 6 active degrees of freedom per node, $u_x$ , $u_y$ , $u_z$, , $\theta_x$ , $\theta_y$ ,and $\theta_z$. Five integration points are used through the thickness of the shell elements (trapezoidal rule). The B31 element is two-node linear-order beam element based on Reissner-Mindlin beam theory, which is compatible with the S4R element. The beam cross-section is modeled by using a five point trapezoidal integration rule through its thickness and width.

The linear spring element SPRING 1 in the ABAQUS element library is used to model the lateral and/or torsional braces. The SPRING 1 element is used to specify a spring element between a node and ground, acting in a fixed direction. The SPRING 1 can be associated with displacement or rotational degrees of freedom.

Through several preliminary analyses, the numbers of elements using in the model are as follows. For the Benchmark Studies LB3, TB1, and CB1, eight shell elements are used

through the flange width and twenty two shell elements are used through the depth of the web. For Richter's (1998) Test No.6, six shell elements are used through the flange width and twenty shell elements are used through the depth of the web. The aspect ratio of the web shell elements is approximately equal to 1.0.

### 5.2.2 Load and Displacement Boundary Conditions

The boundary conditions of the beams in this chapter are modeled as follows. One end of the beam modeled with a hinge support by restraining the displacement in the vertical and longitudinal directions at the juncture of the web and the bottom flange of beam. The other end of the beam is a roller support modeled by restraining the displacement in the vertical direction only at the node at the juncture of the web and the bottom flange of beam. The nodes at the juncture of the web and the top flange of beam at both end is modeled by restraining the vertical direction only. In addition, the nodes at the bottom flange of the beam at both ends are modeled by restraining the lateral displacements.

For the beam subjected to the concentrated load, the applied load is applied as a line load through the width of flange. For the beam subjected to the uniform moment, the moment at the ends is applied as the couple through the nodes at the top and bottom flanges. In case of the uniform bending moment loading, the EQUATION command in ABAQUS is used to constrain both the top and the bottom flange nodes to avoid the local effects. The self weights of beams and bracing members are not included in the analyses.

### 5.2.3 Material Stress-Strain Characteristics

Since the S4R and B31 elements in ABAQUS are based on the large strain formulations, the material response must be defined in terms of true stress and true strain. Mild steel A572 Grade 50 (a yield stress of 50ksi and an ultimate stress of 65ksi), a modulus of elasticity of

29,000ksi, is assumed in the Benchmark Studies LB3, TB1, and CB1. Fig. 5.2.1 illustrates the typical stress-strain relationship for static loading used in the Benchmark Studies LB3, TB1, and CB1.

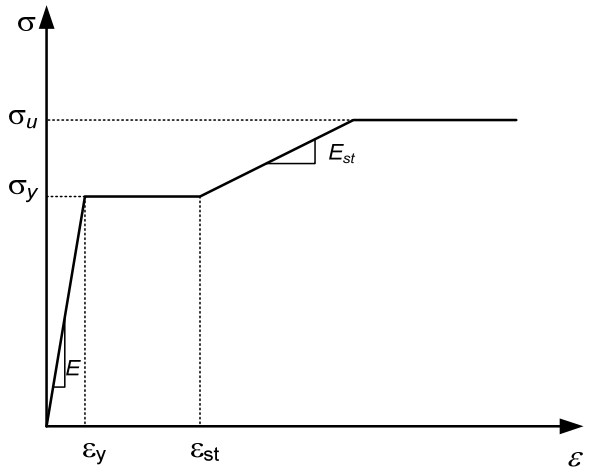


**Fig. 5.2.1. Strain hardening material used in the analyses.**

In Fig. 5.2.1, $\sigma_y$ is the yield stress, $\sigma_u$ is the ultimate stress, $\varepsilon_y$ is the strain at yield, $\varepsilon_{st}$ is the strain at initial strain hardening, $E$ is the elastic modulus, and $E_{st}$ is the strain hardening modulus.

The most common stress-strain relationship in practice is engineering stress versus engineering strain. The engineering stress is calculated by using the original area ($A_o$), undeformed shape of specimen and engineering strain is calculated based on the total elongation over the original value ($L_o$) of the gage length. For the uniaxial tensile or compressive test the engineering stress and strain can be calculated as follows

$$\sigma^{eng} = \frac{F}{A_o} \tag{5-1}$$

$$\varepsilon^{eng} = \frac{L\text{-}L_o}{L_o} = \frac{L}{L_o} - 1 \qquad \therefore \qquad \varepsilon^{eng} + 1 = \frac{L}{L_o} \tag{5-2}$$

where $F$ is the applied force, $L$ is the current length, $A_o$ is the original area, and $L_o$ is the original length.

The true stress can be calculated in terms of the engineering stress and the engineering strain if the elastic strain is negligible when compared to the plastic strain. Assuming the volume of a uniaxial tensile coupon test is constant or $AL = A_oL_o$, where $A$ is the current cross section area, $L$ and $L_o$ are the same meaning as noted above. The true stress $\sigma^{true}$ can be calculated using the follow equation.

$$\sigma^{true} = \frac{F}{A} = \frac{F}{A_o}\frac{A_o}{A} = \frac{F}{A_o}\frac{L}{L_o} = \sigma^{eng}(1+\varepsilon^{eng}) \tag{5-3}$$

The natural strain, $e$, is defined as

$$e = \ln\frac{L}{L_o} = \ln(1+\varepsilon^{eng})$$

The plastic strain, $e^{pl}$, can be written as

$$e^{pl} = \ln(1+\varepsilon^{eng}) - \frac{\sigma^{true}}{E} \tag{5-4}$$

where $E$ is the modulus of elasticity.

The material model used in the finite element analysis is based on the true stress and plastic strain as in Eqs. (5-3) and (5-5). The results for the Benchmark Studies LB3, TB1, and CB1 are shown in the Fig. 5.2.2 and the Table 5.2.1 below.

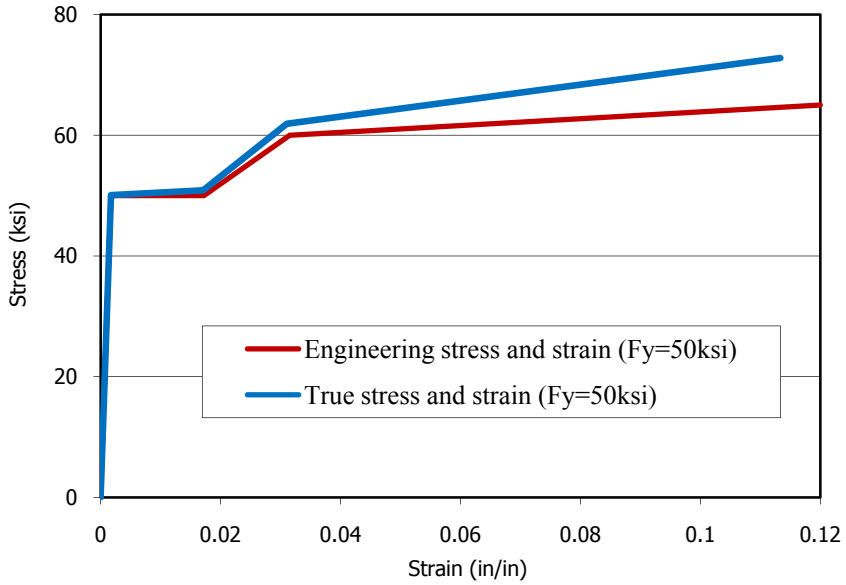


**Fig. 5.2.2. Strain hardening material used in the analyses for Studies LB3, TB1, CB1, and Tapered beam.**

**Table 5.1. True stress-strain data for finite element analysis.**

| True strain (in/in) | True stress (ksi) |
|---|---|
| 0 | 0 |
| 0.00172265 | 50.08620690 |
| 0.01709443 | 50.86206897 |
| 0.03104032 | 61.89162562 |
| 0.11332869 | 72.8 |

The material stress-strain characteristics of Richter's (1998) Test No.6 are applied similarly. The test is addressed in Section 5.3.5.

### 5.2.4 Residual Stress

Steel members are usually heated at some stage during the fabrication process. As they cool down, the part of the cross section for which the surface area to volume ratio is the largest will lose heat more rapidly than the part for which the ratio of surface area to volume is small. This uneven cooling creates a set of self-equilibrating stresses in the cross section. These are called the residual stresses. Residual stresses are one of the main factors that affect the strength of steel members.

The magnitude and distribution of residual stresses in hot-rolled shapes depends on the type of the cross section, rolling temperature, cooling conditions, straightening procedures and metal properties (Beedle and Tall, 1960). For hot-rolled wide-flange shapes, the tips of the flanges have a larger surface area to volume ratio than the regions where the web joins the flanges; hence the tips of the flanges will cool faster. As the junctions of the web and flanges begin to cool and shrink, the tips of the flanges, which have been cooled and hardened already, will prevent the junctions from shrinking, with the result that the juncture web- flange will be left in tension while the toes of the flanges will be left in compression. As for the web, if the height to thickness ration is large, then the central portion will cool much faster than the portion where the web joins the flanges and so a compressive residual stress will be induced at the central portion. On the other hand, if the height to thickness ration is small, then cooling will be more uniform, so that the whole web will be in a state of tension (Chen, Lui, 1987)

In this chapter, the residual stress pattern shown in Fig. 3.5.1 in Chapter 3 is applied for the hot-rolled sections in Studies LB3, TB1, and CB1. The residual stress pattern shown in Fig. 5.2.3 is used for the built up cross section for Richter's (1998) Test No. 6.

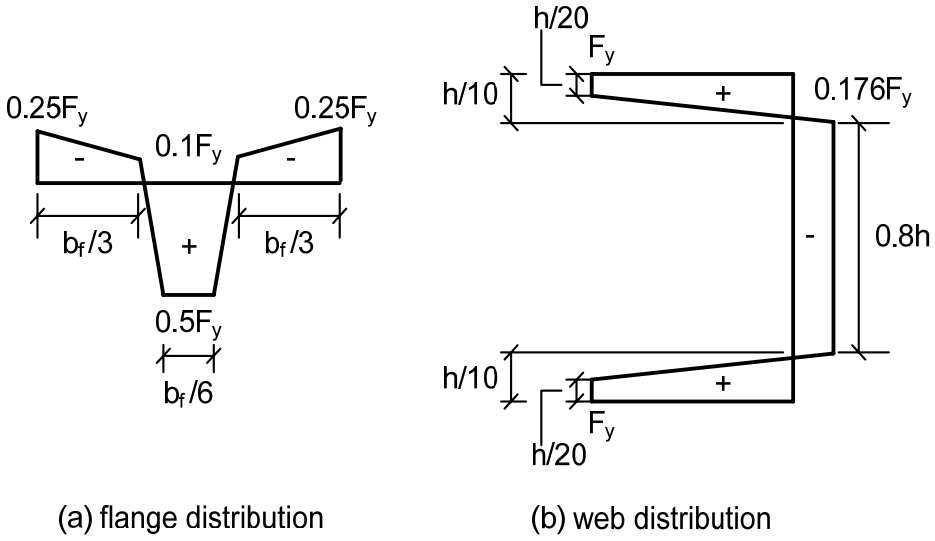


**Fig. 5.2.3. Residual stress distribution of cross section for built up cross section (Kim and White 2007).**

The above residual stress distribution is most effectively introduced into the model by using the ABAQUS User Subroutine feature. This routine is named SIGINI and it assigns initial values of the stress at Gauss points within the shell finite elements prior to the first load increment. Once the routine is active, equilibrium iteration is executed to ensure internal equilibrium of the imposed stress field. The result of residual stresses from ABAQUS is displayed in the Fig. 5.2.4 for Problems LB3, TB1, and CB1 while the results of residual stresses for Richter's (1998) Test No. 6 is shown in Fig. 5.2.5.

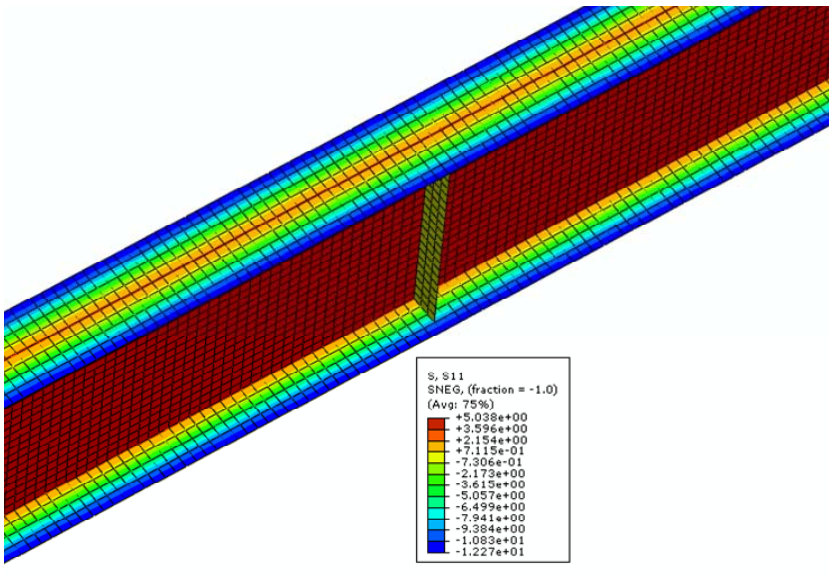


**Fig. 5.2.4. Residual stress distribution for Studies LB3, TB1, and CB1.**

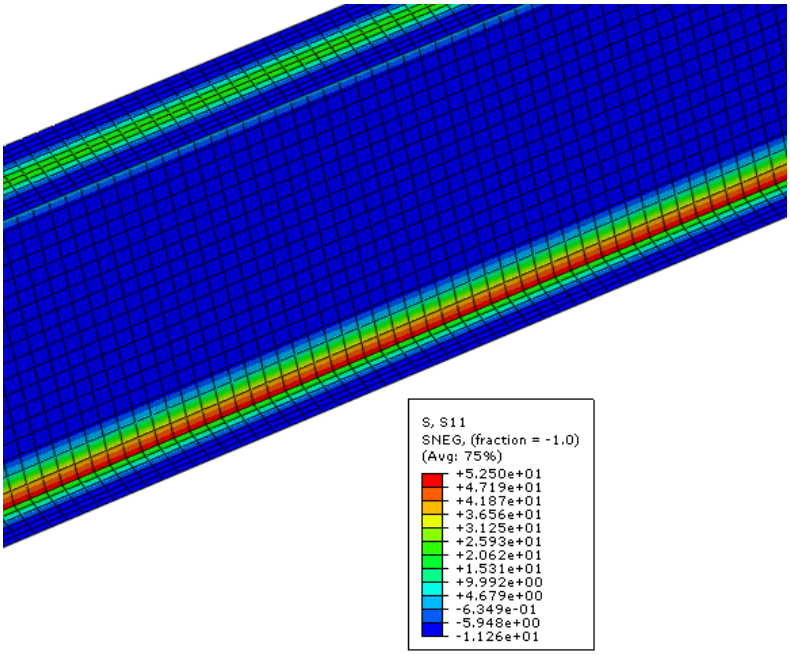


**Fig. 5.2.5. Residual stress distribution for Richter's (1998) Test No. 6.**

### 5.2.5 Geometric Imperfections

Geometric imperfections and residual stresses are the primary factors affecting the strength of steel beams (Galambos, 1998).

The geometric imperfections applied in this chapter similar to those discussed in Section 4.3. The only difference comes from the way in which the geometric imperfections are applied for the analysis model.

In SAP 2000, the imperfections are applied explicitly to produce the "kinked" imperfection geometry shown in the Figs. 4.4.1 through 4.4.3.

In ABAQUS, the geometric imperfections can be based on nodal displacements written to the results file during a previous analysis. The FILE parameter is used to identify the name of the results file from the previous analysis. The STEP parameter must be used to identify the step from the previous analysis containing the results that will define the geometric imperfection. The imperfection shape using ABAQUS is continuous curve as shown in the Fig. 5.2.6.

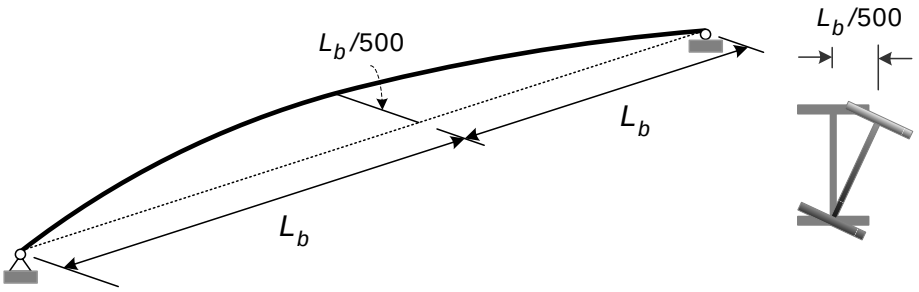


**Fig. 5.2.6. Geometric imperfections in ABAQUS.**

Fig. 5.2.7 shows the geometric imperfection which is used in Studies LB3, TB1, CB1, and Tapered Beam. The geometric imperfection for Richter's (1998) Test No. 6 is shown in Section 5.3.5.

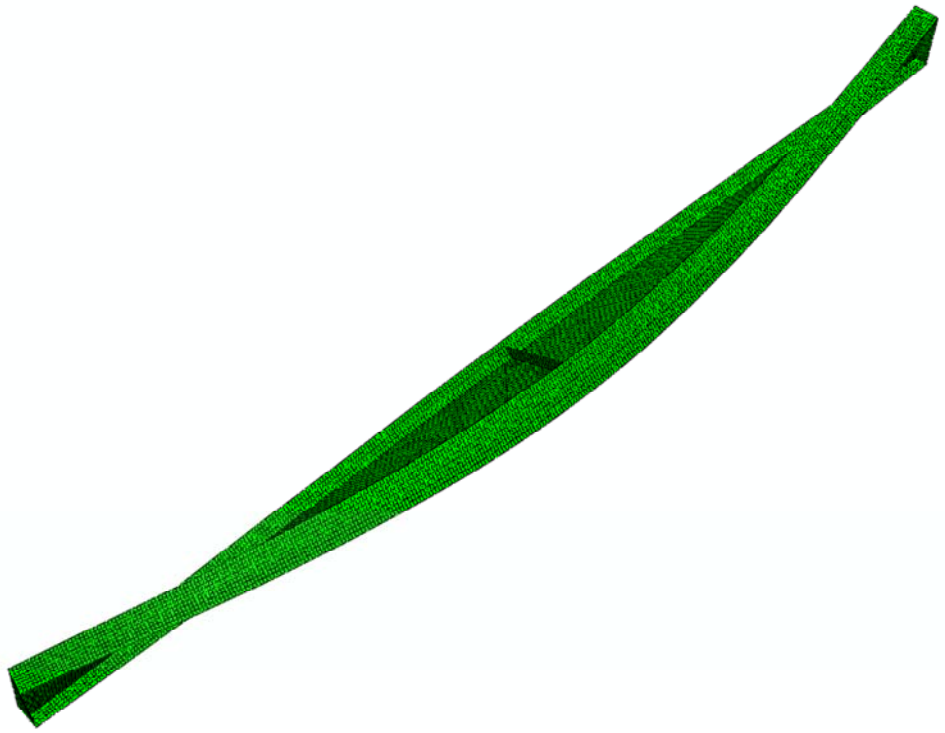

**Fig. 5.2.7. Initial imperfection shape for Benchmark Studies LB3, TB1, CB1 – Scaled 80x.**

## 5.3 Results from Plastic Zone Analyses

The sections below present the results of the plastic zone analyses using ABAQUS for the problems LB3, LB3*, TB1, CB1, Richter's (1998) Test No. 6, and Tapered beam.

### 5.3.1 Lateral bracing: Benchmark Study LB3

The same structural layout in Section 4.6.1.3, the simply supported beam W16x26 with the top flange brace, 4x1/4 stiffener subjected to the concentrated vertical load applied at the top flange shown in Fig. 5.3.1. The nominal flexural strength, $M_n$, based on AISC using $C_b$=1.75 is $M_n = M_p = 2160$ kips-in.

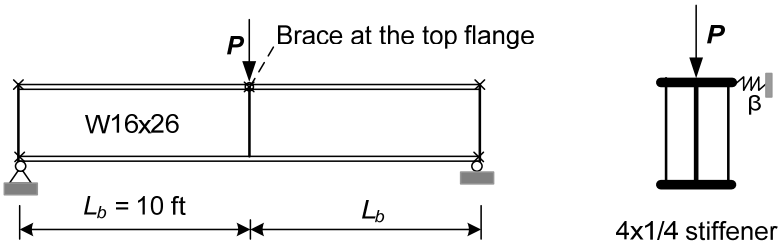


**Fig. 5.3.1. Benchmark Study LB3 - Plastic Zone Solution**

The brace stiffness and strength requirements based on the AISC (2005) Appendix 6 are calculated in Section 5.3.1.1. The results from Plastic Zone Solution with three brace stiffnesses $\beta = (2\beta_{i\,(APP6)})/\phi$, $\beta = 1.9\beta_{i(APP6)}$, and rigid brace $\beta = \infty$ are presented in Section 5.3.1.2.

5.3.1.1 Results from the AISC 2005 Appendix 6 Commentary Equations for $M=M_n$

Similar to Section 4.6.1.3.1, for this problem we have

$$n = 1 \qquad N_i = 4 - \frac{2}{n} = 2 \qquad h_o = 15.355 \text{ inches}$$

$C_b = 1.75$, $C_b = 1.0 + 1.2/1 = 2.2$ (top flange loading), $C_b = 1$, $L_b = 120$ inches

$$P_f = \frac{M_n}{h_o} = \frac{2160}{15.355} = 140.7 \text{ kips}$$

- Required brace stiffness:

$$\beta_i = \frac{N_i P_f}{L_b} C_d C_t \quad ; \qquad \beta_{br} = \frac{2\beta_i}{\phi}$$

$$\beta_i = \frac{2(140.7)}{120}(1)(2.2) = 5.16 \text{ kips/inch}, \qquad \beta_{br} = \frac{2(5.16)}{0.75} = 13.76 \text{ kips/inch}$$

- Required brace strength:

$$P_{br} = \frac{(0.01) M_n}{h_o} C_d C_t = \frac{(0.01)(2160)}{15.355} 1(2.2) = 3.09 \text{ kips} = 0.022 \frac{M_n}{h_o}$$

5.3.1.2 Results from Plastic Zone Analyses

The results from the Finite Element Analysis with three stiffness values are as shown in Fig. 5.3.2.

- For the braces stiffness $\beta = 2\beta_i/\phi = 13.76$ kips/inch, the maximum moment is 0.94 $M_n$
- For the braces stiffness $\beta = 1.9\beta_i = 9.8$ kips/inch, the maximum moment is 0.92 $M_n$
- For the rigid brace, $\beta = \infty$, the maximum moment is 0.98 $M_n$

Fig. 5.3.2 indicates that the bracing force demand is 2.7% of $M_n/h_o$ at the limit load $M_{max}$ when the bracing stiffness of $2\beta_i/\phi$ is used and 3.1% of $M_n/h_o$ when the bracing stiffness of $1.9\beta_i$ corresponding to 2.2% of $M_n/h_o$ based on the AISC (2005) Appendix 6.

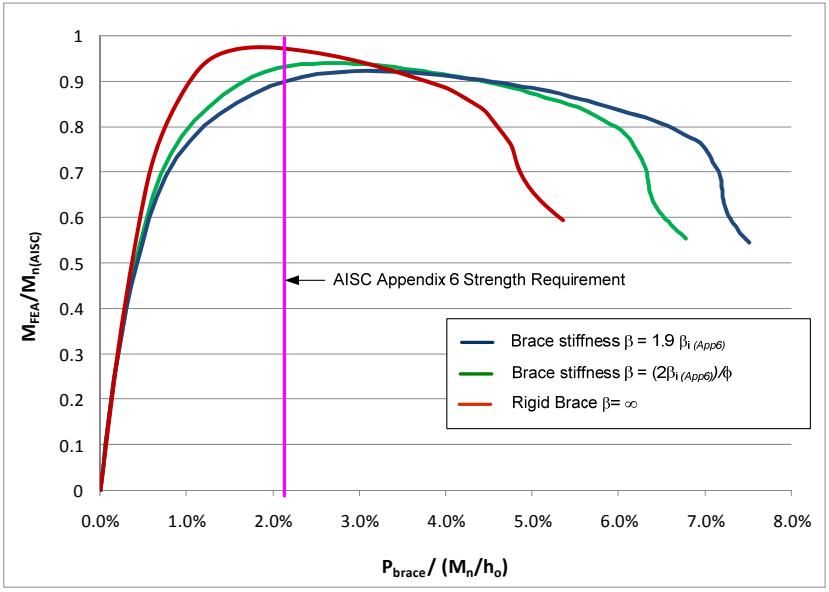


**Fig. 5.3.2. Brace forces for the different brace stiffness, Benchmark Study LB 3.**

The vertical displacements at midspan of the beam corresponding to applied load which are normalized by the nominal flexural strength, $M_n$ are plotted in Fig. 5.3.3. One can observe from Fig. 5.3.3 that the vertical displacement at the maximum load at the mid span is 1.47

inches for the brace stiffness β = 13.76 kips/inch, 1.43 inches for the brace stiffness β = 9.8 kips/inch, and 1.53 inches for the rigid brace.

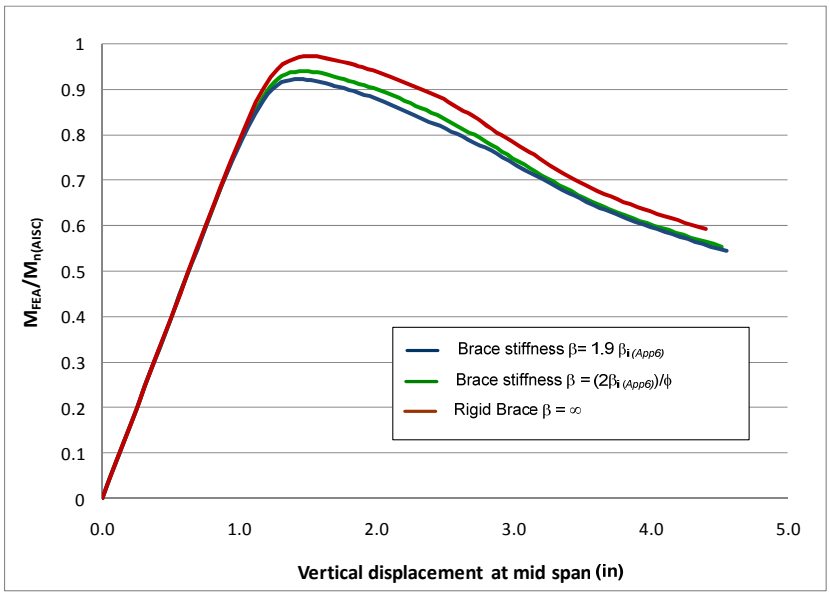


**Fig. 5.3.3. Vertical displacement at the mid span for the different brace stiffness, Benchmark Study LB3.**

The deformed shapes corresponding to the maximum loads for the brace stiffnesses β = $2\beta_i/\phi$ and β = $1.9\beta_i$ are plotted in Figs. 5.3.4 and 5.3.5.

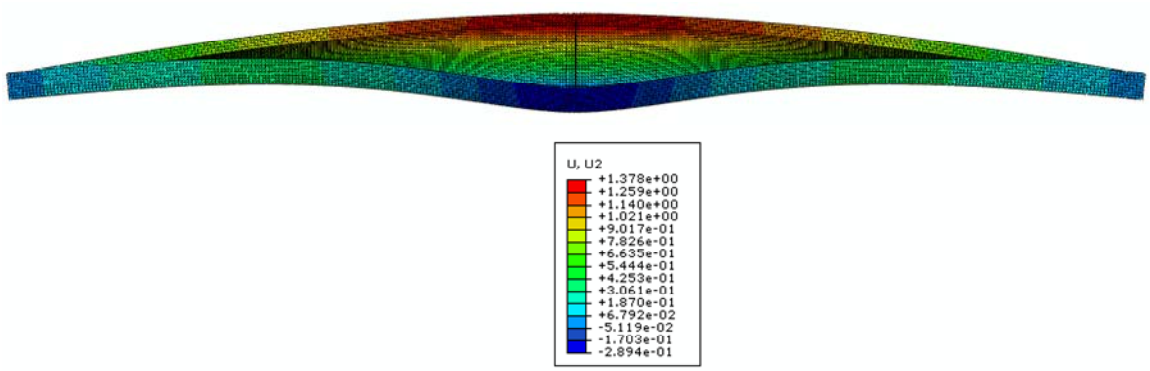


**Fig. 5.3.4. Deformed shape at the maximum load for the brace stiffness β = $2\beta_i/\phi$ – Scaled 10x, Benchmark Study LB3.**

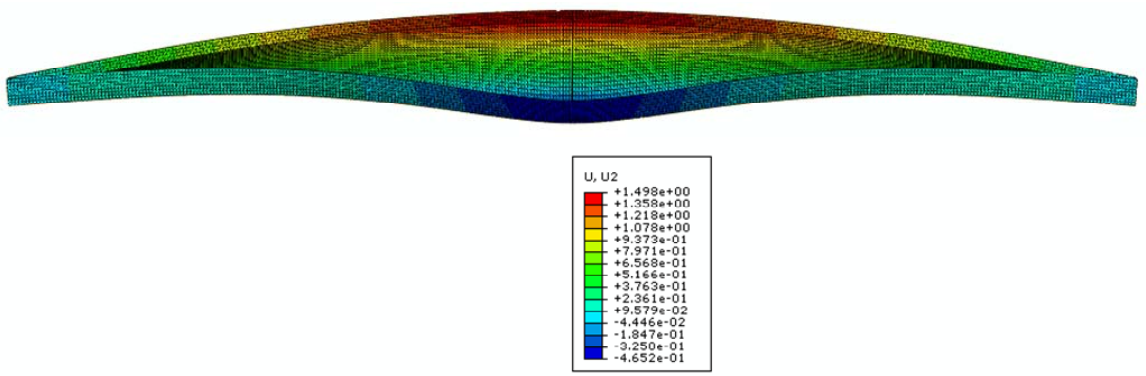


**Fig. 5.3.5. Deformed shape at the maximum load for the brace stiffness $\beta = 1.9\beta_i$ – Scaled 10x, Benchmark Study LB3.**

Fig. 5.3.6 displays the relationship between the brace forces and the moment from the Finite Element Analysis. The deformed shapes corresponding to the four increments labeled in this plot are shown in Fig. 5.3.7.

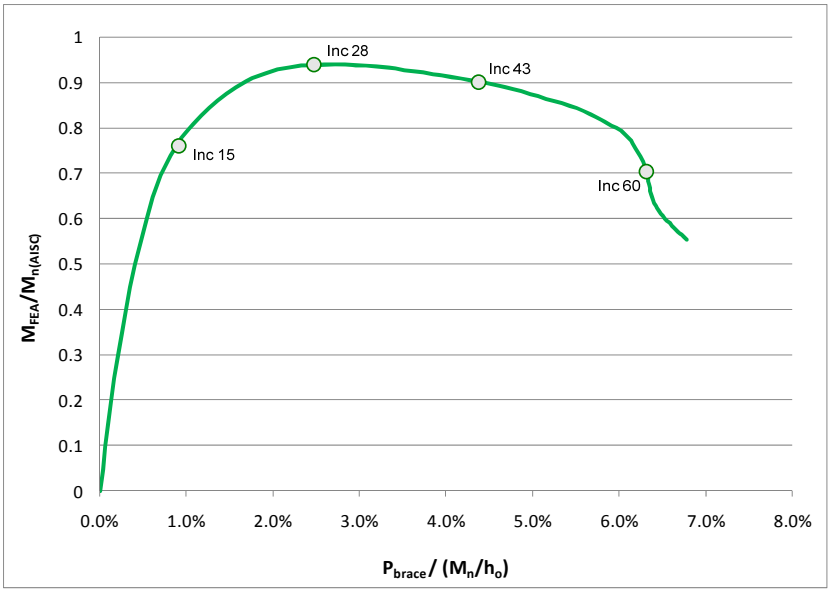


**Fig. 5.3.6. Brace forces for the brace stiffness $\beta = 2\beta_i/\phi$, Benchmark Study LB3.**

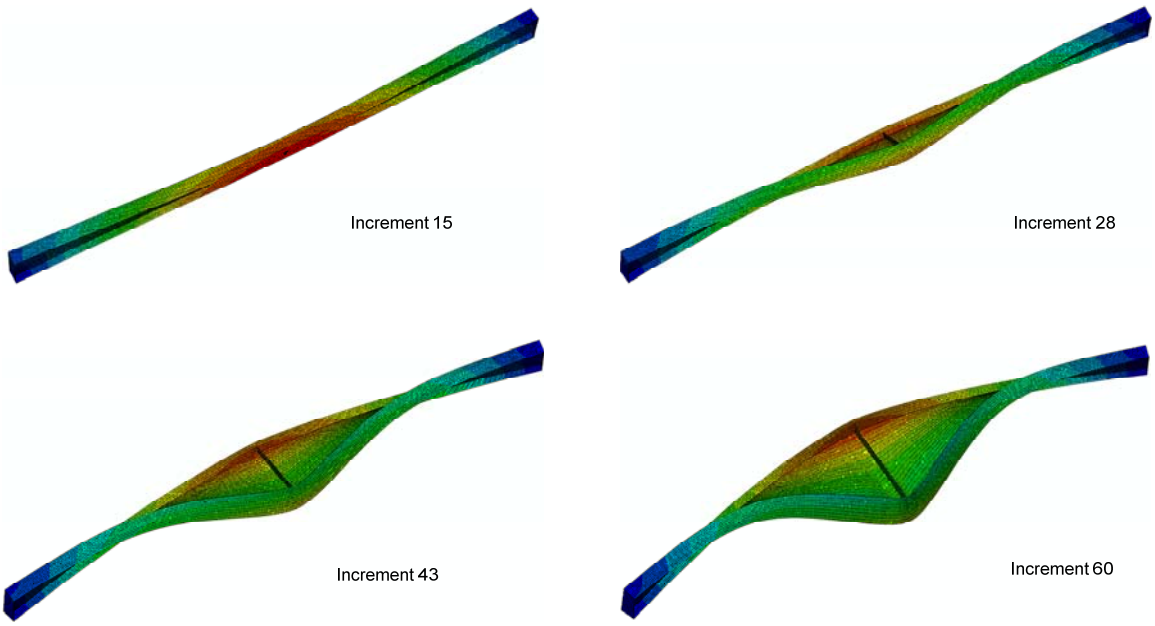


**Fig. 5.3.7. Deformed shape at the different stages for the brace stiffness $\beta = 2\beta_i/\phi$ – Scaled 10x, Benchmark Study LB3.**

The deformed shape in Figs. 5.3.4 and 5.3.5 indicates that the lateral deflection of tension flange of the beam is larger than that of the compression flange. This mode of failure is referred to as web sidesway buckling in the AISC Specification. Web sidesway buckling occurs when the web is subjected to a transverse compression from a concentrated load applied to the braced compression flange, and the tension flange is not sufficient to restrain the web from buckling as a "column" with a maximum sidesway displacement at the tension flange. The web sidesway buckling can be checked based on the 2005 AISC Chapter J as follows.

Since

$$(h/t_w)/(l/b_f) = \frac{15.01/0.25}{240/0.345} = 1.38 < 1.7$$

and the compression flange is not restrained against rotation, the nominal strength, $R_n$, for the limit state of web sidesway buckling is

$$R_n = \frac{C_r t_w^3 t_f}{h^2}\left[0.4\left(\frac{h/t_w}{l/b_f}\right)^3\right] = \frac{480000(0.25^3)(0.345)}{15.01^2}\left[0.4(1.38^3)\right] = 11.97 \text{ kips}$$

The applied load $P$ is

$R_u = P = (4M_n)/L = 4(2160)/240 = 36.01$ kips

Because of $R_n = 11.97$ kips < 36.01 kips = $R_u$, web sidesway buckling is to be expected in this problem. Chapter J addresses two recommendations to prevent web sidesway buckling. The first one is to brace both flanges at the point of application of concentrated load. The other one is to use transverse stiffeners to restrain the rotation of compression flange. Problem LB3 is modified by using the first of these methods in the section below.

### 5.3.2 Lateral bracing: Benchmark Study LB3*

In this section, the above problem is modified by adding the lateral brace at the bottom flange as shown in Fig. 5.3.8.

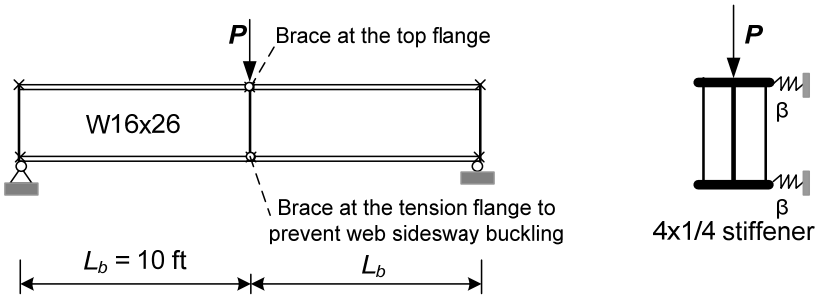


**Fig. 5.3.8. Benchmark Study LB3*.**

It should be noted that if the two braces at the top and bottom flanges are used as shown in the figure, the stiffener is not necessary. However, to compare to the Benchmark Study LB3 the stiffener is retained. Also, the braces at the top and bottom flanges are assumed to have the same stiffness.

5.3.2.1 Results from Plastic Zone Analyses

In the same fashion as Benchmark Study LB3, the results from the Finite Element Analysis with three stiffness values are as shown in Fig. 5.3.9.

- For the braces stiffness $\beta = 2\beta_i/\phi = 13.76$ kips/inch, the maximum moment is 1.021 $M_n$
- For the braces stiffness $\beta = 1.9\beta_i = 9.8$ kips/inch, the maximum moment is 1.016 $M_n$

Fig. 5.3.9 indicates that the bracing force demand is 1.4% of $M_n/h_o$ at the limit load $M_{max}$ when the bracing stiffness of $\beta = 13.76$ kips/inch is used and 1.7 % of $M_n/h_o$ when the bracing stiffness of $\beta = 9.8$ kips/inch corresponding to 2.2% of $M_n/h_o$ based on the AISC (2005) Appendix 6.

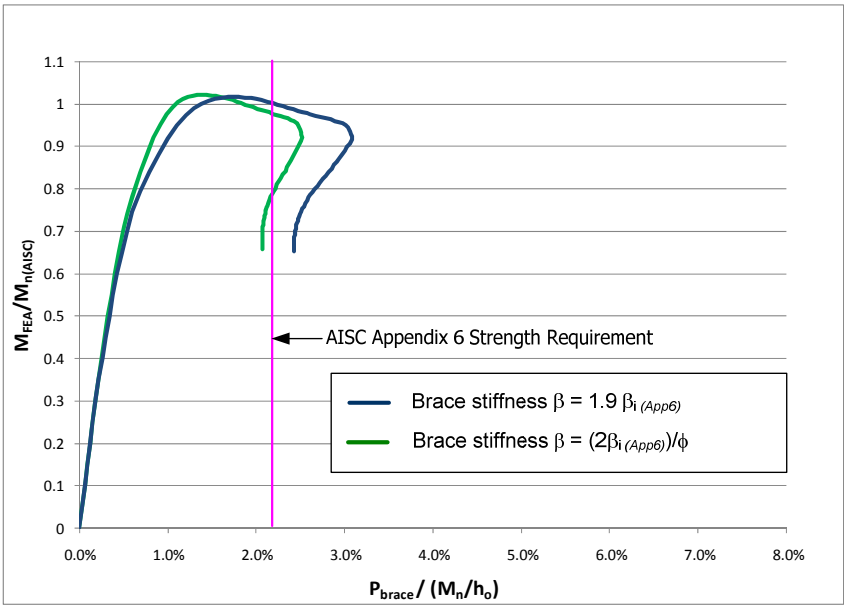


**Fig. 5.3.9. Brace forces for different brace stiffness – Benchmark Study LB3*.**

The vertical displacements at midspan of the beam corresponding to applied load which are normalized by the nominal flexural strength, $M_n$ are plotted in Fig. 5.3.10.

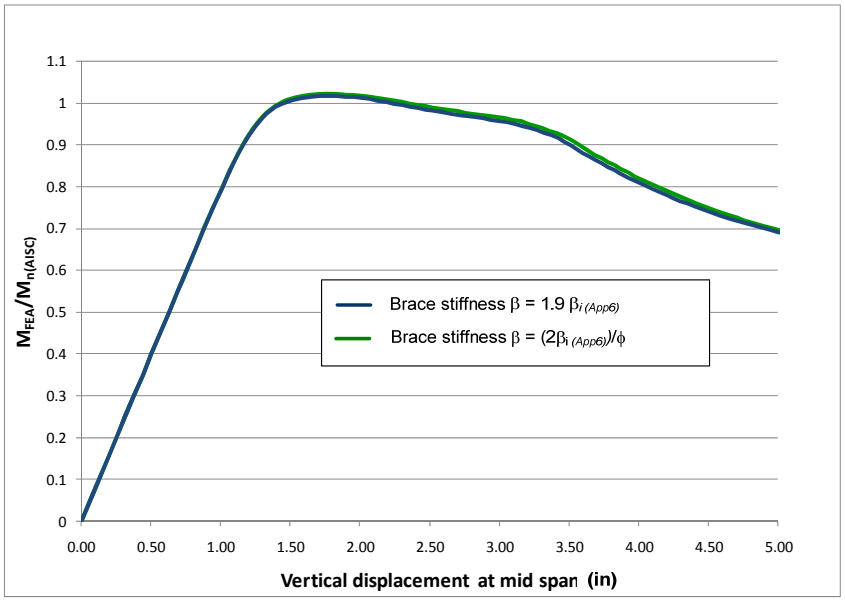


**Fig. 5.3.10. Vertical displacement at the mid span for different brace stiffness - Benchmark Study LB3*.**

The deformed shapes corresponding to the maximum loads for the brace stiffnesses $\beta = 2\beta_i/\phi$ and $\beta = 1.9\beta_i$ are plotted in Figs. 5.3.11 and 5.3.12.

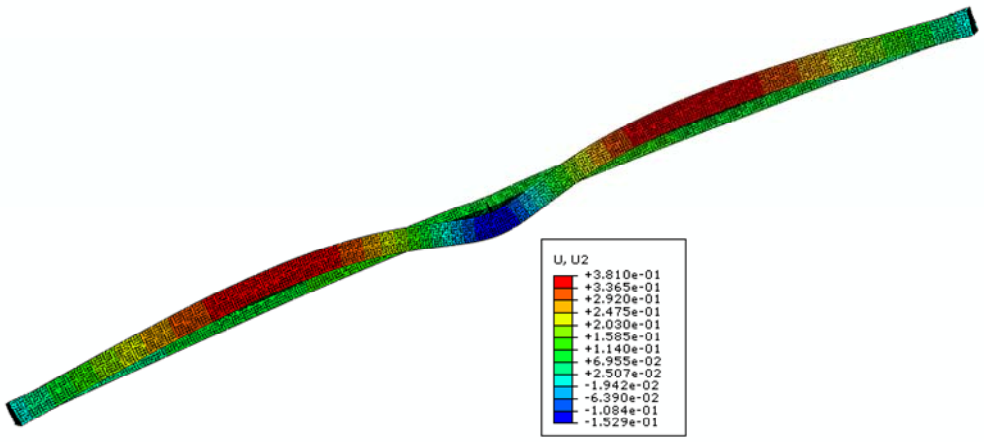


**Fig. 5.3.11. Deformed shape at the maximum load for the brace stiffness, $\beta = 2\beta_i/\phi$ – Scaled 10x, Benchmark Study LB3*.**

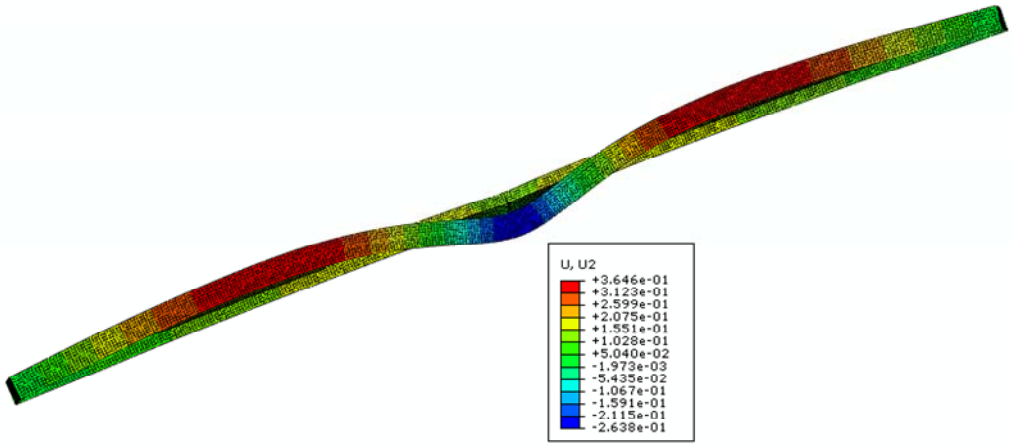


**Fig. 5.3.12. Deformed shape at the maximum load for the brace stiffness, $\beta = 1.9\beta_i$ – Scaled 10x, Benchmark Study LB3*.**

Fig. 5.3.13 displays the relationship between the brace forces and the moment from the Finite Element Analysis. The deformed shapes corresponding to the four increments labeled in this plot are shown in Fig. 5.3.14

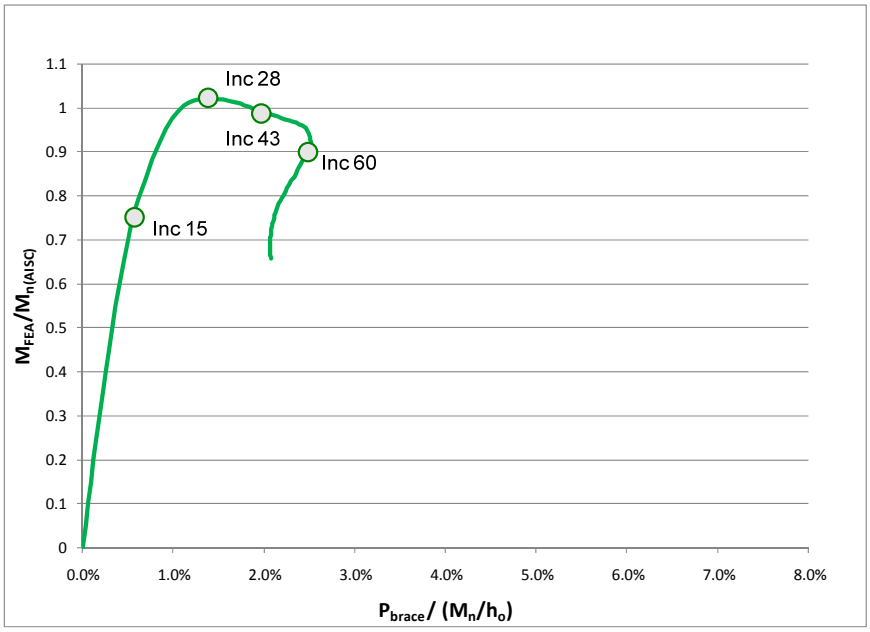


**Fig. 5.3.13. Brace forces for the brace stiffness, $\beta = 2\beta_i/\phi$ - Benchmark Study LB3*.**

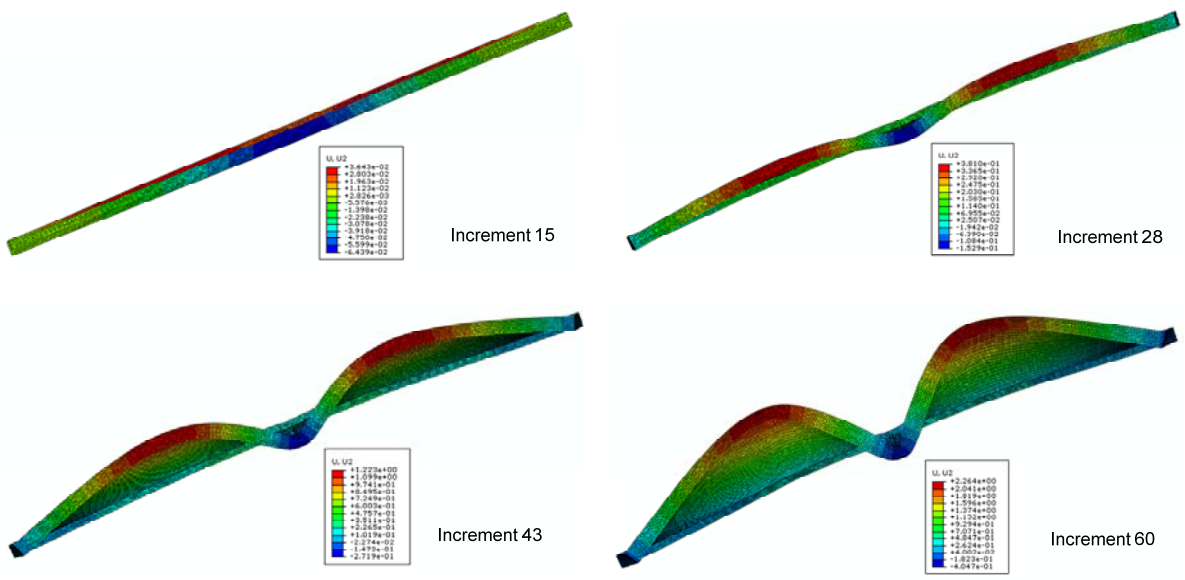


**Fig. 5.3.14. Deformed shape at the different stages for the brace stiffness, $\beta = 2\beta_i/\phi$ – Scaled 10x, Benchmark Study LB3*.**

### 5.3.3 Torsional Bracing: Benchmark Study TB1

Similar to Benchmark Study TB1 in Section 4.6.2.1, the simply supported beam W16x26 with top flange brace, 4x1/4 stiffener subjects to positive uniform bending moment shown in Fig. 5.3.15. The nominal flexural strength, $M_n$, based on AISC is $M_n$ = 1457 kips-in.

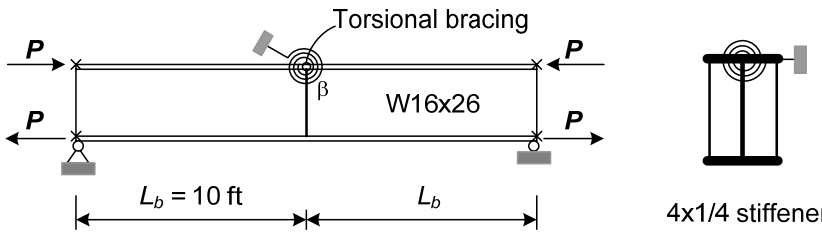


**Fig. 5.3.15. Benchmark Study TB1.**

The brace stiffness and brace force requirements based on the AISC 2005 Appendix 6 Commentary and from the equations from Yura (1992) are performed in Sections 5.3.3.1 and 5.3.3.2. The results from Plastic Zone Solution are considered with three brace

stiffnesses; the first one is based on the AISC 2005 Appendix 6 Commentary Equation, $\beta_{Tb}$ = 11493 kip-inch/rad; the second one is based on refined equations from Yura et al. (1992), $\beta_{Tb}$ = 5207 kip-inch/rad, and the third one is equal to only the ideal stiffness based on Yura et al (1992), $\beta_{Ti}$ = 1211 kip-inch/rad.

5.3.3.1 Results based on the AISC 2005 Appendix 6 Commentary Equations for $M = M_n$

Similar to Section 4.6.2.1.1, the brace requirements are estimated as follow

- The brace stiffness excluding web distortion is

$$\beta_T = \frac{1}{\phi}\left(\frac{2.0LM_n^2}{nEI_yC_b^2}\right)$$

$$\beta_T = \frac{1}{0.75}\left(\frac{2.0(240)(1457)^2}{1(29000)(9.59)(1^2)}\right) = 4885 \text{ kip} - \text{inch/rad}$$

- The web distortional stiffness is

$$\beta_{sec} = \frac{3.3E}{h_o}\left(\frac{1.5h_ot_w^3}{12} + \frac{t_sb_s^3}{12}\right)$$

$$\beta_{sec} = \frac{3.3(29000)}{15.355}\left(\frac{1.5(15.355)0.25^3}{12} + \frac{(0.25)4^3}{12}\right) = 8497 \text{ kip - inch/rad}$$

- Required brace stiffness:

$$\beta_{Tb} = \frac{\beta_T}{\left(1 - \frac{\beta_T}{\beta_{sec}}\right)}$$

$$\beta_{Tb} = \frac{4885}{\left(1 - \frac{4885}{8497}\right)} = 11493 \text{ kip} - \text{inch/rad}$$

- Required brace strength (at $M = M_n$):

$$M_{br} = \frac{0.02 M_n L}{n C_b L_b}$$

$$M_{br} = \frac{0.02(1457)(240)}{1(1)(120)} = 58.28 \text{kip - inch} \quad => \quad \frac{M_{br}}{M_n} = 0.04$$

5.3.3.2 Results based on Refined Equations from Yura and Phillips (1992)

Similar to Section 4.6.2.1.2 in Chapter 4, the brace requirements are calculated as follow

- The ideal discrete torsional brace stiffness is

$$\beta_{Ti} = (M_n^2 - C_{bu}^2 M_o^2) \frac{C_t}{C_{bb}^2 E I_{eff}} \frac{0.75L}{n}$$

$$\beta_{Ti} = (1457^2 - 1^2(502.2)^2) \frac{1}{1^2.(29000)(9.59)} \frac{(0.75)240}{1} = 1211 \text{kip - inch/rad}$$

- The brace stiffness excluding web distortion is

$$\beta_T = \frac{2\beta_{Ti}}{\phi} = 4077 \text{ kip - inch/rad}$$

- The web distortional stiffness, $\beta_{sec}$

$$\beta_{sec} = \frac{3.3E}{h_o}\left(\frac{1.5 h_o t_w^3}{12} + \frac{t_s b_s^3}{12}\right)$$

$$\beta_{sec} = \frac{3.3(29000)}{15.355}\left(\frac{1.5(15.355)0.25^3}{12} + \frac{(0.25)4^3}{12}\right) = 8497 \text{ kip - inch/rad}$$

- Required brace stiffness:

$$\beta_{Tb} = \frac{\beta_T}{\left(1 - \frac{\beta_T}{\beta_{sec}}\right)}$$

$$\beta_{Tb} = \frac{3229}{\left(1 - \frac{3229}{8497}\right)} = 5207 \text{ kip - inch/rad}$$

- Required brace strength:

$$M_{br} = \beta_T \theta_o = \beta_T \frac{L_b}{500 h_o}$$

$$M_{br} = (3229)\frac{120}{500(15.355)} = 50.46 \text{ kip - inch} \quad => \quad \frac{M_{br}}{M_n} = 0.035$$

5.3.3.3 Results from Plastic Zone Analyses

Fig. 5.3.17 shows that although the brace stiffness based on the Appendix 6 ($\beta_{Tb}$ = 11493 kip-inch/rad) almost double the brace stiffness based on the refined equations from Yura et al. (1992) ($\beta_{Tb}$ = 5207 kip-inch/rad), the brace forces are almost the same. At the maximum load, the brace force is equal to 1.75% $M_n$ when brace stiffness is $\beta_{Tb}$ = 11493 kip-inch/rad while the brace force is equal to 1.79% $M_n$ when brace stiffness is $\beta_{Tb}$ = 5207 kip-inch/rad.

If only the ideal brace stiffness is used ($\beta_{Tb} = \beta_{Ti}$ = 1211 kip-inch/rad), the brace force is equal to 1.8% $M_n$ and corresponding to 4% $M_n$ based on the Appendix 6 Strength Requirement. The maximum moment from Finite Element Analysis is equal to 1.03 $M_n$ when using brace stiffness, $\beta_{Tb}$ = 11493 kip-inch/rad, equal to 1.021$M_n$ when using brace stiffness, $\beta_{Tb}$ = 5207 kip-inch/rad, and equal to 0.956 $M_n$ for the brace stiffness, $\beta_{Tb}$ = 1211 kip-inch/rad.

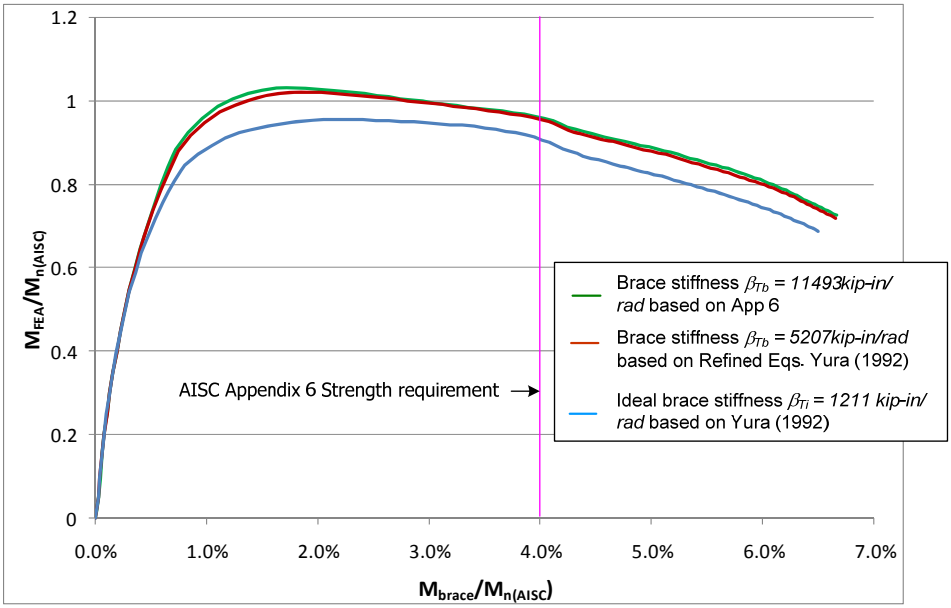


**Fig. 5.3.16. Brace forces for different brace stiffness, Benchmark Study TB1.**

The vertical displacements at midspan of the beam corresponding to applied load which are normalized by the nominal flexural strength, $M_n$ are plotted in Fig. 5.3.17. One can observe from Fig. 5.3.17 that the vertical displacement at the maximum load at the mid span is 1.31 inches for the brace stiffness $\beta_{Tb}$ = 11493 kip-inch/rad, 1.29 inches for the brace stiffness $\beta_{Tb}$ = 5207 kip-inch/rad, and 1.21 inches for the brace stiffness $\beta_{Ti}$ = 1211 kip-inch/rad

The deformed shapes for three brace stiffnesses $\beta_{Tb}$ = 11493 kip-inch/rad, $\beta_{Tb}$ = 5207 kip-inch/rad, and $\beta_{Tb} = \beta_{Ti}$ = 1211 kip-inch/rad are shown from Figs. 5.3.18 to 5.3.20 respectively.

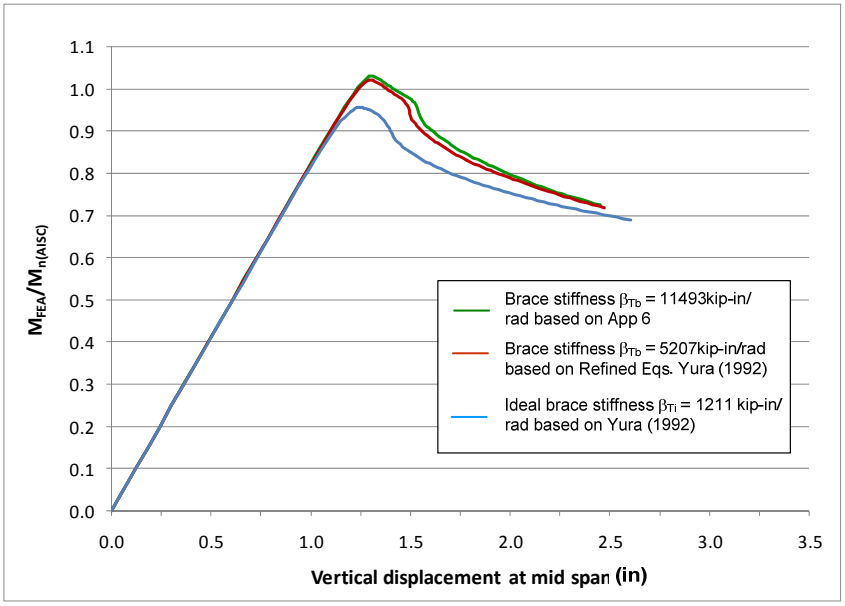


**Fig. 5.3.17. Vertical displacement at the mid span for different brace stiffness, Benchmark Study TB1.**

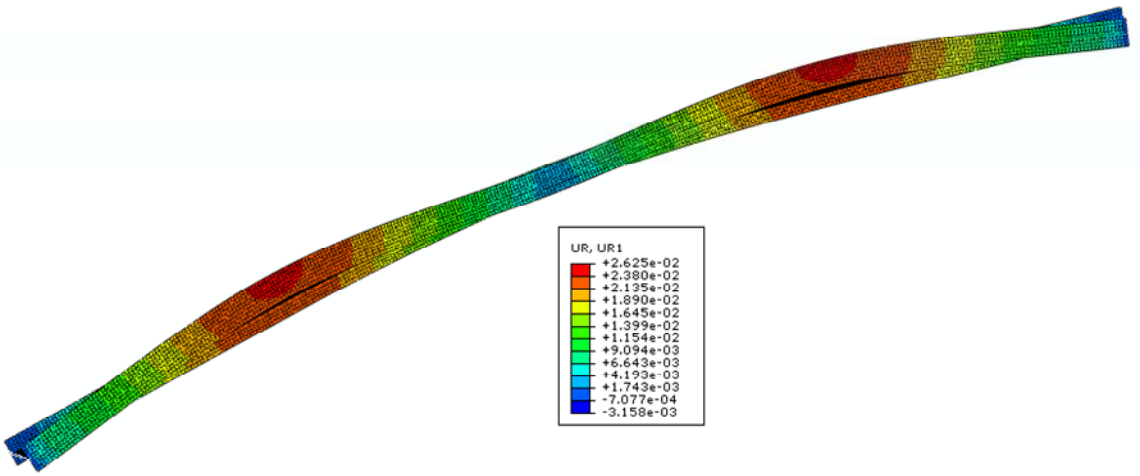


**Fig. 5.3.18. Deformed shape at the maximum load for the brace stiffness $\beta_{Tb}$ = 11493 kip-inch/rad - Scaled 15x, Benchmark Study TB1.**

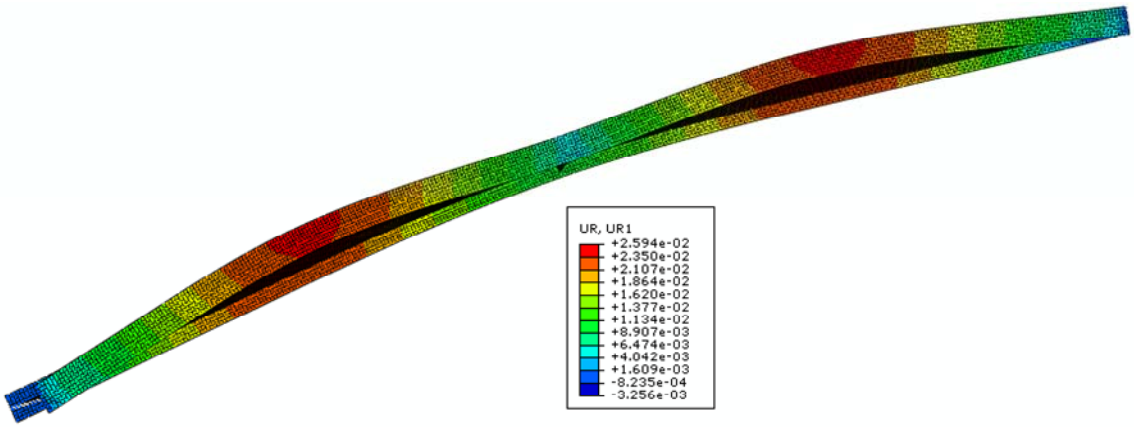


**Fig. 5.3.19. Deformed shape at the maximum load for the brace stiffness $\beta_{Tb}$ = 5207 kip-inch/rad - scaled 15x, Benchmark Study TB1.**

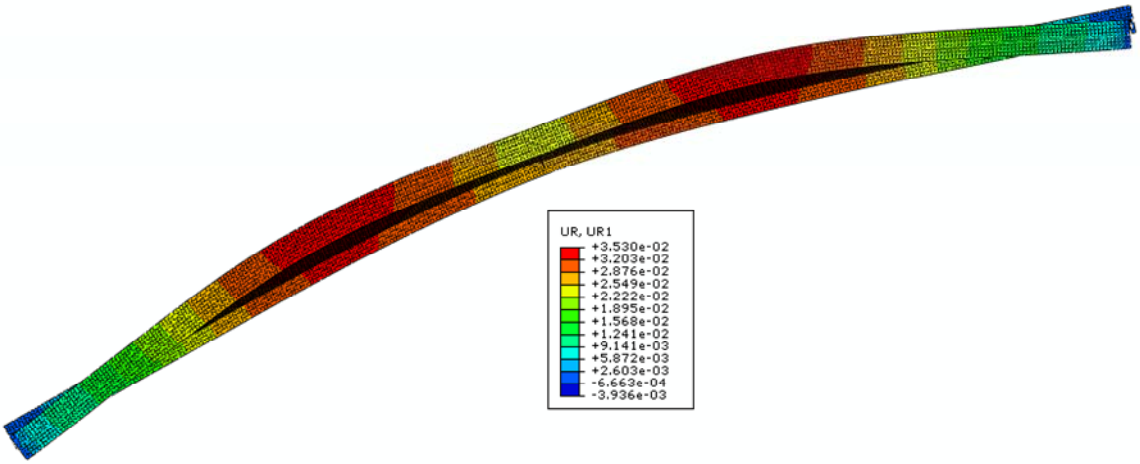


**Fig. 5.3.20. Deformed shape at the maximum load for the brace stiffness $\beta_{Ti}$ = 1412 kip-inch/rad - Scaled 15x, Benchmark Study TB1.**

Fig. 5.3.21 displays the relationship between the brace forces and the moment from the Finite Element Analysis. The deformed shapes corresponding to the four increments labeled in this plot are shown in Fig. 5.3.22

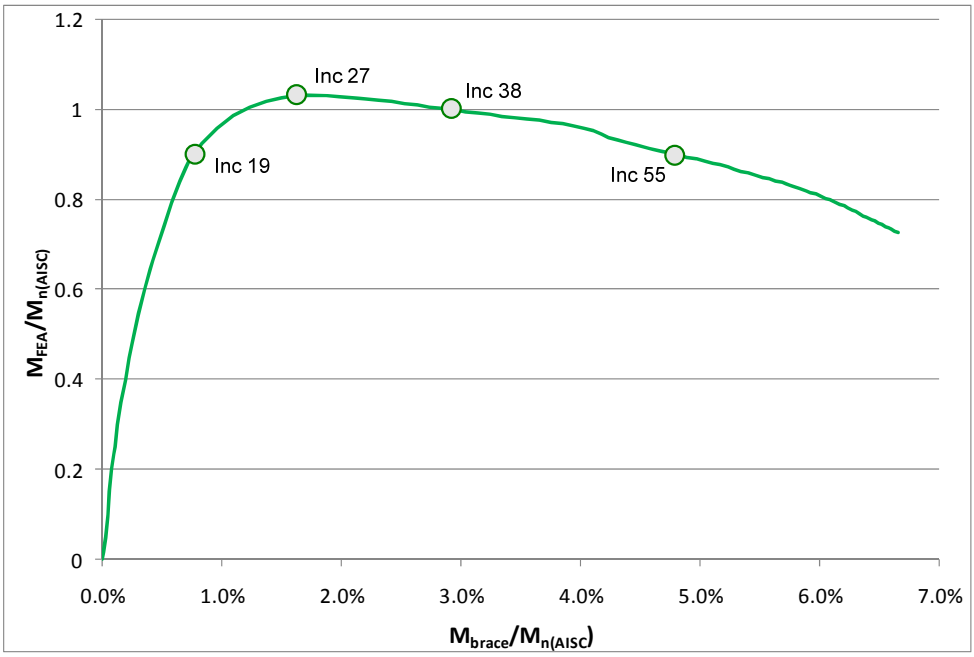


**Fig. 5.3.21. Brace forces for the brace stiffness $\beta_{Tb}$ = 11493 kip-inch/rad, Benchmark Study TB1.**

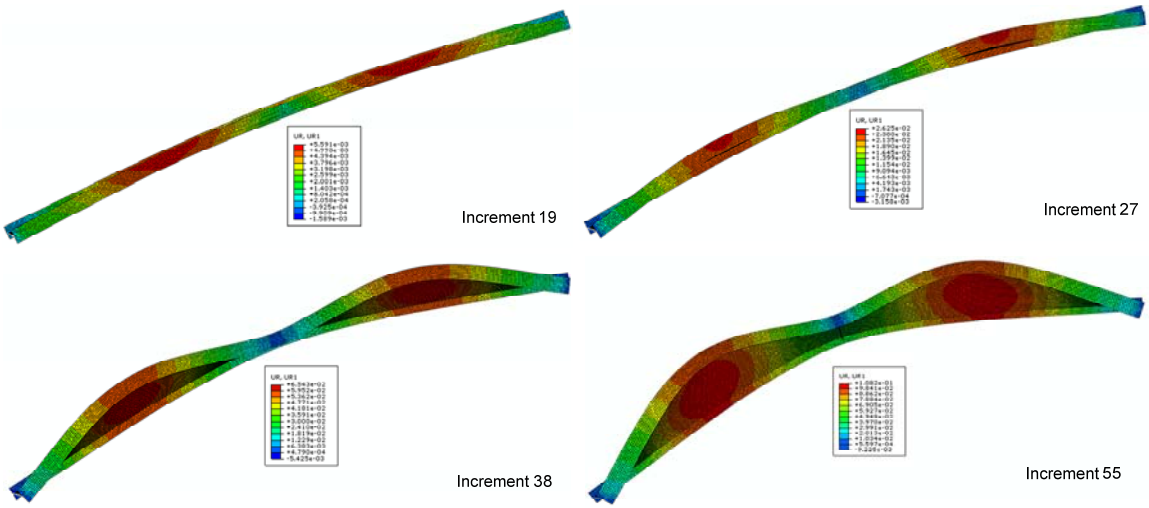


**Fig. 5.3.22. Deformed shape at the different stages for the brace stiffness $\beta_{Tb}$ = 11493 kip-inch/rad - Scaled 15x, Benchmark Study TB1.**

### 5.3.4 Combined Lateral and Torsional bracing: Benchmark Study CB1

Similarly to Benchmark Study CB1 in Section 4.7.3.1, the simply supported beam W16x26 with braces located at 2 in above the top flange is subjected to the positive uniform bending moment as shown in Fig. 5.3.23. The nominal flexural strength, $M_n$, based on AISC is $M_n$ = 1457 kips-in.

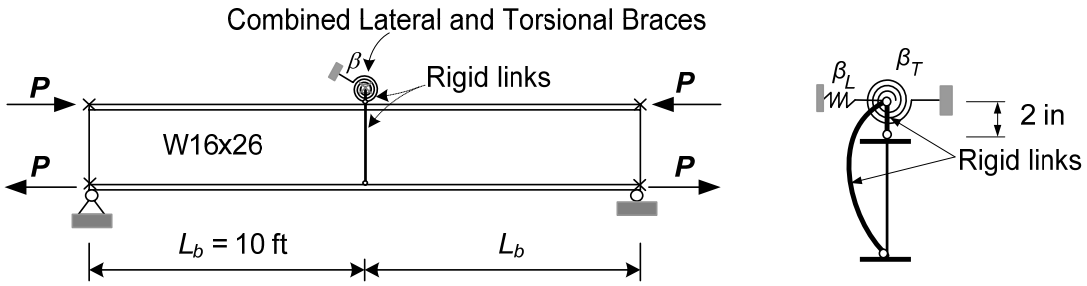


**Fig. 5.3.23. Benchmark Study CB1.**

The results from Plastic Zone Solution will show with the four pairs of the brace stiffnesses based on Fig. 4.7.14 are summarized as follow.

- $\beta_T$ = 781 kip-inch/rad, $\beta_L$ = 0.3 kip/in (Point A in Fig. 4.7.14)
- $\beta_T$ = 1041 kip-inch/rad, $\beta_L$ = 0.4 kip/in (Point B in Fig. 4.7.14)
- $\beta_T$ = 1562 kip-inch/rad, $\beta_L$ = 0.6 kip/in (Point C in Fig. 4.7.14)
- $\beta_T$ = 2083 kip-inch/rad, $\beta_L$ = 0.8 kip/in (Point D in Fig. 4.7.14)

The torsional and lateral brace forces for these pairs of brace stiffnesses are plotted in Figs. 5.3.24 and 5.3.25.

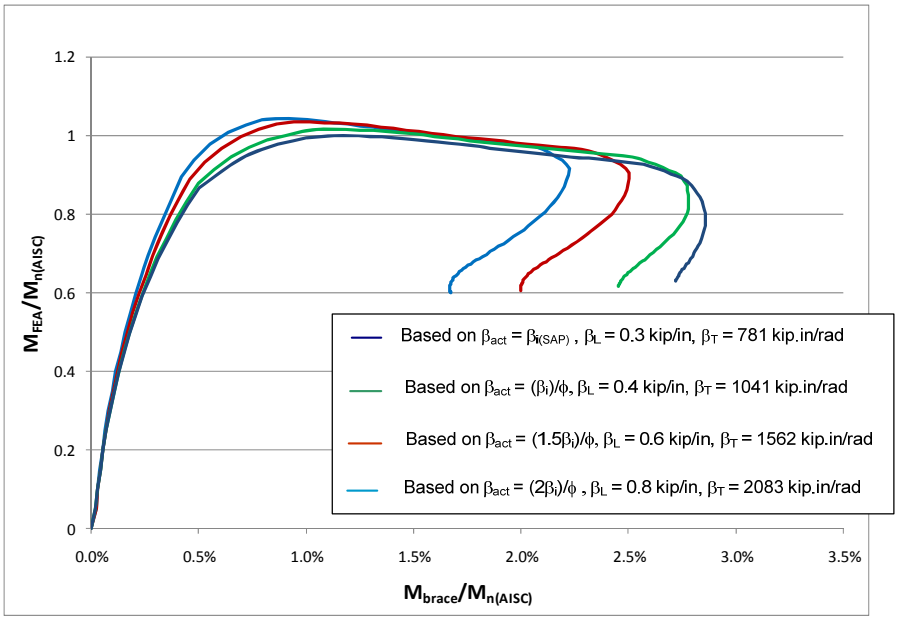


**Fig. 5.3.24. Torsional brace forces for the different brace stiffness, Benchmark Study CB1.**

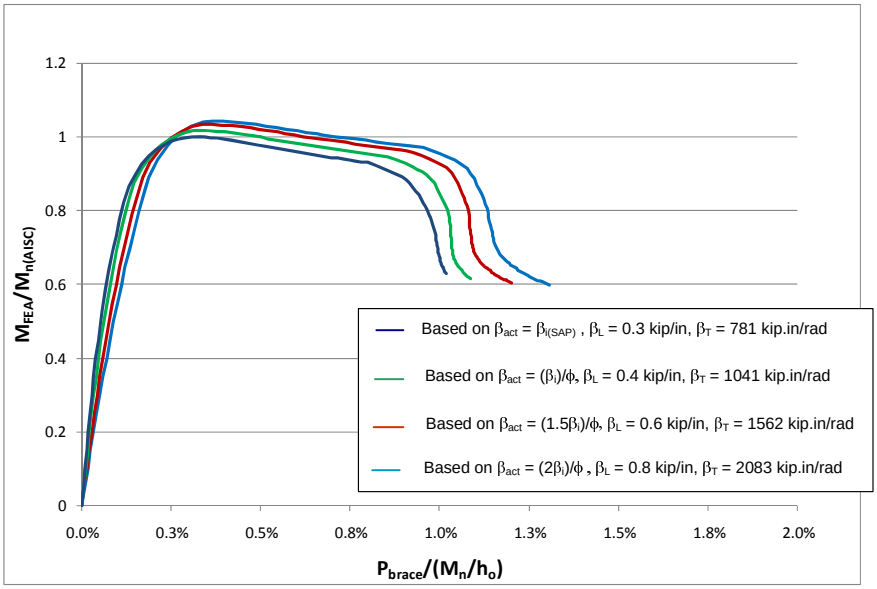


**Fig. 5.3.25. Lateral brace forces for the different brace stiffness, Benchmark Study CB1.**

- For the brace stiffnesses ($\beta_T$ = 781kip-inch/rad, $\beta_L$ = 0.3 kip/in), the lateral brace force at the maximum applied load is equal to 0.34% of $M_n/h_o$, and the torsional brace force at the

maximum applied load is equal to 1.19% of $M_n$. The maximum load obtained from FEA is of 0.99$M_n$.

- For the brace stiffnesses ($\beta_T$ = 1041kip-inch/rad, $\beta_L$ = 0.4 kip/in), the lateral brace force at the maximum applied load is equal to 0.33% of $M_n/h_o$, and the torsional brace force at the maximum applied load is equal to 1.12% of $M_n$. The maximum load obtained from FEA is of 1.02$M_n$.
- For the brace stiffnesses ($\beta_T$ = 1562 kip-inch/rad, $\beta_L$ = 0.6 kip/in), the lateral brace force at the maximum applied load is equal to 0.36% of $M_n/h_o$, and the torsional brace force at the maximum applied load is equal to 1.02% of $M_n$. The maximum load obtained from FEA is of 1.03$M_n$.
- For the brace stiffnesses ($\beta_T$ = 2083 kip-inch/rad, $\beta_L$ = 0.8 kip/in), the lateral brace force at the maximum applied load is equal to 0.37% of $M_n/h_o$, and the torsional brace force at the maximum applied load is equal to 0.87% of $M_n$. The maximum load obtained from FEA is of 1.04$M_n$.

The deformed shapes corresponding to these brace stiffnesses are plotted from Figs. 5.3.26 to 5.3.29 respectively.

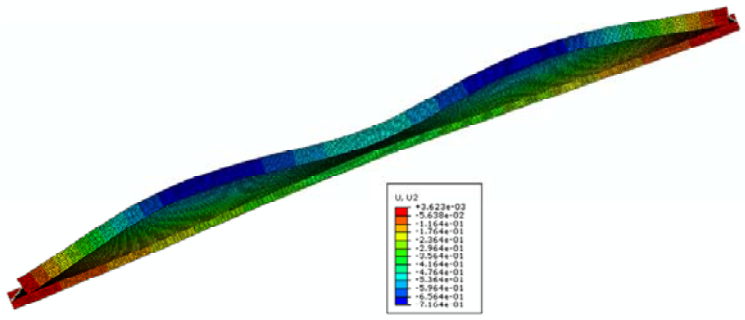

**Fig. 5.3.26. Deformed shape at the maximum load for the brace stiffness $\beta_T$ = 2083 kip-inch/rad, $\beta_L$ = 0.8 kip/in - Scaled 20x, Benchmark Study CB1.**

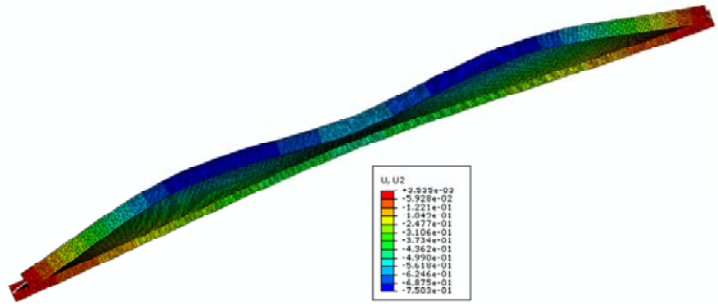

**Fig. 5.3.27. Deformed shape at the maximum load for the brace stiffness $\beta_T$ = 1562 kip-inch/rad, $\beta_L$ = 0.6 kip/in - Scaled 20x, Benchmark Study CB1.**

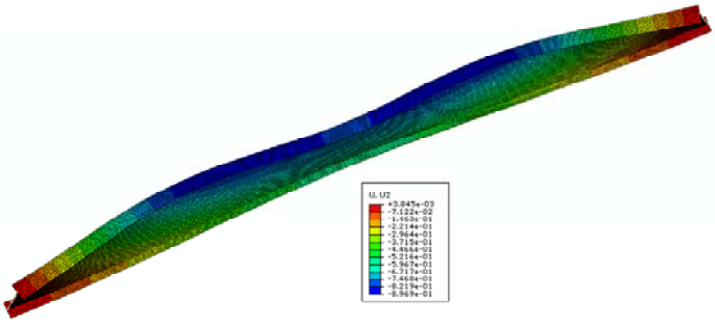

**Fig. 5.3.28. Deformed shape at the maximum load for the brace stiffness $\beta_T$ = 1041 kip-inch/rad, $\beta_L$ = 0.4 kip/in - Scaled 20x, Benchmark Study CB1.**

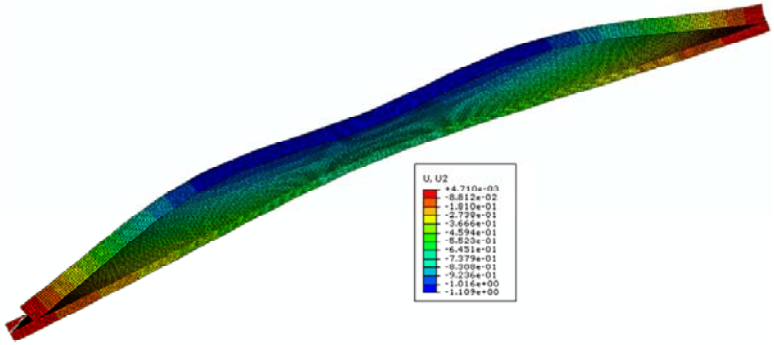

**Fig. 5.3.29. Deformed shape at the maximum load for the brace stiffness $\beta_T$ = 781 kip-inch/rad, $\beta_L$ = 0.3 kip/in - Scaled 15x, Benchmark Study CB1.**

Figs. 5.3.30 and 5.3.31 display the relationship between the brace forces and the moment from the Finite Element Analysis for the brace stiffnesses ($\beta_T$ = 2083 kip-inch/rad, $\beta_L$ = 0.8 kip/in). The deformed shapes corresponding to the four increments labeled in these plots are shown in Fig. 5.3.32.

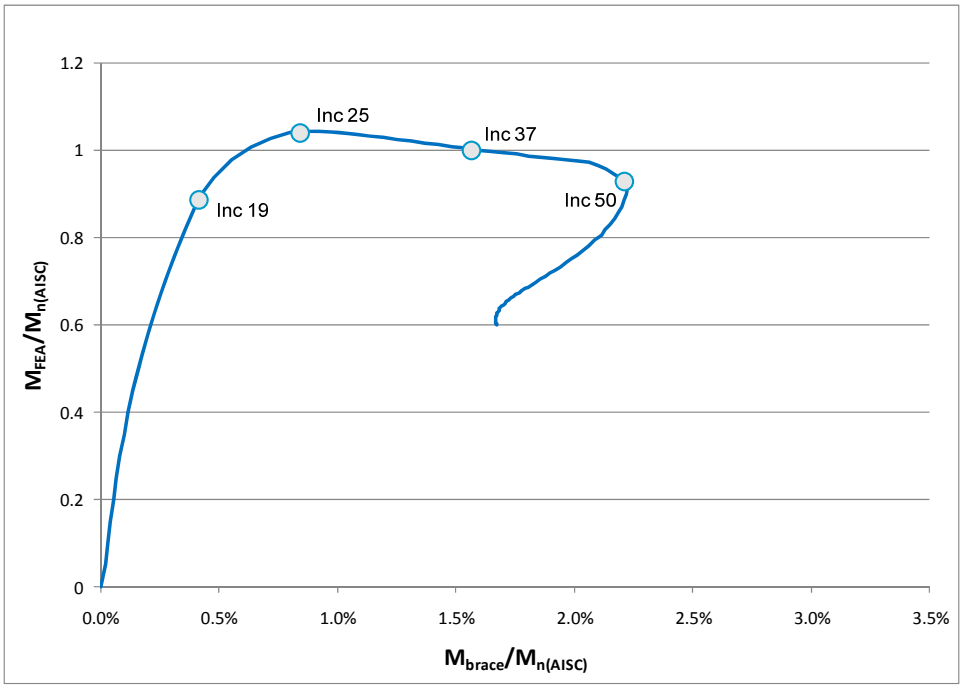


**Fig. 5.3.30. Torsional brace forces for the brace stiffness $\beta_T$ = 2083 kip-inch/rad, $\beta_L$ = 0.8 kip/in, Benchmark Study CB1.**

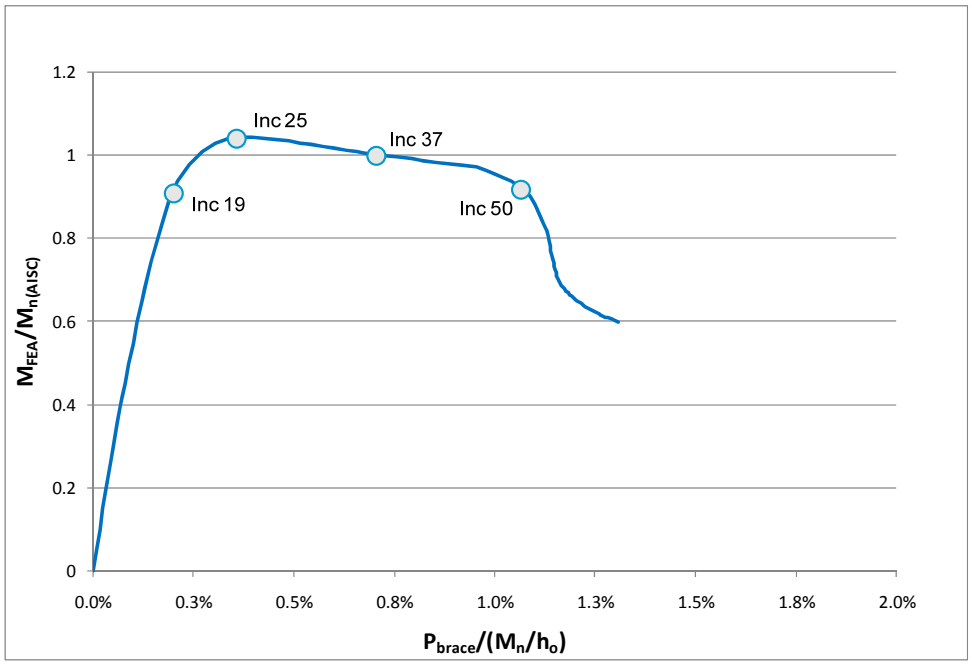


**Fig. 5.3.31. Lateral brace forces for the brace stiffness $\beta_T$ = 2083 kip-inch/rad, $\beta_L$ = 0.8 kip/in, Benchmark Study CB1.**

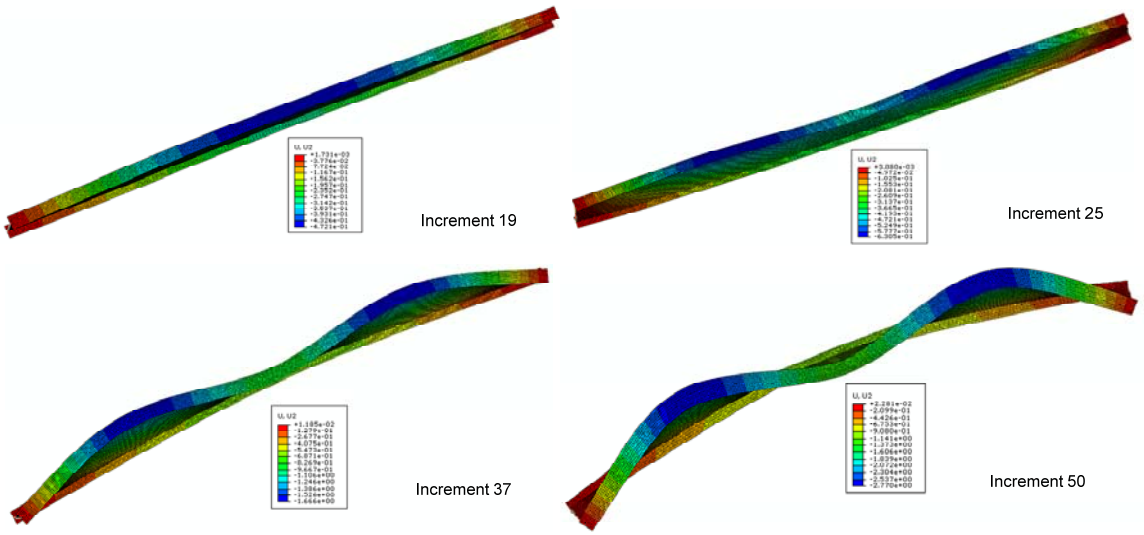


**Fig. 5.3.32. Deformed shape at the different stages for the brace stiffness $\beta = 2\beta_i/\phi$ – Scaled 10x, Benchmark Study CB1.**

### 5.3.5 Lateral Bracing for Richter's (1998) Test No.6

Fig. 5.3.33 shows a configuration of Richter's (1998) Test No. 6: a beam with four intermediate nodal braces under a constant moment, five equal unbraced lengths $L_b$ = 60 inches.

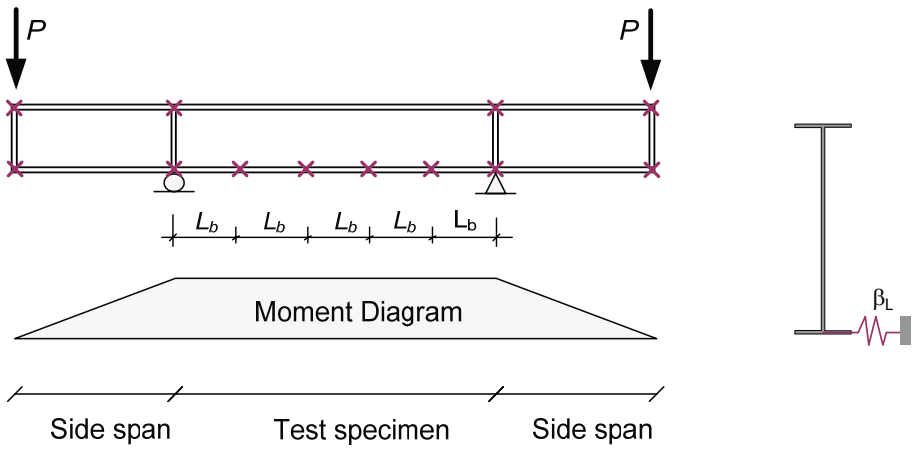


**Fig. 5.3.33. Richter's (1998) Test No.6 - Test configuration, lateral bracing.**

The properties of the cross-section are as follows:

- Tension flange: $b_{ft}$ = 4.99 in x $t_{ft}$= 0.32 in ($F_{yt}$ = 48.4 ksi)
- Compression flange : $b_{fc}$= 4.98 in x $t_{fc}$= 0.31 in ($F_{yc}$ = 48.7 ksi)
- Web : $h$ = 18.00 in x $t_w$= 0.163 in ($F_{yw}$ = 52.5 ksi)

According to the procedure to determine the critical geometric imperfections discussed in Section 4.4, the critical imperfection for this problem is shown in Fig. 5.3.34.

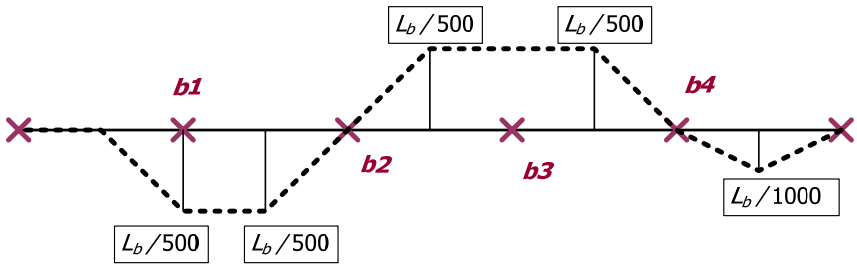


**Fig. 5.3.34. Geometric imperfections, Richter's (1998) - Test No. 6**

The nominal flexural strength, $M_n$, based on AISC is $M_n$ = 1719 kips-in. The brace stiffness and strength requirements based on the Appendix 6 are calculated in Section 5.3.5.1. The results from Plastic Zone Solution with two brace stiffnesses

$\beta = (2\beta_{i\,(APP6)})/\phi$, $\beta = 1.3\beta_{i(APP6)}$ are presented in Section 5.3.5.2.

5.3.5.1 Results from the AISC 2005 Appendix 6 Commentary Equations for $M=M_n$

Based on Eqs. (2-24) and (2-26), for this problem we have

$$n = 4 \quad N_i = 4 - \frac{2}{n} = 3.5 \quad h_o = 18.315 \text{ inches}$$

$$C_t = 1,\ C_d = 1,\ C_b = 1,\ M_n = 1719 \text{kips - inch}$$

$$P_f = M_n/h_o = 93.9 \text{ kips}$$

- Required brace stiffness:

$$\beta_i = \frac{N_i P_f}{L_b} C_d C_t \quad ; \qquad \beta_{br} = \frac{2\beta_i}{\phi}$$

$$\beta_i = \frac{3.5(93.9)}{60} 1(1) = 5.48 \text{ kips/inch}, \qquad \beta_{br} = \frac{2(5.47)}{0.75} = 14.61 \text{ kips/inch}$$

- Required brace strength:

$$P_{br} = \frac{(0.01)M_n}{h_o} C_d C_t = \frac{(0.01)(1719)}{18.315} 1(1) = 0.94 \text{ kips} = 0.01 \frac{M_n}{h_o}$$

5.3.5.2 Results from Plastic Zone Analyses

The brace forces corresponding to the applied load for the outside brace (brace b1 in Fig. 5.3.34) from the Finite Element Analysis are shown in Figs.5.3.35. One can observe from Fig. 5.3.35 that the maximum moment is equal to 0.89 $M_n$ using the brace stiffness $\beta = 2\beta_i/\phi = 14.61$ kips/inch, and equal to 0.88 $M_n$, using the brace stiffness $\beta = 1.3\beta_i = 7.124$ kips/inch.

Fig. 5.3.35 indicates that the bracing force demand is of 1.6 % of $M_n/h_o$ at the limit load $M_{max}$ when using the brace stiffness $\beta = 14.61$ kips/inch and 2.8 % of $M_n/h_o$ when using the brace stiffness $\beta = 7.124$ kips/inch corresponding to 1.0 % of $M_n/h_o$ based on the strength requirement from the AISC Appendix 6.

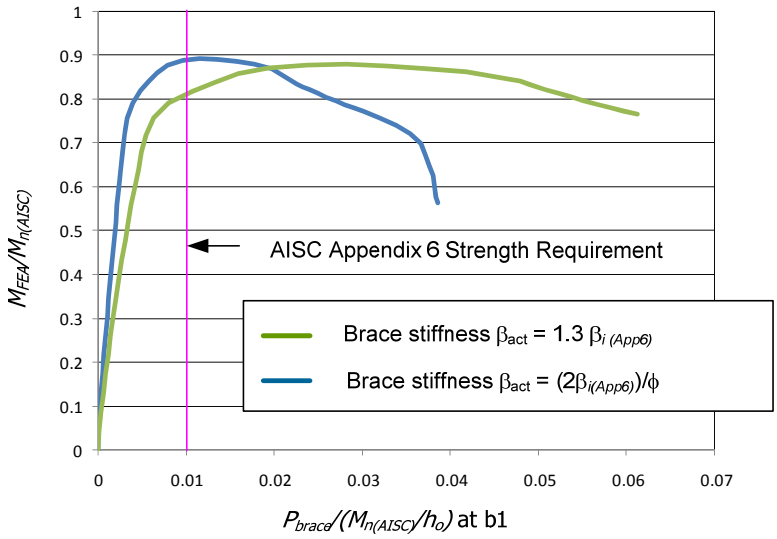


**Fig. 5.3.35. Brace forces for the different brace stiffness – Richter's (1998) Test No. 6.**

The vertical displacements at midspan of the beam corresponding to applied load are plotted in Fig. 5.3.36. This figure shows that the vertical displacement at the maximum load at the midspan is 2.7 inches using the brace stiffness $\beta = 2\beta_i/\phi = 14.61$ kips/inch and 2.3 inches using the brace stiffness $\beta = 1.3\beta_i = 7.124$ kips/inch

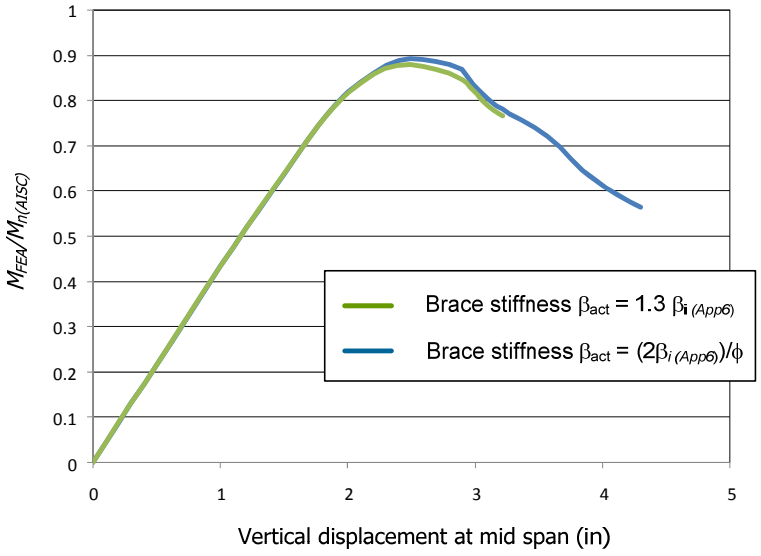


**Fig. 5.3.36. Vertical displacement at the mid span for the different brace stiffness, Richter's (1998) Test No. 6.**

The deformed shapes corresponding to the maximum load for the brace stiffnesses $\beta = 2\beta_i/\phi = 14.61$ kips/inch and $\beta = 1.3\beta_i = 7.124$ kips/inch are plotted in Figs. 5.3.37 and 5.3.38.

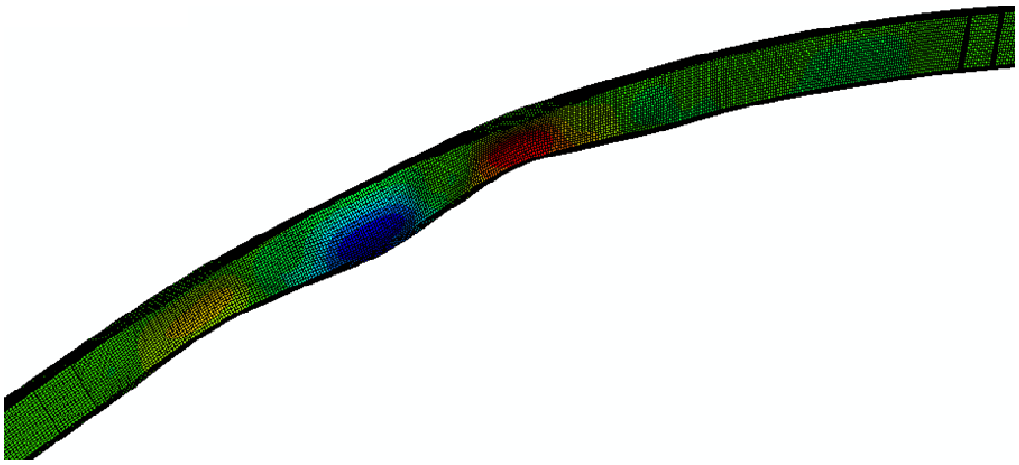

**Fig. 5.3.37. Deformed shape at the maximum load for the brace stiffness $\beta = 2\beta_i/\phi$ – Scaled 10x, Richter's (1998) Test No. 6.**

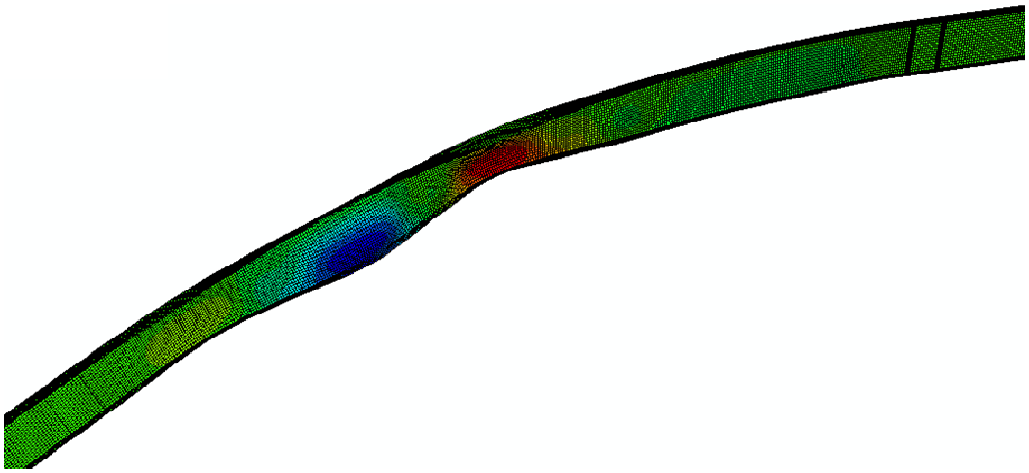

**Fig. 5.3.38. Deformed shape at the maximum load for the brace stiffness $\beta = 1.3\beta_i$ – Scaled 10x, Richter's (1998) Test No. 6.**

Fig. 5.3.39 shows the relationship between the brace forces and the moment from the Finite Element Analysis for the brace stiffness $\beta = 2\beta_i/\phi = 14.61$ kips/inch. The deformed shapes corresponding to the four increments labeled in this plot are shown in Fig. 5.3.40.

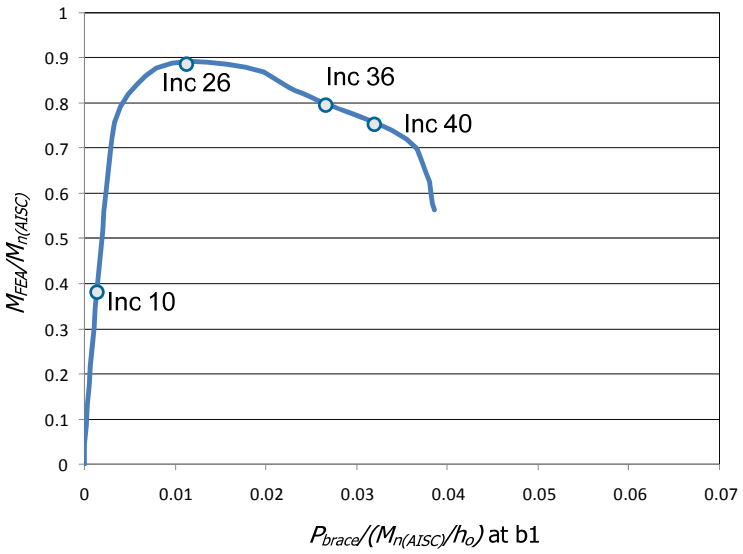


**Fig. 5.3.39. Brace forces for the brace stiffness $\beta = 2\beta_i/\phi$, Richter's (1998) Test No. 6.**

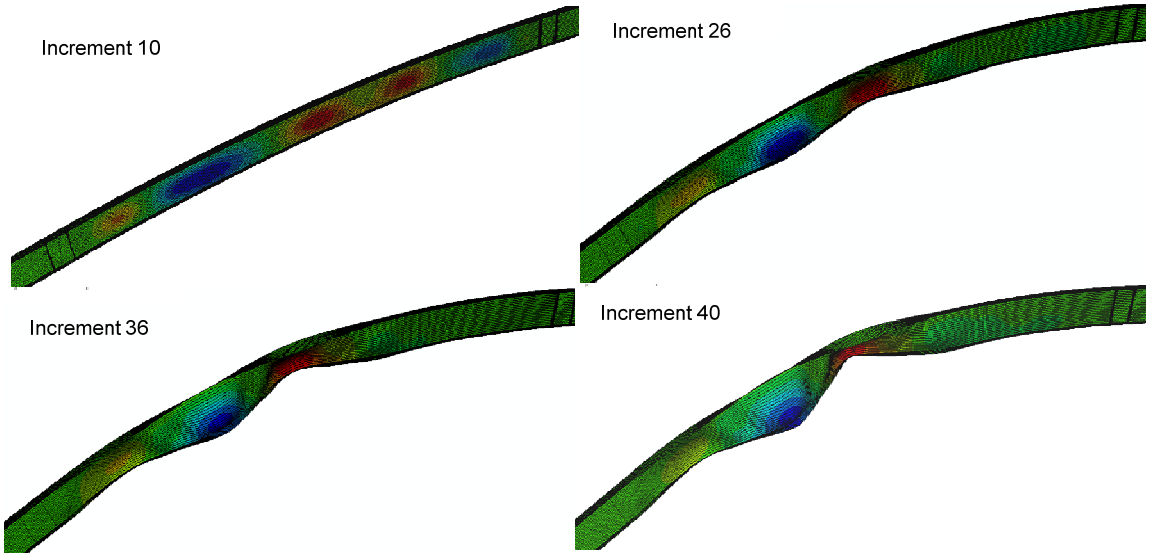


**Fig. 5.3.40. Deformed shape at the different stages for the brace stiffness $\beta = 2\beta_i/\phi$ – Scaled 10x, Richter's (1998) Test No. 6.**

### 5.3.6 Torsional Bracing for Richter's (1998) Test No.6

In this section, Richter's (1998) Test No.6 is analyzed by using four intermediate torsional braces as shown in Fig. 3.5.41. The brace points are located at 3 in above the

centroid of the top flange and they are connected by two rigid links. One rigid link is pin connected to the top flange at the web-flange juncture and one is pin connected to the bottom flange at the web-flange juncture. The test configuration and cross-section properties are the same as those in Section 5.3.5.

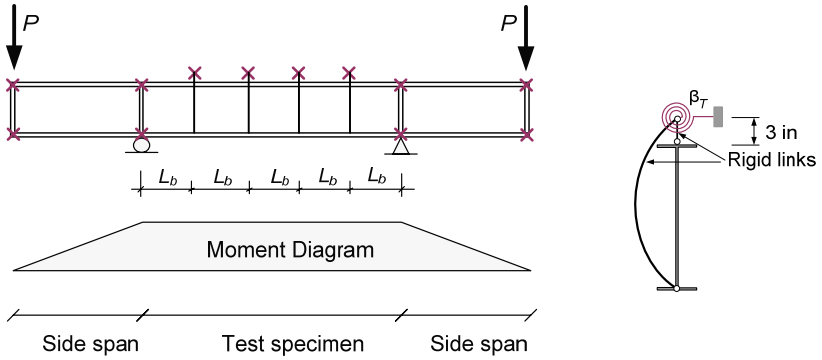


**Fig. 5.3.41. Richter's (1998) Test No.6 - Test configuration for torsional bracing.**

The brace stiffness and strength requirements based on the Appendix 6 are calculated in Section 5.3.6.1. The results from Plastic Zone Solutions with a brace stiffnesses $\beta = (2\beta_{i\,(APP6)})/\phi$ are presented in Section 5.3.6.2.

5.3.6.1 Results from the AISC (2005) Appendix 6 Commentary Equations for $M=M_n$

With $n = 4, L = 5L_b = 300$ inches, $C_b = 1$, $M_n = 1719$ kips - inch the brace stiffness and brace strength requirements can be estimated as follows:

- Required brace stiffness:

$$\beta_T = \frac{1}{\phi}\left(\frac{2LM_n^2}{nEI_yC_b^2}\right)$$

$$\beta_T = \frac{1}{0.75}\left(\frac{2.0(300)(1719)^2}{4(29000)(6.48)(1^2)}\right) = 3145 \text{ kips} - \text{inch/rad}$$

- Required brace strength:

$$M_{br} = \frac{0.02 M_n L}{n C_b L_b}$$

$$M_{br} = \frac{0.02(1719)(300)}{4(1)(60)} = 43.0 \text{ kips - inch} = 0.025 M_n$$

5.3.6.2 Results from Plastic Zone Analyses

Using the same critical imperfection as in Fig. 5.3.34, the results from the Finite Element Analysis are presented as follows.

The brace forces corresponding to the applied load for the inside brace (brace b3 in Fig. 5.3.34) are plotted in Figs.5.3.42. One can observe from Fig. 5.3.42 that the maximum moment is equal to 0.85 $M_n$ using the brace stiffness $\beta = 2\beta_i/\phi = 3145$ kip-inch/rad. Fig. 5.3.42 also indicates that the bracing force demand is equal to 1.8% of $M_n$ at the limit load $M_{max}$ when using bracing stiffness $\beta = 3145$ kip-inch/rad while the brace force demand is equal to 2.5% of $M_n$ based on the AISC (2005) Appendix 6.

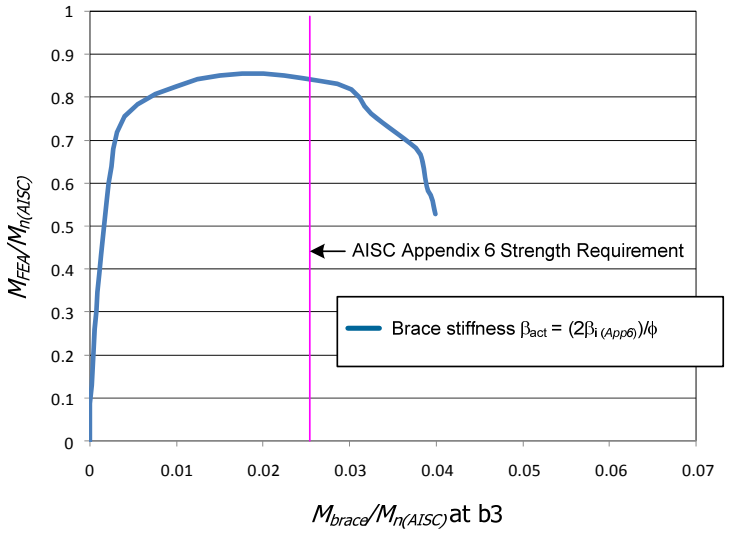


**Fig. 5.3.42. Brace forces for the different brace stiffness, Richter's (1998) Test No.6.**

The vertical displacements at midspan of the beam corresponding to applied load are plotted in Fig. 5.3.43. This figure shows that the vertical displacement at the maximum load at the midspan is 2.2 inches using the brace stiffness $\beta = 2\beta_i/\phi = 3145$ kip-inch/rad.

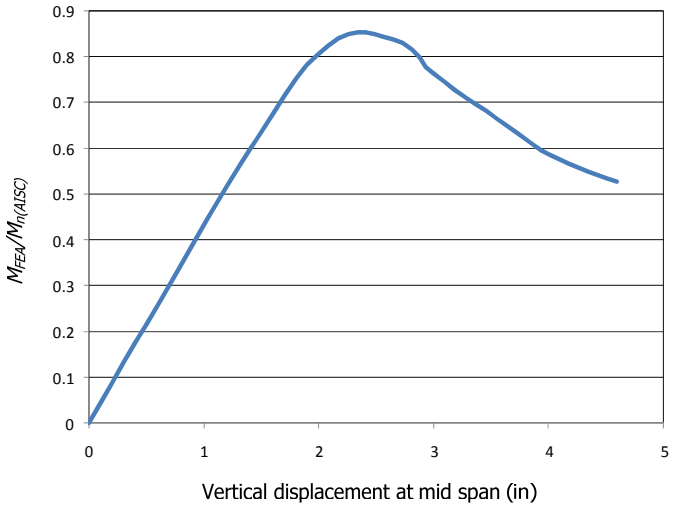


**Fig. 5.3.43. Vertical displacement at the mid span for the brace stiffness $\beta = (2\beta_{i\,(APP6)})/\phi$, Richter's (1998) Test No.6.**

The deformed shapes corresponding to the maximum load for the brace stiffness $\beta = 2\beta_i/\phi = 3145$ kip-inch/rad is plotted in Fig. 5.3.44. The relationship between the brace forces and the moment from the Finite Element Analysis is shown in Fig. 5.3.45. The deformed shapes corresponding to the four increments labeled in this plot are shown in Fig. 5.3.46.

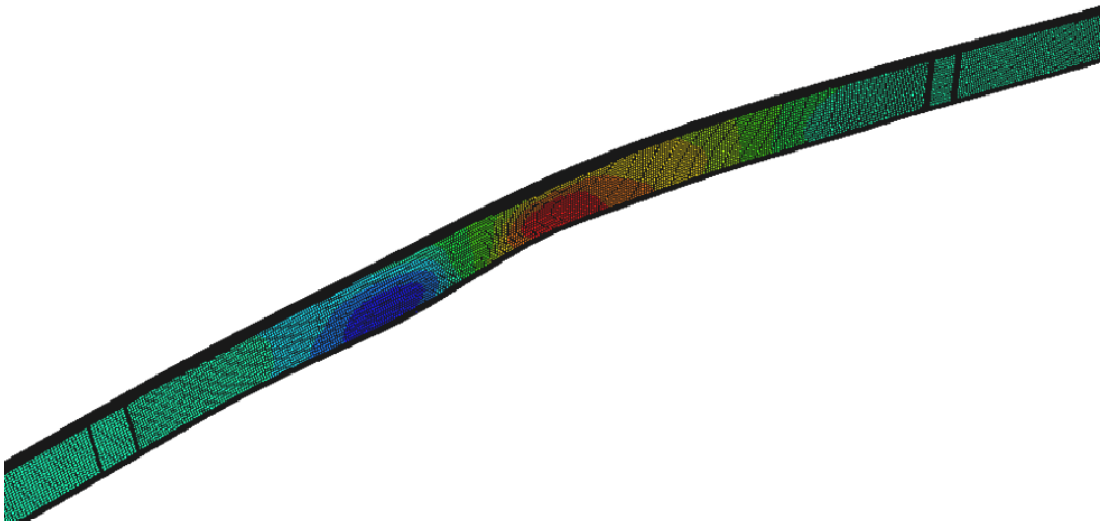

**Fig. 5.3.44. Deformed shape at the maximum load for the brace stiffness $\beta = 2\beta_i/\phi$ – Scaled 5x, Richter's (1998) Test No.6.**

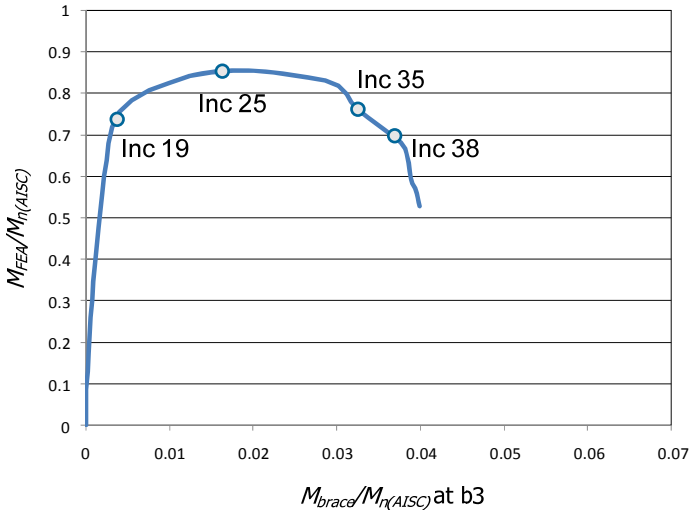


**Fig. 5.3.45. Brace forces for the brace stiffness $\beta = 2\beta_i/\phi$, Richter's (1998) Test No.6.**

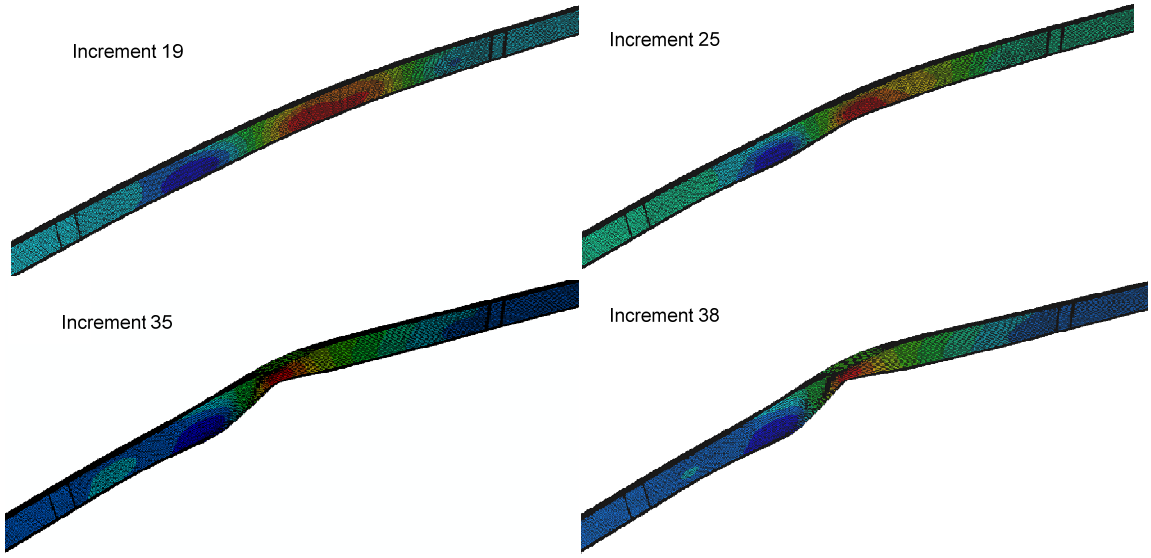


**Fig. 5.3.46. Deformed shape at the different stages for the brace stiffness $\beta = 2\beta_i/\phi$ – Scaled 5x, Richter's (1998) Test No.6.**

### 5.3.7 Combined Lateral and Torsional Bracing for Richter's (1998) Test No.6.

Fig. 5.3.47 shows the configuration of Richter's (1998) Test No.6 with combined lateral and torsional braces. The test configuration and cross-section properties are the same as those in Section 5.3.5. Similar to Section 5.3.6, the brace points are located at 3 in above the centroid of the top flange and they are connected by two rigid links. One rigid link is pin connected to the top flange at the web-flange juncture and one is pin connected to the bottom flange at the web-flange juncture.

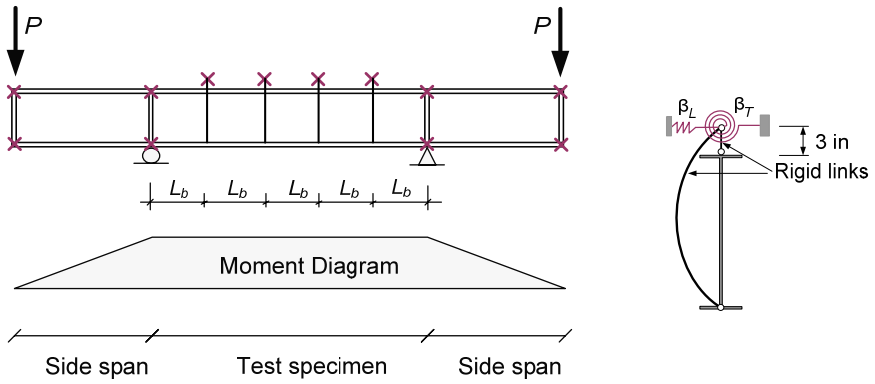


**Fig. 5.3.47. Richter's (1998) Test No.6 - Test Configuration, combined lateral and torsional bracing.**

Section 5.3.5 shows that the brace stiffness requirement based on the AISC (2005) Appendix 6 Commentary is $\beta$ = 14.5 kips/inch for using only the lateral brace system. And Section 5.3.6 shows that the brace stiffness requirement based on the AISC (2005) Appendix 6 Commentary is $\beta_T$ = 1345 kips-inch/rad for using only the torsional brace system. In this section, the results from Plastic Zone Solution for combined lateral and torsional braces using the lateral brace stiffness $\beta_{CL} = 5.5\%\beta_L = 0.8$ kips/inch and the torsional brace stiffness $\beta_{CT} = 60\%\beta_T = 1887$ kip-inch/rad are presented.

5.3.7.1 Results from Plastic Zone Analyses

The torsional brace moments corresponding to the applied load for the brace "b3" in Fig. 5.3.34 from the Finite Element Analysis are shown in Figs.5.3.48. This figure shows that that the maximum moment is equal to 0.84 and the bracing force demand is of 1.7% of $M_n$ at the limit load $M_{max}$. One can observe that these results are very close to the results from Section 5.3.6 using the torsional brace only with stiffness $\beta_T$ = 1345 kips-inch/rad.

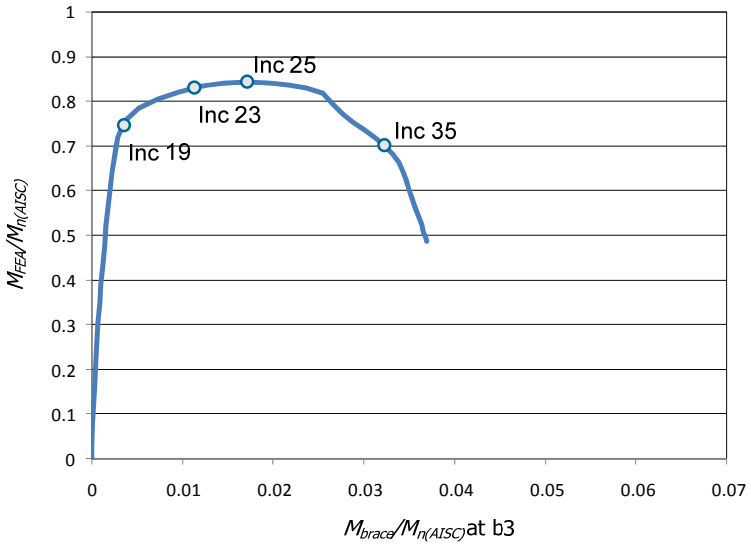


**Fig. 5.3.48. Torsional brace forces, Richter's (1998) Test No.6.**

The lateral brace forces corresponding to the applied load for the brace "b1" in Fig. 5.3.34 from the Finite Element Analysis are shown in Figs.5.3.49. This figure shows that that the maximum moment is equal to $0.84M_n$ and the bracing force demand is of 2.2% of $M_n /h_o$ at the limit loads $M_{max}$.

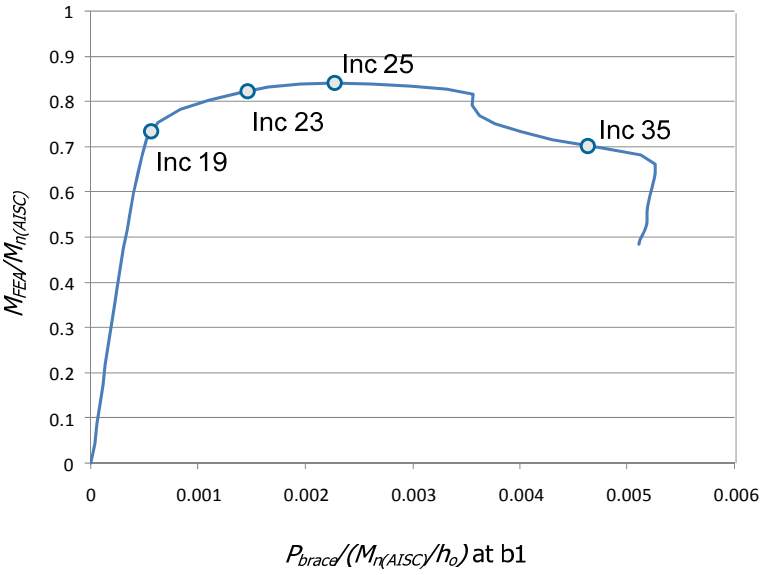


**Fig. 5.3.49. Lateral brace forces, Richter's (1998) Test No.6.**

The vertical displacements at midspan of the beam corresponding to applied load are plotted in Fig. 5.3.50. This figure shows that the vertical displacement at the maximum load at the midspan is 2.3inches. The deformed shapes corresponding to the maximum load is plotted in Fig. 5.3.51.

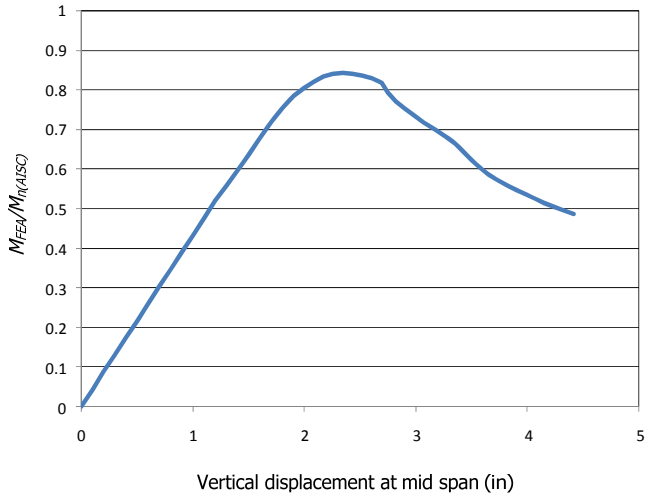


**Fig. 5.3.50. Vertical displacement at the mid span, Richter's (1998) Test No. 6.**

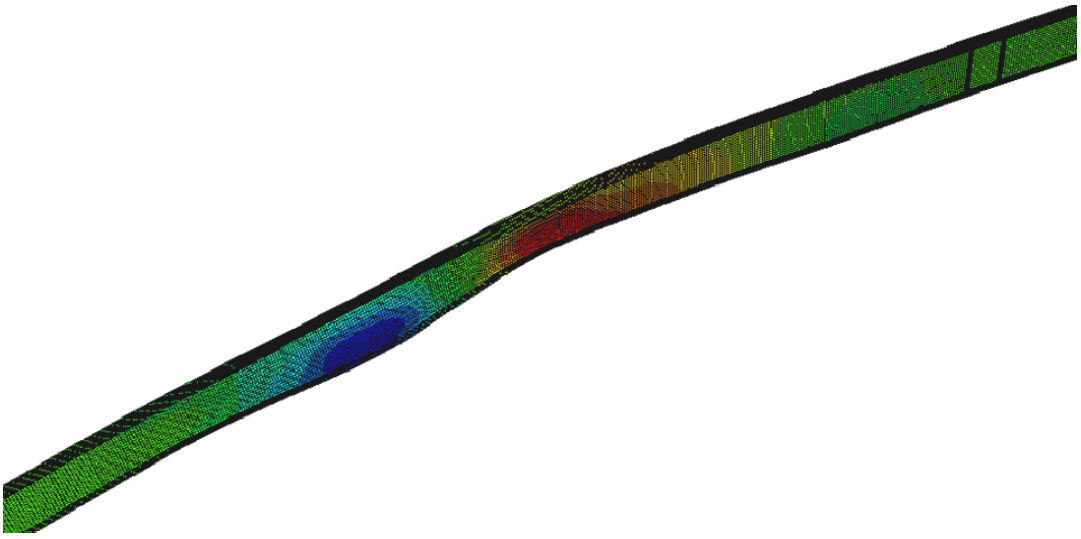

**Fig. 5.3.51. Deformed shape at the maximum load - Scaled 5x, Richter's (1998) Test No. 6.**

Figs. 5.3.48 and 5.3.49 show the relationship between the brace forces and the moment from the Finite Element Analysis. The deformed shapes corresponding to the four increments labeled in this plot are shown in Fig. 5.3.52.

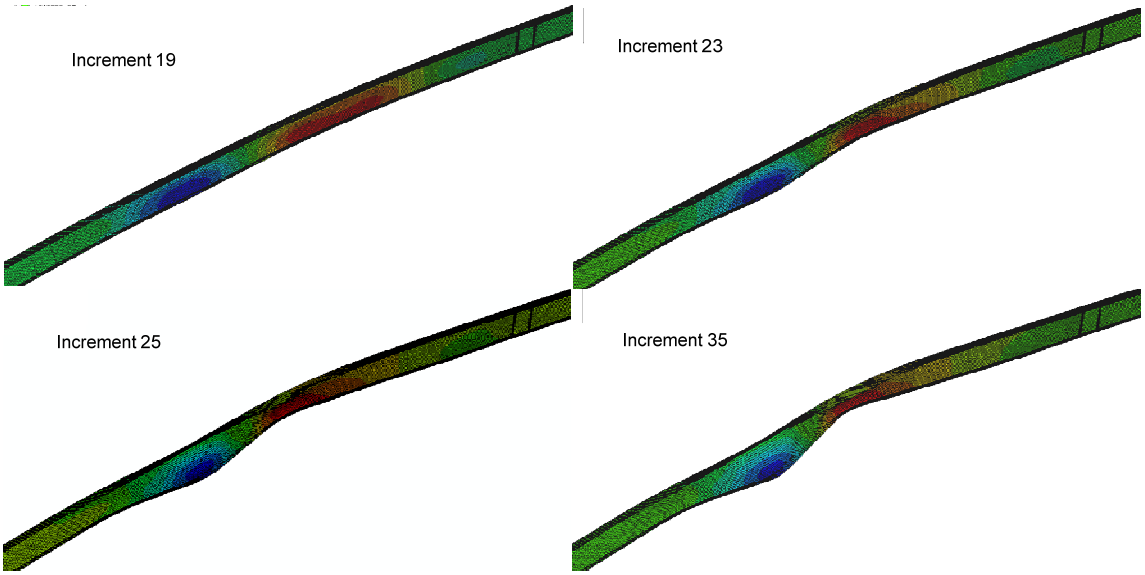


**Fig. 5.3.52. Deformed shape at the different Stages – Scaled 5x, Richter's (1998) Test No. 6.**

### 5.3.8 Tapered Beam

The beam bracing studies investigated so far are the prismatic beams. In this section, beam bracing for a tapered beam is considered. Fig. 5.3.53 shows a tapered beam with a torsional brace at its midspan. The centroid of the torsional brace is assumed to be located at 2 inches above the top flange. The brace is connected to the beam by two rigid links. One rigid link is pin connected to the top flange at the web-flange juncture and one is pin connected to the bottom flange at the web-flange juncture.

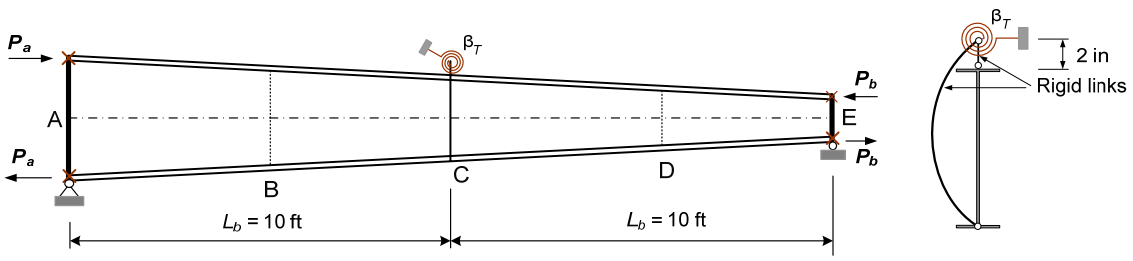


**Fig. 5.3.53. Tapered beam, torsional bracing.**

The cross-section is based on the section W16x26. The web of the beam varies linearly through the length. The cross-section properties are shown in Table 5.2.

**Table 5.2. The cross-section properties of tapered beam.**

| Section | Web | | Flanges | |
|---|---|---|---|---|
| | $h$ (in) | $t_w$ (in) | $b_f$ (in) | $t_f$ (in) |
| A | 23.01 | 0.25 | 5.5 | 0.345 |
| B | 19.01 | 0.25 | 5.5 | 0.345 |
| C | 15.01 | 0.25 | 5.5 | 0.345 |
| D | 11.01 | 0.25 | 5.5 | 0.345 |
| E | 7.01 | 0.25 | 5.5 | 0.345 |

The beam is subjected to moment $M_A$ at the left end and $M_B$ at the right end. The moment $M_A$ is assigned equally the yielding moment at A and moment $M_B$ is assigned equally the yielding moment at E.

The beam is modeled by 22 elements through the web depth and 8 elements through the flange width. The other parameters such as material, residual stress, geometric imperfections are used the same as the Benchmark Study TB1 in Section 5.3.3.

The critical unbraced moment is calculated based on the Steel Design Guide – Frame Design Using Web-Tapered Members (Kaehler, White, and Kim 2008). The results are summarized as follow.

**a) For the left unbraced length (Segment AC)**

The critical moment for the left unbraced length, segment AC is

$M_{cr}$ = 1980.4 kips-inch

The critical stress for segment AC is

$$F_{crA} = \frac{M_{crA}}{S_{xA}} = \frac{1980.4}{50.62} = 39.13\text{ksi}$$

The ratio of the member elastic buckling load or moment to the required strength for segment AC is (consider cross section at the left end)

$$\gamma_{eA} = \frac{F_{crA}}{f_{bmaxA}} = \frac{39.13}{53.57} = 0.730$$

The web plastification factor $R_{pc}$ is

$$\text{Since } \lambda_{pw} = 3.76\sqrt{\frac{E}{F_y}} = 90.55 < h_c/t_w = 92.04 < \lambda_{rw} = 5.7\sqrt{\frac{E}{F_y}} = 137.27$$

$$R_{pc} = \frac{M_p}{M_{yc}} - \left(\frac{M_p}{M_{yc}} - 1\right)\left(\frac{\lambda - \lambda_{pw}}{\lambda_{rw} - \lambda_{pw}}\right) = 1.183 < \frac{M_p}{M_{yc}} = 1.189$$

(5.3, AISC F4-9b)

The web bend buckling factor $R_{pg}$ is

$$\text{Since } h_c/t_w = 92.04 < \lambda_{rw} = 5.7\sqrt{\frac{E}{F_y}} = 137.27\text{ , } R_{pg} = 1.0$$

Because of $8.2 > \frac{\gamma_{eA} f_{bmaxA}}{F_y} = \frac{0.73(50)}{50} = 0.73 > 0.7 = \frac{F_L}{F_y}$, the inelastic lateral-torsional buckling nominal strength is

$$M_n = R_{pg} R_{pc} M_{yc} \left[ 1 - \left( 1 - \frac{F_L}{R_{pc} F_y} \right) \left( \frac{\pi \sqrt{\frac{F_y}{\gamma_{eA} f_{bmaxA}}} - 1.1}{\pi \sqrt{\frac{F_y}{F_L}} - 1.1} \right) \right] \tag{5.4}$$

$$M_n = 1.0(1.183)(3254.64) \left[ 1 - \left( 1 - \frac{35}{1.183(50)} \right) \left( \frac{\pi \sqrt{\frac{50}{0.73(50)}} - 1.1}{\pi \sqrt{\frac{50}{35}} - 1.1} \right) \right]$$

$M_n$ = 3272.7 kips-inch

The ratio, $\left( \frac{M_r}{M_n} \right)_A$ for the left unbraced length is $\left( \frac{M_r}{M_n} \right)_A = \frac{3254.64}{3272.7} = 0.994$

**b) For the right unbraced length (Segment CE)**

The critical moment for segment CE is

$M_{crB}$ = 1264.2 kips-inch

The critical stress for segment BC is

$$F_{crB} = \frac{M_{crB}}{S_{xB}} = \frac{1264.2}{25.67} = 49.25\text{ksi}$$

The ratio of the member elastic buckling load or moment to the required strength for segment BC is (Consider cross section at the braced point)

$$\gamma_{eB} = \frac{F_{crB}}{f_{bmaxB}} = \frac{49.25}{54.02} = 0.912$$

The web plastification factor $R_{pc}$ is

Since $h_c/t_w = 60.04 < \lambda_w = 3.76\sqrt{\frac{E}{F_y}} = 90.55$

$$R_{pc} = \frac{M_p}{M_{yc}} = 1.15 \qquad \text{(5.5, AISC F4-9a)}$$

The web bend buckling factor $R_{pg}$ is

$$\text{Since } h_c/t_w = 60.04 < \lambda_{rw} = 5.7\sqrt{\frac{E}{F_y}} = 137.27\text{, } R_{pg} = 1.0$$

Because of $8.2 > \frac{\gamma_{eB} f_{bmaxB}}{F_y} = \frac{0.912(54.02)}{50} = 0.985 > 0.7 = \frac{F_L}{F_y}$, the inelastic lateral-torsional buckling nominal strength is

$$M_n = R_{pg} R_{pc} M_{yc}\left[1 - \left(1 - \frac{F_L}{R_{pc} F_y}\right)\left(\frac{\pi\sqrt{\frac{F_y}{\gamma_{eB} f_{bmaxAB}}} - 1.1}{\pi\sqrt{\frac{F_y}{F_L}} - 1.1}\right)\right]$$

$$M_n = 1.0(1.15)(1873.78)\left[1 - \left(1 - \frac{35}{1.15(50)}\right)\left(\frac{\pi\sqrt{\frac{50}{0.912(54.02)}} - 1.1}{\pi\sqrt{\frac{50}{35}} - 1.1}\right)\right]$$

$M_n$ = 1936.24 kip-in

The ratio, $\left(\frac{M_r}{M_n}\right)_B$ for the left unbraced length is $\left(\frac{M_r}{M_n}\right)_B = \frac{2007.44}{1936.24} = 1.037$

Because of $\left(\frac{M_r}{M_n}\right)_A = 0.994 < \left(\frac{M_r}{M_n}\right)_B = 1.037$, the lateral-torsional buckling strength of this beam is $M_n$ = 1936.24 kip-in

The brace stiffness using in this analysis is based on the torsional brace stiffness calculated in Section 5.3.3.1 ($\beta_T$ = 4885 kip-inch/rad). The reason to select this specific brace stiffness is that the cross-section at the brace point is the same as cross section in problem

TB1 in Section 5.3.3 (section W16x26). One should be noted that in this case the web distortional stiffness $\beta_{sec} = 0$ since the brace is connected to the beam by two rigid links. Therefore, based on the AISC 2005 Appendix 6 Commentary equations, the required brace stiffness is equal to the brace stiffness excluding web distortion, $\beta_T = \beta_{Tb} = 4885$ kips-inch/rad (see Section 5.3.3.1 for more detail).

Fig. 5.3.54 shows the relationship between the brace forces and the moment from the Finite Element Analysis for the brace stiffness $\beta_T = 4885$ kip-inch/rad and the rigid brace, $\beta = \infty$. This figure indicates that the brace moment is equal to 0.15% $M_n$ for the brace stiffness $\beta_T = 4885$ kip-inch/rad. The maximum moment from Finite Element Analysis is equal to 0.746 $M_n$ when using brace stiffness, $\beta_T = 4885$ kip-inch/rad and equal to 0.748$M_n$ when using the rigid brace.

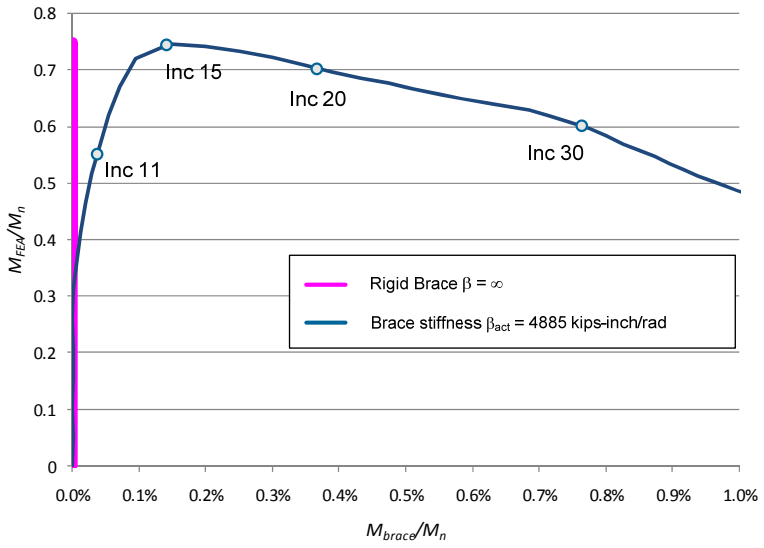


**Fig. 5.3.54. Torsional brace forces with brace stiffness β = 4885 kips-inch/rad and rigid brace, Tapered beam bracing.**

The deformed shapes corresponding to the four increments labeled in Fig. 5.3.54 using the brace stiffness $\beta_T = 4885$ kip-inch/rad are shown in Fig. 5.3.55.

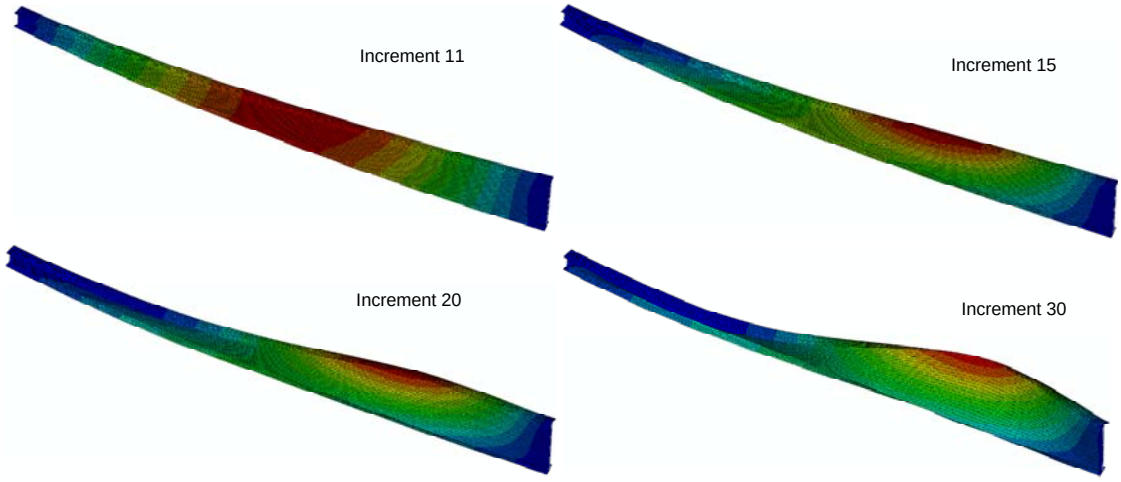


**Fig. 5.3.55. Deformed shape at the different stages for the brace stiffness β = 4885 kips-inch/rad, Scaled 5x, Tapered beam bracing.**

### 5.3.9 Summary

The Plastic Zone Solutions are conducted up to the nominal strength of beam $M_n$ for beams with a single intermediate nodal brace as well as for beams with the four intermediate nodal braces. The Benchmark Study LB3 shows that use of $\beta_{br} = 2\beta_i / \phi$ is not sufficient to develop $M_n = M_p$, although $M_n = 0.94M_p$ is developed. The behavior of the beam shows the similar response using brace stiffness $\beta_{br} = 2\beta_i / \phi$ or $\beta_{br} = 1.9\beta_i$. The Benchmark Study CB1 shows the effectiveness of using combined lateral and torsional bracing. This same beam performs well in uniform bending with a lateral brace stiffness of only 19 % of the Appendix 6 compression flange lateral bracing requirement and a torsional brace stiffness of only 51 % of the Appendix 6 torsional bracing requirement.

The Test No.6 from Richter (1998) performs well using Lateral bracing with $\beta_L = 1.3\beta_i$, torsional bracing with $\beta_T = 2\beta_i / \phi$, and combined bracing with $\beta_L = 0.15\beta_i$ (using the

compression flange lateral bracing $\beta_i$) and $\beta_T = 1.6\beta_i$ (60% of the Appendix 6 torsional brace stiffness requirement).

The tapered beam problem shows that the behavior of bracing system is rather complex than the behavior of prismatic beams. More research needs to be conducted to understand this type of bracing system.

### 5.4 Summary and Conclusions for Beam Bracing

Based on the result from analyses in Chapter 4 and Chapter 5, the conclusion and summary for beam bracing are summarized as follows.

1) Application of the Direct Analysis Method and other more refined methods to the assessment of beam stability bracing.
   - In the column strength solutions of part (*A*), the elastic stiffness was factored by 0.8 and the member strengths were factored by 0.9 to obtain brace force calculations compatible with the AISC member design strengths. Unfortunately, the application of these rules in the context of beam lateral torsional buckling is not as straightforward. Therefore, the beam bracing studies in this research are conducted with nominal stiffness and nominal strength values. As such, the beam load-deflection solutions may be considered as virtual experimental tests conducted for test members and bracing having nominal material properties.
   - In SAP2000 and in programs with similar shell FEA capabilities, web distortion effects can be approximated, and complications associated with separating web bend buckling modes from overall buckling modes can be alleviated in eigenvalue buckling solutions, by using a simplified analysis model with beam elements for the flanges and stiffeners and a single shell element through the depth of the web.

Rotational continuity is released between the web shell elements and the flange beam elements to account for the influence of web distortional flexibility that this coarse FEA approach would otherwise miss. The web bending effects at brace points are approximated by a separate beam element connecting the two flanges and having a width of $1.5h_o$. This is referred to in the following as the simplified model.

- The above simplified model gives errors in the prediction of $M_{cr}$ ranging from -14 to +8 %. It gives unconservative errors in the prediction of brace forces up to 21 %. Therefore, the approximation is reasonable compared to other design-analysis approximations, but better accuracy is desirable if one goes to the trouble of conducting an assessment by structural analysis.
- For load-deflection analysis studies, geometric imperfections may be applied in a fashion similar to the approach used in the prior column studies; however, for beams subjected to single-curvature bending, the tension flange is kept straight. This produces an overall twist in the cross-section of $(L_b/500)/h_o$ in addition to the compression flange sweeps of $L_b/500$ and is consistent with recommendations by Wang and Helwig (2005). For beams subjected to double-curvature bending both of the flanges may be displaced by $L_b/500$ in opposite directions or the initial displacements may be taken as one-half of these values (overall relative sweep between the two flanges of $L_b/500$). The selection of one or the other of these imperfection magnitudes is a judgment call.

2) Benchmarking comparisons to eigenvalue buckling solutions previously conducted by Yura (1992)

- Refined models of various test beams match closely with the prior eigenvalue buckling predictions by Yura.
- Simplified models of these same beams give reasonable approximate buckling solutions with similar trends in the responses.

3) Second-order elastic load-deflection analyses to determine beam bracing forces for the above benchmark cases
   - To the knowledge of the authors, complete load-deflection solutions of the beam brace forces have not been published for the benchmark beams in prior research.
   - For the single-curvature $n = 1$ lateral bracing cases studied, Appendix 6 gives a reasonable rough prediction of the brace forces obtained from the refined analysis models.
   - For the single-curvature $n = 1$ torsional bracing cases studied, the AISC Appendix 6 torsional bracing stiffness requirement is substantially conservative. Yura (1992) gives more detailed alternative equations that provide a reasonable approximation of the torsional brace stiffness requirement. The torsional bracing force demands are also predicted very conservatively by the Appendix 6 equations for the case of uniform bending. They are predicted reasonably well by the Appendix 6 equations for moment gradient and top flange loading. The more detailed equations specified by Yura and Phillips generally give better predictions in all cases.
   - Torsional brace moments $M_{br}$ as high as 3.8 % are predicted by the Yura (1992) equations and are observed in the refined analysis solutions. The Appendix 6 estimates can be higher than this.

- For single curvature bending and $n = 1$, the use of $1.9\beta_i$ roughly doubles the nodal lateral brace force demand relative to the Appendix 6 estimate. The brace force is still less than 2 % of $M_u/h_o$ though using this stiffness.
- For double-curvature bending and $n = 1$, the beam performs adequately with a nodal brace stiffness of 1.9/2.67 = 0.7 of the Appendix 6 requirement. The brace forces are approximately 1 % of $M_u/h_o$ for equal and opposite flange sweeps of $L_b/1000$, and are approximately twice this value for equal and opposite flange sweeps of $L_b/500$.

4) Benefits of combined light lateral bracing in reducing torsional bracing demands
   - The torsional brace stiffness and force demands are substantially reduced by providing a small amount of lateral bracing stiffness.
   - For the cases studied having light lateral bracing combined with torsional bracing, the combined stiffnesses may be reduced to 1.0 of the ideal bracing stiffness (i.e., the combined stiffnesses at which the bracing system buckles at the applied load level causing $M_u = M_{cr(K=1)}$) while still maintaining acceptable structural response. The maximum torsional brace moment in these extreme cases is 2.7 % of $M_{cr}$.

# CHAPTER 6

# CONCLUSIONS AND RECOMMENDATIONS

## 6.1 Summary

This thesis presents an extensive effort to establish a much clearer understanding of the actual demands on flange bracing in metal building systems. A wide range of column and beam case studies accounting for the influence of various attributes of metal building systems are investigated. These attributes include:

- Unequal brace spacing and stiffness,
- Partial bracing and continuity effects in members with large numbers of braces points,
- Nonprismatic member geometry,
- Variable axial load along the member length,
- Flexibility of end brace points,
- Load height effect and cross-section distortion,
- Combined nodal and relative bracing (Hybrid bracing system),
- Combined torsional and lateral bracing.

Second-order elastic analyses by the Direct Analysis Method and refined Distributed Plasticity Analysis are used to assess the bracing requirements for columns and beams. Also, procedures to determine the critical geometry imperfections are addressed in detail in this research. Both the column and beam case studies are investigated by using eigenvalue buckling analysis and load-deflection analysis solutions. In addition, the beam

bracing problems have been studied by using both refined and simplified analysis models. The advantage of using the simplified analysis model, other than the economy of the calculations, is to avoid complexities associated with the bend-buckling or compression buckling behavior of slender webs. The analysis results from the Direct Analysis Method and the Distributed Plasticity Analysis Method are compared with each other as well as with the bracing requirements from AISC 2005 Appendix 6. Key observations and findings from the DM and DP methods are summarized in the following sections.

## 6.2 Findings and Recommendations

- **Reduced bracing stiffness requirements due to continuity effects**
  - This research shows good performance of columns and of beams with bracing stiffnesses as low as $1.3\beta_i$ (1.3 times the ideal bracing stiffness corresponding to buckling of the bracing system) in members containing a large number of intermediate brace points. These benefits appear to be due to continuity effects in the member being braced, as well as load sharing among multiple intermediate brace points.
  - Members with only one intermediate brace require larger brace stiffnesses. It appears that good performance is still achieved with the use of lateral bracing stiffnesses of $1.9\beta_i$ in the worst-cases with single intermediate braces. The reduced bracing stiffness due to continuity effects can be reasoned as follows: When the bracing system stiffness is reduced to a value less than the *ideal bracing stiffness* for *full bracing* in a member that has multiple intermediate braces, the

reduction in the load capacity with reduced stiffness is much more gradual than in a member that has only a single intermediate brace. Hence, it makes sense that the increased force demands on the bracing are not as great with reduced bracing stiffness when there are multiple intermediate braces.

- Smaller bracing stiffnesses generally lead to larger bracing forces. The bracing forces for column bracing and beam lateral bracing using the above smaller bracing stiffnesses are still in the neighborhood of 2% of $P_u$ or $M_u/h_o$ at the critical load level.
- The current beam torsional bracing moment requirements reflect these larger percentages. It appears that the current AISC torsional bracing requirements should not be reduced any further unless other factors (such as combined lateral and torsional bracing) are considered.

- **Reduced torsional bracing stiffness requirements due to light lateral bracing**
  - The studies in this research show that dramatic reductions in the torsional bracing stiffness requirements occur with only a small amount of lateral bracing stiffness. The torsional bracing stiffness requirement is a function of the lateral bracing stiffness.
  - It is noted that typical metal building systems have stiffer bracing at the panel point locations of the cable or rod bracing, whereas the lateral bracing from the roof diaphragm at the purlin locations between these panel points is generally more flexible.

- **Potential improved analysis and design procedures**

Potential directions regarding synthesis of the research into design procedures, guidelines and/or rules are as follows.

- The current AISC Appendix 6 equations are based largely on the selection of a sufficient bracing stiffness for simplified nodal and relative bracing models. The corresponding force requirements are based on very simplified models that provide a reasonable but only a very coarse estimate of the force demands observed from refined models of nodal bracing systems.
- The Direct Analysis Method and other more refined procedures provide a means to assess the stiffness and strength requirements of any type of bracing system via analysis. However, there are significant complexities associated with the proper modeling of geometric imperfections and structural stiffnesses to determine the bracing demands in general structural systems. This is particularly the case when we consider the extension from more basic member or component bracing models to larger subassembly or complete system models. One option to alleviate some of these complexities is to focus on ***refined*** calculation of the buckling load multiplier ($\gamma_e$) for appropriate models (complete or subassembly models) of frames and their and bracing systems. The important keyword here is ***refined***. Refinements can include:
  - Consideration of the contribution of the flexural rigidity (*EI*) in the member that is being braced in solutions commonly analyzed as relative bracing.
  - Consideration of various contributions to stiffness and in analysis models of the structure at higher levels of sophistication than in the present basic relative

and nodal bracing models.

- Sufficient multiples of the ideal bracing stiffness, or sufficient $\gamma_e$ values greater than one, can be determined for different categories of bracing systems to ensure adequate performance, i.e.,
  - Maintaining bracing strength requirements to a tolerable level, e.g., 2 % in lateral bracing and 4 % in torsional bracing.
  - Maintaining the second-order amplification of the bracing system displacements and forces to levels sufficiently small such that the response will not be overly sensitive to changes in load or changes in stiffness.
- Upper bound force levels, which must be withstood in the bracing systems for selected minimum required stiffness levels, can be determined in the research studies for the different categories of systems, e.g., 2 % in lateral bracing and 4 % in torsional bracing.

## 6.3 Future Work

This research provides a reasonably comprehensive assessment of stability bracing requirements for columns and beams. Nevertheless, further studies are needed to cover all the bases relating to the complexities in physical metal building frame systems. The worthwhile areas for future work are as follows:

- **Local versus global influences on bracing stiffness and strength demands**

  Metal building frames are always designed to a loading envelope. Therefore, for a given loading causing say maximum moment at a particular location of the frame, a number of the other locations will tend to be less heavily stressed. As a result,

particularly when the limit state of the critical unbraced segment or segments involves substantial inelasticity, the bracing demands will tend to be significantly larger within the vicinity of the critical segment or segments. Obviously, design engineers will find it rather odd if they need to consider the bracing stiffness at some other remote location of a metal building frame when sizing the flange bracing at a selected location. For instance, in a clear-span frame, should the moment at the ridge, or the bracing system at the ridge, influence the bracing requirements at the knee? We need to sort out how to strike a balance between the physical behavior, design economy, and design simplicity.

It should be noted that for systems with weak partial bracing, the demands on any individual brace will be more sensitive to variations in all the different bracing stiffnesses and strengths. However, for cases approaching full bracing, it is expected that the demands on any individual brace will be much less sensitive to variations in bracing stiffnesses and strengths that are not local to the brace point being considered. Unfortunately, the most cost effective solutions often do not involve full bracing, e.g., the use of $L_q$ results in partial bracing. Localized member inelasticity also tends to lead to more localized brace demands and reduced sensitivity of brace stiffness and strength requirements to non-local changes in other brace stiffnesses and strengths. However, generally speaking, the elastic behavior of the system prior to development of yielding can result in significant non-local bracing interactions and sensitivities. The sensitivity to non-local changes in various brace stiffnesses and strengths also can depend significantly on whether the members are loaded close to their strength limit or not; unfortunately, the member strength limit can be influenced by partial

bracing, so the general determination of brace stiffness and strength requirements is quite complex.

- **Increased demands at the inside of the knee region of clear-span frames and at the exterior roof girder-to-column joints in modular frames**

The knee region of the clear-span frames should be examined carefully. A number of variables may influence the bracing requirements at the inside of the knee. These include:

  - The angle between the member centroidal axes.
  - The location of the centroid and shear center of the column and of the roof girder framing into the joint.
  - The dimensions of the end-plates at end-plate connections.
  - The size of the stiffeners on the other inside edge of the panel zone as well as whether the stiffeners are full height or half height.
  - The web panel zone thickness and the extent of post-buckling action being relied upon from the panel zone at the strength limit.
  - The ratio of the axial forces in the column and roof girder to the moment transferred at the knee joint.
  - The stiffness and offset of the eave strut, with the out-of-plane lateral bracing stiffness delivered at the eave strut by the diaphragm and cable or rod bracing systems being the most important stiffness attribute at this location.
  - The positioning of purlins or girts close to the end-plate connections and the stiffeners at the edges of the panel zone and the development of torsional bracing from the framing action of the stiffeners and end plates in

combination with these girts and purlins.

The future work would need to address how the design of bracing at the knee could be achieved without the need to consider a model of the entire structure.

- **Combined effects of bending plus axial force in the primary framing members.**

The axial force in the roof girders and/or exterior columns is typically small compared to the bending moment, and the effects of the axial force are expected to be smaller than a number of other effects that are typically ignored in many cases. Also, the use of beam bracing designed using $L_q$ implies that $\Omega M_a/M_n = 1$ (ASD) or $M_u/\phi M_n = 1$ (LRFD); hence, there is conceptually (and simplistically) no member capacity left to resist axial force when the bracing is designed using $L_q$. In addition, torsional bracing is not effective to allow a given brace point to be considered as a lateral brace for axial compression. Future research should address when the influence of bending plus axial force needs to be considered in the design of bracing.

# REFERENCES


AISC (1999*). Load and Resistance Factor Design Specification for Structural Steel Building*, American Institute of Steel Construction, Chicago, IL.

AISC (2005*). Specification for Structural Steel Building*, ANSI/AISC 360-05, American Institute of Steel Construction, Chicago, IL.

Chen, W.F, and Lui, E.M (1987), *Structural Stability: Theory and Implementation*, Elsevier, New York.

Chen, S., and Tong, G. (1994), "Design for Stability: Correct Use of Braces," Steel Structures, *Journal of the Singapore Structural Steel Society*, 5(1), 15-23.

Computer and Structures, Inc. (CSI). SAP2000 Analysis Reference, Version 11.

Dassault Systèmes (2007). ABAQUS Analysis Users Manual, Version 6.7.

Galambos, T.V (ed). (1998), *Guide to Stability Design Criteria for Metal Structures 5th Ed*., John Wiley and Sons, New York.

Galambos, T.V. (1963), "Inelastic Lateral Buckling of Beams," *ASCE Journal of Structural Division*, 89(5), 217-244.

Green, G., Winter, G. and Cuykendall, T. (1947), "Light gage steel columns in wall-braced panels", *Cornell Engineering Experiment Station*, Bulletin No. 35, Part 2, Ithaca, NY.

Griffis, L., and White, D.W. (2008). *Stability Design of Steel Buildings*, AISC Design Guide (to appear).

Gil, H. (1996), "Bracing Requirements for Inelastic Steel Members," thesis, presented to University of Texas at Austin, Austin, TX, in partial fulfillment of the requirements for the degree of Doctor of Philosophy.

GT-Sabre (Chang 2006).

Helwig, T.A. and Yura, J.A. (1999), "Torsional Bracing of Columns," *Journal of Structural Engineering*, American Society of Civil Engineers, 125(5), 547-555.

Helwig, T.A. (1994), "Lateral Buckling of Bridge Girders by Metal Deck Forms," thesis, presented to University of Texas at Austin, Austin, TX, in partial fulfillment of the requirements for the degree of Doctor of Philosophy.

Helwig, T.A., Yura, J. A., and Frank, K. H. (1993), "Bracing Forces in Diaphragms

and Cross Frames," *SSRC Conference, Is Your Structure Suitably Braced?* Milwaukee, Wisconsin, 129-140.

Kaehler, R., White, D.W. and Kim, Y.D. (2008). *Design of Frames Using Web-Tapered Members*, AISC/MBMA Design Guide (to appear).

Kemp, A.R. (1986), "Factors Affecting the Rotation Capacity of Plastically Designed Members," *The Structural Engineer*, 64B(2), 28-35.

Kemp, A.R. (1985), "Interaction of Plastic Local and Lateral Buckling," *Journal of Structural Engineering*, ASCE, 111(10), 2181-2196.

Lay, M.G. and Galambos, T.V. (1996), "Bracing Requirements for Inelastic Steel Beams," *ASCE Journal of Structural Division*, 92(ST2), 207-228.

Lukey, A.F. and Adams, P.F. (1969), "Rotation Capacity of Wide-Flange Beams under Moment Gradient," *ASCE Journal of Structural Division*, 95 (ST6), 1173-1188.

Lutz, A.L., and Fisher, J. (1985), "A Unified Approach for Stability Bracing Requirements," *AISC Engineering Journal*, 22(4), 163-167.

Li, G. (2002), "Bracing Design Requirements for Inelastic Members," thesis, presented to University of Texas at Austin, Austin, TX, in partial fulfillment of the requirements for the degree of Doctor of Philosophy

Mutton, B.R., and Trahair, N.S. (1973), "Stiffness Requirements for Lateral Bracing," *ASCE Journal of Structural Division*, 99 (ST10), 2167-2182.

McGuire, W. (1968). *Steel structures.* Prentice-Hall, Englewood Cliffs, N.J.

Medland, I. C. (1977). "A basis for the design of column bracing." *Struct. Engr.*, 55(7), 301-307.

Mutton, B. R., and Trahair, N. S. (1975). "Design requirements for column braces." *Or. Engrg. Trans.*, Australia, 17(1), 30-36.

Nair, R. S. (1992). "Forces on bracing systems," *Engrg. J., Am. Inst. Steel Constr.*, 29(1), 45-4.

Newman, A. (2004), *Metal Building System: Design and Specification,2nd* Ed, McGraw-Hill, New York.

Nethercot, D. A. and Trahair, N. S.,(1975). " Design of Diaphragm-braced I-Beams", *ASCE Journal of Structural Division* 101(ST10), 2045-2061.

Nethercot, D.A. and Trahair, N.S. (1976), "Inelastic Lateral Buckling of Determinate Beams," *ASCE Journal of Structural Division*, 102(ST4), 701-717.

O'Connor, C. (1979). "Imperfectly braced columns and beams," *Cir. Engrg. Trans.*, Institution of Engineers, Australia, 21(2), 69-74.

Plaut, R.H., and Yang, J.W. (1995). "Behavior of Three-Span Braced Columns with Equal or Unequal Spans." *Journal of Structural Engineering*, ASCE, 121(6): 986-994.

Plaut, R.H. (1993), "Requirements for Lateral Bracing of Columns with Two Spans," *ASCE Journal of Structural Division*, 119(10), 2913-2931.

Plaut, R.H., and Yang, J.G. (1993). "Lateral Bracing Forces in Columns with Two Unequal Spans." *Journal of Structural Engineering*, ASCE, 119(10), 2896-2912.

Riks, E. (1979), "An Incremental Approach to the solution of Snapping and Buckling Problems," *International Journal of Solids and Structures*, 15, 529-551.

Salmon, C.S., and Johnson, J. E. (1996), *Steel Structures: Design and Behavior, 4th* Ed, Harper & Row, New York.

Shanley, F.R. (1946), "The Column Paradox." *Journal of Aeronautical Science*, 13(5), 678.

Shanley, F.R. (1947), "Inelastic Column Theory," *Journal of Aeronautical Science*, 14(5), 261-267.

Stanway, G. S., Chapman, J. C., and Dowling, P. J. (1992). "A simply supported imperfect column with a transverse elastic restraint at any position. Part 1: behaviour." *Proc. lnstn. Civ. Engrs., Strucs. and Bldgs.*, 94(2), 205-216.

Taylor, A. C. and Ojalvo, M. (1966), "Torsional Restraint of Lateral Buckling," *Journal of the Structural Division*, ASCE, ST2, 115-129.

Timoshenko, S. and Gere, J., (1961), *Theory of Elastic Stability*, New York: McGraw-Hill.

Tong, G. S., and Chen, S. H., 1988, "Buckling of Laterally and Torsionally Braced Beams", *Journal of Constructional Steel Research*, 11, 41-55.

Trahair, N. S. and Nethercot, D. A. (1982), "Bracing Requirements in Thin-Walled Structures," *Developments in Thin-Walled Structures*, 2, 93-129.

Wang, L., and Helwig, T. A (2005), Critical Imperfections for Beam Bracing Systems, *ASCE Journal of Structural Division*, 131(6), 933-940.

Waltz M. E., McLain T.E., Miller T.H, Leichti R.J. (1999) Discrete Bracing Analysis for Light-Frame Wood-Truss Compression Webs, *J. Struct. Engrg.*, ASCE, 126(9)

Wakabayashi, M. and Nakamura, T. (1983),"Buckling of Laterally Braced Beams", *Eng. Struct.*, 5, 108-118.

Wang, Y. C. and Nethercot, D. A., (1989), "Ultimate Strength Analysis of Three-Dimensional Braced I-Beams", *Proceedings, Institution of Civil Engineers*, London, Part 2, 87,87-112.

Wang, L. (2002), "Cross-Frame and Diaphragm Behavior for Steel Bridges with skewed supports," thesis, presented to University of Houston, TX, in partial fulfillment of the requirements for the degree of Doctor of Philosophy.

Winter G. (1958), "Lateral Bracing of Columns and Beams", *Trans. ASCE*, Part 1, 125,809-925

White, D.W. (2008a). "Structural Behavior of Steel," Chapter 6, *Steel Bridge Design Handbook*, National Steel Bridge Alliance (to appear).

White, D.W., and Jung, S.-K. (2008). "Unified Flexural Resistance Equations for Stability Design of Steel I-Section Members – Uniform Bending Tests," *Journal of Structural Engineering*, ASCE, (to appear).

White, D.W., and Kim, Y.D. (2008). "Unified Flexural Resistance Equations for Stability Design of Steel I-Section Members – Moment Gradient Tests," *Journal of Structural Engineering*, ASCE, (to appear).

White, D.W., and Griffis, L.G..(2007) "Stability Design of Steel Buildings (Main Text and Appendices)"

White, D.W., and Griffis, L.G..(2007), "Stability design of steel buildings: Highlights of a new AISC design guide"

White, D.W., Surovek, A.E. and Kim, S.-C (2007a). "Direct Analysis and Design Using Amplified First-Order Analysis, Part 1 – Combined Braced and Gravity Framing Systems," *Engineering Journal*, AISC, 44(4), 305-322.

White, D.W., Surovek, A.E. and Chang, C.-J (2007b). "Direct Analysis and Design Using Amplified First- Order Analysis, Part 2 – Moment Frames and General Rectangular Framing Systems," *Engineering Journal*, AISC 44(4), 323-340.

White, D.W., and Chang, C.-J. (2007). "Improved Flexural Stability Design of I-Section Members in AISC (2005) – A Case Study Comparison to AISC (1989) ASD," *Engineering Journal*, AISC, 44(4), 291-304.

White, D.W., Surovek, A.E., Alemdar, B.N., Chang, C.-J., Kim, Y.D., and Kuchenbecker, G.H. (2006). “Stability Analysis and Design of Steel Building Frames Using the AISC 2005 Specification,” *International Journal of Steel Structures*, 6, 71-91.

Yura, J.A. (2001). “Fundamentals of Beam Bracing,” *Engineering Journal*, AISC, 38(1), 11-26.

Yura, J. A. (1996). ‘‘Winter’s bracing approach revisited.’’ *Engineering Structures* 8(10), 821–825.

Yura, J. A. (1995), “Bracing for Stability – State-of-the-Art”, Proceedings of the ASCE *Structures Congress XIII*, Boston, Ma., 88-103.

Yura, J. A. (1995a),”Bracing for Stability-State-of-the-Art”, *Proceedings*, Structures Congress XIII, ASCE, Boston, MA, 1793-1797

Yura, J.A. (1993b), “Fundamentals of Beam Bracing,” Is Your Structure Suitably Braced? 1993 Conference, Milwaukee, Wisconson, *Structural Stability Research Council*, Bethlehem, PA, 1-40.

Yura, J. A. and Phillips, B. (1992), “Bracing Requirements for Elastic Steel Beams,” *Report No. 1239-1*, Center for Transportation Research, University of Texas at Austin, May, 73.

Yura, J. A., Phillips, B., Raju, S., and Webb, S. (1992), “Bracing of Steel Beams in Bridges,” *Report No. 1239-4F*, Center for Transportation Research, University of Texas at Austin, October, 80.

Ziemian, R.D. and McGuire, W. (2007). Mastan 2, Version 3.0, www.mastan2.com .

Zuk, W. “Lateral bracing forces on beams and columns”, J. *Engng Mech., ASCE* 1956, 82 (EM3), 1032-1-1032-16.